Observational study of inflammatory profiles in patients with ST-elevation myocardial infarction stratified by plaque erosion or rupture identified by optical coherence tomography:

The Plaque Erosion Pilot Study

Dr Sujay Chandran

MBBS, BSc, MRCP (London)

Cardiology Department

Norfolk and Norwich University Hospital

Colney Lane

Norwich

NR4 7UY

Submitted for the degree of

Doctor of Medicine (MD)

To the University of East Anglia

2017

Supervisors:

Dr Alisdair Ryding

Professor Marcus Flather

University of East Anglia

ABSTRACT

Background

Plaque erosion is responsible for 30–40% of ST-elevation myocardial infarction (STEMI) cases, but the underlying cause is unknown. Autopsy studies suggest that inflammatory infiltrates are less abundant in erosion compared to plaque rupture, which suggests that other pathological mechanisms are important. So far, different inflammatory profiles have not been demonstrated in vivo.

Objectives

We sought to characterise the inflammatory profiles of plaque rupture and plaque erosion in patients with STEMI undergoing primary percutaneous coronary intervention (PPCI).

Methods

Forty STEMI patients undergoing PPCI with less than six hours of chest pain were recruited in a single-centre observational study. Blood samples were taken from the infarct-related artery and a peripheral artery. Culprit plaques were imaged using optical coherence tomography (OCT) before PCI and classified by three blinded observers as ruptured fibrous cap (RFC) or intact fibrous cap (IFC). The expression profiles of 102 cytokines were measured using an array, and comparisons of the two pathological groups were performed using the Significance Analysis of Microarrays (SAM) methodology. Significant cytokines were validated with enzyme-linked immunosorbent assay (ELISA) and this was confirmed statistically using Wilcoxon rank-sum tests. Thrombectomy samples were analysed for differential mRNA expression using real-time polymerase chain reaction (RT-PCR).

Results

Twenty-three lesions were classified as RFC (58%), fifteen as IFC (38%) and two were undefined (4%). Overall, 12% (12/102) of cytokines were differentially

expressed in both coronary and peripheral plasma. We selected the most significant differences and confirmed that IFC was associated with preferential expression of epidermal growth factor (EGF) (coronary samples: SAM adjusted $P < 0.001$; ELISA IFC 7.42 vs RFC 6.63 $\log_2$ pg/ml, $P = 0.036$) and Thrombospondin-1 (TSP-1) (coronary samples: SAM adjusted $P = 0.03$; ELISA IFC 10.4 vs RFC 8.65 $\log_2$ ng/ml, $P = 0.0041$). Interferon-inducible T-cell alpha chemoattractant (I-TAC) was preferentially expressed in RFC (coronary samples: SAM adjusted $P <0.001$; ELISA IFC 10.2 vs RFC 10.8 $\log_2$ pg/ml; $P = 0.042$). Thrombectomy mRNA demonstrated significantly elevated EGF expression in IFC ($P = 0.0264$) and I-TAC in RFC ($P = 0.0007$), but no differences in expression of TSP-1.

Conclusions

Distinct inflammatory profiles for RFC and IFC are demonstrable in coronary plasma and thrombectomy specimens in STEMI patients. IFC is associated with elevated intracoronary EGF and TSP-1. These results may help to further understand the pathophysiology of plaque erosion and to potentially tailor future treatment strategies.

(Chandran S, Watkins J, Abdul-Aziz A, Shafat M, Calvert PA, Bowles KM, et al. Inflammatory differences in plaque erosion and rupture in patients with ST-segment elevation myocardial infarction. J Am Heart Assoc. 2017 May 3;6(5).)

DECLARATION

This thesis is the result of my own work and has not been submitted for a degree elsewhere. The help and contributions of others to this work are specified in the acknowledgements section. Where information has been derived from other sources, I confirm that this has been indicated in the thesis.

The thesis does not exceed the prescribed word limit for the relevant degree committee.

The work described in this thesis has been conducted primarily in the cardiac catheter laboratories within the cardiology department of Norfolk and Norwich University Hospital and the Bob Champion Research and Education Centre, University of East Anglia.

I drafted the protocol for the Plaque Erosion Pilot Study and progressed the study through research and development at Norfolk and Norwich University Hospital and the Camden and Islington Research Ethics Committee for approval.

I actively screened and recruited participants and was personally present during the recruitment of all forty patients recruited for the Plaque Erosion Pilot study. I collected all of the data and personally undertook cytokine analysis by learning and performing the techniques of cytokine arrays and ELISAs. In addition, I anonymously analysed each of the OCT images from all of the patients recruited into the study. The clinical, angiographic and OCT statistical measurements were all performed by myself. With Alisdair Ryding, I drafted and managed revisions for the manuscript summarising this work, which has been published.

DEDICATION

I would like to dedicate this thesis firstly to my wife, Selina: thank you for all your love, encouragement and support during my MD. Thank you for listening and taking an interest in something you knew very little about! The last few years, beginning with my time in Norwich, have been some of the happiest times of my life, ending with us finally getting married.

To my sister, Shruthi: thank you for continually being very supportive and caring throughout my career and during my MD. You are the best little sister I could ever have wished for. I hope that I can try to provide the same level of understanding and support during what I know will be a very successful career for you.

Finally, to my parents, Jaya and Subash: thank you for absolutely everything you have done for me. You have both been incredible parents to Shruthi and myself and have provided us with anything and everything we have ever needed. You have always encouraged and guided me through difficult times. I hope one day I can emulate you both by being as doting a parent as you have been to me.

ACKNOWLEDGEMENTS

The last couple of years have been thoroughly enjoyable, fulfilling and rewarding, and several people deserve special mention.

Firstly, I would like to thank my primary supervisor, Dr Alisdair Ryding. Thank you for developing the idea of the PEPS project and for taking me on board as your first research fellow. I am truly indebted to you for your support, guidance, teaching and mentorship since I have known you. You have helped me develop into a better researcher and interventional cardiologist. I hope we can continue to work together in the future.

Secondly, I would like to thank Professor Marcus Flather. Thank you for believing that I was the right candidate to come to Norwich to continue your vision of improving and developing the exciting research possibilities within the Norfolk and Norwich University Hospital. I have thoroughly enjoyed learning from you and have fully appreciated all of the constructive feedback and guidance you have given me.

I am very thankful for the guidance of Dr Stuart Rushworth and Professor Kristian Bowles at the Bob Champion Research and Education Centre. Thank you both for allowing us to collaborate and letting me use the facilities for cytokine analysis. I am particularly grateful to Stuart for teaching me the laboratory techniques, including cytokine arrays and ELISAs, and how to be a good basic science researcher. Thank you also for your help in performing the mRNA analysis of the thrombectomy specimens.

I would like to extend my gratitude to Stuart's PhD students, Amina Abdul Aziz and Manar Shafat, for their help and supervision in performing the laboratory-based experiments.

I would particularly like to thank Johnathan Watkins for his help in performing complex multivariate statistical analysis on the results of the cytokine array analysis and ELISAs. Thank you also for providing additional statistical support for the project.

I am very grateful to both cardiac research nurses, Ian Gallagher and Mary Ilsley, for their support and help with record keeping and documentation.

I would like to thank all of the interventional cardiologists at the Norfolk and

Norwich University Hospital, Dr Timothy Gilbert, Dr Sarev, Dr Simon Eccleshall, Dr Trevor Wistow and Dr Liam Hughes, for allowing me to recruit STEMI patients from their lists. I would also like to extend my thanks to all of the cardiac catheter laboratory staff for their help and patience during recruitment.

I am also very grateful to Professor Roger Hall, Professor Andreas Baumbach and Dr Thomas Johnson for their oversight of the study.

Finally, I would like to thank all of the patients who participated in the study.

Publications arising from MD (Res) thus far

Abstracts

Chandran SS, Watkins J, Abdul-Aziz A, Calvert P, Rushworth S, Bowles K, et al. Abstract 14288: Differential cytokine expression in plaque erosion and rupture in ST segment elevation myocardial infarction. Circulation. 2016 Nov 11; 134(Suppl 1):A14288 LP-A14288. Presented at the American Heart Association, November 2016 as a moderated poster.

Chandran SS, Watkins J, Abdul-Aziz A, Calvert P, Rushworth S, Bowles K, et al. Abstract: Plaque erosion pilot study. Heart 2017; 103:A3. Presented at Advanced Coronary Intervention, January 2017 as a moderated poster.

Chandran SS, Watkins J, Abdul-Aziz A, Calvert P, Rushworth S, Bowles K, et al. Abstract 89232: Differential cytokine expression between the coronary and peripheral circulation in patients with ruptured and intact fibrous caps presenting with ST segment myocardial infarction. European Heart Journal, Volume 38, Issue suppl_1, 1 August 2017, ehx502. P1779. Presented at ESC congress, Barcelona, August 2017 as a moderated poster.

Publications

Chandran S, Watkins J, Abdul-Aziz A, Shafat M, Calvert PA, Bowles KM, et al. Inflammatory differences in plaque erosion and rupture in patients with ST-segment elevation myocardial infarction. J Am Heart Assoc. 2017 May 3;6(5).

Table of Contents

List of Tables

List of Tables

List of Abbreviations

ACS	–	Acute coronary syndrome
AHA	–	American Heart Association
AMI	–	Acute myocardial infarction
Apo E	–	Apolipoprotein E
AU	–	Arbitrary units
BDNF	–	Brain-derived natriuretic peptide
BTC	–	Betacellulin
CECs	–	Circulating endothelial cells
CHD	–	Coronary heart disease
CRP	–	C-reactive protein
CS	–	Coronary sinus
CT	–	Cycle threshold
cTnI	–	Cardiac troponin I
CXCR3	–	Chemokine receptor 3
DRLA	–	Distal reference luminal area
DS	–	Diameter stenosis
ECM	–	Extracellular matrix
ECs	–	Endothelial cells
EF	–	Ejection fraction
EGF	–	Epidermal growth factor
ELISA	–	Enzyme-linked immunosorbent assay
EMPs	–	Endothelial circulating microparticles
EPCs	–	Endothelial progenitor cells
EREG	–	Epiregulin
ESS	–	Endothelial shear stress

FBC	–	Full blood count
FD	–	Frequency domain
FGF-7	–	Fibroblast growth factor-7
GADPH	–	Glyceraldehyde 3-phosphate dehydrogenase
Gp2b3a	–	GlycoproteinIIbIIIa
GPx-1	–	Glutathione peroxidase
Hb	–	Haemoglobin
HB-EGF	–	Heparin-binding epidermal growth factor
HGF	–	Hepatocyte growth factor
HOCL	–	Hypochlorous acid
I-TAC	–	Interferon-inducible T-cell alpha chemoattractant
ICAM	–	Intercellular adhesion molecule
IFC	–	Intact Fibrous Cap
IL	–	Interleukin
IL-19	–	Interleukin-19
IRA	–	Infarct-related artery
IVUS	–	Intravascular ultrasound
JAM	–	Junction adhesion molecules
LAD	–	Left anterior descending
LAO	–	Left anterior oblique
LCx	–	Left circumflex
LDL	–	Low-density lipoprotein
LMWH	–	Low molecular weight heparin
LP	–	Lipid pool
Lp-PLA2	–	Lipoprotein-associated phospholipase A2
LPS	–	Lipopolysaccharides

LV	–	Left ventricular
Lym	–	Lymphocytes
MACCE	–	Major adverse cardiac and cerebrovascular event
MAPK	–	Mitogen-activated protein kinase
MCP-1	–	Macrophage-chemotactic protein-1
MCSF	–	Macrophage colony stimulating factor
MI	–	Myocardial infarction
MiRs	–	MicroRNAs
MLD	–	Minimal luminal diameter
MMLV	–	Moline murine leukaemia virus
MMPs	–	Matrix metalloproteinases
MnCl2	–	Manganese (II) chloride
MPO	–	Myeloperoxidase
mRNA	–	Messenger RNA
MVO	–	Microvascular obstruction
NC	–	Necrotic core
NETs	–	Neutrophil extracellular traps
Neu	–	Neutrophils
NFkB	–	Nuclear transcription factor kappa-B
NNUH	–	Norfolk and Norwich University Hospital
OCT	–	Optical coherence tomography
ORW	–	Offline review workstation
OSI	–	Oscillatory shear index
PAI-1	–	Plasminogen activator inhibitor-1
PAPP-A	–	Pregnancy-associated plasma protein-A
PCI	–	Percutaneous coronary intervention

PEPS	–	Plaque Erosion Pilot Study
PIGF	–	Placental growth factor
PIT	–	Pathologic intimal thickening
PKB	–	Protein kinase B
Plts	–	Platelets
PCI	–	Percutaneous coronary intervention
PPCI	–	Primary percutaneous coronary intervention
PR	–	Plaque rupture
PRLA	–	Proximal reference luminal area
QCA	–	Quantitative coronary angiography
RANTES	–	Regulated on activation normal T-cell expressed and secreted
RAO	–	Right anterior oblique
RBCs	–	Red blood cells
RCA	–	Right coronary artery
RDB	–	RNA dilution buffer
RFC	–	Ruptured fibrous cap
ROS	–	Reactive oxygen species
RT	–	Reverse transcription
RT-PCR	–	Real-time PCR
RVD	–	Reference vessel diameter
RWA	–	RNA wash solution
SAA	–	Serum amyloid A
SAM	–	Significance analysis of microarrays
sCD40L	–	Soluble CD40 ligand
SMCs	–	Smooth muscle cells

sPLA2	–	Secretory type II phospholipase A2
SRA	–	Scavenger receptor A
STEMI	–	ST segment myocardial infarction
TCAD	–	Transplant coronary artery disease
TCFA	–	Thin-cap fibroatheroma
Thr	–	Thrombus
TIMI	–	Thrombolysis in myocardial Infarction
TIMPs	–	Tissue inhibitors of MMPS
TLR2	–	Toll-like receptor-2
TLRs	–	Toll-like receptors
TMB	–	Tetramethylbenzidine
TNF-α	–	Tumour necrosis factor
TOTAL	–	Trial of Routine Aspiration Thrombectomy With PCI Versus PCI Alone in Patients With STEMI
TrkB	–	Tropomyosin-related kinase receptor B
TSP-1	–	Thrombospondin-1
UH	–	Unfractionated heparin
VCAM-1	–	Vascular cell-adhesion molecule
VH-IVUS	–	Virtual histology-intravascular ultrasound
VHTCFA	–	Virtual histology thin-cap fibroatheroma
VSMC	–	Vascular smooth muscle cell
WBCC	–	White blood cell count
WBCs	–	White blood cells
WCC	–	White cell count
WSS	–	Wall shear stress

Chapter 1: Introduction

1.1 Epidemiology of myocardial infarction

Despite improvements in medical care, atherosclerotic cardiovascular disease remains a significant cause of morbidity and mortality worldwide. Cardiovascular disease causes 27% of all deaths in the UK, and coronary heart disease (CHD) itself is the UK's single biggest cause of death, accounting for nearly 160,000 deaths per year (1). Acute myocardial infarction (AMI) is responsible for most deaths from coronary heart disease, with approximately 188,000 hospital admissions annually attributed to AMI in the UK every year (2). CHD is projected to remain a leading cause of mortality and morbidity, not only in affluent countries but also globally, for many years to come (3). The aetiology of CHD is multifactorial but the trilaminar arterial vessel wall is key to understanding the initiation and progression of atherosclerosis.

1.2 The trilaminar arterial vessel wall

The normal arterial wall consists of three distinct layers. The inner most layer – the tunica intima – comprises a single layer of squamous epithelium termed the endothelium, which lines the lumen, and a layer of connective tissue bound by the internal elastic lamina. The intima also comprises a proteoglycan layer interspersed with smooth muscle cells. The endothelial layer has many important functions as a barrier layer, as well as inhibition of thrombus formation, angiogenesis and the regulation of vascular tone and growth.

The internal elastic lamina separates the tunica intima from the tunica media, the middle layer. The underlying tunica media contains circularly arranged multiple layers of vascular smooth muscle cells (VSMC). VSMCs permit changes in blood vessel diameter (vasoconstriction and vasodilatation) regulated by sympathetic vasomotor nerve fibres.

The tunica adventitia is the outermost layer and is separated from the tunica media by the external elastic lamina. This layer consists of a layer of collagen-rich, loose connective tissue, fibroblasts and perivascular nerves. It also consists of the vasa vasorum, a microvasculature providing nutrients and oxygen to the arterial wall.

1.2.1 Atherosclerosis

Atherosclerosis is a chronic disease of the large and medium-sized muscular arteries and is characterised by endothelial dysfunction, vascular inflammation and the build-up of lipids, cholesterol, calcium and cellular debris within the intima of the vessel wall (4). The word atherosclerosis originates from the Greek ‘athero’, meaning gruel or wax and ‘sclerosis’, meaning hardening or induration. Pathologically, ‘athero’ refers to the core necrotic base and ‘sclerosis’ to the fibrous cap at the luminal edge of the atherosclerotic plaque (5). This is a dynamic process involving the progression of early lesions to advanced plaques that are responsible for the majority of acute ischaemic cardiovascular events (6). Systemic risk factors for atherosclerosis include genetic predisposition, hyperlipidaemia, hypertension, cigarette smoking, diabetes mellitus and chronic inflammatory conditions (7).

1.2.2 Role of shear stress

Although the entire arterial tree is exposed to the atherogenic effect of systemic risk factors, atherosclerotic lesions form at specific arterial loci and this is influenced by the points at which low- and high-oscillatory endothelial shear stresses (ESS) occur. Regions with low-oscillatory shear stresses appear to be more prone to atherosclerotic lesions and, conversely, regions of high-stress are relatively protected (8). Therefore, plaque tends to develop at specific sites in the arterial tree: at side-branches, the outer wall of bifurcations and the inner curve of large arteries (9).

1.2.3 Classification of atherosclerosis

Initially, Stary et al. (10) classified atherosclerosis, proposing a classification of both early intimal lesions and more advanced atheromatous plaques, which led to the American Heart Association (AHA) classification, first published in 1994 and revised in 1995. This was modified by Virmani et al. (11) to take into account post mortem data of plaques responsible for sudden cardiac death and also the recognition from other studies (12) that plaque rupture was not the only mechanism responsible for coronary thrombosis (Table 1).

1.2.3.1 Intimal thickening and fatty streaks

The earliest vascular change described microscopically was intimal thickening (AHA Type I lesion), which consists mainly of smooth muscle cells (SMCs) and the proteoglycan matrix with little or no infiltration of inflammatory cells. 'Fatty streaks' represent lesions composed primarily of foamy macrophages and, to a lesser extent, lipid-laden smooth muscle cells within the intima. This entity is considered by the AHA classification as the earliest lesion of atherosclerosis, although studies have shown that this is a reversible process with few progressive tendencies (13).

1.2.3.2 Pathological intimal thickening

The earliest progressive and potentially persisting lesions is pathologic intimal thickening (PIT, AHA Type III lesion). This lesion is characterised by the presence of SMCs interspersed within the extra cellular matrix (ECM) towards the lumen and areas of extracellular lipid accumulation with an absence of SMCs (lipid pool) close to the media. They are further divided into two groups based on the presence or absence of macrophage infiltration (PIT without macrophages and PIT with macrophages) (11).

1.2.3.3 Fibroatheroma

Fibroatheromas (AHA Type IV lesion) are characterised by a dense fibrous cap overlying a necrotic core, and this lesion is further divided into two different stages: early and late fibroatheromas (14). Early fibroatheroma is defined as a lesion consisting of macrophage infiltration in the lipid pool, forming focal areas of necrosis, with loss of proteoglycans. Late fibroatheroma consists of a necrotic core with discrete collections of cellular debris, an increase in free cholesterol crystals, and complete depletion of ECM (proteoglycans and collagen).

Stage		Stary *et al.*	Virmani *et al.*
Early plaque	"Fatty streaks"	Type I: microscopic collections of lipid and foam cells, seen in infants	Intimal thickening
		Type II: macroscopic 'fatty streak' visible with naked eye containing inflammatory cells, seen in the aorta of infants and adolescents	Intimal xanthoma
		Type III: extracellular lipid pools within layers of vascular smooth muscle cells	Pathological intimal thickening
Intermediate plaque		Type IV: well-defined lipid-rich core	Fibrous cap atheroma
			Thin-capped fibroatheroma (TCFA)
	Atheroma	Type Va: New fibrous cap overlying lipid core	Healed plaque rupture
Late plaque		Type Vb: calcific lesion	
	Fibrous plaque	Type Vc: fibrotic lesion with minimal lipid	Fibrous plaque
Complicated plaque	Miscellaneous	Type VIa: surface disruption	
		Type VIb: intraplaque haemorrhage	
		Type VIc: adherent intraluminal thrombosis	
			Calcified nodule

Table 1: Classification of atherosclerotic lesions (adapted from Stary et al. (10) and Virmani et al. (11)) AHA classification of atherosclerotic lesions

1.3 Atherothrombosis

Whilst most coronary artery plaques are asymptomatic, some cause obstruction with stable angina and others may become unstable leading to an acute coronary syndrome (ACS). Patients with ACS present with unstable angina, acute myocardial infarction, with or without ST elevation, and sudden coronary death. Most of the acute coronary syndromes are believed to result from luminal coronary artery thrombosis with numerous autopsy studies conducted ascribing most fatal coronary events to a physical disruption of coronary arterial plaques (Figure 1) (15).

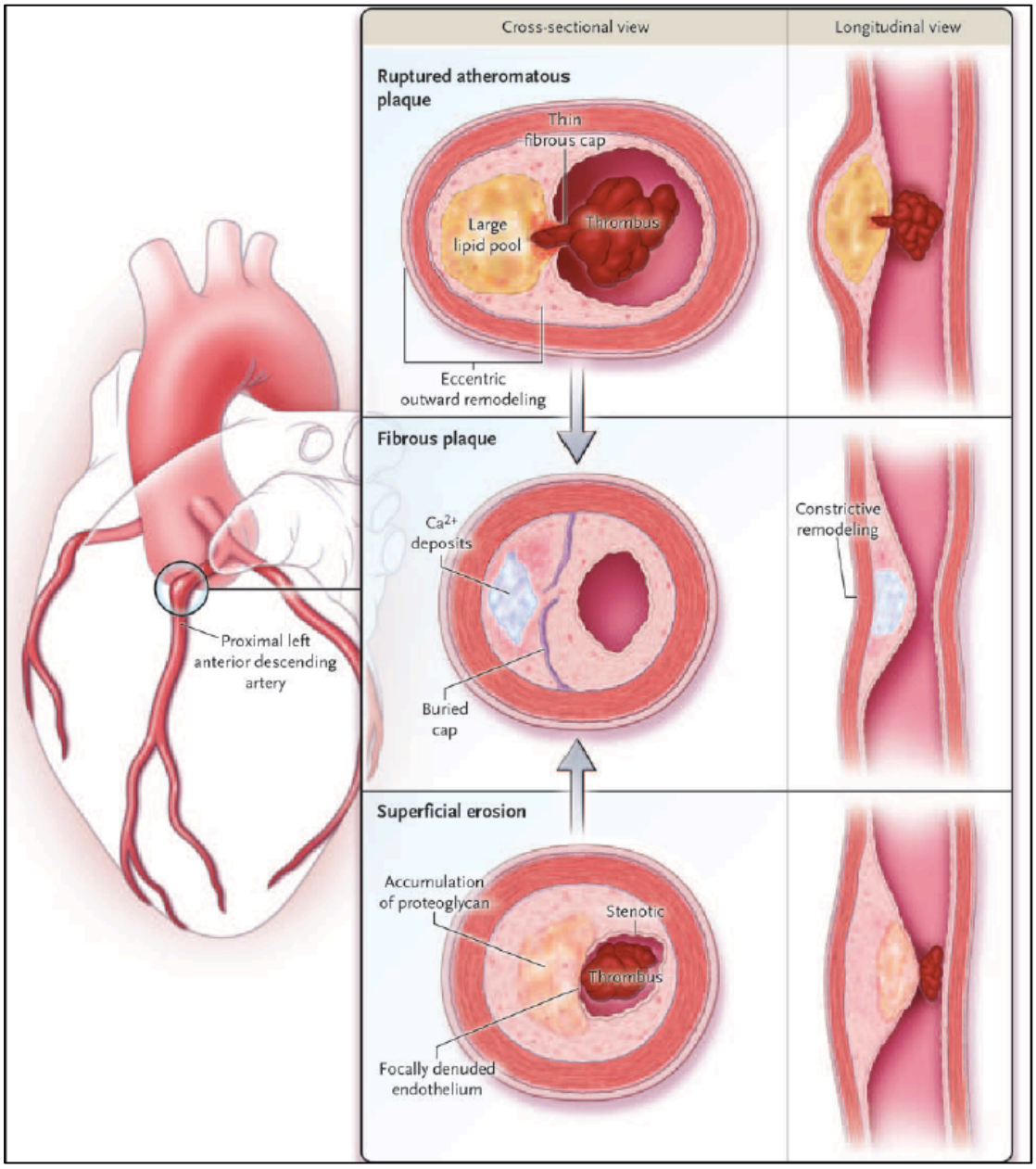

Figure 1: Atherosclerotic plaques with various presentations of coronary artery disease

This figure illustrates lesion types at the plaque level in both cross sectional and longitudinal views. The top two images demonstrate an eccentric, positively remodelled atheromatous plaque in which the fibrous cap is thin and has ruptured, provoking thrombus formation. The middle two images demonstrate healing of disrupted atheromatous plaques. This healing process can encourage the development of a non-occlusive atheromatous, lipid-rich plaque to a stenotic, more fibrous, calcified plaque. The bottom two images illustrate a proteoglycan-rich plaque, in which superficial erosion of the intimal surface has caused an occlusive thrombus (reproduced from Libby et al. (15)).

1.4 Plaques underlying coronary thrombi

Pathological studies of the thrombosed coronary artery attribute sudden death to three distinct morphologic entities: plaque rupture, plaque erosion and calcified nodules. The most frequent underlying mechanism of sudden coronary death from thrombi is from plaque rupture (55-65%), followed by erosions (30-35%) and most infrequently from calcified nodules (2-7%)(16). Each will be discussed in turn in greater detail.

1.4.1 Plaque rupture

Plaque rupture is the most common cause of fatal acute coronary syndromes (11). In a consensus statement by Schaar et al., plaque rupture was defined as a 'structural defect (gap) in the fibrous cap that separates the lipid-rich necrotic core of a plaque from the lumen of the artery' (Figure 2) (17). The fibrous cap consists mainly of type I collagen, with significant numbers of macrophages and lymphocytes, and with sparse distribution of smooth muscle cells. In spite of common belief that fibrous cap rupture occurs at its weakest point, which is commonly near shoulder regions, autopsy studies have used serial sections to demonstrate that a similar number of ruptures occur at the mid portion of the fibrous cap, particularly following exercise (18). Such plaques often, but not always, have thin fibrous caps (50–65 μm thick) (19). A disruption of the thin fibrous cap allows circulating cellular and non-cellular elements within the lumen of the artery to come into direct contact with the highly thrombogenic components of the necrotic core, and this contact results in thrombus formation. Focal calcification, or spotty calcification, is frequently observed in ruptured plaques, and is most commonly located towards the abluminal surface of the necrotic core (20).

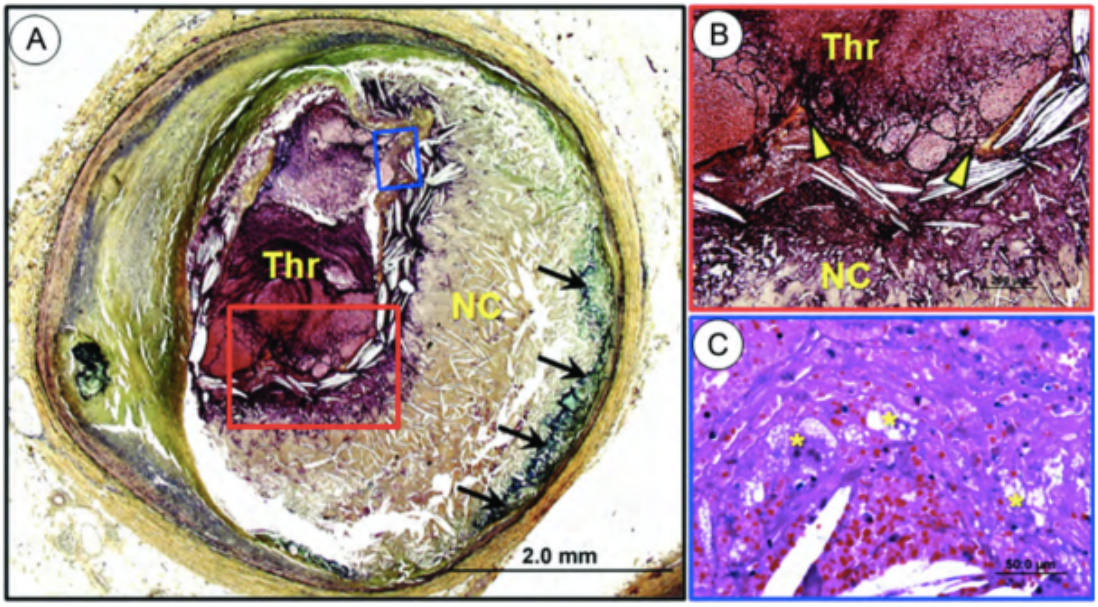

Figure 2: Plaque rupture. Cross-sectional photomicrograph of a coronary artery showing plaque rupture

A) An acute occlusive luminal thrombus characterised by a large necrotic core (NC) and thin fibrous cap. Note calcification near the NC base (arrows) and destruction of the medial wall. (B) (Red box within A) Higher magnification of the rupture site, demonstrating disruption of the thin fibrous cap (yellow arrows). (C) (Blue box within A) Higher magnification image of thrombus with cholesterol clefts, red cells and foamy macrophages (asterisks) (reproduced from Falk et al. (21)).

1.4.2 Plaque erosion

From the 1990's, the term 'plaque erosion' was used to describe the process of coronary thrombosis without associated plaque rupture (22). Plaque erosion is the second most prevalent cause of thrombosis. The fibrous cap is not disrupted and the luminal surface beneath the thrombus lacks endothelium, macrophages and T-cell infiltrates. However, it is rich in proteoglycans and smooth muscle cells (23).By contrast with ruptured plaques, where the media is necrotic and often destroyed, plaque erosion has pathological intimal thickening and sometimes calcification with an intact media.

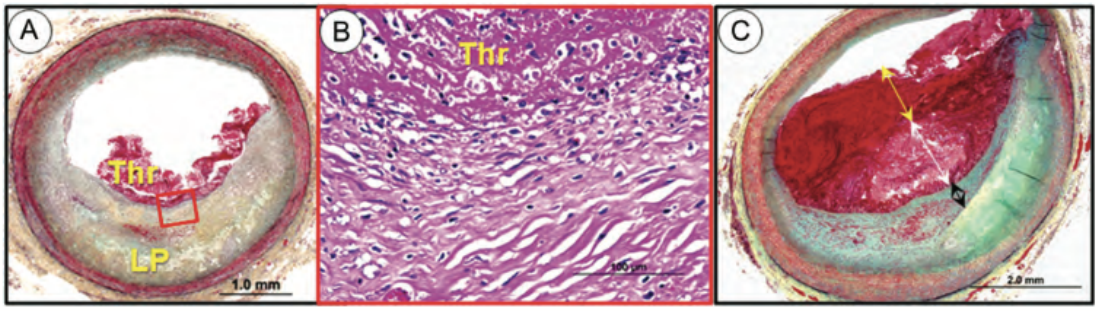

Figure 3: Plaque erosion. Cross-section of a coronary artery showing plaque erosion

(A) A non-occlusive thrombus (Thr) is present on the surface of a plaque, consisting of pathological intimal thickening. There is no connection between the thrombus and the lipid pool (LP), and the media is intact. (B) Higher-magnification image of the red box in (A). Presence of thrombus and the underlying plaque, consisting of smooth muscle cells in a proteoglycan–collagen-rich matrix. (C) Another case of plaque erosion. The oldest layer of the plaque (black double arrow) is an organising thrombus and is being replaced by smooth muscle cells in a proteoglycan-rich matrix, and there is an overlying acute thrombus present in the lumen of varying ages (white and yellow double arrows) (reproduced from Falk et al. (21)).

1.4.3 Calcified nodule

The term ‘calcified nodule’ was introduced by Virmani et al. (11) to describe a rare type of coronary thrombosis not caused by plaque rupture but related to disruptive nodular calcifications protruding into the lumen (Figure 4). The calcified nodule is the least frequent cause of luminal thrombus, accounting for approximately 5% of acute thrombotic cases (11). It usually occurs in older individuals and in tortuous heavily calcified arteries. Calcified nodules are composed of fibrocalcific plaque with little or no underlying necrotic core and a luminal surface that is disrupted by nodules of dense calcium, with overlying thrombus. They have large plates of calcified matrix with surrounding areas of fibrosis, inflammation and neo-vascularisation. The precise nature of this lesion remains poorly understood, although fragmentation of calcified plates is believed to be the aetiology of the nodular calcification.

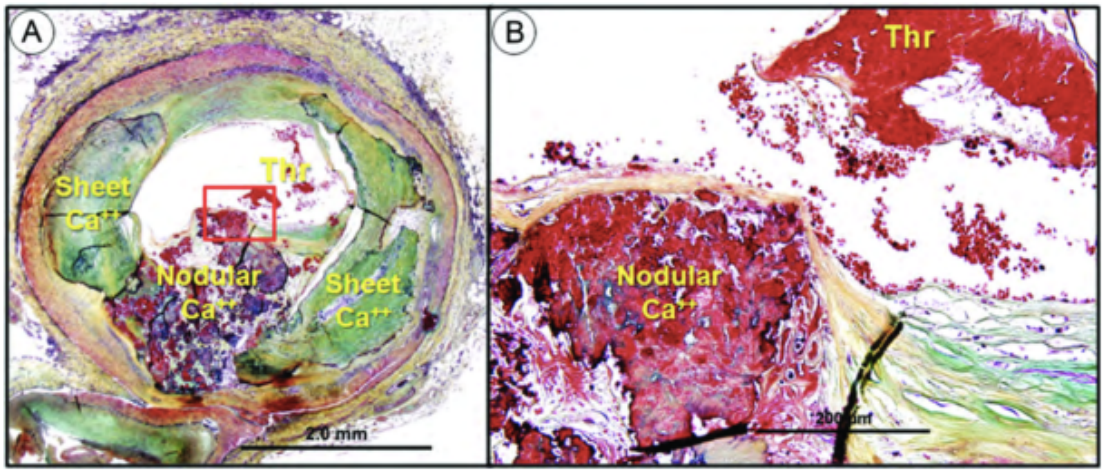

Figure 4: Cross-section of the coronary artery showing the presence of calcified nodule

Nodular calcifications (Ca++) are identified between sheets of calcification. (B) Higher-magnification image of the red box in (A). The nodular calcification is protruding into the lumen area with an overlying non-occlusive thrombus (reproduced from Falk et al. (21)).

1.5 Risk factors for coronary thrombosis

1.5.1 Vulnerable plaque

The term vulnerable plaque has been used for plaques assumed to be at high risk of thrombosis (24). There is significant interest in the identification of these plaques prior to the occurrence of thrombosis since early detection could lead to research into preventative methods. Although recognised as a cause of thrombosis, calcified nodules are not thought of as high-risk lesions (25), leaving two major types of vulnerable plaque: rupture-prone and erosion-prone.

1.5.2 Rupture-prone plaques

Pathological and clinical studies have revealed that the atherosclerotic plaque type at the greatest risk of rupture is a thin-cap fibroatheroma (TCFA), characterised by a large necrotic core covered by a thin layer of fibrous cap (16). TCFA is recognised by its morphologic resemblance to a ruptured plaque. The main differences are the absence of a luminal thrombus, an intact thin fibrous cap, a smaller necrotic core, expansive remodelling, spotty calcification, less plaque burden, less luminal encroachment (mild stenosis by angiography) and fewer macrophages infiltrating the

thin fibrous caps (26). The thin fibrous cap is made up mostly of type I collagen and there is either an absence of, or only a few SMCs observed. The thin fibrous cap is traditionally defined as being <65μm thick, an indicator of plaque vulnerability (11).

1.5.3 Erosion-prone plaques

Erosion-prone plaques are very difficult to identify and are usually defined only by the thrombosed event. The surface endothelium is missing, but whether it has gone before or after thrombosis remains difficult to determine. No specific morphological features have been identified but, in general, eroded plaques with thrombosis are scarcely calcified, rarely associated with expansive remodelling, and only sparsely inflamed (11).

1.5.4 Prospective detection of vulnerable plaques

PROSPECT (Providing Regional Observations to Study Predictors of Events in the Coronary Tree) was a follow-up study of 697 patients treated with percutaneous coronary intervention after an ACS using multimodality imaging to identify vulnerable plaques (27). Using virtual histology-intravascular ultrasound (VH-IVUS), the study was able to identify 595 TCFAs in non-culprit coronary arteries and found a three-fold increase in the risk of recurrent cardiovascular events in the subsequent three-year follow-up period.

Similar observations were reported in the VIVA (VH-IVUS in Vulnerable Atherosclerosis) study (28). The purpose of this study was to determine whether TCFA identified by VH-IVUS are associated with major adverse cardiac events (MACCE) based on individual plaque or whole-patient analysis. One hundred and seventy patients with stable angina or troponin-positive acute coronary syndrome referred for percutaneous coronary intervention (PCI) were prospectively enrolled and underwent 3-vessel VH-IVUS pre-PCI and also post-PCI in the culprit vessel. Eighteen MACCE occurred in 16 patients over a median follow-up of 625 days; 1,096 plaques were classified, and 19 lesions resulted in MACCE (13 non-culprit lesions and six culprit lesions). Non-culprit lesion factors associated with non-restenotic MACCE included VHTCFA (hazard ratio [HR]: 7.53, p = 0.038) and plaque burden >70% (HR: 8.13, p = 0.011). VHTCFA (HR: 8.16, p = 0.007), plaque

burden >70% (HR: 7.48, p < 0.001), and minimum luminal area <4 mm^2 (HR: 2.91, p = 0.036) were associated with total MACCE. Three-vessel non-calcified VH-IVUS TCFA was associated with non-restenotic total MACCE based on whole-patient analysis (HR: 1.79, p = 0.004).

There are, however, some limitations to the concept of the vulnerable plaque. The predictive power of VH-IVUS-defined TCFA in the PROSPECT study suggests that imaging of the vulnerable plaque may have a limited specificity for the prediction of cardiovascular events. Although 595 TCFAs were identified by IVUS in 313 of 623 patients, only 26 of these plaques were sites of subsequent events at three years, and almost all events were related to rehospitalisation for unstable or progressive angina.

A further study of coronary plaque with VH-IVUS suggests that the plaque phenotype is dynamic, with 15 out of 20 of the TCFAs identified healing over a 12-month follow-up period (29).

Furthermore, post mortem data suggest that ruptured coronary plaques do not inevitably lead to clinical events. Eight per cent of coronary plaques that cause over 50% diameter stenosis have evidence of old, healed plaque rupture with incorporation of thrombus into the atheroma (30).

1.6 Mechanisms of plaque rupture

1.6.1 Inflammation in atherosclerosis

Vessel wall inflammation is thought to play a role in the pathological progression of atherosclerosis, in particular plaque destabilisation and rupture (see Figure 5) (31). The role of inflammatory processes in plaque erosion is less clear (32).

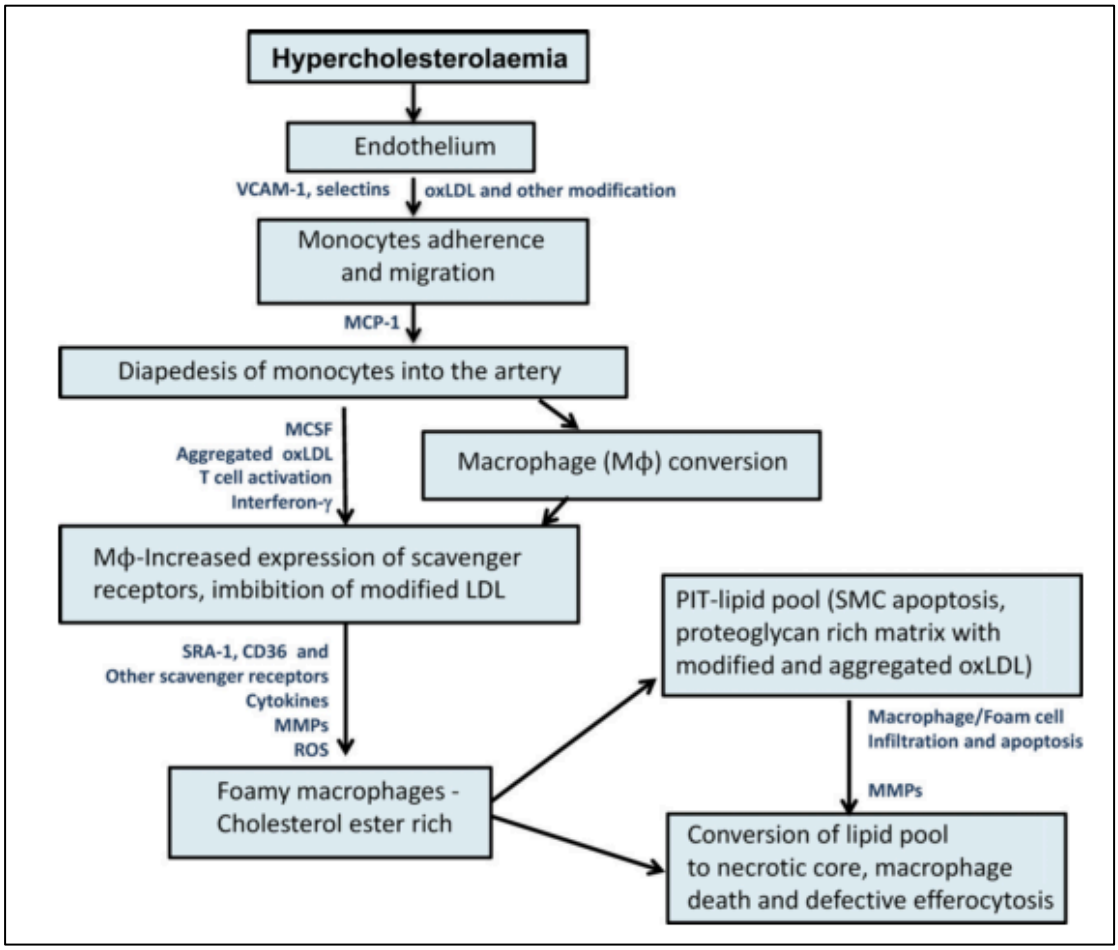

Figure 5: Events that lead to atherosclerotic change and progression

Hypercholesterolaemia is the trigger for the initiation of atherosclerosis. The monocyte migration and adherence to the endothelium is facilitated by the expression of vascular cell-adhesion molecule-1 (VCAM-1), and selectins. Oxidisation and other modifications of low-density lipoprotein (LDL) induce the secretion of macrophage-chemotactic protein-1 (MCP-1). In the arterial intima, the monocytes undergo maturation into macrophages. Macrophages express scavenger receptors such as scavenger receptor A (SRA) and CD36, which facilitate the uptake of modified LDL and the conversion to foamy macrophages that are rich in cholesterol esters. Monocytes/macrophages proliferate in the presence of MCP-1 and macrophage colony stimulating factor (MCSF). Macrophages excrete matrix metalloproteinases (MMPs), which are further enhanced by the presence of reactive oxygen species (ROS), which then facilitate the breakdown of collagen to allow migration of cells within the plaque. Foamy macrophages infiltrate pathological intimal thickening (PIT) lesions and the lipid pool areas that are formed by the smooth muscle cell (SMC) apoptosis and proteoglycan accumulation. Aggregation of oxidised LDL and macrophage infiltration induces the conversion of the lipid pool to the necrotic core, and, within the necrotic core, macrophage death and defective efferocytosis (reproduced from Sakakura et al. (31)).

1.6.2 Inflammation in atherosclerotic plaque progression

Atherosclerosis occurs as a result of the deposition of low-density lipoproteins (LDL) within the arterial wall, where they bind to the extracellular proteoglycan-rich matrix, resulting in diffuse intimal thickening (33). LDL deposition in the intima eventually results in oxidation and increasing expression of adhesion molecules on the endoluminal surface (34). LDL oxidation is promoted in vitro by monocytes, endothelial cells and smooth muscle cells (35). Oxidised LDL induces dysfunctional endothelial cells to secrete macrophage-chemotactic protein 1 (MCP-1) to recruit circulating monocytes, which adhere to endothelial cells expressing vascular cell adhesion molecule-1 (VCAM-1) (36). Once inside the intima of the arterial wall, these inflammatory cells participate in and perpetuate a local inflammatory response. Macrophage colony-stimulating factor (M-CSF) also contributes to the differentiation of the blood monocyte into the macrophage foam cell (37).

1.6.3 Endothelial activation and monocyte recruitment

The first step in the initiation of monocyte recruitment is activation of the endothelium. Multiple factors may lead to endothelial damage and activation, including oxidative stress, hypercholesterolaemia, long-term hyperglycaemia, as well as increased plasma levels of both native and oxidised LDL (38). The endothelium normally releases nitric oxide; however, the presence of oxidised LDL reduces its activity (39). Platelets are also involved in the activation of the endothelium, by producing platelet factor 4 and P-selectin, which attract monocytes to the endothelium, forming monocyte–platelet aggregates (40).

Once activated, endothelial cells overexpress chemokines (e.g. CCL5 and CCL2), as well as toll-like receptors (TLRs) and adhesion molecules (41). Blood monocytes are recruited to the activated/damaged endothelium. The expression of adhesion molecules, such P- and E-selectins, VCAM-1 and ICAM-1 facilitates an initial adhesion followed by the firm attachment of activated monocytes expressing reciprocal ligands such as Mac-1 and VLA-4 onto endothelial cells (42).

The monocytes transmigrate across the endothelium via diapedesis to the subendothelial space. Junction adhesion molecules (JAM) -A and -C have been shown to be involved in the control of vascular permeability and thus leukocyte

transmigration across endothelial cell surfaces (43).

1.6.4 Macrophage receptors

In the subendothelial space, monocytes differentiate macrophages promoted by factors such as M-CSF. Macrophages express two types of receptor: scavenger receptors and toll-like receptors (TLR). Scavenger receptors such as scavenger receptor A (SRA) and CD36 facilitate the uptake of modified LDL and the conversion to foamy macrophages that are rich in cholesterol esters and free fatty acids (44). The lipid laden macrophages apoptose and become foam cells. They also stimulate an inflammatory response through the release of cytokines, growth factors, MMP, reactive oxygen species and tissue factor. In addition there is smooth muscle migration and proliferation across the intima. The result of these processes is a lesion with a lipid-rich atherosclerotic core and fibrous cap. The lipid-laden macrophages also release cytokines, growth factors, MMP, reactive oxygen species (ROS) and tissue factor, all perpetuating the inflammatory response and vascular remodelling (45). This also activates and attracts platelets, thus increasing plaque susceptibility to thrombus formation.

TLRs are the most characterised members of the pattern recognition receptor family. TLRs recognise molecular patterns foreign to the body, including lipopolysaccharides, bacterial pathogens and oxidised lipoproteins (46). TLRs activate the proinflammatory transcription factor nuclear factor kappa-B (NFkB) and the mitogen-activated protein kinase (MAPK) pathway, resulting in the production of cytokines that augment local inflammation and smooth muscle cell proliferation (47).

The main TLRs implicated in the atherosclerotic process are TLR2 and TLR4 (48). Lipopolysaccharides (LPS) induce the macrophage expression of MMP-9 via TLR4, while MMP-9 has been shown to degrade collagen fibrous caps, thus predisposing to plaque rupture (49). TLR4 was also increased systematically in patients following myocardial infarction (MI) and locally at sites of plaque rupture, yet suggesting that monocyte TLR4 has a role in plaque destabilisation and rupture (50).

1.6.5 Immune response by T-cells

T-lymphocytes are also prompted via chemokines induced by interferon-γ to move into the intima (51). The initial activation of T-cells requires a strong stimulus delivered by dendritic cells or via memory T-cells (52). T-cell activation leads to the expression of CD40, which then binds to its CD40 receptor on the macrophage cell surface, resulting in increased macrophage expression of CD40 and TNF receptors that help to increase the level of macrophage activation as well as vascular endothelial cells and SMCs (52).

As the inflammatory process continues, the activated leukocytes and macrophages release various cytokines, chemokines, growth-factors and disintegrins (listed in Figure 6), leading to the activation and proliferation of smooth muscle cells, lesion progression, and finally to the weakening of a vulnerable plaque by matrix degradation of its fibrous cap (53).

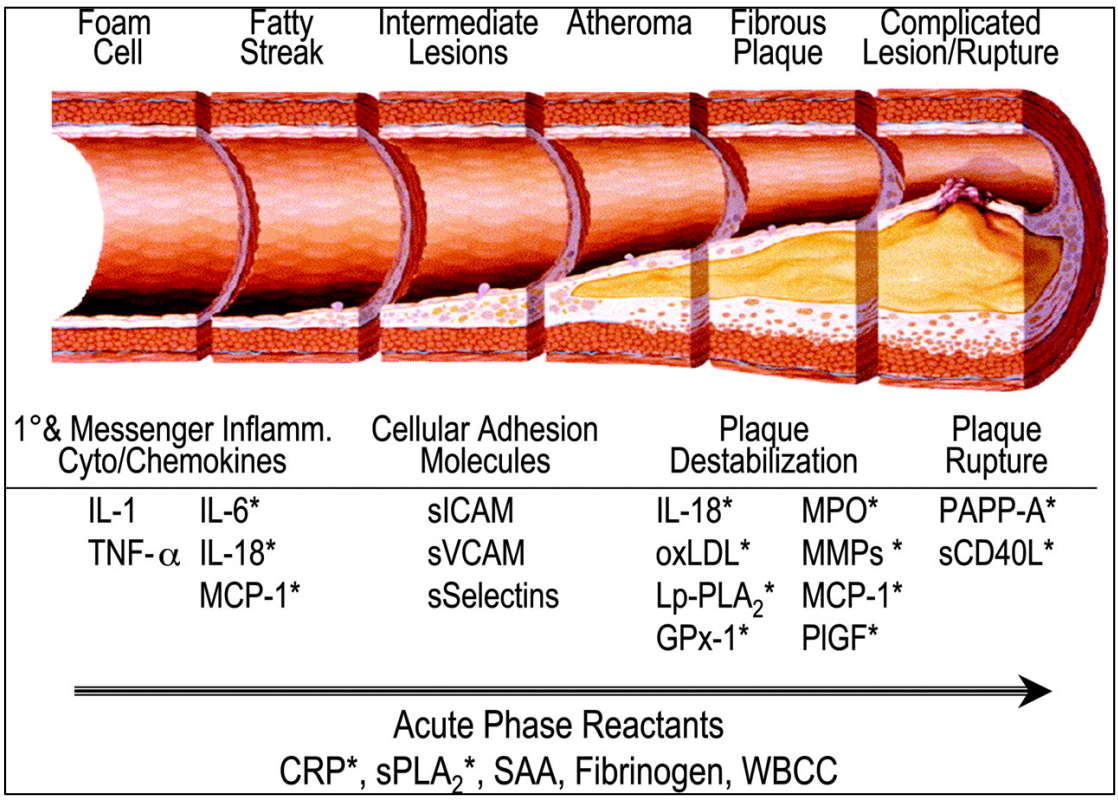

Figure 6: Markers of inflammation and plaque instability

From foam cell to plaque rupture: IL = interleukin, TNF-α = tumour necrosis factor-α; MCP-1 = monocyte chemoattractant protein-1; sICAM = soluble intercellular adhesion molecule-1; sVCAM = soluble vascular cell adhesion molecule; oxLDL = oxidised low-density lipoprotein; Lp-PLA2 = lipoprotein-associated phospholipase A2; GPx-1 = glutathione peroxidase; MPO = myeloperoxidase; MMPs = matrix metalloproteinases; PlGF = placental growth factor; PAPP-A = pregnancy-associated plasma protein-A; sCD40L = soluble CD40 ligand; CRP = C-reactive protein; sPLA2 = secretory type II phospholipase A2; SAA = serum amyloid A; WBCC = white blood cell count (reproduced from Koenig et al. (53)).

1.6.6 Inflammation and degradation of the fibrous cap

Vascular smooth muscle cells (VSMCs) synthesise collagen, which gives tensile strength to the fibrous cap and protects it from rupture. Plaque inflammation, and specifically inflammatory macrophages in the shoulder regions of atherosclerotic plaques, release matrix metalloproteinases (MMPs) that degrade collagen, thereby contributing to the thinning and eventual disruption of the fibrous cap and exposure of the thrombogenic lipid core to the blood stream (54). In addition, activated T-cells secrete the cytokine interferon-γ, which inhibits the production of new interstitial

collagen, further contributing to the weakening of the fibrous cap.

Interstitial collagen is usually very stable and resists degradation by most proteolytic enzymes, with MMPs being only a handful of proteinases capable of breaking down fibrillar collagen. MMPs are expressed by monocytes, macrophages, foam cells, mast cells and, to a lesser extent, VSMCs and endothelial cells. The various MMPs that are found in macrophage-rich regions include MMPs-1, -2, -3, -8, -9, -11, -12, -13, -14 and -16. However, MMPs-1, -8 and -13 are overproduced by macrophages in advanced plaques and are thought to play a role in catalysing the initial breakdown of collagen (Figure 7) (15). T-cells also activate the macrophages in the intimal lesion by expressing CD40 ligand (CD154), which engages its cognate receptor (CD40) on the macrophage (55).

MMP activity is inhibited by the tissue inhibitors of MMPs (TIMPs), which help to prevent excessive proteolytic activity. TIMPs are also regulated by T-cell-derived cytokines. In a study of human carotid plaques obtained at the time of carotid endarterectomy, Muller et al. (56) found that TIMP-3 expression was highest in stable plaques and low in vulnerable plaques, suggesting that this particular TIMP is down-regulated in vulnerable plaques.

1.6.7 Alternative explanations for plaque rupture

A weakened fibrous cap is clearly a key determinant in rendering plaques susceptible to rupture, but alone it is not enough to explain all instances of plaque rupture. A study by Ohayon et al. (57) investigated the change in plaque vulnerability as a function of necrotic core size and plaque morphology. Using idealised morphological models as references, 24 patients underwent IVUS imaging of non-ruptured plaques. They demonstrated that plaque instability risk is due to cap thickness, necrotic core thickness and the arterial remodelling index, combined. Plaque rupture might also be prompted by coronary vasospasm and punctate calcifications. Additional contributors to the triggering of plaque rupture may also include coronary vasospasm and punctate calcifications (15).

1.6.8 Thrombosis

When the fibrous cap does eventually rupture, blood in the lumen of the artery comes into contact with thrombogenic material in the plaque's lipid-rich necrotic core. Thrombosis then ensues, as described below:

1. Blood enters the core of the plaque, activating platelets and the coagulation cascade. The resulting intraplaque mass is known as an intraplaque thrombus (58). This thrombus prevents the further entry of blood into the core.

2. Fibrin accumulates over the intra-plaque thrombus. It becomes bigger and partially occludes the lumen. The flow and sheer force within the vessel will determine the size of the accumulating thrombus. As the thrombus is still exposed to blood flow, dislodged parts may result in distal emboli (59).

3. Finally the thrombus enlarges sufficiently enough to completely occlude the vessel. This occurs as further fibrin and red blood cells mesh together on the external surface (60).

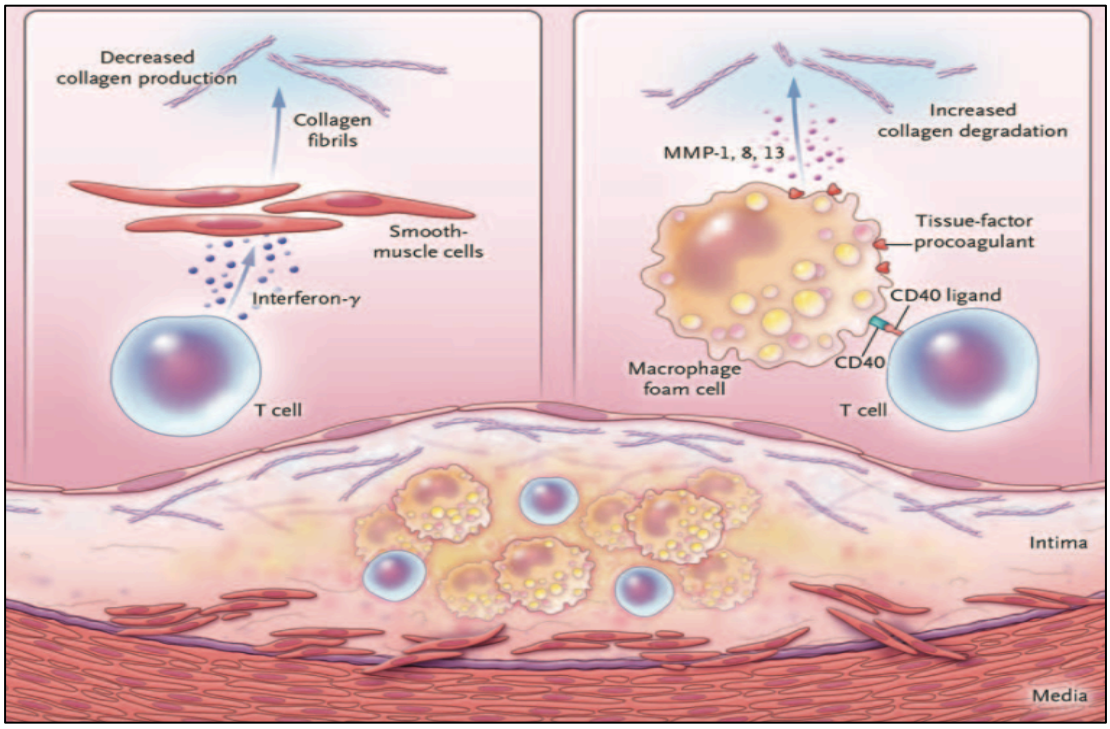

Figure 7: Inflammatory Pathways Predisposing Coronary Arteries to Rupture and Thrombosis

Bottom: A cross-section of an atheromatous plaque shows the central lipid core that contains macrophage foam cells (yellow) and T-cells (blue). The intima and media also contain arterial smooth muscle cells (red), which are the source of arterial collagen (depicted as triple helical coiled structures).

Upper left: Activated T-cells (of the type 1 helper T-cell subtype) secrete cytokine interferon-γ, which inhibits the production of the new, interstitial collagen, required to repair and maintain the plaque's protective fibrous cap.

Upper right: The T-cells can also activate the macrophages in the intimal lesion by expressing CD40 ligand (CD154), which engages its cognate receptor (CD40) on the phagocyte. This inflammatory signalling causes overproduction of interstitial collagenases (matrix metalloproteinases [MMPs] -1, -8 and -13) that catalyse the initial rate-limiting step in collagen breakdown (reproduced from Libby (15)).

1.7 Mechanisms in plaque erosion

Despite the identification of plaque erosion as an important alternative mechanism for coronary thrombosis and a major cause of sudden death, its underlying pathophysiological mechanisms are not well understood. Whereas plaque rupture is thought to be an inflammatory process, as cells such as macrophages and lymphocytes that may induce apoptosis are prevalent in ruptured plaques, these same

cells are not as widespread in eroded plaques (16). In coronary thrombotic lesions caused by plaque erosion, there is an increase in smooth muscle and proteoglycan deposition, specifically containing more versican and the glycosaminoglycan, hyaluronan, and less biglycan (23). Therefore, a better understanding of the factors leading to plaque erosion is needed. The leading hypothesis for erosion suggests that endothelial denudation of an atherosclerotic plaque exposes thrombogenic extracellular matrix to the blood (61). The cause of this focal denudation is not known, but possibilities include vasospasm and high shearing flow (22) inducing endothelial apoptosis, leading to denudation of the intimal surface of the vessel. Durand et al. confirmed that endothelial loss could be sufficient to precipitate thrombus by inducing apoptosis with intravascular staurosporine in a rabbit model (62).

1.7.1 Endothelial shear stress

High laminar blood flow is a potent endogenous antiatherosclerotic factor, as illustrated by the focal distribution of atherosclerotic lesions in areas with low or turbulent flow (63). Studies have shown that endothelial cells cultured under static conditions undergo apoptosis, whereas normal levels of shear stress are protective (64). A study by Tricot et al. (65) examined 42 human carotid atherosclerotic plaques. Quantitative analysis of endothelial cell apoptosis in these plaques showed a systematic preferential occurrence of apoptosis in the downstream parts of plaques, where low flow and low shear stress prevail, in comparison with the upstream parts ($18.8 \pm 3.3\%$ versus $2.7 \pm 1.2\%$, respectively, $P < 0.001$) (Figure 8).

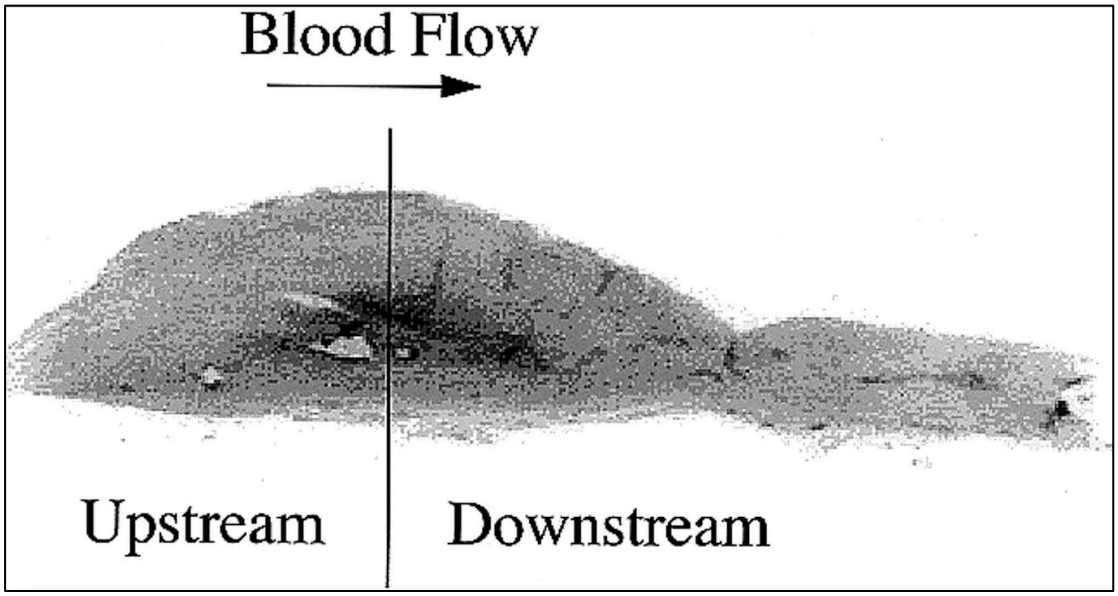

Figure 8: Longitudinal section of a carotid plaque showing upstream and downstream parts

Stenotic atherosclerotic plaques would be expected to experience significantly elevated shear stress on the upstream face of the plaque, modifying endothelial behaviour. Similarly, on the downstream surface of the plaque, the endothelium would be expected to experience disturbed flow, promoting higher rates of apoptosis (reproduced from Tricot et al. (65)).

Campbell et al. (66) investigated whether local haemodynamics was associated with sites of plaque erosion. They generated 3D, patient-specific models of coronary arteries from biplane angiographic images in three human patients with plaque erosion diagnosed by optical coherence tomography (OCT). Using computational fluid dynamics, they simulated pulsatile blood flow and calculated both wall shear stress (WSS) and oscillatory shear index (OSI). Neither high nor low magnitudes of mean WSS were associated with sites of plaque erosion. OSI and local curvature were also not associated with erosion. Although the sample size was small, hence lowering the significance of the study, the data suggested that there was no significant association between erosion and shear stress.

Another study by Campbell et al. (61) examined a total of 74 human coronary plaque specimens obtained at autopsy. Using histology-based, lesion-specific computational modelling techniques to calculate the distribution of stresses and strains in the walls of atherosclerotic plaques, they studied the spatial relationship between stress/strain and markers of inflammation. Consistent with previous studies, inflammatory markers were positively associated with increasing strain in specimens with rupture

and thin-cap fibroatheromas. Conversely, overall staining for inflammatory markers and apoptosis were significantly lower in erosion, and there was no relationship with mechanical strain. Samples with plaque erosion most closely resembled those with the stable phenotype. The data suggests that plaque erosion is a distinct pathophysiological process with a different aetiology.

1.7.2 Apoptosis and detachment of endothelial cells

Programmed cell death (apoptosis) and desquamation of luminal endothelial cells (ECs) exposing platelets and coagulation factors to the basement membrane provide two possible mechanisms of plaque erosion (Figure 9) (67).

Apoptosis can lead to the detachment of ECs from the ECM in vivo, as described above (62). On the other hand, loss or weakening ECM contacts may provoke endothelial anoikis (apoptosis triggered by loss of cell contacts), most likely owing to the disruption of signals from focal adhesions to the protein kinase B (PKB/c-Akt) pathway (Figure 9) (68).

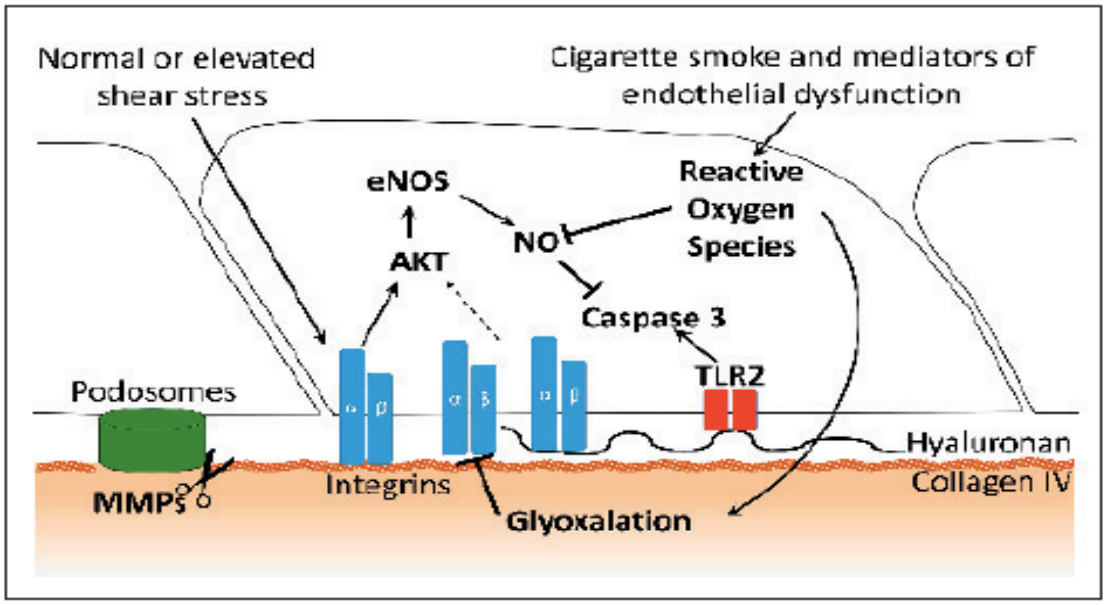

Figure 9: Mechanisms that potentially contribute to endothelial erosion

Normal or elevated shear stress activates adhesion of integrins, increasing survival signalling through AKT. Integrin adhesion can be reduced in low-shear environments, or via glyoxalation of collagens and modification of the subcellular matrix to include high proportions of hyaluronan, thereby diminishing AKT signalling. Activation of TLR 2 by hyaluronan may activate caspase 3, increasing apoptotic drive and pro-inflammatory signalling. Reactive oxygen species from cellular and

extracellular sources (e.g. cigarette smoke) scavenge nitric oxide, preventing the inhibition of activated caspases. Endothelial dysfunction may promote aberrant turnover basement membrane components, with endothelial and sub-endothelial cells increasing the production, or activation, of MMPs or other proteases contributing to an increase in subcellular protease activity (reproduced from White et al. (67)).

A variety of factors have been shown to promote endothelial apoptosis in vitro or in vivo. These include depletion of growth/survival factors, such as VEGFA, or disruption of cell-to-cell contacts mediated by VE-cadherin, which interfere with signalling through the mitogen-activated protein kinase and c-Akt pathways (69).

1.7.2.1 Endothelial cell apoptosis and Toll-like Receptor-2 (TLR2)

A study by Quillard et al. (70) suggests that TLR2 ligation is a potential activator of endothelial apoptosis in vitro and in vivo. ECs exposed to TLR2 agonists or plated on hyaluronic acid (also a TLR2 ligand) in vitro showed increased apoptosis, measured by the rise in cleaved caspase 3 (the hallmark of apoptotic cells) and also cell detachment. The mechanisms involved in cell detachment involve increased matrix metalloproteinase activity, and downregulation of VE-cadherin complexes, disrupting cell junctions (67). It has been postulated that overproduction of active forms of non-fibrillar collagenases MMP-2 and MMP-9 and the activator of MMP-2, MMP-14, could sever the tethers between endothelial cells and the underlying basement membrane, facilitating their desquamation and consequent local thrombosis (71).

1.7.2.2 Neutrophil extracellular traps (NETs)

Once the endothelial cell has desquamated, the dying endothelial cell can release tissue factor that can accelerate the activity of factors VII and X to augment thrombin formation and ultimately the conversion of fibrinogen to fibrin, provoking thrombosis and coagulation. Exposure of the sub-endothelial matrix can provide a substrate for granulocyte adhesion, activation and degranulation. Granulocytes are a source of reactive oxygen species such as hypochlorous acid, HOCI, a product of myeloperoxidase (MPO). Dying granulocytes release DNA and histones contributing

to the formation of neutrophil extracellular traps (NETs) (72). Exposure of the sub-endothelial extracellular matrix can activate platelets, causing them to degranulate and release pro-inflammatory mediators such as interleukin-6 and RANTES. Activated platelets also release plasminogen activator inhibitor-1 (PAI-1), a major inhibitor of endogenous fibrinolytic enzymes. PAI-1 can thus reduce fibrinolysis and increase clot stability (15).

ECs exposed to TLR2 agonists also show modestly increased expression of the inflammatory markers, E-selectin, VCAM-1 and IL-8, which could also act together to recruit neutrophils (73). Examination of human carotid endarterectomy specimens ex vivo suggests that TLR2 and activated neutrophils expressing NETs co-localise with areas of endothelial denudation downstream of plaques (70). NETs can form a nidus for extension of thrombosis and entrapment of further blood leukocytes, amplifying the local inflammatory response.

These studies illustrate the possible interaction between the endothelial dysfunction mediated by TLR-2 and neutrophil recruitment in provoking erosions, emphasising the two-way connection between adhesion and apoptosis of ECs.

1.7.3 Myeloperoxidase in plaque erosion

An in vitro study by Sugiyama et al. (74) looked at the relationship between macrophages at erosive sites of human coronary atheroma producing myeloperoxidase (MPO), an enzyme that produces hypochlorous acid (HOCL). They tested the hypothesis that HOCL affects endothelial viability and that it modifies thrombogenicity in the endothelium, thereby leading to superficial erosion and occlusive thrombosis. Their results demonstrated that MPO-positive macrophage-derived HOCL in the subendothelium of the atheromata may initiate or propagate endothelial cell loss and local thrombosis in coronary arteries.

Increased systemic levels of MPO were also demonstrated in patients with plaque erosion compared to plaque rupture in a small study of 25 patients with ACS (75). In addition, the density of myeloperoxidase-positive cells within thrombi overlying plaques in post mortem coronary specimens retrieved from sudden coronary death victims was significantly higher in lesions with erosion (n=11) than ruptures (n=11).

1.8 Thrombus aspiration

The foremost therapeutic goal during the treatment of STEMI is to re-establish normal coronary blood follow. Treatment strategies for reperfusion therapy focus on dissolving, mechanically disrupting or surgically bypassing occlusive thrombus in the epicardial infarct-related artery. Primary percutaneous coronary intervention (PPCI) is recognised as the preferred treatment of STEMI, if logistically feasible, and has been proven to be a very effective method to restore patency of the infarct-related artery (IRA) (76). However, even after epicardial arterial patency has been established, microvascular dysfunction with diminished myocardial perfusion is seen in a significant proportion of patients and has been associated with an increased infarct size, less recovery of left ventricular ejection fraction and increased mortality (77).

The main two mechanisms for causing microvascular dysfunction are considered to be reperfusion injury and microvascular obstruction (MVO). Reperfusion injury refers to necrotic myocardium unable to be reperfused (78). MVO is caused by the embolisation of soft plaque and/or thrombotic material downstream, in the bed of the IRA. Studies emphasise mechanical disruption and fragmentation of the culprit lesion during PCI as the major cause (77).

To overcome this clinical problem, the technique of thrombus aspiration is used, which involves passing a fine catheter over the coronary angioplasty wire and aspirating thrombus at the site of the lesion.

1.8.1 Evidence for thrombus aspiration

Although thrombus aspiration during PPCI for STEMI may improve microvascular reperfusion, its impact on clinical outcomes has yielded contrasting results. A recent meta-analysis by Jolly et al. (79) compared manual thrombectomy and PCI alone in patients with ST-segment-elevation myocardial infarction. Included were three large (n>1,000) controlled, randomised trials: TAPAS (Thrombus Aspiration During Percutaneous Coronary Intervention in Acute Myocardial Infarction); TASTE (Thrombus Aspiration in ST-Elevation Myocardial Infarction in Scandinavia); and TOTAL (Trial of Routine Aspiration Thrombectomy With PCI Versus PCI Alone in Patients With STEMI). They found that routine thrombus aspiration during PCI for

ST-segment-elevation myocardial infarction did not improve clinical outcomes. In the subgroup with high thrombus burden, thrombus aspiration was associated with fewer cardiovascular deaths and with more strokes or transient ischemic attacks.

1.8.2 Thrombus yield

Systematic thrombectomy yields thrombus samples for histopathological evaluation of intracoronary thrombi in PPCI cases. In the TAPAS trial, coronary thrombotic material was successfully retrieved in 72.9% of patients (80). A study by Kramer et al. (81) sought to establish the histopathological characteristics of material aspirated during PPCI in a STEMI population. Material could be aspirated in 74% of patients. Components of plaque were found in 395 of these patients (39%). Fresh thrombus was found in 577 of 959 patients (60%) compared to 382 patients (40%) with lytic or organised thrombi. These studies highlight the feasibility of obtaining thrombus samples in approximately two-thirds of patients undergoing PPCI for STEMI.

1.8.3 Thrombus types

Histological analysis of aspirated thrombi usually reveals a variety of thrombus types, which can be classified according to the accepted definitions of thrombus age (82):

Fresh thrombus (<1 day old) is composed of platelet aggregates, erythrocytes, intact granulocytes and fibrin (Figure 10B).

Lytic thrombus (1 to 5 days old) is characterised by areas of colliquation necrosis and karyorrhexis of granulocytes (Figure 10C).

Organised thrombus (>5 days old) is characterised by the presence of smooth muscle cells, homogenous or hyaline fibrin and depositions of connective tissue and capillary vessel ingrowth (Figure 10D).

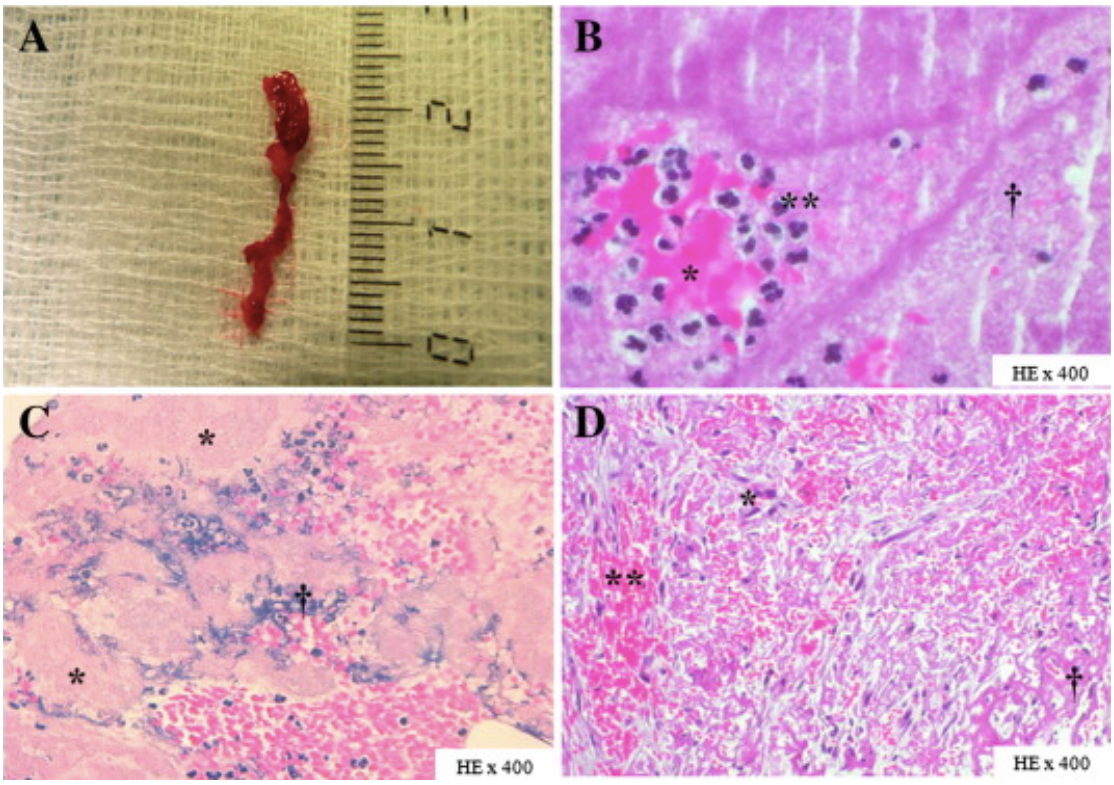

Figure 10: (A) Macroscopic appearance of aspirated thrombus after thrombectomy. (B) Microphotograph of a fresh thrombus (HE staining, ×400). *Nonhomogeneous fibrin, **leukocytes, †platelet aggregates. (C) Microphotograph of a lytic thrombus (HE staining, ×400). *Colliquative necrosis, †granulocytes with karyorrhexis. (D) Microphotograph of an organised thrombus (HE staining, ×400). *Endothelial cells, **erythrocytes, †hyaline and homogenised fibrin (reproduced from Carol et al. (83)).

Rittersma et al. (82) studied the age of intracoronary thrombi, aspirated during angioplasty, in 211 consecutive patients with acute STEMI presenting within six hours. The aspirated material was histologically screened on thrombus and plaque components, and thrombus age was classified as fresh, lytic thrombus and organised thrombus. Thrombus was identified in 199 (95%) of 211 patients. In 12 patients (5%), only plaque components were identified, and in 85 patients (41%), both thrombus and plaque material were aspirated.

Kramer et al. (81) performed a larger study of thrombus aspiration during PPCI in 1,362 STEMI patients. Thrombus age was classified as above into fresh, lytic and organised. Components of plaque were found in 395 of these patients (39%). Fresh thrombus was found in 577 of 959 patients (60%), compared to 382 patients (40%) with lytic or organised thrombi.

In both studies, at least 40% of patients presenting with STEMI had coronary

thrombus aged older than 24 hours and in some cases days or weeks old, indicating that plaque disruption and thrombus formation occur significantly earlier than the onset of symptoms in many patients.

1.8.4 Coronary thrombus and plaque morphology

Post mortem studies suggest that coronary thrombi may differ according to the underlying plaque pathology. Sato et al. (84) investigated the proportion of fibrin and platelets in the thrombi of ruptured and eroded coronary atherosclerotic plaques obtained from patients who had died of acute MI within three days of onset. They found that fibrin was more abundant than platelets in the thrombi of ruptured plaques, whereas platelets tended to be more abundant than fibrin in the thrombi of eroded plaques.

In a different type of study, Kramer et al. (85) aimed to study the relationship between thrombus age (healing) and plaque morphology in sudden coronary death victims. The results showed that late-stage thrombi were present in 79 (69%) of the 115 culprit plaques and that the majority of early thrombi (＜1 day) and lytic thrombi (1 to 3 days) were present in plaque ruptures compared with erosions, whereas the majority of thrombi in erosions were infiltrating (4 to 7 days) or healing (＞7 days). Moreover, women more frequently had erosions with a greater incidence of late-stage thrombi (44 of 50, 88%) than ruptures (35 of 65, 54%, $p < 0.0001$).

Ferrante et al. (75) analysed the relationship between coronary plaque morphology and the density of MPO-positive cells within thrombi overlying plaques in 22 sudden coronary death victims. The results showed that the number of MPO-positive cells (neutrophils and some macrophages) within thrombi were significantly higher in the lesions with erosion (n=11) than in the lesions with rupture (n=11) ($p = 0.0012$).

There have been more recent assessments of culprit plaque morphology using imaging modalities such as IVUS and OCT, and analysis of intracoronary thrombi in living patients.

The OCTAVIA study (Mechanisms of Atherothrombosis and Vascular Response to Primary Percutaneous Coronary Intervention in Women Versus Men with Acute Myocardial Infarction) sought to assess, in vivo, sex differences in the

pathophysiology of STEMI using OCT to determine plaque morphology. It was found that there were no sex differences in the composition of aspirated thrombus (86).

Saia et al. (87) evaluate the pathophysiological features and response to primary percutaneous coronary intervention (PCI) of non-ruptured/eroded plaque versus ruptured plaque as a cause of STEMI, again using OCT to determine plaque pathology. They also found that there were no significant differences in thrombus components and thrombus age between the plaque rupture and plaque erosion groups.

In routine clinical practice, the thrombectomy specimen is not analysed and is usually discarded. Although the most recent studies have not shown any relationship between plaque morphology and thrombus type, there is clearly scope for undertaking further immunohistopathological assessment of thrombus specimens now that we have the technology to assess plaque morphology in vivo.

1.9 Detection of plaque morphology

1.9.1 Optical coherence tomography (OCT)

OCT is an intravascular catheter-based imaging modality that uses infrared light to create cross-sectional images of the coronary arteries. It is recognised as the optimum modality for in vivo imaging of coronary arteries and enables visualisation of the vessel wall and related structures due to its ultra-high resolution (15μm). Compared to traditional intra-vascular ultrasound (IVUS), OCT has a ten-fold higher image resolution (Table 2). The first use of an OCT catheter for in vivo imaging of coronary arteries was in 1996 by Tearney et al. (88).

Image acquisition requires blood to be transiently displaced with an intra-coronary injection of x-ray contrast, while the fibre optic lens is rapidly rotated and withdrawn through a transparent shaft. Tomographic images are reconstructed almost instantaneously.

Characteristic	OCT	IVUS
Energy source	Near-infrared light	Ultrasound (20–45Mhz)
Wave-length, µm	1.3	35–80
Resolution, µm	15–20 (axial); 20–40 (lateral)	100–200 (axial); 200–300 (lateral)
Frame rate, frame/s	100–200	30
Pull-back rate, mm/s	25	0.5–1
Maximum scan diameter, mm	7	15
Tissue penetration, mm	1–2.5	10

Table 2: Characteristics of OCT vs IVUS (adapted from Prati et al. (89)).

OCT can discriminate three layers of the coronary artery wall, demonstrating the intima as the signal-rich layer nearest the lumen, the media as the signal-poor middle layer, and the adventitia as the signal-rich layer surrounding the signal-poor layer of the media (Figure 11) (90).

This advantage has seen OCT successfully applied to the assessment of atherosclerotic plaque, stent apposition and tissue coverage.

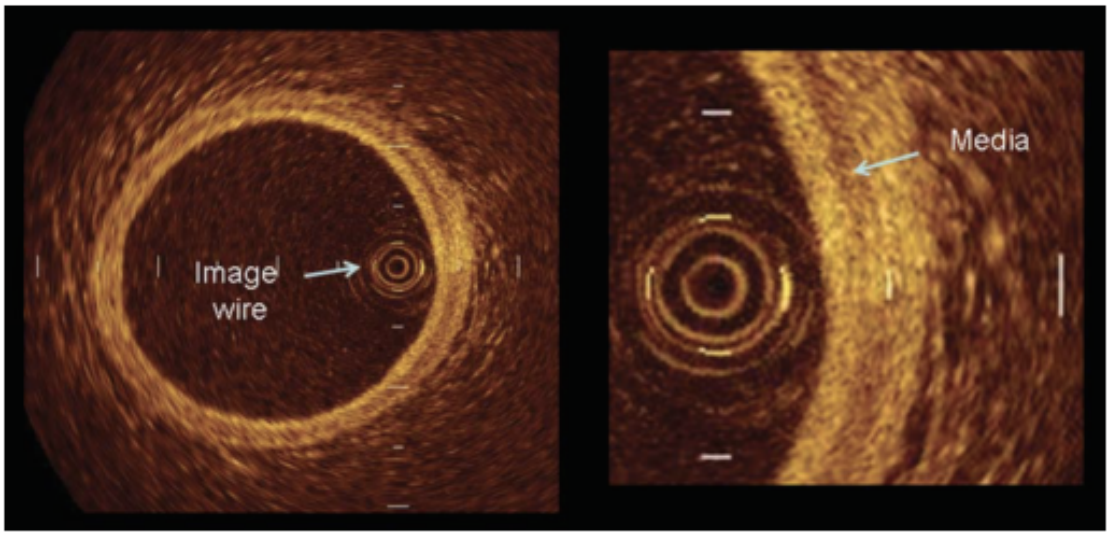

Figure 11: Optical coherence tomography showing the trilaminar appearance of a normal coronary artery

The muscular media is revealed as a low signal layer comprised between internal and external lamina (reproduced from Prati et al. (89)).

1.9.2 Limitations of OCT

In coronary arteries, the high scattering of red blood cells causes significant signal attenuation (89) and blurring of the image when using optical imaging, thereby precluding visualisation of the related structures and underlying vessel wall. Consequently, blood must be displaced from the imaging field during OCT examination. This is achieved by flushing the vessel during image acquisition with either saline or contrast medium. Saline has a low viscosity and is not very effective at displacing blood. Using saline, therefore, requires an 'occlusive technique', which involves the simultaneous occlusion of the vessel with a balloon proximal to the lesion of interest during infusion. The 'non-occlusive technique' uses a flush of high-viscosity contrast to displace blood during image acquisition. This method uses very small additional contrast volumes (10–14ml).

A drawback remains when imaging large vessels, lesions near large side branches and in the aorto-ostial junction, where it is often difficult to obtain satisfactory image quality.

Imaging depth is another limitation, with the new-generation frequency domain (FD) OCT systems limited to a scan diameter of 8–10mm inside the arterial wall in a blood-free environment. The imaging depth is further influenced by the amount of light penetration, which is dependent on the composition of the vessel wall and the optical properties (backscatter and attenuation) of the tissues (89). Backscattering refers to the amount of light waves reflected back in the direction from which they came, while attenuation describes the loss of signal intensity across the scan line. The limited penetration depth into the vessel wall can reduce the sensitivity of OCT for different plaque components. Fibrous and fibrocalcific tissues allow a high light penetration, whereas lipid-rich and macrophage accumulations attenuate OCT light significantly, resulting in limited penetration.

1.9.3 Safety of OCT

OCT is a safe procedure with an extremely low risk of complications. Image acquisition does not involve ionising radiation. The main safety concerns are vessel trauma due to passage of the catheter within an extremely tortuous vessel, additional x-ray contrast volume and procedural delay. In the PPCI setting, OCT can only be

performed following successful thrombectomy and re-established TIMI III flow, so that there is no delay to reperfusion or significant interference with the PPCI procedure (91).

1.9.4 Plaque composition

In comparison with histology, OCT has been demonstrated to be highly sensitive and specific for characterising different types of atherosclerotic plaques.

Fibrous plaque is characterised by signal-rich, homogenous lesions, fibrocalcific plaque by well-delineated, signal-poor, sharp-border lesions, and lipid-rich plaques as signal-poor, diffuse-border lesions (Figure 12) (92).

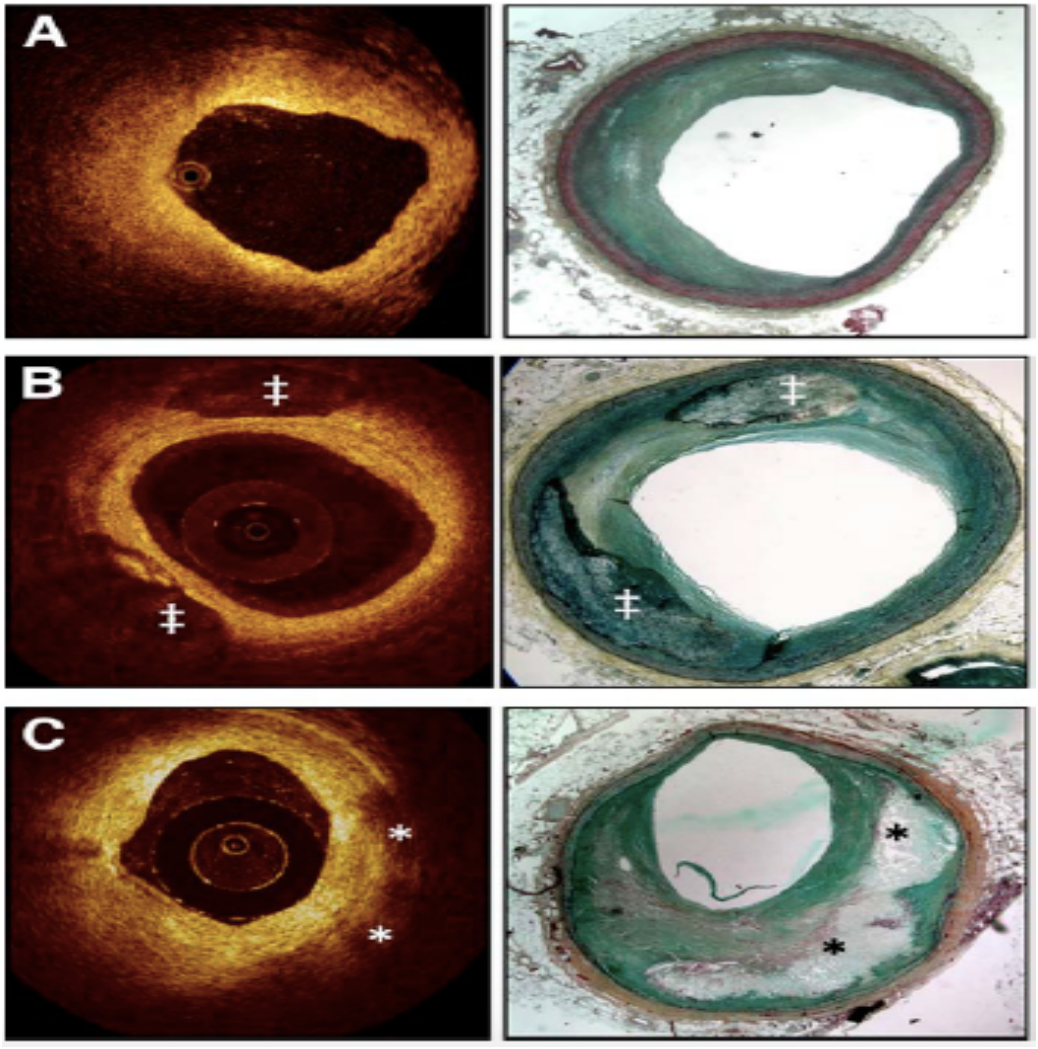

Figure 12: OCT: histology correlation

(A) Fibrotic plaque: characterised by high signal (high backscattering) and low attenuation (deep penetration). (B) Predominantly calcified plaque: calcified regions have a sharp border, low signal and low attenuation permitting deeper penetration. (C) Lipid-rich plaque: the lipid core has a diffuse border. High light attenuation results in poor tissue penetration (in contrast to calcified regions). ‡Calcified region; *lipid core (reproduced from Rollins et al. (92)).

A study by Yabushita et al. (93) aimed to establish objective OCT image criteria for atherosclerotic plaque characterisation. OCT images of 357 atherosclerotic arterial segments obtained at autopsy were correlated with histology. When compared to histological examination, OCT had a sensitivity and specificity of 71–79% and 97–98% for fibrous plaques, 95–96% and 97% for fibrocalcific plaques, and 90–94.5% and 90–92% for lipid-rich plaques, respectively. Further, the inter-observer and intra-observer reproducibility of OCT measurements were high (κ values of 0.88 and 0.91,

respectively).

The high resolution of OCT provides more detailed structural information of the coronary artery wall and coronary atherosclerotic plaque composition compared with other imaging modalities. Kubo et al. (94) compared OCT, IVUS and coronary angioscopy (CAS) in 30 patients in acute myocardial infarction (AMI). They found that the incidence of plaque rupture observed by OCT was 73% and it was significantly higher than that by CAS (47%, $p = 0.035$) and IVUS (40%, $p = 0.009$). In addition, OCT was superior (23%) to CAS (3%, $p = 0.022$) and IVUS (0%, $p = 0.005$) in the detection of plaque erosion. Intracoronary thrombus was observed in all cases by OCT and CAS, but only in 33% by IVUS (vs OCT, $p < 0.001$). OCT was also the only modality that could estimate fibrous cap thickness.

Kume et al. demonstrated that OCT might be able to distinguish between white and red thrombus (95). At histologic examination, red thrombus (Figure 13) appears as a dark-red mass protruding into the vessel lumen, consisting of mainly RBCs and fibrin, while white thrombus (Figure 14) can be observed as a willow-like structure composed of platelets and white blood cells (WBCs), with a small amount of RBCs (95). In this study, the researchers examined 108 coronary arterial segments of 40 consecutive human cadavers and obtained OCT images of red and white thrombi. Red and white thrombi were found in 16 (17%) and 19 (18%) of the 108 arterial segments, respectively. Red thrombi were identified as high-backscattering structures inside the lumen of the artery, with signal-free shadowing in the OCT image, while white thrombi were identified as signal-rich, low-backscattering structures projecting into the lumen. There were no significant differences in peak intensity of OCT signals between red and white thrombi (130 ± 18 μm vs 145 ± 34 μm, $p = 0.12$). However, the $\frac{1}{2}$ attenuation width of the signal intensity curve, which was defined as the distance from peak intensity to its $\frac{1}{2}$ intensity, was significantly different between red and white thrombi (324 ± 50 μm vs 183 ± 42 μm, $p = 0.0001$), and the cut-off value of 250μm in the $\frac{1}{2}$ width of signal intensity attenuation can differentiate white from red thrombi with a sensitivity of 90% and a specificity of 88%.

It would, therefore, seem plausible that OCT could be helpful to identify the culprit lesion in ACS and might also provide additional information about the underlying causes that lead to coronary thrombosis.

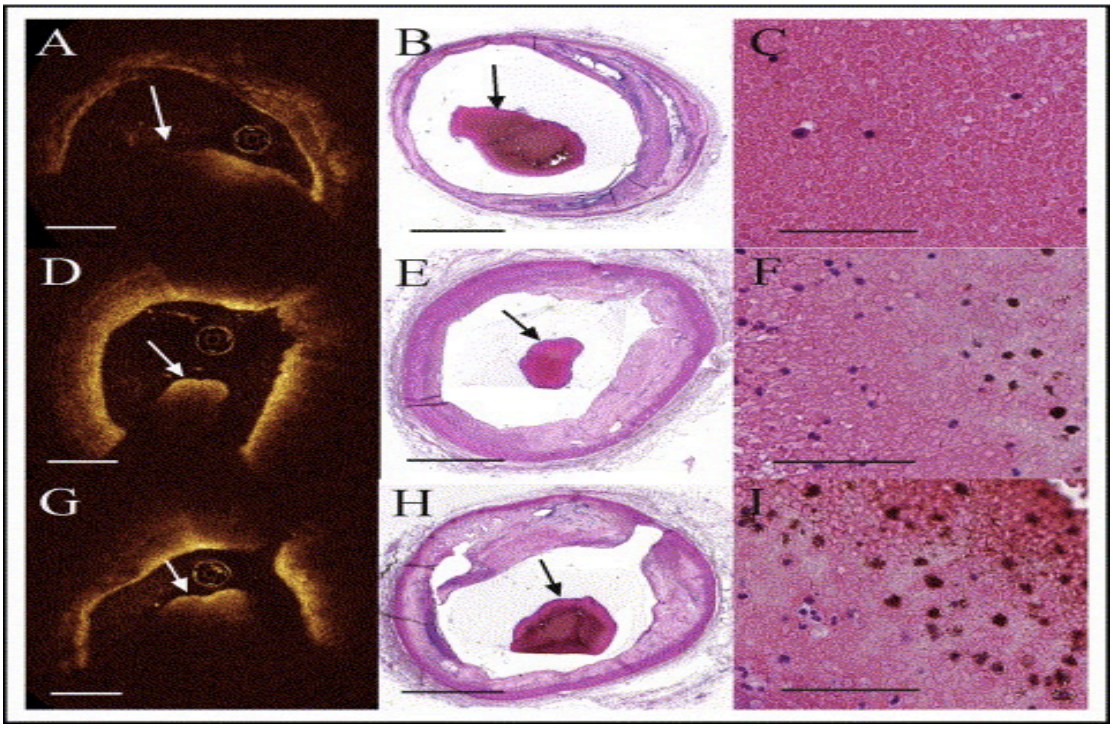

Figure 13: Correlation between OCT images and histologic (haematoxylin and eosin stain) examinations of human coronary red thrombi obtained at autopsy

OCT images of red thrombi are characterised as high-backscattering protrusions with signal-free shadowing (arrows) (reproduced from Kume et al. (95)).

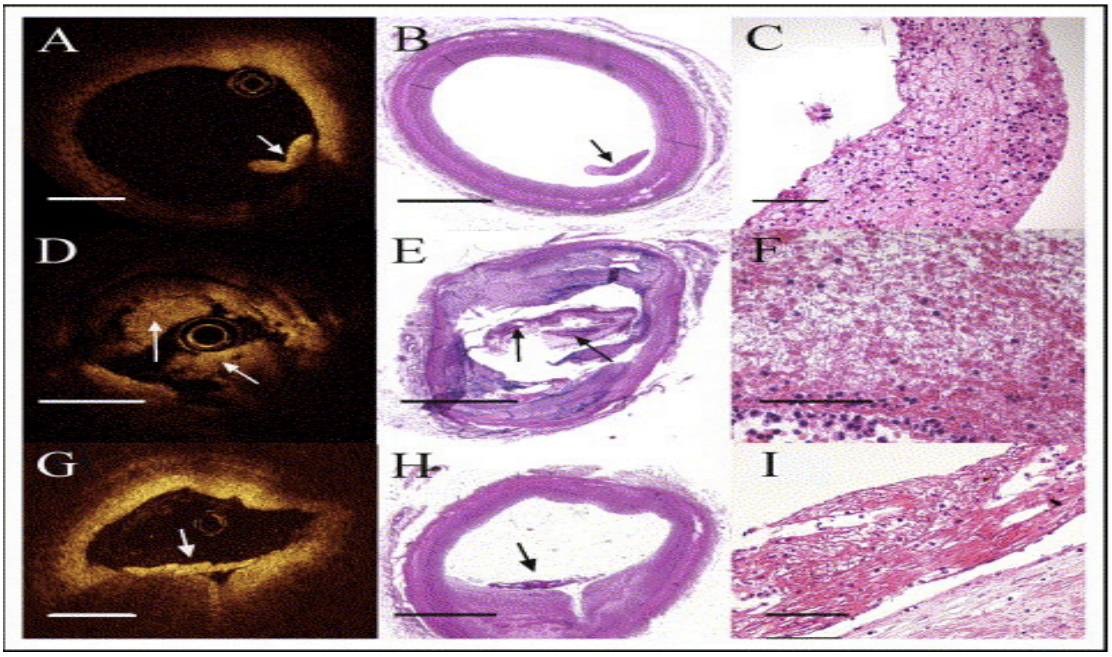

Figure 14: Correlation between OCT images and histological (haematoxylin and eosin stain) examinations of human coronary white thrombi obtained at autopsy

OCT images of white thrombi were visualised as signal-rich, low-backscattering projections (arrows) (reproduced from Kume et al. (95)).

1.9.4.1 Fibroatheroma

Fibroatheroma are the first distinguishable plaque consisting of a demarcated lipid-rich necrotic core encapsulated by surrounding fibrous tissue. They can be further subdivided into the early and late stage. The early stage is characterised by macrophage infiltration into the lipid pool, together with focal loss of proteoglycans and collagen. In the late stage, discrete collections of cellular debris and increased amounts of free cholesterol exist, and the extracellular matrix is almost completely depleted. This stage can result in substantial luminal stenosis from episodes of intraplaque haemorrhage (11). OCT images of fibroatheroma are characterised by a superficial high backscattering bright signal (Figure 15), with pronounced signal attenuation of light in the deeper plaque regions (96).

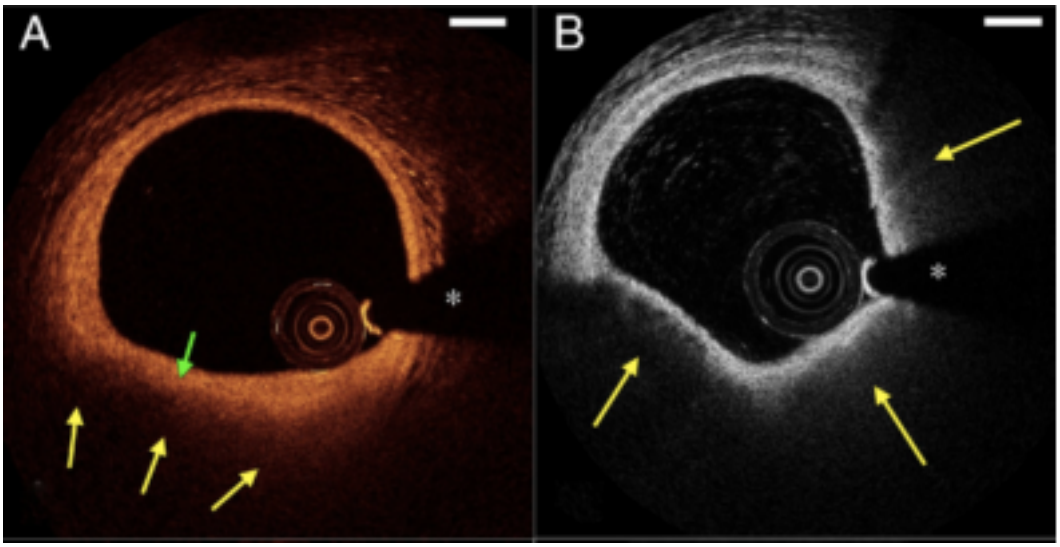

Figure 15: OCT Fibroatheroma

(A) Low OCT signal (yellow arrows) with poorly delineated borders and a cap (green arrow) characterise this fibroatheroma. (B) Signal-poor and poorly delineated regions can be seen in more than three quadrants circumferentially (yellow arrows) (reproduced from Tearney et al. (97)).

1.9.4.2 Thin-cap fibroatheroma

The TCFA, often referred to as a 'vulnerable plaque', is characterised by a large necrotic core encased by a thin fibrous cap. This is traditionally defined as being <65μm thick and is heavily infiltrated by macrophages, T-lymphocytes, but contains few smooth muscle cells (21). OCT can be used to measure fibrous cap thickness and, therefore, can be employed to identify TCFA using a threshold of 65μm, similar to the cut-off established by histopathology (89).

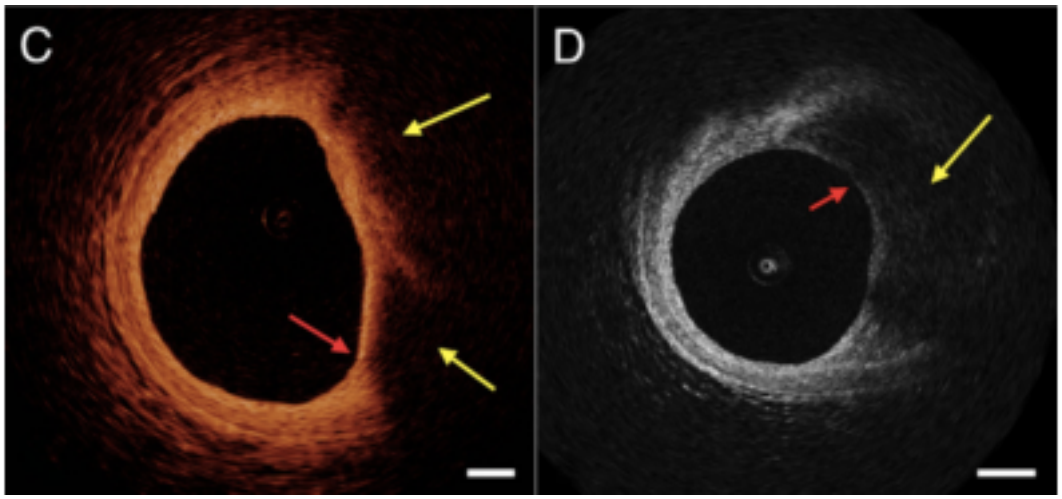

Figure 16: OCT Thin-cap fibroatheroma

C. OCT thin-capped fibroatheroma (TCFA) lesion that shows regions with low backscattering (yellow arrows) and a thin fibrous cap (red arrow). (D) OCT-TCFA that shows low backscattering (yellow arrow) covered by a thin fibrous cap (red arrow) (reproduced from Tearney et al. (97)).

1.9.4.3 Plaque rupture

Ruptured plaques are distinguished from TCFA by the presence of a luminal thrombus overlying a thin, disrupted fibrous cap. The fibrous cap consists mainly of Type I collagen, with greater numbers of macrophages and lymphocytes than in TCFA and with a limited distribution of smooth muscle cells.

Several OCT imaging studies have confirmed plaque rupture as the most frequent event-causing lesion identified in patients with ACS (19,98). Plaque rupture (Figure 17) is characterised by the presence of fibrous cap discontinuity and cavity formation within the plaque, being detected on OCT in 50～70% of culprit lesions of ACS (94). An important difference in the definition of plaque rupture by histology versus OCT is the presence of an intraplaque cavity. Whereas most contemporary imaging studies applied a definition of plaque rupture covering a disrupted thin fibrous cap along with an intraplaque cavity, the mandatory presence of an intraplaque cavity has not been reported in histopathology studies (96).

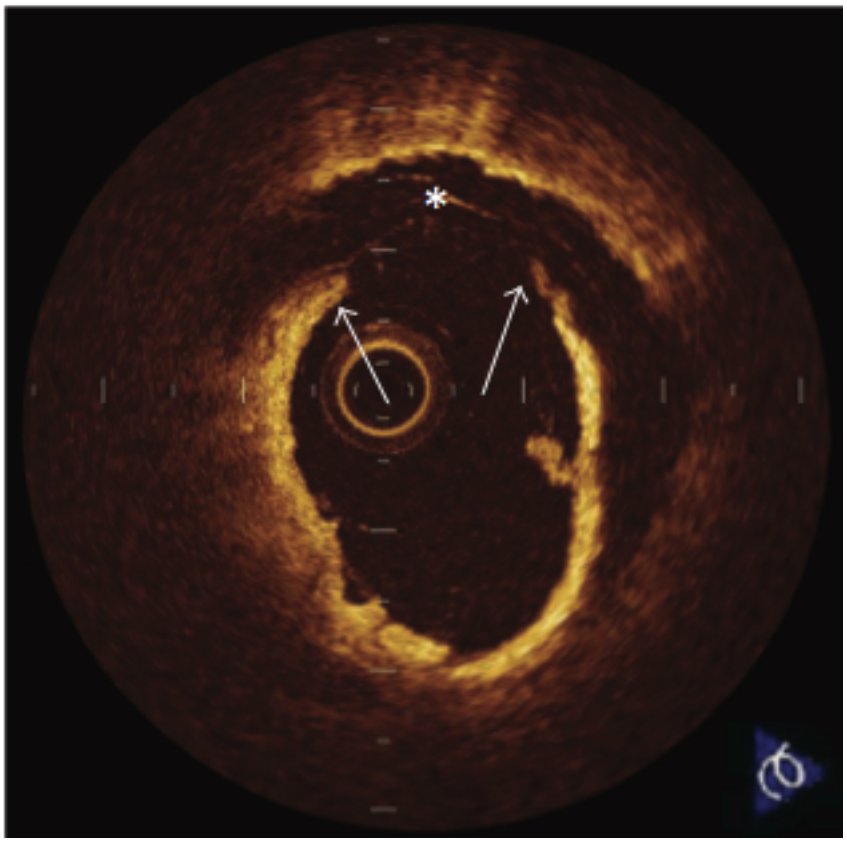

Figure 17: OCT plaque rupture

Defined as a presence of fibrous cap discontinuity (white arrows) and a cavity formation (*) in the plaque (reproduced from Kubo et al. (99)).

1.9.4.4 Plaque erosion

Plaque erosion (Figure 18) is the second most prevalent cause of coronary thrombosis. OCT characterises plaque erosion by the presence of a thrombus, an irregular luminal surface and no evidence of cap rupture, or the presence of an intact fibrous cap (IFC) evaluated in multiple adjacent frames (97). The clinical utility of OCT in reliably distinguishing plaque erosion is reduced due to its limited axial resolution in detecting a disrupted endothelial monolayer. The presence of a luminal thrombus further amplifies the hindrance of light into deeper tissue regions of the underlying plaque, making a reliable judgement of plaque morphology extremely difficult in some cases. Clinical OCT studies have suggested that, in the setting of an acute coronary event, the presence of a luminal thrombus over an intact fibrous cap is indicative of plaque erosion (72).

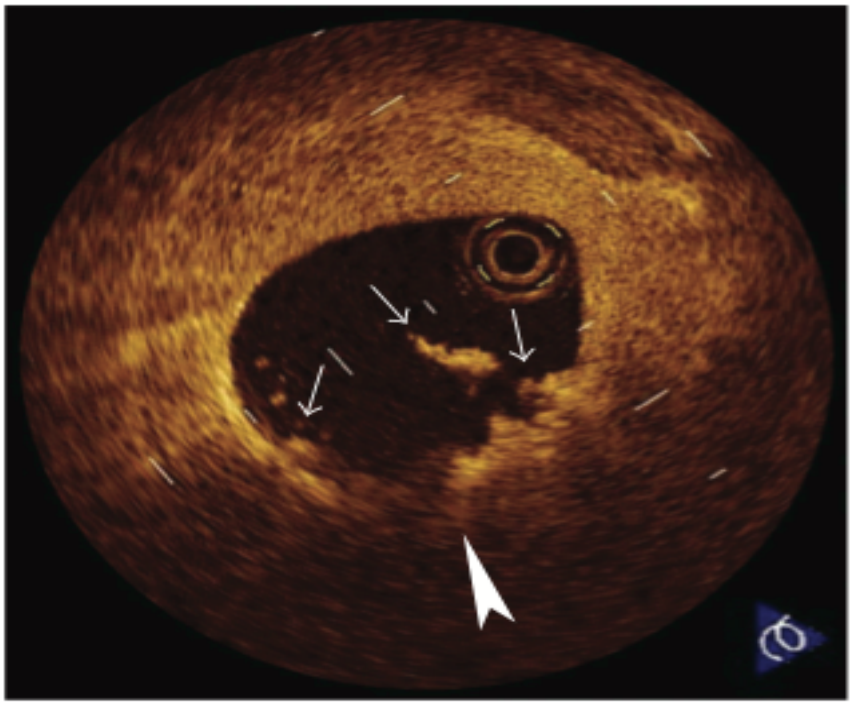

Figure 18: OCT plaque erosion

Erosion (arrowhead) is usually comprised of OCT evidence of thrombi (white arrows), an irregular luminal surface and no evidence of cap rupture evaluated in multiple adjacent frames (reproduced from Kubo et al. (99)).

1.9.4.5 Calcified nodule

A calcified nodule (Figure 19) is the least frequent cause of coronary thrombosis. OCT imaging defines these nodules as fibrous cap disruption over sites of calcified plaque characterised by protruding areas of calcification as well as superficial calcium deposition with substantive calcium accumulation proximal and/or distal to the lesion (101). However, by definition, calcified nodules have an overlying thrombus and disruption of the luminal surface, which helps to differentiate this type of plaque from nodular calcification, a more stable form of calcified plaque.

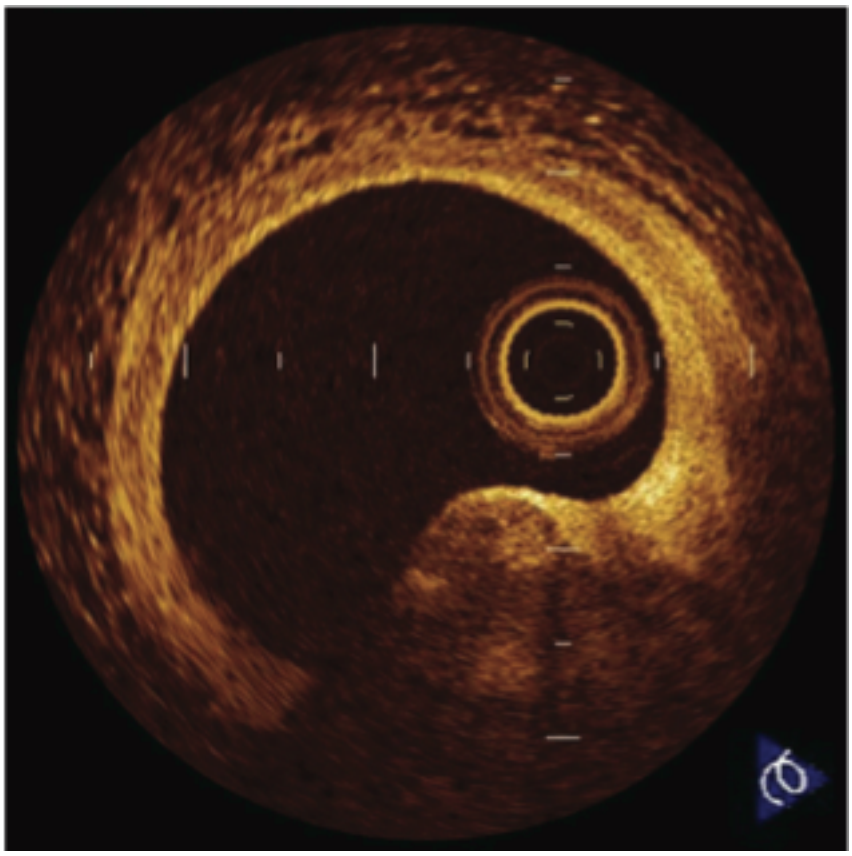

Figure 19: OCT calcified nodule

Defined as a protrusion of a signal-poor or heterogenous region with a sharply delineated border (reproduced from Kubo et al. (101)).

1.9.5 OCT in STEMI studies

Intracoronary OCT has been established as the best modality for detailed analysis of plaque morphology, including discriminating between plaque rupture and erosion. Plaque rupture and erosion in the culprit lesions of patients with ACS can be defined as 'ACS with Ruptured Fibrous caps (RFCs)' or 'ACS with Intact Fibrous Caps (IFC)' (100).

There have been a few studies in ACS that have directly compared RFC versus IFC using OCT and subsequently reported on the distinguishing features between the two pathologies.

The OCTAVIA study assessed in vivo sex differences in the pathophysiology of STEMI (86). In this prospective, multi-centred study, 140 men and women with STEMI undergoing primary PCI were age matched. All patients were investigated

with intravascular OCT of the culprit artery, histopathology-immunohistochemistry of thrombus aspirates and serum biomarkers from a venous sample. The study found no significant differences in culprit plaque morphology and factors associated with coronary thrombosis between age-matched men and women.

Saia et al. (87) focused on the comparison of patients presenting with IFC versus RFC at the culprit site of STEMI, representing a pre-specified analysis of the OCTAVIA trial. In this study, patients underwent OCT of the IRA before PCI, after everolimus-eluting stent implantation and at nine-month follow-up. Similarly, the histopathology-immunohistochemistry of thrombus aspirates and serum biomarkers were assessed at baseline. An IFC was observed at the culprit lesion site of one third of STEMIs. IFC compared to RFC presented more frequently with a patent IRA (56.2% vs 34.9%, p = 0.047), fewer lipid areas (lipid-rich areas: 75.0% vs 100%, p <0.001) and less residual thrombus (white thrombus: 0.41mm^3 vs 1.52mm^3, p = 0.001; red thrombus: 0mm^3 vs 0.29mm^3, p = 0.001) before stenting. Both groups had similar clinical characteristics and biomarker profiles. The finding of the more patent IRA in this study is supported by the previous work done by Farb et al. (23). They compared the incidence and morphological characteristics of coronary thrombosis associated with plaque rupture versus thrombosis in eroded plaques without rupture in post mortem samples of 50 consecutive sudden cardiac death cases. They described a significant difference in the luminal percentage stenosis between the two groups. The mean percent luminal area stenosis was 78 ± 12% in plaque rupture and 70 ± 11% in erosion cases (*P* <0.03). The evidence does, therefore, suggest that luminal patency, both post mortem and in vivo, are greater in plaque erosion compared to rupture.

A study by Niccoli et al. (102) compared the prognostic value of RFC versus IFC in patients with ACS. The study comprised 139 consecutive ACS patients each of whom underwent coronary angiography followed by OCT imaging of the culprit lesion. They found no significant differences between clinical, angiographic, procedural or biomarker data between the two groups. However, they did demonstrate major adverse cardiac events (MACCE) occurring more frequently in RFC when compared to IFC (39% vs 14%, p = 0.001). This is further supported by a study by Yonetsu et al. (103) in which a total of 318 patients with ACS underwent OCT of a culprit lesion. Lesions were defined as RFC, IFC and those with massive

thrombus precluding plaque visualisation (MT group). Adverse cardiac event-free survival was significantly higher in the IFC group compared with the RFC and MT groups (log rank $X^2 = 8.87$, $p = 0.012$). These two studies suggest that, in ACS patients, the underlying pathological coronary substrate has major prognostic value.

Another study by Niccoli et al. (104) sought to investigate the biohumoral correlations between RFC and IFC groups in patients with ACS. They found that patients with RFC displayed a marked elevation of CRP and MMP-9 in comparison to IFC (OR 1.48, 95% CI 1.10–1.98, $p = 0.009$ and OR1.10, 95% CI 1.02–1.19, $p = 0.008$) and patients presenting with IFC had higher levels of MPO compared to IFC (OR 1.04, 95% CI 1.01–1.05, $p = 0.04$). This supports the studies previously described, which have demonstrated increased MPO levels in sudden death patients with plaque erosion.

1.9.6 Demographic characteristics of plaque erosion compared to rupture

In addition to the underlying morphological differences between the two plaque types described above, differences in the demographics have also been observed.

A higher rate of smoking has been observed in cases of endothelial erosion compared to plaque rupture (16). Smoking is known to induce endothelial dysfunction (105), which offers further insight into the mechanisms of endothelial erosion.

Several studies have shown that a higher proportion of plaque erosions compared to plaque ruptures occurs in females compared to males (23, 85). This is consistent with data showing that fibroatheromas without lipid cores are most commonly found in women (106). Interestingly, however, the higher proportions of erosions are only true for females below the age of 50, where they account for the majority of coronary thrombotic events (107). Whether this reflects an active process precipitated by the effects of female sex hormones in premenopausal women or simply protection from plaque rupture is unknown.

Obesity is also now well recognised as a chronic inflammatory process characterised by arterial wall inflammatory cell infiltration, cytokine production and cell death (108). There are limited studies that have been performed to investigate a potential association between obesity and plaque morphology. However, a recent study by De Rosa et al. using OCT, demonstrated a significant association of obesity with a thin

fibrous cap and with macrophage infiltration, in addition to increased plaque burden and the amount of lipid-rich plaque (109). Obese patients in this study therefore demonstrated an association with a phenotype more consistent with plaque rupture.

1.10 Alternative treatment strategies for plaque erosion

Prati et al. (91) demonstrated an alternative treatment strategy for patients with ACS and OCT-verified IFC. In a study of 31 patients who were identified as having an IFC-causing STEMI, based on clinical criteria, 40% of patients with subcritically occlusive plaque were treated with dual antiplatelet therapy without PCI and the remaining 60% of patients underwent angioplasty and stenting. At a median follow-up of 753 days, all patients were asymptomatic, regardless of stent implantation. The current study suggests further research is indicated to identify a potential subgroup of patients that might not require stent implantation.

A larger study by Jia et al. (110) aimed to assess whether patients with ACS caused by plaque erosion might only require anti-thrombotic therapy, therefore also potentially avoiding stent deployment. Patients diagnosed with plaque erosion by OCT and residual diameter stenosis <70% on coronary angiogram were treated with anti-thrombotic therapy without stenting. OCT was repeated at one month and thrombus volume was measured. The primary endpoint was >50% reduction of thrombus volume at one month compared with baseline. The secondary endpoint was a composite of cardiac death, recurrent ischaemia requiring revascularisation, stroke, and major bleeding. Among 405 ACS patients with analysable OCT images, plaque erosion was identified in 103 (25.4%) patients. Sixty patients enrolled and 55 patients completed the one-month follow-up OCT. Forty-seven patients (47/60, 78.3%; 95% confidence interval: 65.8–87.9%) met the primary endpoint, and 22 patients had no visible thrombus at one month. Thrombus volume decreased from 3.7 (1.3, 10.9) mm^3 to 0.2 (0.0, 2.0) mm^3 (P <0.001). Minimal flow area increased from 1.7 (1.4, 2.4) mm^2 to 2.1 (1.5, 3.8) mm^2 (P = 0.002). One patient died of gastrointestinal bleeding, and another patient required repeat percutaneous coronary intervention. The rest of the patients remained asymptomatic. This study supports the preliminary evidence that conservative treatment with antithrombotic therapy without stenting may have a role for ACS patients presenting with plaque erosion.

1.11 Potential areas for research

Research into the fundamental processes triggering plaque erosion is important as an improved understanding of this important pathological process may allow the development of new strategies for the prevention and treatment of myocardial infarction. For example, novel anti-inflammatory treatments such as canakinumab (111) may be more relevant to plaque rupture than plaque erosion. Preliminary data suggests that patients with IFC tend to have better long-term outcomes, less luminal stenosis, potential avoidance of stent deployment and expression of different biomarkers in comparison to RFC patients. OCT has also emerged as the key modality in helping us to distinguish between plaque morphologies in vivo and also to provide unique information about plaque composition, fibrous cap thickness, the presence or absence of macrophages and thrombus characteristics.

The pathophysiology of plaque erosion is best studied in comparison to plaque rupture. The inflammatory differences between erosion and rupture seen at autopsy may be difficult to demonstrate in vivo due to the localised nature of coronary lesions and the secondary inflammatory changes in response to myocardial infarction. Thus far, clinical studies have examined a limited number of cytokines in peripheral plasma samples, and, apart from Niccoli et al. (104), have failed to reveal any significant differences (86,87).

To the best of our knowledge, there are no studies that have determined plaque pathology by OCT within the first hours of the acute infarct and correlated this with molecular differences in coronary plasma proteins using array technology.

We have, therefore, designed an observational study to compare the inflammatory profiles of plaque rupture and erosion using OCT to determine plaque morphology, thrombectomy to obtain coronary samples and cytokine arrays to screen a broad range of inflammatory mediators (the Plaque Erosion Pilot Study (PEPS)). We targeted patients presenting with short ischemic times in order to minimise the impact of secondary inflammatory changes. We also sought to explore the possibility that the inflammatory profile of intracoronary blood samples taken from the vicinity of the culprit lesion would be distinct from peripheral blood samples, and might reflect the underlying pathological substrate more closely. We hypothesised that differential cytokine expression would provide insights into the underlying cause of

plaque erosion, and would validate our methodology as an approach to studying the aetiology of plaque erosion.

1.12 Hypotheses and Aims

1.12.1 Hypotheses

1. The primary hypothesis is that plaque rupture and plaque erosion are associated with differential expression of intra-coronary cytokines.
2. The secondary hypothesis is that the coronary and peripheral circulations are associated with differential expression of cytokines.

1.12.2 Aims

1. The primary aim is to provide new insights into the possible mechanisms that lead to plaque erosion.
2. The secondary aim is to understand more about the local culprit artery environment and compare this to the peripheral circulation.

1.12.3 Study objectives

1. To demonstrate the feasibility and utility of this combined methodology.
2. To correlate expression of cytokines in coronary blood samples with plaque morphology during myocardial infarction by OCT.
3. To compare expression of cytokines between the coronary and peripheral circulation during myocardial infarction.

Chapter 2: Methods

2.1 Introduction

This is a prospective observational study to assess the feasibility of studying the pathobiological differences between coronary atherosclerotic plaque rupture and plaque erosion and to correlate expression of cytokines with plaque morphology during myocardial infarction by OCT in patients presenting with STEMI.

2.2 Ethics

This thesis is based upon the study of patients recruited prospectively into the Plaque Erosion Pilot Study (PEPS) at Norfolk and Norwich University Hospital, UK. The study was given ethical approval by the Camden and Islington Research and Ethics committee (N° 14/LO/1901). Subsequently, the study was given full permission for research by the Norfolk and Norwich University Hospitals National Health Service Foundation Trust (Research and Development Reference Number: 2014CARD06L).

2.3 Patient recruitment

Patients were recruited following a diagnosis of STEMI based on a history of chest pain and characteristic ECG changes of ST elevation. All patients were treated at the Norfolk and Norwich University Hospital NHS Foundation Trust. Patients were identified in the community by East of England ambulance paramedics or by medical staff in the Accident and Emergency departments of Norfolk and Norwich University Hospital or nearby district general hospitals (James Paget University Hospital, Great Yarmouth and Queen Elizabeth Hospital, King's Lynn). All of the patients were given 300mg of aspirin and 600mg of clopidogrel prior to arriving at the cardiac catheter laboratory of Norfolk and Norwich University Hospital for Primary Percutaneous Coronary Intervention (PPCI) for emergency treatment of the acute myocardial infarction.

2.4 Eligibility

Eligible patients included were those who presented:

1. Within six hours following the onset of pain
2. With ST-segment elevation of >1 mm in at least two contiguous leads
3. With new left bundle branch block, or true posterior myocardial infarction (MI) on the 12-lead electrocardiogram
4. And who were able to give verbal assent for study participation. Written informed consent was given later.

Exclusion criteria were:

1. Cardiogenic shock prior to PPCI – defined as systolic blood pressure <90mmHg for 30 minutes with signs of tissue hypoperfusion (e.g. blood lactate >2mmol/L) or a requirement for vasoconstrictor medication (e.g. adrenaline) or mechanical support (e.g. intra-aortic balloon pump)
2. STEMI due to stent thrombosis
3. Patients who suffered cardiac arrest prior to hospitalisation, requiring mechanical ventilation
4. Failed coronary thrombectomy (e.g. very tight stenosis or tortuosity) and therefore unable to collect intracoronary samples
5. Failed OCT examination of the culprit lesion (inadequate flow, inability to pass OCT catheter)
6. Patients with known severe renal impairment (eGFR <30ml/min/1.73m^2) who were not on renal replacement therapy.

2.5 Primary percutaneous coronary intervention (PPCI)

All aspects of the PPCI procedure were at the discretion of the consultant cardiologist responsible for the patient's procedure. Diagnostic coronary angiography was performed largely via the right radial artery or, in some circumstances, the right femoral artery through a 6 French (Fr) sheath following administration of 1% lignocaine for local anaesthesia. Peripheral arterial blood samples were aspirated from the sheath: 5ml was transferred to a heparinised tube (Fisher Scientific) for study purposes, and 10ml was collected for routine emergency blood tests (full blood count, urea and electrolytes, liver function tests, CRP, and troponin).

Coronary angiography was performed using diagnostic 5 Fr catheters to investigate the likely non-culprit artery(s) based on the presenting ECG. An appropriate 6 Fr guiding catheter was then used to identify the culprit artery, after which the patient was given weight-adjusted unfractionated heparin before the lesion was subsequently crossed with a suitable angioplasty wire (0.014 inch).

2.6 Thrombectomy

Following successful passage of a coronary guide wire across the culprit lesion, a thrombus extraction catheter (either PRONTO®V3 or PRONTO®LP, Vascular Solutions, Minneapolis, USA) was advanced to the lesion site. Using the 30ml syringe, approximately 10–20mls of coronary aspirate was extracted and a filter basket (70 micron mesh) was used for filtering the thrombus from the blood. The coronary blood was then transferred into a separate 5ml heparinised tube. The thrombus collected in the filter basket was carefully transferred to a 1.5ml Eppendorf tube (SigmaAldrich). Approximately 1ml of Allprotect® Tissue Reagent (Qiagen, Hilden, Germany) was added to this for immediate stabilisation of DNA, RNA and proteins in the collected thrombus.

If, due to technical reasons, passage of the thrombectomy catheter was difficult, predilation of the lesion with a small balloon (no greater than 2mm in diameter) was performed in order to facilitate thrombus aspiration.

2.7 Optical coherence tomography (OCT)

OCT pullback of the infarct-related artery (IRA) was then performed after thrombectomy but before PCI, using an ILUMIEN™ PCI Optimization™ OCT System (St Jude Medical, Inc. Minnesota, USA). This involved the passage of a 2.7 Fr optical Dragonfly™ Duo OCT Imaging Catheter (St Jude) (Figure 1), along the coronary guide wire beyond the culprit lesion. Radiopaque markers at the distal tip, imaging lens and 50mm proximal to the lens of the catheter helped to align the OCT pullback to the region of interest.

OCT image acquisition was then performed by injecting 10–14mls of x-ray contrast medium (Iohexol/Omnipaque, GE Healthcare, Wisconsin, USA) into the coronary

artery. During injection, the optical sensor is automatically withdrawn 54mm over 2 seconds. The images and data obtained were then stored digitally on the OCT system for offline analysis.

OCT was only performed after effective thrombus aspiration before stent placement, with re-established intracoronary TIMI II/III flow. If the OCT catheter could not cross the culprit lesion, predilation of the lesion with a small balloon (no greater than 2mm in diameter) was permitted to facilitate image acquisition. Patients were excluded from the study if adequate images were unable to be obtained.

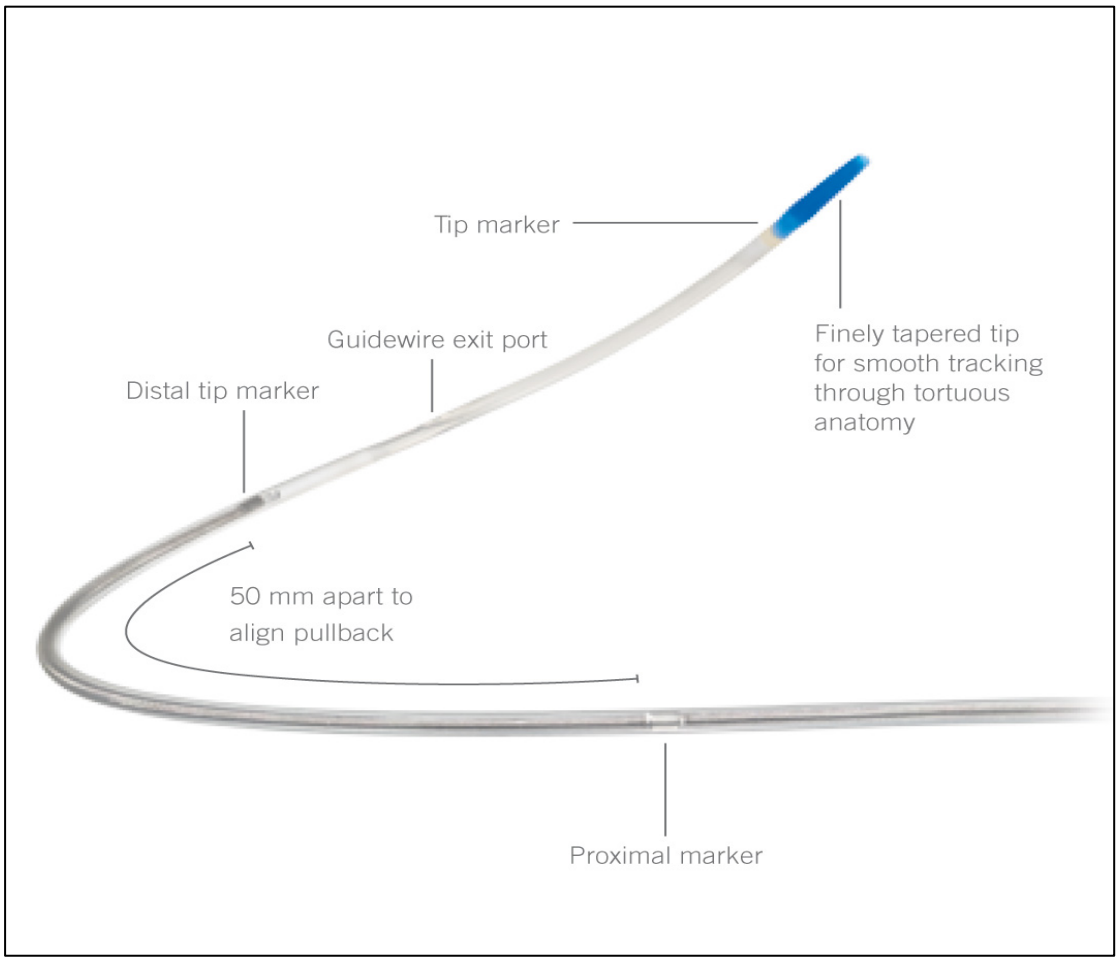

Figure 20: Dragonfly™ Duo OCT Imaging Catheter, St Jude Medical

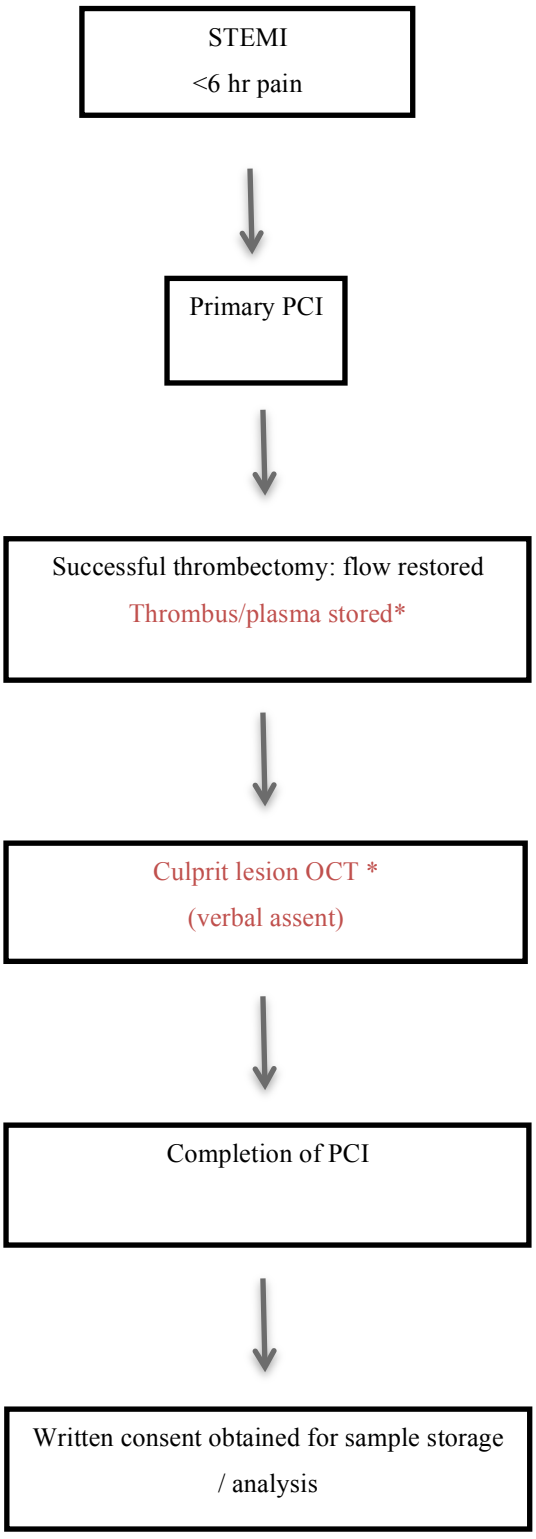

* indicates study specific procedures

Figure 21: Schematic of study recruitment and methodology for plaque erosion

2.8 Sample preparation

The peripheral and coronary blood samples were immediately put onto ice and transported in a polystyrene box to the haematology laboratory in the Bob Champion Research and Education Building, University of East Anglia. To ensure consistency, the samples were transported as soon as possible and no longer than 30 minutes following collection of the coronary aspirate. The blood samples were centrifuged at 2500g for five minutes at room temperature. One millilitre of the resultant supernatant plasma was aspirated and transferred to a 1.5ml Eppendorf tube. Samples were then stored at -20°C.

2.9 Consent

Verbal assent for study participation was obtained prior to the PPCI procedure. Consent for study participation, sample retention and analysis was sought retrospectively. Written study information and a detailed explanation of the study were given to the patients within 12 hours of completion of the PPCI procedure. Within 24 hours of providing this information, a member of the study team approached the patients to obtain informed written consent. If patients had provided verbal assent but not subsequent written consent, they were not eligible to participate in the study. Patients were also made to understand that they were free to withdraw from the study at any point.

Copies of the signed, informed written consent forms were given to the patient as well as filed in the patient's clinical notes and Trial Master File. A copy of the consent form for sample retention and analysis was also sent to the Norfolk Biorepository for sample storage permission and to generate a unique identification code for each participant in lieu of a name to protect the subject's identity. The original signed consent forms were stored in a specific study folder in a locked research office.

Letters were sent to the patients' General Practitioners outlining the study and confirming the patients' participation once written consent was provided.

2.10 Baseline demographic and clinical data

Baseline data about the study participants was collected following written consent and stored on a password-protected computer in the Norfolk and Norwich University Hospital cardiology research office. Data included age, gender, past cardiovascular history (previous myocardial infarctions, PCI procedures, or coronary artery bypass grafting, hypertension, hyperlipidaemia, stroke, transient ischaemic attack, peripheral vascular disease), smoking status, diabetes and chronic kidney disease.

Clinical data specific to each patient's presentation was also recorded, including time from symptom onset to cardiac catheterisation laboratory, door to balloon time, call to balloon time, Killip Class (I-IV), presence of anaemia and TIMI risk score.

Results of routine inpatient investigations were also recorded, including post-MI echocardiography (left ventricular ejection fraction), full blood count (FBC), renal function, high sensitive troponin I and C-reactive protein (CRP).

Post-MI echocardiography was carried out one day post MI by an experienced echo sonographer with British Society of Echo Accreditation to establish left ventricular ejection fraction (LV function). LV function is categorised into good or normal, mildly impaired, moderately impaired and severely impaired left ventricular systolic function based on the ejection fraction (EF). The EF is calculated using the Simpson biplane method (112). The Simpson method enables determination of the volume of the left ventricle. EF can be calculated by measuring the end-diastolic and end-systolic volumes in both the apical four-chamber and two-chamber views using the following formula:

$$\text{EF} = \frac{\text{End diastolic Volume} - \text{End systolic volume}}{\text{End diastolic Volume}} \text{ x } 100$$

Normal values of EF are shown in the following table (113):

Good or Normal	≥55%
Mild	45–54%
Moderate	36–44%
Severe	≤35%

Table 3: Categorisation of LV function according to ejection fraction

FBC was performed according to the established standard operating procedures in the haematology laboratory, and in accordance with the Sysmex-XE2100^{TM} (Kobe, Japan) manufacturer's instruction.

The reference clinical biochemistry laboratory measured creatinine and CRP using the ARCHITECT c800 autoanalyser (Abbott Diagnostics, Maidenhead, UK) and absolute plasma cardiac troponin I (cTnI) concentrations using the ARCHITECT Troponin I STAT assay (Abbott Diagnostics, Maidenhead, UK).

2.11 Angiographic and procedural data

Angiographic and procedural data was recorded for each patient participating in the study. The parameters included the number of lesions treated, the infarct-related artery, the presence or absence of multivessel disease (>1 significantly diseased vessel was defined as ≥70% in luminal diameter stenosis), the presence or absence of pre-procedural thrombus, use of glycoprotein IIb/IIIa inhibitors, arterial access route (radial versus femoral), number of stents implanted, total number of stents implanted per patient, total stent length, use of direct stenting without predilatation, use of predilatation to facilitate OCT use, maximum balloon diameter, initial and final TIMI flow, procedural success, reference vessel diameter pre and post intervention, pre and post thrombectomy minimal luminal diameter and percentage stenosis (see section 2.14).

2.12 Clinical outcomes

Major adverse cardiac or cerebrovascular events (MACCE), including cardiac death, recurrent myocardial infarction, stroke, target-lesion revascularisation, and stent thrombosis, were assessed at three, six and 12 months. This information was

ascertained initially through the Trust Patient Administration System database to determine if any unexpected deaths or admissions had occurred, followed by telephone calls by the investigator to the patient directly. In some instances, patients would notify the research team directly if there were any concerns or hospital admissions. If information was not obtainable through the sources described above, the patient's GP was contacted to establish more information. For any unexpected deaths in the community, the patient's GP was contacted to ascertain more information including cause of death written on the death certificate. The electronic records from NNUH are linked to NHS digital and therefore an up to date status on mortality data was available. Adverse events and clinical endpoints were assessed from the time of verbal assent until the 12-month follow-up was completed.

2.13 Quantitative coronary angiography

Quantitative coronary angiography (QCA) was performed retrospectively after the PPCI procedure using the CAAS II analysis system (PIE Medical, Maastricht, The Netherlands). Coronary angiograms were analysed offline by two interventional cardiologists independently of each other. Before taking measurements, the guiding catheter was used for calibration to enable quantification of the vessel size as accurately as possible. The absolute diameter of the coronary artery could therefore be compared to the size of the guiding catheter. The specific parameters – reference vessel diameter (RVD), minimum luminal diameter (MLD) and diameter stenosis (DS) – were measured pre (TIMI 0/I flow) and post thrombectomy (TIMI III flow) in two orthogonal views. Reference vessel diameter (RVD) is defined as the luminal diameter of a comparable segment and in this case referred to the segment of the target vessel proximal to the lesion or occlusion. The reference vessel diameter was measured in millimetres as an average of the sum of the diameters in one left anterior oblique (LAO) view and right anterior oblique view (RAO). Minimum luminal diameter (MLD) is defined as the smallest measured luminal diameter across the site of the target lesion at which it is most severe. Diameter stenosis (DS) is calculated as MLD/RVD X 100% with the result expressed as a percentage.

We were unable to perform these measurements in six of the 40 PPCI cases as their procedures were done in a cardiac catheter laboratory without suitable QCA software.

2.14 OCT analysis

All OCT data were exported, after having been anonymised, onto a St Jude OCT Offline Review Workstation (ORW). Each OCT was analysed independently by two operators (based at NNUH) both of whom were blinded to other study data. The analysis was undertaken using previously standardised criteria (97) but using a systematic approach to ensure consistency. Specific measurements of OCT cross-sectional images were performed with dedicated OCT system software (B.0.1, Light Lab Imaging).

Steps:

1. The first step for each OCT was to assess whether the lesion was interpretable. In some cases, excessive thrombus, very tight stenosis or indeed poor opacification of the vessel were factors that made some images very difficult to interpret.
2. For each run, the region of interest was defined and marked with markers on the longitudinal run and this defined segment was measured in millimetres.
3. To avoid ambiguity and reduce variable interpretations of pathology, OCT images were categorised into RFC, IFC/eroded plaque and undefined. RFC (Figure22a) was defined by the presence of a cavity formation in the plaque beginning at the luminal-intimal border with a clear discontinuity of the thin fibrous cap; IFC (Figure 22b) was defined by no evidence of cap rupture at the culprit site, evaluated in multiple adjacent frames, and the presence of thrombus on an irregular luminal surface (87). Plaque morphology was classed as undefined when OCT was unable to distinguish the lesion type because of an excess of thrombus obscuring the underlying structures, or where the images were simply too unclear to interpret.
4. Culprit plaques were classified as fibrous, fibrocalcific or lipid-rich if these components were present in two or more quadrants of an OCT cross-section. Plaque composition could be two classifications if two adjacent quadrants

fulfilled the criteria for one plaque component and two adjacent criteria fulfilled the criteria for another component. Fibrocalcific plaques were identified as well-delineated, signal-poor regions with sharp borders; fibrous plaques as homogeneous, signal-rich regions with low attenuation; and lipid plaques as signal-poor regions with high attenuation and diffused borders (86).

5. The proximal reference luminal area (PRLA) and distal reference luminal area (DRLA) were defined as the largest luminal areas within 5mm of the region of interest. The areas were measured three times for both reference points and the average of the three recorded.
6. Within the lumen of the culprit plaque, the presence or absence of thrombus was recorded.
7. If the presence of thrombus was recorded, this was identified as red, white or mixed thrombus. Red thrombus was identified as a high-backscattering protrusion inside the lumen of the artery, with signal-free shadowing in the OCT image, while white thrombi was identified as signal-rich, low-backscattering structures projecting into the lumen. Mixed encompassed characteristics of both red and white thrombus in equal measure.
8. Measurements were taken within the lesion of the culprit plaque with and without thrombus. Luminal area stenosis, minimal luminal diameter and maximal luminal area diameter were measured, yielding a total of six measurements.
9. In ruptured plaques, minimum fibrous cap thickness was measured at the thinnest point of the remnant cap, whereas mean cap thickness was computed as the mean of three evenly distributed measurements along the fibrous cap.

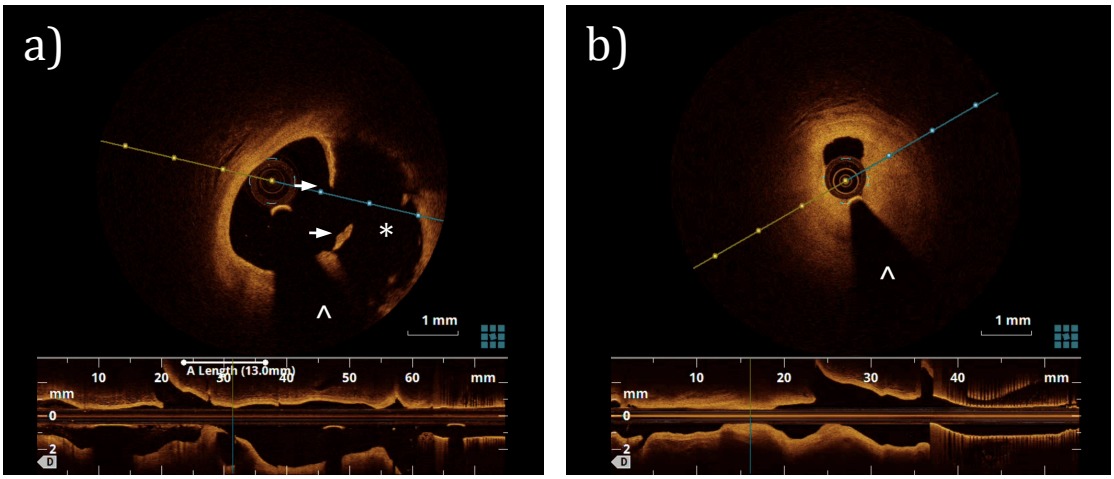

Figure 22: Examples of atheromatous plaque pathology using optical coherence tomography

a) Ruptured fibrous plaque: note the fibrous cap discontinuity (→), with cavity formation (*): ∧ wire shadow artefact.

b) Intact fibrous plaque/eroded plaque: note the absence of fibrous cap discontinuity: ∧ wire shadow artefact.

2.15 OCT consensus

The anonymised raw OCT data was sent to an experienced independent operator at Birmingham University Hospitals for qualitative assessment of the culprit plaque. The operator was blinded to patient details and previous analyses. The operator was asked solely to categorise the plaque morphology of the 40 culprit plaques into RFC, IFC and undefined. The results of this interpretation were then compared with the initial analysis done at NNUH. In circumstances in which a consensus could not be reached with regard to classification of a culprit plaque, this then became categorised as undefined.

2.16. Cytokine array

The Proteome Profiler™ Human XL Cytokine Array Kit (R&D Systems, Abingdon, UK) ARY022 is a membrane-based antibody array used to simultaneously detect the relative expression and differences of 102 cytokines, chemokines and acute-phase proteins between samples. This particular kit was chosen since it is composed of cytokines, chemokines and adipokines, therefore encompassing a large range of proteins. Secondly, we had significant experience with this array kit in the Bob

Champion Research and Education Centre, having done multiple arrays on acute myeloid leukaemia (AML) cells (114). Each kit was stored at 2°C in the haematology laboratory after purchase, with each array kit containing four membranes with 102 different cytokine antibodies. A complete list of the cytokines (with abbreviations) included on this array is found in section 3.0 of the Appendix.

2.16.1 Principle of cytokine array

Each of the 102-cytokine antibodies is spotted in duplicate on nitrocellulose membranes. Plasma samples are diluted and mixed with a cocktail of biotinylated detection antibodies. The sample/antibody mixture is then incubated with the array. Any cytokine/detection antibody complex present is bound by its cognate immobilised capture antibody on the membrane. Streptavidin-horseradish peroxidase and chemiluminescent detection reagents are added, and a signal is produced in proportion to the amount of cytokine bound (115) (Figure 23). Chemiluminescence is detected after a 10-minute exposure to x-ray film. Profiles of mean spot pixel density are created using a transmission-mode scanner and array capture spots are then quantified using imaging software.

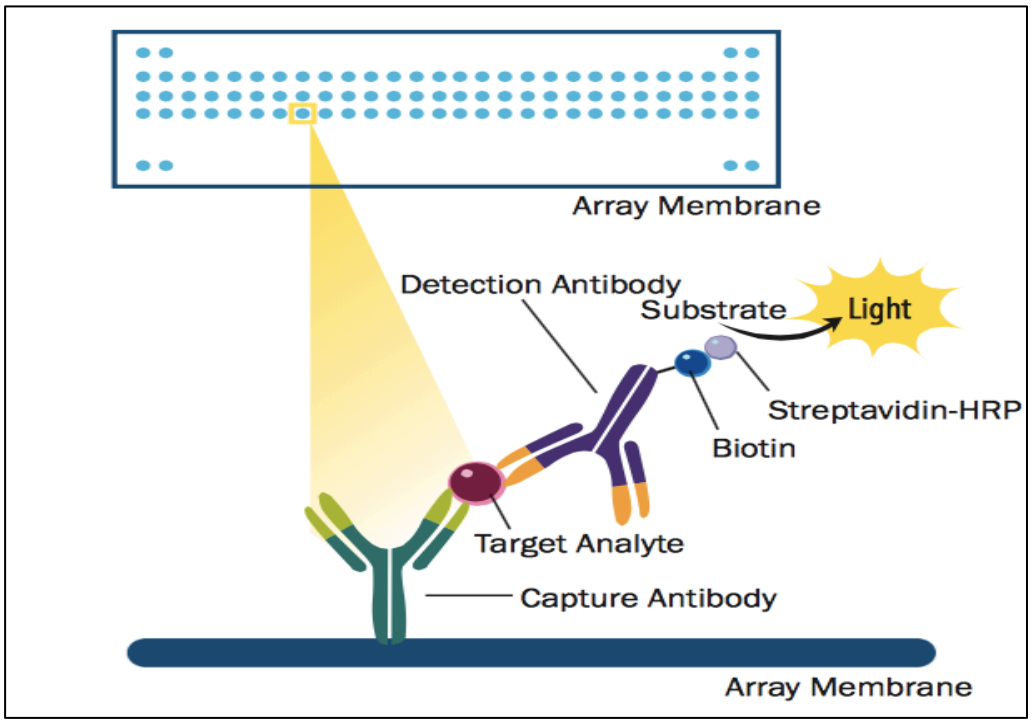

Figure 23: Schematic to demonstrate cytokine array methodology

Reproduced from Ary, CN 2012: 16 Proteome Profiler Array (115).

2.16.2 Cytokine array experiment

Coronary and peripheral arterial plasma samples were analysed using the Proteome Profiler™ Human XL Cytokine Array Kit (ARY022) as per the manufacturer's instructions. Before commencing, all reagents including the plasma samples were brought to room temperature. Four plasma samples were used for each kit (four nitrocellulose membranes per kit), therefore enabling the testing of paired coronary and peripheral samples from two separate patients. The vial of detection antibody cocktail (lyophilised biotinylated antibodies) was reconstituted in 100µl of deionised water. The bottle of 40ml of 25x wash buffer concentrate was diluted into 960ml deionised water.

Two millilitres of array buffer 6 was pipetted into each well of the four-well multi-dish. Each nitrocellulose membrane was removed from between the protective sheets using flat-tip tweezers and placed in one well of the dish. The array number was kept facing upward. The membranes were then incubated for one hour on a rocking platform shaker to block non-specific bindings. While the arrays were blocking, patient samples were prepared by diluting 200µl of the plasma sample with 1.3ml of array buffer 6 to give a final volume of 1.5ml. After one hour of blocking, array buffer 6 was aspirated from the wells of the four-well multi-dish and the prepared samples were added. The four-well multi-dish was then incubated overnight at 2–8°C on a rocking platform with the lid on.

The following day, each membrane was carefully removed and placed into individual plastic containers with 20ml of 1x wash buffer. The four-well multi-dish was rinsed with deionised water and dried thoroughly. Each membrane was washed with 1x wash buffer for 10 minutes on a rocking platform shaker, a total of three times. For each array, 30µL of detection antibody cocktail was added to 1.5ml of 1x array buffer 4/6. 1.5ml of the reconstituted detection antibody cocktail was pipetted into each well of the four-well multi-dish. Each membrane was then removed carefully from the wash container, returning the array to the four-well multi-dish containing the diluted detection antibody cocktail, and covered with the lid. This was then incubated for one hour on a rocking platform shaker.

After incubation, the membranes were washed as before up to a total of three times, each for 10 minutes. The four-well multi-dish was again rinsed with deionised water

and dried thoroughly. Two millilitres of 1x streptavidin-HRP was pipetted into each well of the four-well multi-dish. Each membrane was again removed from its wash container and returned to the four-well multi-dish containing the 1x streptavidin-HRP with the lid used to cover the wells. The dish was incubated for 30 minutes on a rocking platform.

After incubation, each membrane was washed as before and blot-dried to allow excess wash buffer to drain off. Each membrane was then placed on the bottom sheet of a plastic sheet protector with the identification number facing up. One millilitre of the prepared chemi reagent mix (0.5ml of chemi reagent 1 and 0.5ml of chemi reagent 2) was pipetted evenly onto each membrane. The top sheet of the plastic sheet protector was used to carefully cover each membrane and gently smooth out any air bubbles to ensure the chemi reagent mix was spread evenly to all corners of each membrane. This was left to incubate for one minute. Paper towels were positioned on the top and sides of the plastic sheet protector containing the membranes and excess chemi reagent mix was squeezed out. Leaving membranes on the bottom plastic sheet protector and taking the top plastic protector off, the membranes were covered with plastic wrap to gently smooth out any air bubbles. Membranes were placed with the identification numbers facing up and imaged using the Chemdoc-It^2 Imager, UVP (Figure 24). Array capture spots were then quantified using HL++ imaging software (Western Vision Software, Salt Lake City, UT, USA).

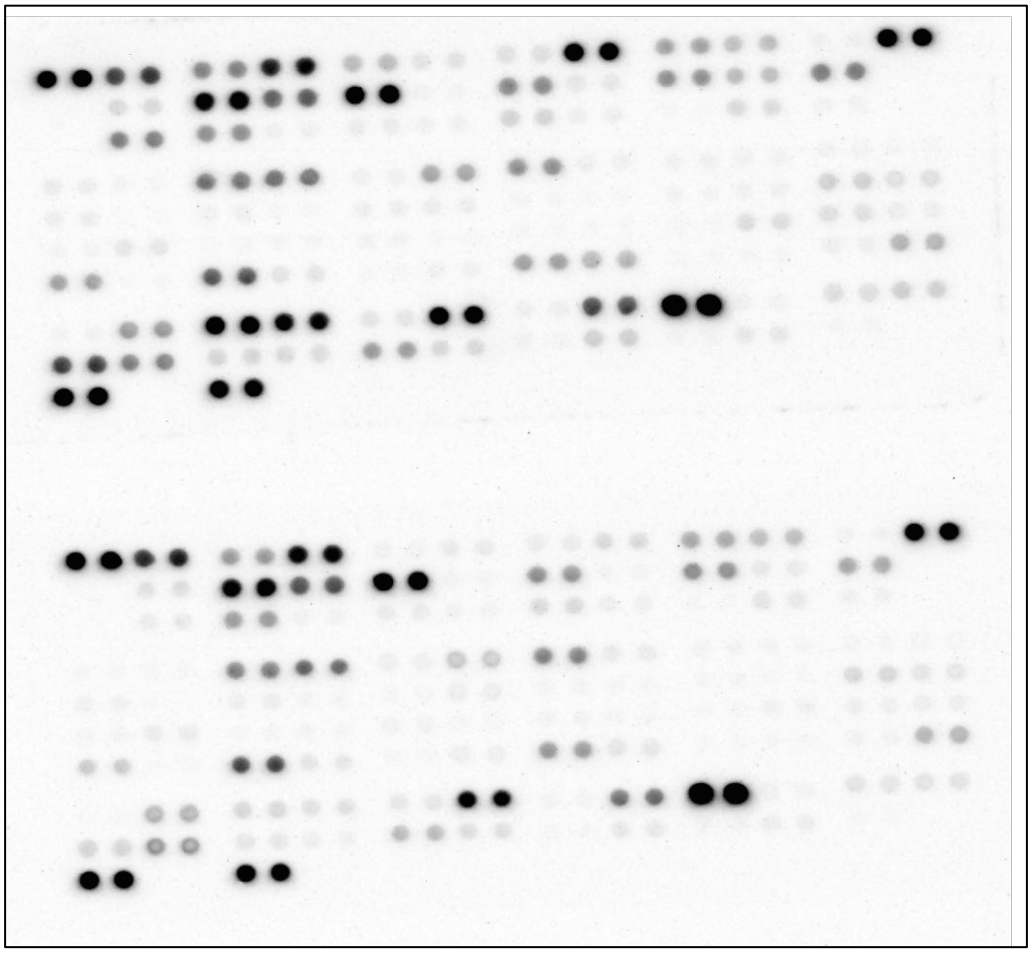

Figure 24: Representative membranes post-chemiluminiscent imaging demonstrating varying intensities of individual dots (cytokines)

2.16.3 Cytokine data analysis

Pixel intensities of individual dots captured using the Chemdoc-It^2 Imager were quantified by densitometric analysis using HL ++ imaging software (Western Vision Software, Salt Lake City, UT, USA). The quantification tool in the software enabled a relative reading to be taken for each spot and the average of each pair was considered as the reading for each cytokine. Signals were normalised using internal, positive and negative controls included on the array. A value of approximately 65,000 represented a spot intensity as demonstrated in the positive control, while a value of zero represented the spot intensity as seen in the negative control. The data was saved in a Microsoft Excel (version 14.7.1) spreadsheet for each patient.

This process was done for a total of 40 patients (peripheral and coronary samples), using a total of 20 cytokine array kits.

2.17 Enzyme-linked immunosorbent assays (ELISA)

ELISA was performed using Quantikine ELISA kits purchased from R&D Systems (Abingdon, UK) for EGF, TSP-1, BDNF, MIG, I-TAC, MMP-9, MPO, growth hormone and leptin (see Appendix).

The rationale for selecting these cytokines for ELISA validation is described in the results section.

2.17.1 Principle of Quantikine Sandwich ELISA methodology

Quantikine sandwich ELISA kits are quantitative enzyme immunoassay kits used to detect and quantify specific proteins. The sandwich ELISAs use a pair of antibodies, as capture and detector, directed against two or more distinct epitopes on antigens. A capture antibody binds to its typical antigen, while a detector antibody linked to an enzyme provides detection and enhancement of the signal.

The capture antibodies specific to the antigens are first coated on the microtiter plate. After coating, a series of dilutions of the antigens in the sample solution and antigen standard are added and captured by the antibodies on the plate. The bound antigens are subsequently detected by adding a specific amount of detector antibodies whereby the antigens become trapped and sandwiched between the capture and detector antibodies.

Multiple washing steps are performed between each step in order to remove the excess or unbound proteins. As with other ELISAs, the bound antigen-antibody complexes are detected by the addition of the enzyme-conjugated secondary antibodies (second antibody that will bind specifically to the detector antibody), followed by incubation of the enzyme substrate (Figure 25). As a result, the colorimetric signal produced during the enzymatic reaction is proportional to the amount of enzyme-conjugate bound to the plate as measured with the ELISA plate reader. A direct relationship exists between the concentration of the antigen-antibody and the intensity of the signal (or colour). As the concentration of antigen in the sample increases, the colour becomes more intense.

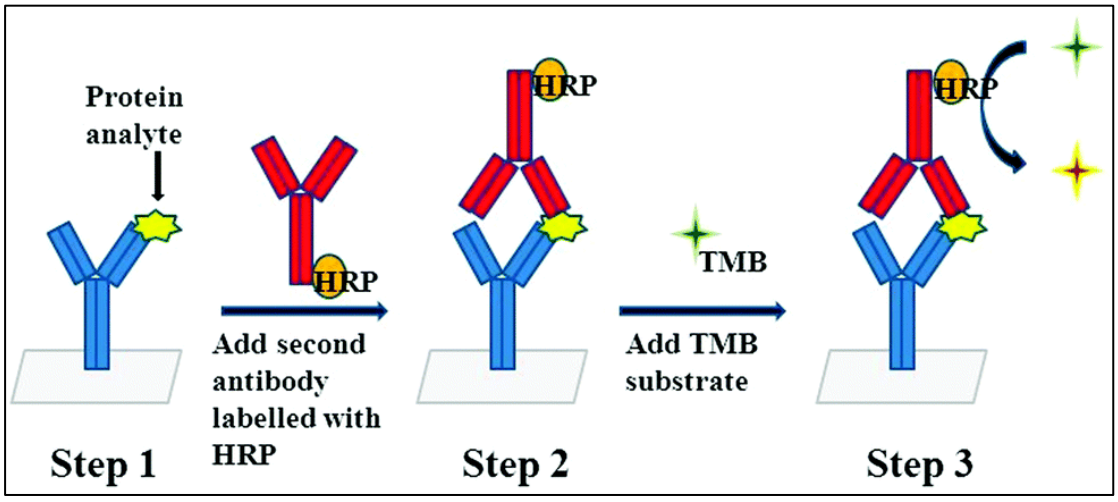

Figure 25: Schematic to demonstrate sandwich ELISA (reproduced from Zhang et al. (116)).

HRP – horseradish peroxidase, TMB – tetramethylbenzidine

2.17.2 ELISA experiment

The ELISA for MMP-9 was performed using the Human MMP-9 Quantikine ELISA kit (DMP900) as per the manufacturer's instruction. This was representative of all the other ELISAs undertaken.

Before commencing, all reagents, including the plasma samples, were brought to room temperature, with all samples, standards and controls assayed in duplicate. The bottle of 20ml of 25x wash buffer concentrate was diluted into 500ml of deionised water. MMP-9 standard was reconstituted with deionised water, producing a stock solution of 20ng/ml. With the stock solution, a dilution series using calibrator RD5-10 diluent was made up. The undiluted standard 20ng/ml served as the high standard to the lowest standard of 0.313ng/ml. 100µL of assay diluent RD1-34 was added to each well of the 96-well plate microtitre (monoclonal antibody was already pre-coated onto the plate). 100µL of standard, control or sample solution was then added to each well, covered with a plate sealer and then incubated at room temperature for two hours on a horizontal orbital microplate shaker. Each well was then aspirated and washed three times using 400µL of 25x wash buffer solution. After the last wash, the plate was inverted and blotted against clean paper towels to remove any remaining wash buffer. 200µL of human MMP-9 conjugate was then added to each well, covered with a plate sealer and incubated for one further hour on the shaker. Each well was again aspirated, washed and blotted as described above, followed by

the addition of 200µl of substrate solution to each well followed by 30 minutes of incubation at room temperature on the benchtop, protected from light using a black lid cover. 50µl of stop solution was then added to each well, turning the colour in the wells from blue to yellow. The optical density of each well was determined within 30 minutes, using a microplate reader (Tecan, Infinite® 200 PRO) set at 450nm. Optical density readings were also determined at 570nm and these were subtracted from 450nm to correct for optical imperfections in the plate. The readings were stored on a Microsoft Excel (version 14.7.1) spreadsheet for subsequent analysis.

2.17.3 ELISA analysis

Using the data stored on the Excel spreadsheet, a standard curve was constructed by plotting the mean absorbance for each standard on the y-axis against the concentration on the x-axis and a best fit curve was drawn through the points on the graph. The data was linearised by plotting the log of the cytokine concentrations versus the log of optical density and the best fit line was determined by regression analysis. The data was analysed using a four-parameter curve fit using software from www.elisaanalysis.com (see Figure 26).

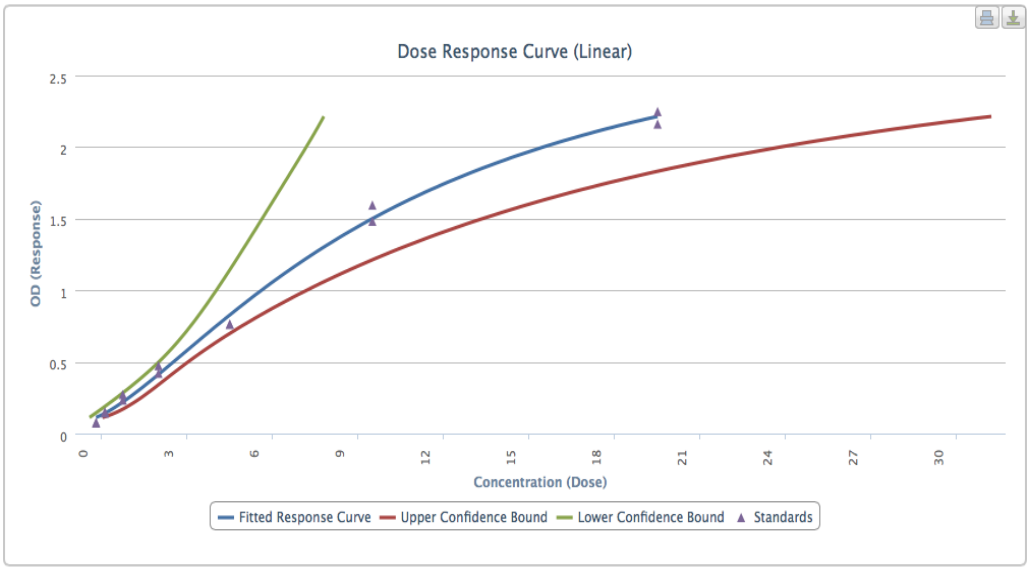

Figure 26: Dose response curve

2.18 Thrombectomy analysis

To confirm the expression data generated by cytokine array analysis, and validated

by ELISA, we performed a real-time polymerase chain reaction (RT-PCR) for EGF, TSP-1, I-TAC and MPO on the messenger RNA (mRNA) extracted from the thrombectomy specimens.

2.18.1 RNA extraction

Previously stored particulate matter was thawed and total RNA was extracted from homgenised thrombectomy specimens using the ReliaPrep™ RNA Cell Miniprep system (Promega, Southampton, UK) according to the manufacturer's instructions.

Frozen thrombectomy samples were placed in a sterile centrifuge tube containing 200µl lysis buffer solution (LBA) + thioglycerol (TG). The lysis was followed by pipetting 7–10 times to shear the DNA using a P1000 pipette to homogenise and disrupt the nucleoprotein complexes.

130µl of RNA dilution buffer (RDB) was added to each homogenate and vortexed for 10 seconds to mix, followed by centrifugation at 12,000rpm for two minutes. The cleared homogenate was carefully transferred to a clean 1.5ml tube, avoiding transfer of any pelleted material. 400µl of 100% isopropanol was added to each cleared homogenate and mixed by vortexing.

For each sample, a ReliaPrep™ Minicolumn was placed into a collection tube. The homogenate was transferred to the minicolumn and centrifuged at 12,000rpm for 30 seconds. The minicolumn was removed and the liquid in the collection tube discarded before replacing the minicolumn with the remaining homogenate back into the collection tube. 500µl of RNA wash solution (RWA) was added to each column and centrifuged at 12,000rpm for two minutes before discarding the collection tube and transferring the minicolumn into a 1.5ml elution tube. 40µl of nuclease-free water was added to each column and centrifuged at 12,000rpm for one minute. The minicolumn was discarded at this point.

5µl of DNase I and 5µl DNase 10x buffer was transferred to each eluate, followed by incubation for five minutes at room temperature. 150µl of LBA solution + TG buffer was added to the DNase treatment tube, followed by the addition of 300µl of 95% ethanol to the mixture and vortexing for 10 seconds to mix.

500µl of this mixture was then transferred to a new minicolumn and collection tube assembly. This mixture was then centrifuged at 12,000rpm for 30 seconds with the liquid in the collection tube discarded after. The minicolumn was transferred to a new collection tube and 500µl of RWA was added to each column, followed by centrifugation at 12,000rpm for 30 seconds. The minicolumn was removed and the liquid in the collection tube discarded before replacing the minicolumn back into the collection tube. 500µl of RWA was again added to each column, followed by centrifugation at 12,000rpm for two minutes.

The collection tube was discarded and the minicolumn transferred into a 1.5ml elution tube. 15µl of nuclease-free water was added to each column and centrifuged at 12,000rpm for one minute. The minicolumn was finally discarded and the elution tube capped. The elution tube with RNA was then stored at -70°C.

2.18.2 cDNA synthesis

For mRNA expression analysis, cDNA was synthesised from the total RNA using the Moline Murine Leukaemia Virus (MMLV) reverse transcriptase cDNA synthesis kit (PCR Biosystems, London, UK), as per the manufacturer's guidelines.

Reverse transcription was performed on a 96-well PCR plate (Thermo Scientific) and was prepared on ice. Total RNA was diluted into aliquots at 2ng/µl using nuclease-free water. A master mix comprised of 5x cDNA synthesis mix (containing anchored oligo deoxy-thymidine (DT) complementary primers) 20x reverse transcriptase (RT), nuclease-free water and RNA was made up into a 20µl reaction (Table 4).

Reagent	**Volume (µl)**
5x cDNA synthesis mix	4.0
20x RTase	1.0
Total RNA	2.5
Deionised water (dH_20)	12,5

Table 4: Reverse transcription master mix used in cDNA synthesis reactions

Reverse transcription was performed at 42°C for 30 minutes to permit cDNA synthesis, followed by enzyme denaturation at 85°C for 10 minutes.

The final cDNA products were stored at -20°C until required for RT-PCR.

2.19 Quantitative real-time polymerase chain reaction

2.19.1 The principle of RT-PCR

Real-time PCR is based on the detection and quantification of fluorescence where the signal increases in direct proportion to the amount of PCR product in the reaction. The method quantitates the initial amount of the template specifically, sensitively and reproducibly, and is a preferred method over standard PCR that detects the amount of final amplified product by gel electrophoresis at the end-point. Real-time PCR monitors the fluorescence emitted during the reaction as an indicator of product accumulation during each PCR cycle (117).

2.19.2 RT-PCR reaction

RT-PCR was performed on the cDNA reverse transcribed from purified RNA, using SYBR Green technology (PCR Biosystems, London, UK) on a 384-well light cycler 480 (Roche, Burgess Hill, UK). mRNA was analysed for EGF, MPO, I-TAC and TSP-1 expression and was normalised to either GADPH (glyceraldehyde 3-phosphate dehydrogenase) or beta actin. Primer sequences were designed using KicqStart (Sigma Aldrich, UK). The sequence of primers is shown in Table 5.

Protein	**Primers: Forward (F) and Reverse (R)**
β actin	F: 5'- gacgacatggagaaaatctg – 3' R: 5' – atgatctgggtcatcttctc – 3'
EGF	F: 5' – ggtggtgaagttgatctaaag – 3' R: 5' – tagcatgtgttgagattctg – 3'
GADPH	F: 5' – ctccttgttcgacagtcagcc – 3' R: 5' – gactccgaccttcaccttcc – 3'
I-TAC	F: 5' – ctacagttgttcaaggcttc – 3' R: 5' – cactttcactgcttttaccc – 3'

MPO	F: 5' – ccatggaactcctatcctac – 3' R: 5' – ttgacttggacaacacattc – 3'
TSP-1	F: 5' – gtgactgaagagaacaaagag – 3' R: 5' – cagctatcaacagtccattc – 3'

Table 5: Primers used in RT-PCR

Reactions for each cytokine were performed using 384-well PCR plates. Each well contained a master mix of 10µl of 2x qPCRBIO Sybr Green Blue Mix, 0.8µl of diluted forward and reverse primer (1/20 dilution), 1µl cDNA mixed with 4µl dH_2O and 3.4µl of dH_2O. The plates were run using the SYBR Green detection system under the following cycle conditions: 95°C for two minutes (pre-amplification), 45 cycles of 95°C for 15 seconds (amplification), 60°C for 10 seconds (annealing) and 72°C for 10 seconds (extension).

Using the comparative CT (cycle threshold) method, delta (d)-Ct values were determined by subtracting the Ct of the appropriate endogenous control (GADPH or β actin) from the Ct of the mRNA (EGF, MPO, I-TAC and TSP-1) in question.

Two-sided Wilcoxon rank-sum tests were used to assess the significance of any difference between the Ct values of IFC and RFC cases for each cytokine. P-values below 0.05 were considered significant. dCt values for all of the analysable samples for the four cytokines normalised to GADPH and β actin are listed in the Appendix.

2.20 Statistical analysis

Continuous variables were reported as median and first to third quartiles. Categorical data were reported as numbers and relative percentages. Overall comparisons across groups were based on the non-parametric Wilcoxon rank-sum test for continuous variables and Fisher's exact test for categorical variables. All p-values are two-sided. P-values less than 0.05 were considered significant unless otherwise stated. Power calculations were not undertaken since this was a pilot study with a limited number of patients, with the aim of generating preliminary data to plan for a larger study. Statistical analysis was performed using the Real Statistics Excel package (www.real-statistics.com).

2.21 Statistical analysis of cytokine arrays

Intensities of the negative control of each sample were subtracted from the intensity of each cytokine-sample pair (118). To remove variation originating from systematic, technical biases rather than from biological differences between cytokines or samples, relative intensity values were quantile-normalised (119). Next, data were $\log_2$ transformed to allow for direct comparisons to be made between cytokines by homogenising their variances.

Differential expression was assessed using the Significance Analysis of Microarrays (SAM) method (120) with the Benjamini–Hochberg procedure for multiple testing correction yielding q-values. The output of this included assignment to either a group comprising cytokines with an average expression higher in patients with plaque erosion or a group comprising cytokines with an average expression higher in patients with plaque rupture. A differential expression score (D-score) and average $\log_2$ fold change in expression were captured for each cytokine, in addition to a q-value.

For the meta-analysis approach, Stouffer's z-score method was used to combine the q-values from the coronary and peripheral sample analyses. This was only deployed for cytokines that were assigned to the same plaque-defined group of cytokines in both the coronary and peripheral blood samples. Cytokines with assignments that were discordant were not included in the meta-analysis.

Chapter 3: Clinical results

3.1 Baseline and angiographic characteristics

Between 2 February and 14 October, 2015, 40 STEMI patients were recruited to the PEPS (Figure 27), representing approximately 30% of all potentially eligible patients. An additional five patients were not enrolled in the study due to unsuitable anatomy and the inability to obtain adequate OCT images. A fully identifiable culprit plaque was adjudicated (adjudication process described in methods section) in 38 patients. Table 6 shows that RFC was identified in 23 (57.5%) patients and IFC in 15 (37.5%). Two (5%) were undefined. Figure 28 shows examples of the culprit plaque morphology as visualised with OCT.

There were no differences in baseline characteristics between patients with RFC and IFC except for age (65 [59.5 to 75] yrs RFC vs 60 [52 to 64.5] yrs IFC, $p = 0.03$) (Table 7). Both groups had very similar ischaemic times. Baseline echo characteristics (Table 8) did not show any significant differences between the groups: the majority of patients in both groups post STEMI had good left ventricular systolic function.

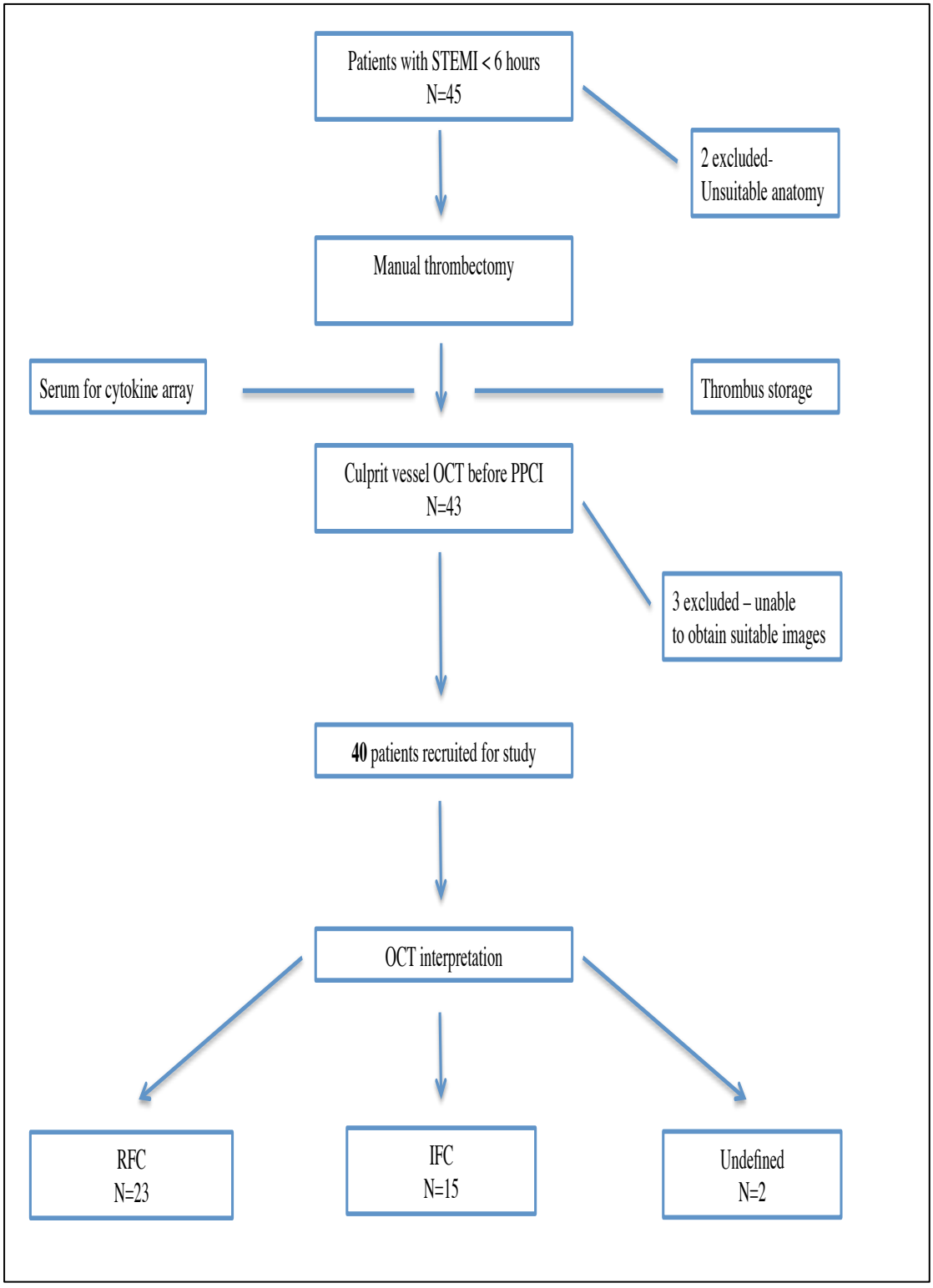

Figure 27: Study enrolment

STEMI – ST segment myocardial infarction; OCT – optical coherence tomography; PPCI – primary percutaneous coronary intervention; RFC – ruptured fibrous cap; IFC – intact fibrous cap.

Key number	First Reviewer	Second Reviewer	Consensus Pathology	Comments	Sex	Initial Consensus	Final Consensus
2279	Erosion	Erosion	Erosion		M	**Y**	
6710	Erosion	Erosion	Erosion		M	**Y**	
7191	Erosion	Erosion	Erosion		M	**Y**	
7369	Erosion	Erosion	Erosion		M	**Y**	
7775	Erosion	Erosion	Erosion		F	**Y**	
7911	Erosion	Erosion	Erosion		M	**Y**	
7816	Erosion	Erosion	Erosion		M	**Y**	
8843	Erosion	Erosion	Erosion		F	**Y**	
1022	Rupture	Rupture	Rupture		M	**Y**	
1177	Rupture	Rupture	Rupture		F	**Y**	
1309	Rupture	Rupture	Rupture		M	**Y**	
1819	Rupture	Rupture	Rupture		M	**Y**	
1845	Rupture	Rupture	Rupture		F	**Y**	
2053	Rupture	Rupture	Rupture		F	**Y**	
2058	Rupture	Rupture	Rupture		M	**Y**	
3204	Rupture	Rupture	Rupture		M	**Y**	
3460	Rupture	Rupture	Rupture		M	**Y**	
3766	Rupture	Rupture	Rupture		M	**Y**	
4872	Rupture	Rupture	Rupture		F	**Y**	
5430	Rupture	Rupture	Rupture		M	**Y**	

5452	Rupture	Rupture	Rupture		F	**Y**	
5670	Rupture	Rupture	Rupture		M	**Y**	
6219	Rupture	Rupture	Rupture		M	**Y**	
7600	Rupture	Rupture	Rupture		M	**Y**	
8203	Rupture	Rupture	Rupture		M	**Y**	
8258	Rupture	Rupture	Rupture		M	**Y**	
8521	Rupture	Rupture	Rupture		F	**Y**	
9802	Rupture	Rupture	Rupture		M	**Y**	
8715	Rupture	Rupture	Rupture		M	**Y**	
4201	Undefined	Undefined	Undefined	Heavily calcified – unable to classify	F	**Y**	
6787	Undefined	Undefined	Undefined	Unclassifiable	M	**Y**	
8053	Erosion	Rupture	Erosion	Pre-dilated – no evidence of rupture	M	**N**	**Y**
1243	Erosion	Undefined	Erosion	Intact fibrous cap, calcified	M	**N**	**Y**
1608	Erosion	Undefined	Erosion	Pristine vessel, thrombus but no obvious rupture	F	**N**	**Y**
4027	Rupture	Undefined	Erosion	Intact cap – no evidence of rupture	M	**N**	**Y**
5266	Erosion	Undefined	Erosion	Intact fibrous cap – clear OCT definition	M	**N**	**Y**

6894	Erosion	Undefined	Erosion	Pre-dilated – no evidence of rupture	F	**N**	**Y**
9989	Erosion	Undefined	Erosion	Intact TCFA, with thrombus	F	**N**	**Y**
5660	Undefined	Rupture	Rupture	Disruption of fibrous cap	F	**N**	**Y**
8437	Rupture	Undefined	Rupture	Definite rupture	M	**N**	**Y**

Table 6: OCT culprit plaque morphology adjudication

This table demonstrates the results of the adjudication process for all 40 patients by both interventional cardiologists. Two cases were not classifiable. Nine cases initially had different consensus, but after discussion, a final consensus was reached. Comments for these cases are included in the table to illustrate the reasons for the final consensus.

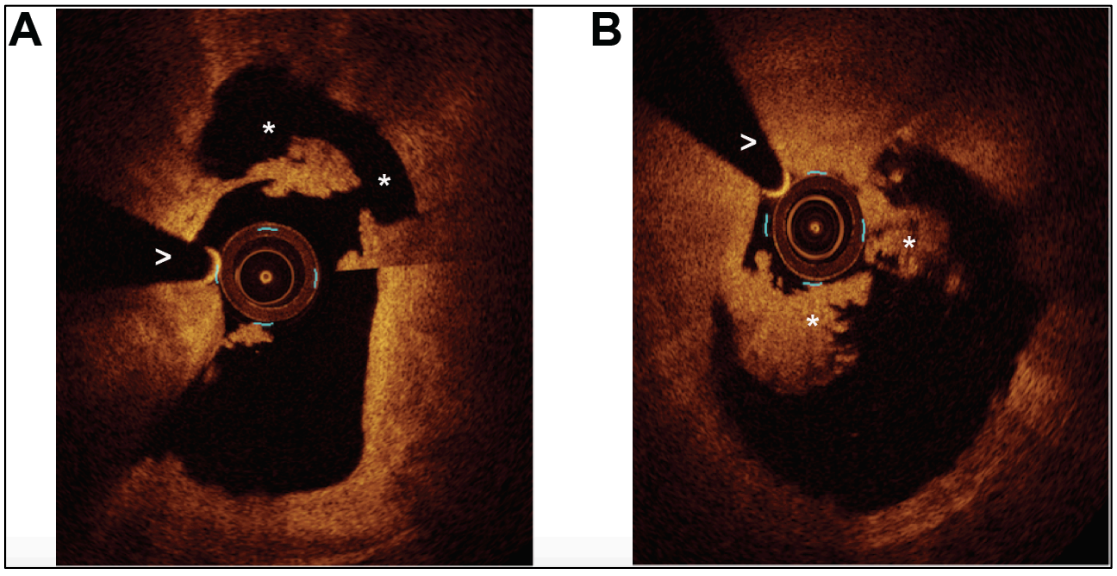

Figure 28: Examples of ruptured and intact fibrous cap appearance using OCT from enrolled patients

(**A**) Ruptured fibrous cap. * rupture cavity. > wire artefact.

(**B**) Intact fibrous cap.* thrombus. > wire artefact.

There were no differences in baseline blood characteristics (Table 7). Radial access was used in almost every patient (97.4%). Angiographic and procedural findings

were similar between the two groups, except for the finding that there was significantly lower use of stents in the IFC group (18 (78%) RFC vs 9 (60%) IFC, p = 0.01) (Table 10). Differences in the number of stents implanted per patient (1.09 [0.73] RFC vs 0.6 [0.63] IFC, p = 0.06) and total stent length (27 [22 to 38] vs 23 [17 to 28], p = 0.06) did not reach statistical significance when comparing the two groups, but did also suggest a lower use of stents in the IFC group. Proportionally, there was a higher use of drug-coated balloon therapy in the IFC group (5 (21.7%) RFC vs 6 (40%) IFC), supporting the data that there was lower use of stents in the IFC group; although, again, this did not reach statistical significance. Baseline lesion severity was not significantly different between the two groups (% diameter stenosis 100% RFC vs 100% IFC, p = 0.88).

	RFC (n=23)	IFC (n=15)	P value
Age (years)	65 (59.5–75)	60 (52–64.5)	0.03
Sex (males)	16 (69.6)	10 (66.7%)	1.00
Hypertension	8 (34.8%)	3 (20%)	0.47
Hyperlipidaemia	8 (34.8%)	4 (26.7%)	0.44
Smoker	12 (52.2%)	8 (53.3%)	1.00
Diabetes	0 (0%)	2 (13.3%)	0.15
Previous MI	0 (0%)	0 (0%)	
Previous PCI	0 (0%)	0 (0%)	
Time onset to lab (mins)	160 (125–207.5)	190 (145–247.5)	0.24
Door to balloon time	37 (29–61)	44 (29–46)	0.47
Call to balloon time	125 (95–147)	134 (99–142)	0.71
Killip Class			0.15
Class 1	23 (100%)	13 (86.7%)	
Class 2	0 (0%)	2 (13.3%)	
TIMI risk score	2 (1–4)	2 (1–2)	0.46
Anaemia	0 (0%)	0 (0%)	1.00

Table 7: Baseline characteristics

Values are median (first to third quartile) or n (%). IFC – intact fibrous cap; MI – myocardial infarction; PCI – percutaneous coronary intervention; RFC – ruptured fibrous cap; TIMI – thrombolysis in myocardial infarction.

Echocardiographic LV function	RFC	IFC	P value
			0.87
Good LV function	16 (69.6)	6 (40%)	
Mildly impaired LV function	6 (26.1%)	4 (26.7%)	
Moderately impaired LV function	1 (4.3%)	3 (20%)	
Severely impaired LV function	0 (0%)	2 (13.3%)	

Table 8: Baseline echo characteristics post PCI

Values are n (%)

LV – left ventricular

	RFC (n=23)	IFC (n=15)	P value
Hb (135–170g/L)	150 (140–154)	142 (135–152.5)	0.4
Plts (150–410 $x10^9$/L)	252 (233–302.5)	331 (237.5–362.5)	0.09
WCC (4.00–10.00 $x10^9$/L)	10.9 (8.7–14.1)	12.1 (10.3–16.3)	0.08
Neu (2.0–7.0 x $x10^9$/L)	7.42 (5.6–10.4)	8.81 (7.6–13.1)	0.07
Lym (1.0–3.0 $x10^9$/L)	1.47 (1.2–2.2)	2.0 (1.8–2.5)	0.14
Creatinine (59–104 μmol/L)	76 (69.5)	75 (65–81.5)	0.53
CRP (0–10mg/dL)	3 (2–7.3)	8 (1.8–14)	0.3
Troponin I (0–34.3ng/L)	7321 (851–2863.5)	26350 (5315–39915.5)	0.3

Table 9: Baseline blood characteristics including normal ranges

Values are median (first to third quartile)

CRP – C-reactive protein; Hb – haemoglobin; Lym – lymphocytes; Neu – neutrophils; Plts – platelets; WCC – white cell count.

	RFC (n=23)	IFC (n=15)	P value
Number of lesions treated			1.00
1	22 (95.7%)	15 (100%)	
2	1 (4.3%)	0 (0%)	
Infarct-related artery			0.64
LAD	7 (30.4%)	9 (60%)	
LCX	4 (17.4%)	2 (13.3%)	
RCA	12 (52.2%)	4 (26.7%)	
Multivessel disease	9 (39.1%)	4 (26.7%)	0.5
Thrombectomy	23 (100%)	15 (100%)	1.00
Gp2b3a use	9 (39.1%)	8 (53.3%)	0.51
Radial access	23 (100%)	14 (93.3%)	0.39
Dilatation pre-OCT	4 (17.4%)	5 (33%)	0.44
Stents implanted	18 (78.3%)	9 (60%)	0.01
Stents implanted per patient	1.09 (0.73)	0.6 (0.63)	0.06
Total stent length (mm)	27 (22–38)	23 (17–28)	0.06
Drug-coated balloon	5 (21.7%)	6 (40%)	0.28
Direct stenting	11 (47.8%)	5 (33.3%)	0.51
Maximum balloon/stent diameter (mm)	4 (3.375–4)	3.5 (3.125–3.875)	0.20
Base TIMI flow			0.63

0	14 (60.9%)	10 (66.7%)	
1	0 (0%)	0 (0%)	
2	3 (13.3%)	3 (20%)	
3	6 (26.8%)	2 (13.3%)	
Final TIMI flow			0.82
0	0 (0%)	0 (0%)	
1	1 (4.3%)	0 (0%)	
2	0 (0%)	0 (0%)	
3	22 (95.6%)	15 (100%)	
Procedural success	22 (95.6%)	15 (100%)	
QCA at baseline			
Reference vessel diameter (mm)	3.28 (2.81–3.62)	3.17 (2.73–3.33)	0.44
Minimal luminal diameter (mm)	0 (0–0.97)	0 (0–0.84)	0.96
Diameter stenosis (%)	100 (75.6–100)	100 (75.2–100)	0.88
QCA post-thrombectomy			
Reference vessel diameter (mm)	3.38 (2.85–3.76)	3.22 (2.58–3.49)	0.39
Minimal luminal diameter	1.1 (0.88–1.45)	0.94 (0.7–1.2)	0.40
Diameter stenosis	66.5 (46.4–77.3)	68.8 (62.3–73.6)	0.75

Table 10: Angiographic and procedural characteristics

Values are median (first to third quartile) or n (%), except for stents implanted per patient, which is expressed as a mean (standard deviation)

Gp2b3a – glycoprotein$_{IIbIIIa}$; IFC – intact fibrous cap; LAD – left anterior descending; LCx – left circumflex; OCT – optical coherence tomography; PCI – percutaneous coronary intervention; QCA – quantitative coronary angiography; RCA – right coronary artery; RFC – ruptured fibrous cap. TIMI – thrombolysis in myocardial infarction.

3.2 OCT characteristics

We next examined whether OCT analysis would reveal any differences in lesion structure between RFC and IFC (Table 11). We found significant differences for minimum cap thickness (40 [30 to 40] μm RFC vs 80 [70 to 95] μm IFC, p <0.001) and for mean cap thickness groups (52 [40 to 59] μm RFC vs 100 [99 to 134] μm IFC, p <0.001), demonstrating that cap thickness was significantly lower in the RFC group. There were no significant differences in other plaque parameters, though there was a trend towards a more fibrous phenotype in IFC (2 (8.7%) RFC vs 6 (40%) IFC). The residual thrombus burden after thrombectomy and thrombus type were similar between groups, with white thrombus and mixed thrombus predominating. Representative OCT images from patients enrolled have also been included in this section to further demonstrate plaque morphology and measurements obtained. Figures 29, 30 and 31 illustrate cases of RFC. In addition, Figures 30 and 31 demonstrate lipid-rich and fibrocalcific characteristics. Figures 32, 33 and 34 demonstrate IFC cases, with Figures 33 and 34 highlighting fibrocalcific and fibrous plaque characteristics. Figures 35 and 36 demonstrate luminal area measurements with and without thrombus in order to calculate area stenosis. Figure 37 demonstrates minimum cap thickness measurement in an RFC case, and Figure 38 demonstrates lesion length measurement.

3.3 Clinical outcomes

Twelve-month clinical outcome data (Table 12) reports only one death and one TIA occurring during follow-up. There were no statistical differences between the two groups.

	RFC (n=23)	IFC (n=15)	P value
Residual thrombus	19 (82.6%)	12 (80%)	1.00
Minimum cap thickness (µm)	40 (30–40)	80 (70–95)	<0.001
Mean cap thickness (µm)	52 (40–59)	100 (99–134)	<0.001
Length of lesion (mm)	11.3 (9.75–12.55)	11.4 (9.9–15.1)	0.82
Plaque characteristics			0.93
Fibrocalcific	1 (4.34%)	1 (4.34%)	
Fibrous	2 (8.7%)	6 (40%)	
Lipid-rich	20 (86.7%)	8 (53.3%)	
Area stenosis (%)	79.0 (52.5–83.1)	74.3 (70.4–77.1)	0.16
Residual thrombus characteristics			0.54
Red	1 (4)	1 (7)	
White	12 (52)	5 (33)	
Mixed	9 (39)	5 (33)	
None	1 (4)	4 (27)	

Table 11: Optical coherence tomography analysis

Values are median (first to third quartile) or n (%). IFC – intact fibrous cap; RFC – ruptured fibrous cap.

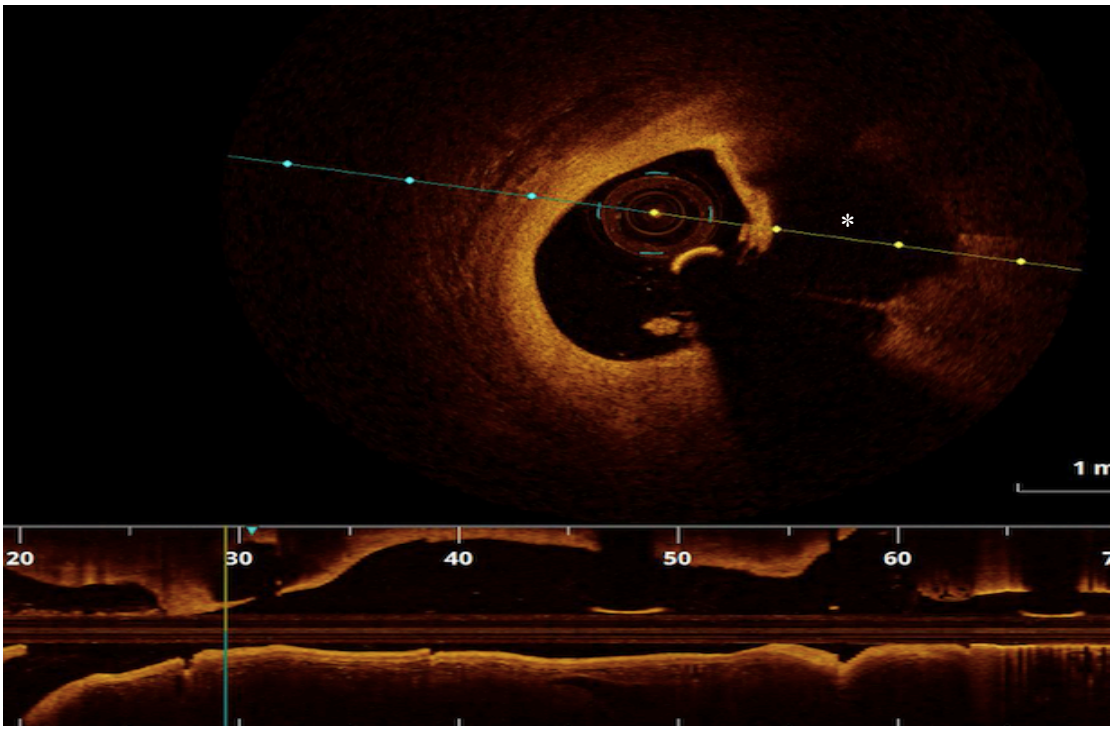

Figure 29: Example of RFC showing disruption of fibrous cap and rupture cavity formation

* rupture cavity

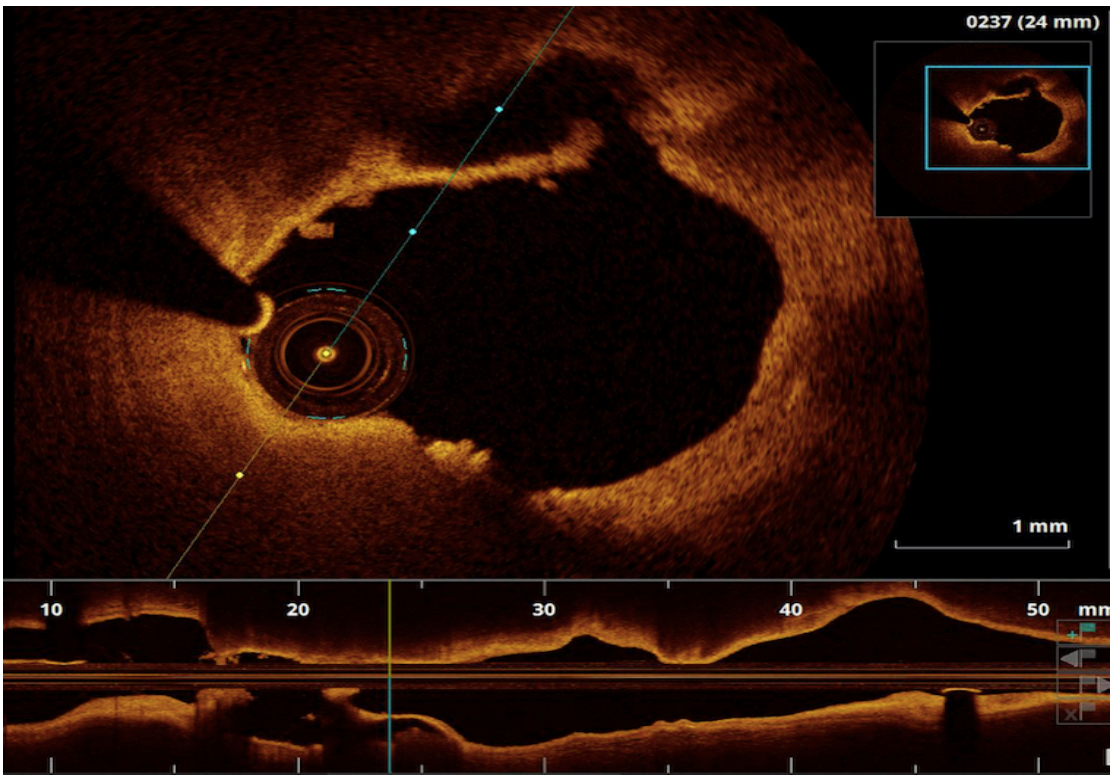

Figure 30: Further example of RFC with lipid-rich characteristics – signal-poor regions with high attenuation and diffuse borders

* rupture cavity

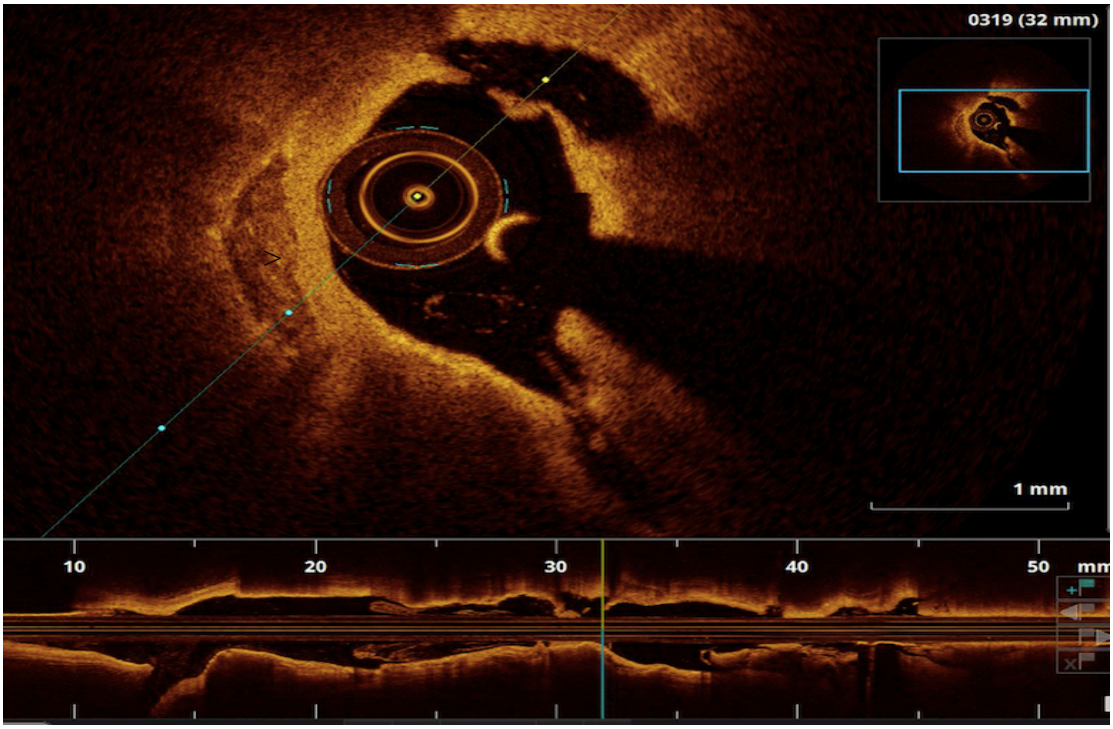

Figure 31: Example of RFC with lipid-rich and fibrocalcific characteristics

Fibrocalcific plaques are identified as well-delineated, signal-poor regions with sharp borders.

* rupture cavity. > fibrocalcific region.

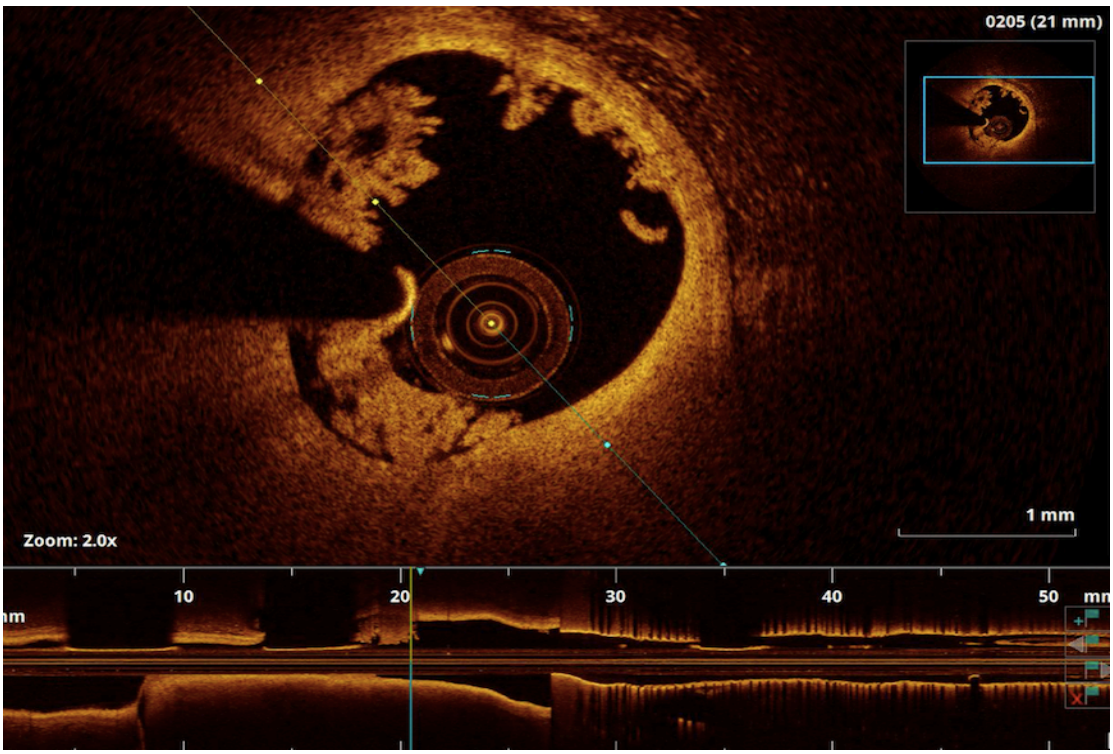

Figure 32: IFC example with intact fibrous cap and thrombus adherent to vessel wall

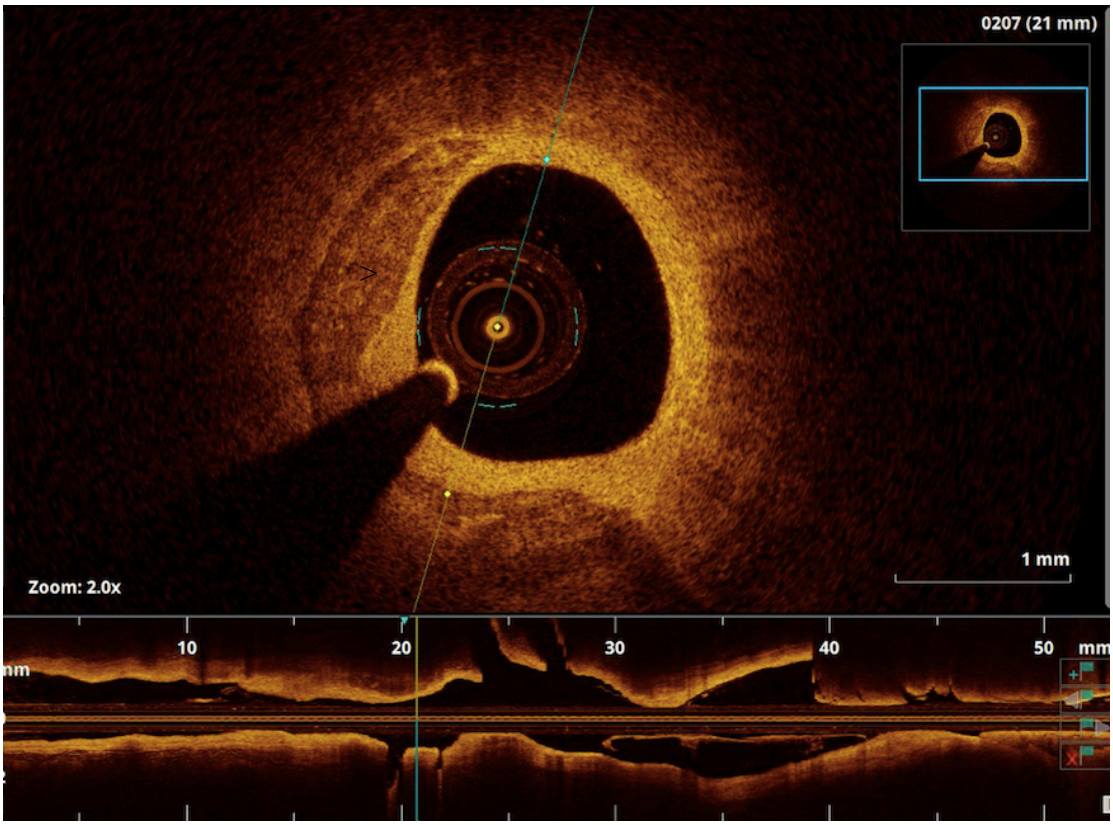

Figure 33: IFC with fibrocalcific characteristics

> fibrocalcific region

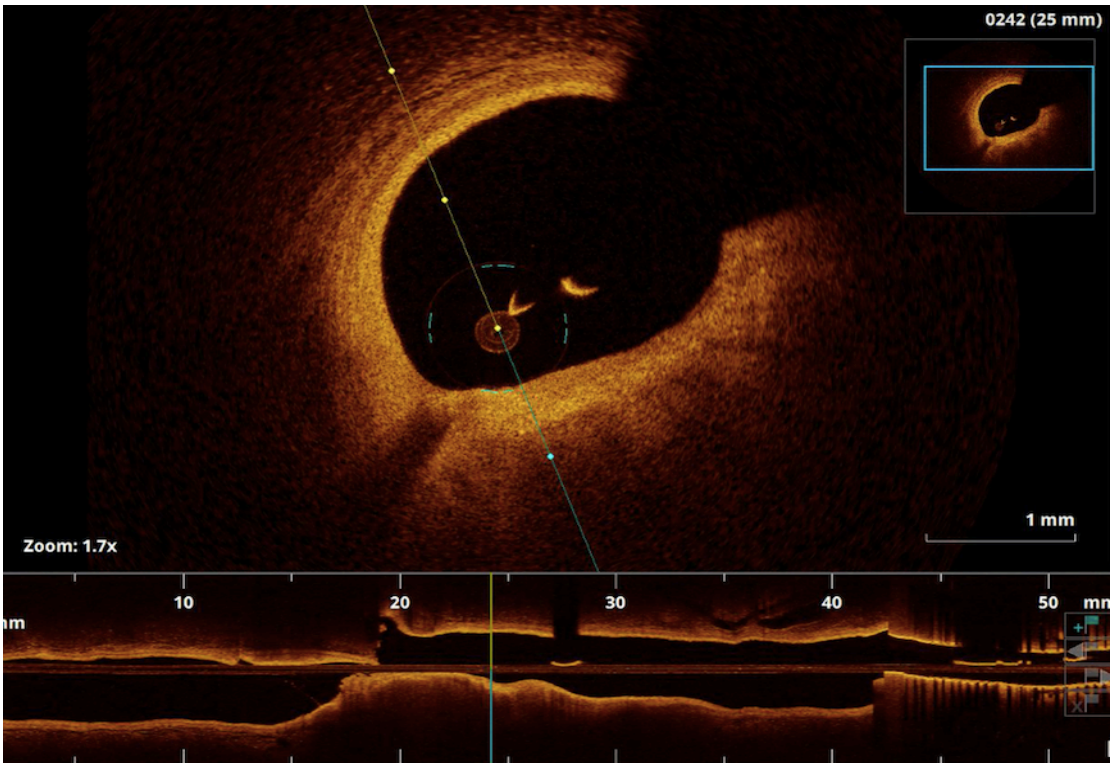

Figure 34: IFC with predominantly fibrous phenotype – homogenous, signal-rich with low attenuation

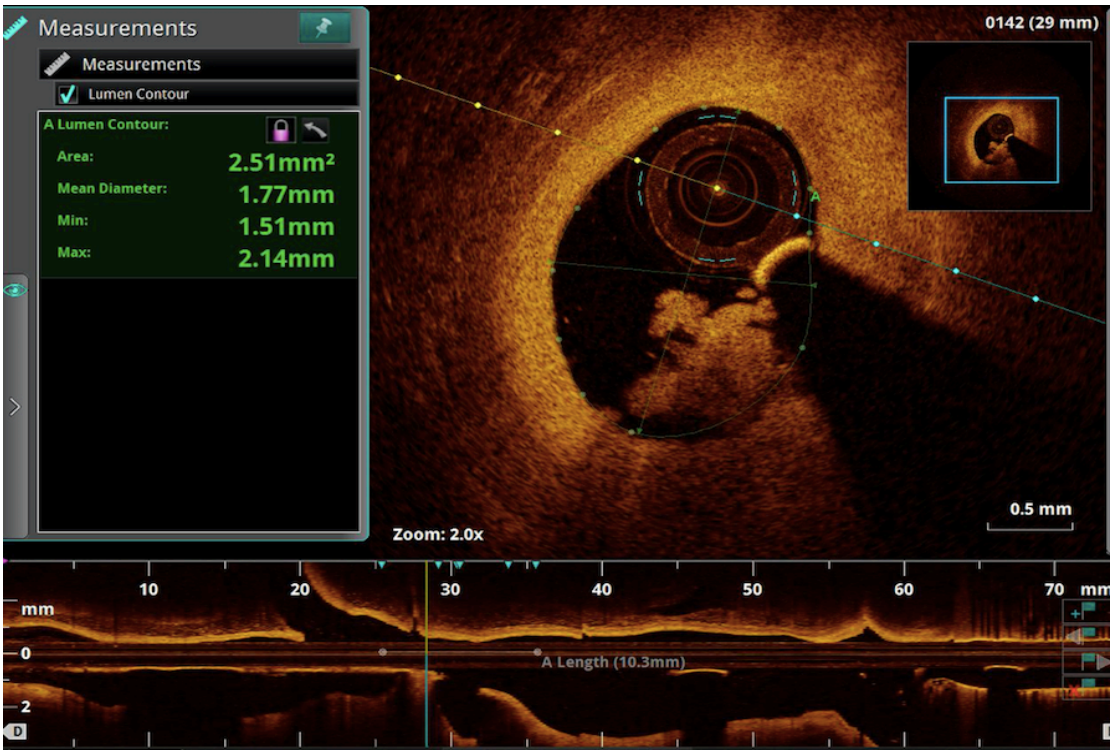

Figure 35: An example of IFC case with luminal area measurement including thrombus

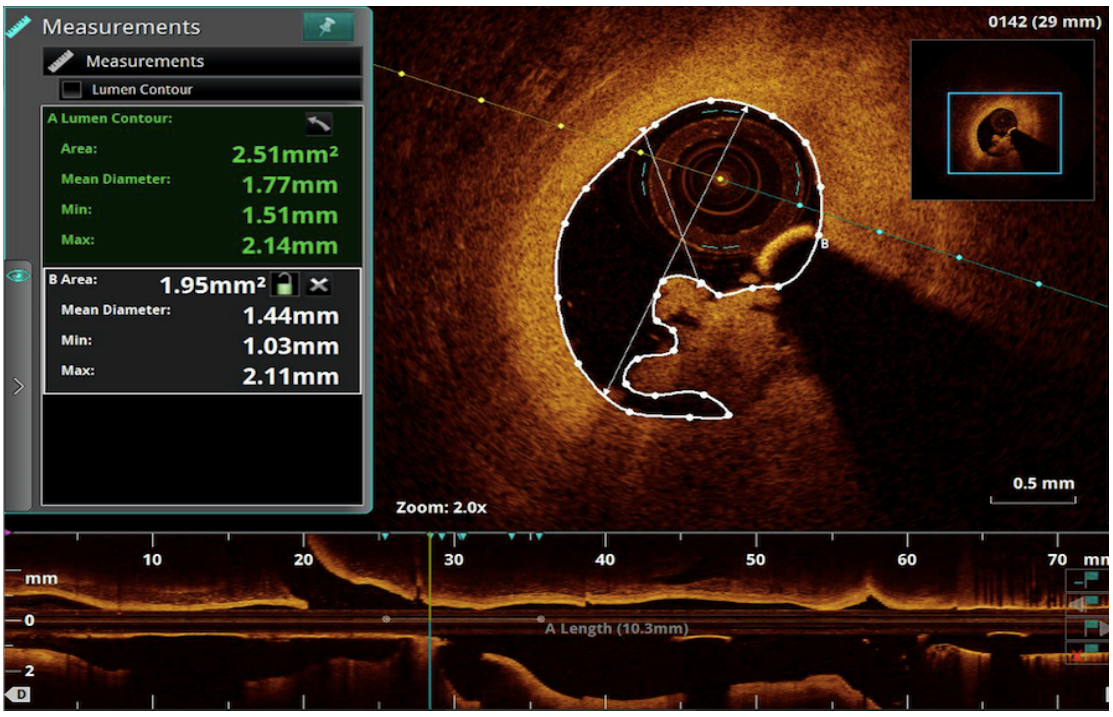

Figure 36: Same IFC case with luminal area measurement excluding thrombus to calculate area stenosis

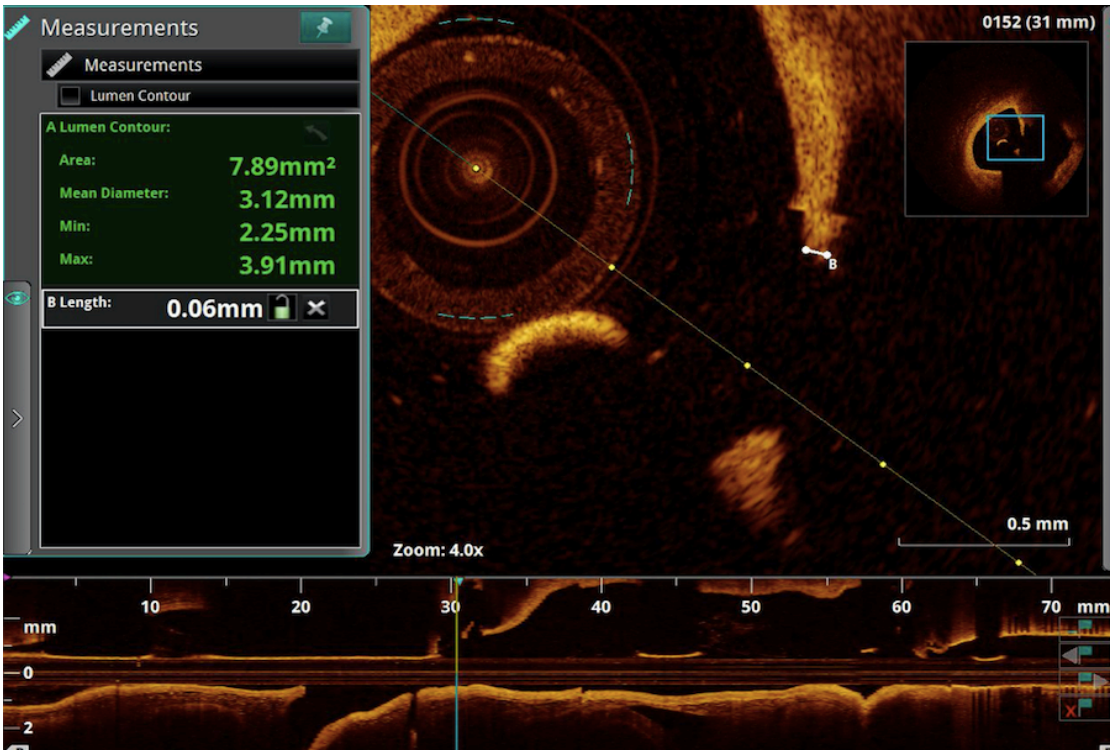

Figure 37: Measurement of minimum cap thickness in RFC case

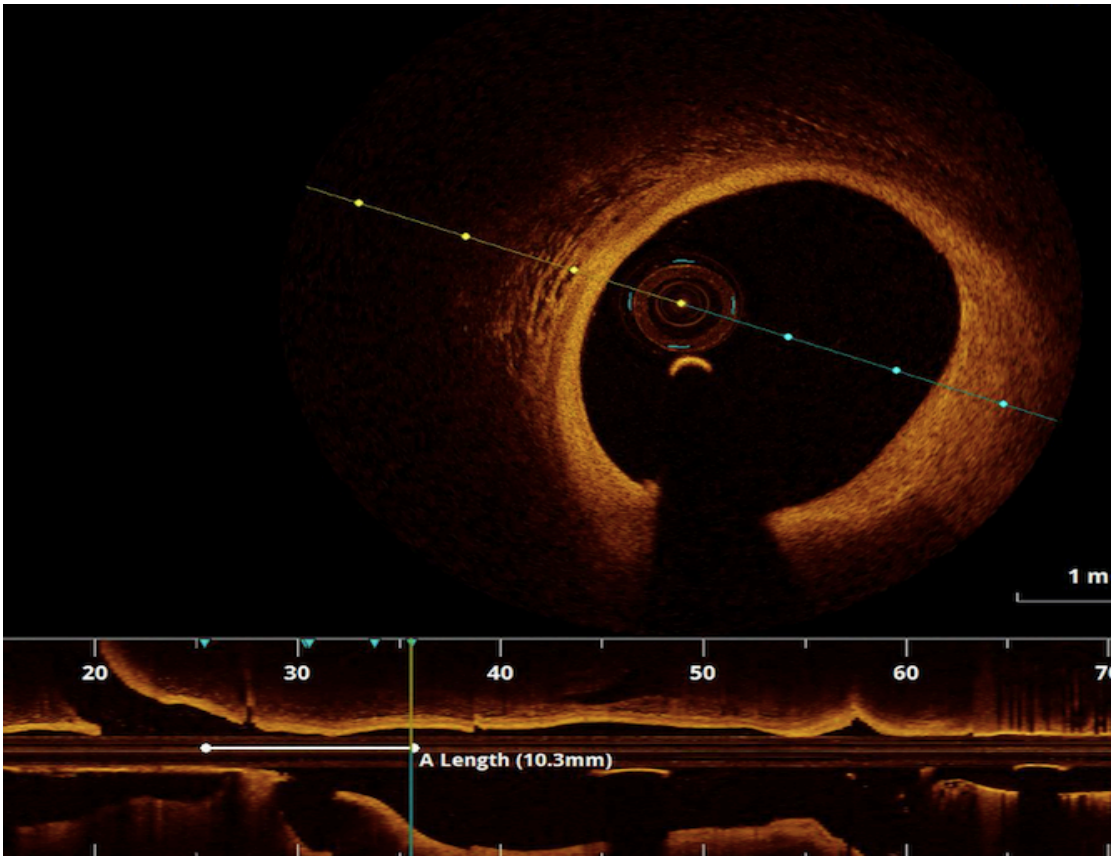

Figure 38: Assessment of lesion length

	RFC (n=23)	IFC (n=15)	P value
6 months			
MACCE	1 (4.35%)	1 (6.67%)	1.00
Death	1 (4.35%)	0	0.6
Cardiac	0	0	1.00
Non-cardiac	0	0	1.00
Reinfarction	0	0	1.00
Stroke	0	1 (6.67%)	0.39
Stent thrombosis	0	0	1.00
Target vessel revascularisation	0	0	1.00
12 months			
MACCE	1 (4.35%)	1 (6.67%)	1.00
Death	1 (4.35%)	0	0.6
Cardiac	0	0	1.00
Non-cardiac	0	0	1.00
Reinfarction	0	0	1.00
Stroke	0	1 (6.67%)	0.39
Stent thrombosis	0	0	1.00
Target vessel revascularisation	0	0	1.00

Table 12: Clinical outcomes

Values are n (%). MACCE – major adverse cardiac and cerebrovascular event

Chapter 4: Cytokine results

4.1 Cytokine analysis

The next stage of our study was to identify cytokines that were differentially expressed between RFC and IFC cases. Cytokine arrays on all the coronary and peripheral samples were performed, yielding mean spot pixel densities, which were then analysed. The SAM analysis was conducted for coronary and peripheral blood samples separately to determine preferential expression. Just under 40.2% (41/102) of cytokines were more highly expressed on average (only two cytokines demonstrating significantly higher expression (see below)) in IFC cases than in RFC cases for both coronary and peripheral samples. By contrast, 47.1% (48/102) were more highly expressed on average (10 cytokines demonstrating significantly higher expression (see below)) in RFC patients than in IFC patients for both coronary and peripheral samples (Figures 39 and 40). For the remaining cytokines (12.7% [13/102]), preferential expression was discordant between coronary and peripheral samples (Figures 39 and 40).

Overall, there was high concordance of cytokines between coronary and peripheral samples (odds ratio = 46.03 [95% CI: 13.33 to 198.59], $p < 0.001$) (Figure 40).

The SAM methodology was also conducted to identify cytokines in each plaque morphology group that were differentially expressed between coronary and peripheral samples (Table 13). Within RFC cases, nine cytokines were more highly expressed in coronary samples and 11 in peripheral samples. Within IFC cases, 21 cytokines were each expressed in both the coronary and peripheral circulations. Within the coronary samples, three cytokines – HGF, FGF-7 and IL-19 – were expressed in both the RFC and IFC groups. Similarly, within the peripheral samples, two cytokines – MIG and MIP-3α – were expressed in both the RFC and IFC groups.

Epidermal growth factor (EGF) and thrombospondin-1 (TSP-1) were the only cytokines with significantly higher expression in IFC cases than in RFC cases in both coronary and peripheral samples (adjusted $p < 0.05$) (Figure 41). The average $\log_2$ fold change in expression was greater than 1.75 for both (Figure 41).

By contrast, 10 cytokines demonstrated significant preferential expression in patients with RFC for both coronary and peripheral samples, including MIG, I-TAC, MMP-9, aggrecan, lipocalin-2, IL-18/BPα, TFF3, complement factor D, RANTES and adiponectin (adjusted $p < 0.05$) (Table 14).

The full list of cytokines demonstrating preferential expression with associated q-values, d-score and log fold changes are listed in sections 4.0 and 5.0 of the Appendix.

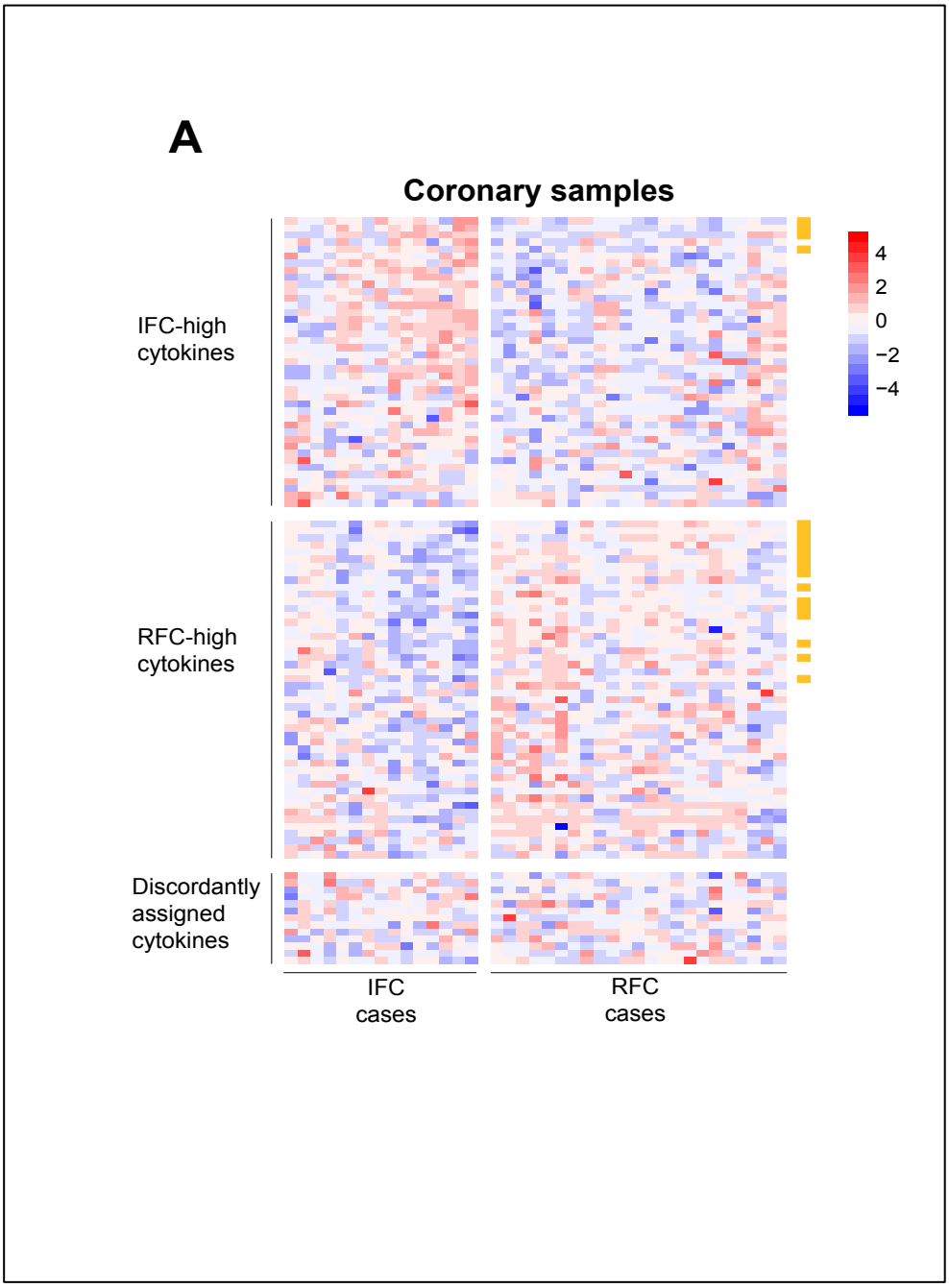

Figure 39: Heatmaps of the cytokines differentially expressed between the two plaque pathologies within coronary samples. Samples (columns) are sorted from left to right in ascending order within the IFC (left-hand panels) and RFC (right-hand panels) case groups. The cytokines (rows) are ordered from top to bottom by descending average fold change within the IFC-assigned cytokine group (top panels), the RFC-assigned group (middle panels) and the discordantly assigned group (bottom panels). Heatmap colours represent $\log_2$ expression values standardised across the data set. A legend that maps colour to standardised expression value is shown to the side of the heatmaps. The gold bars on the side of each heatmap indicate significant hits.

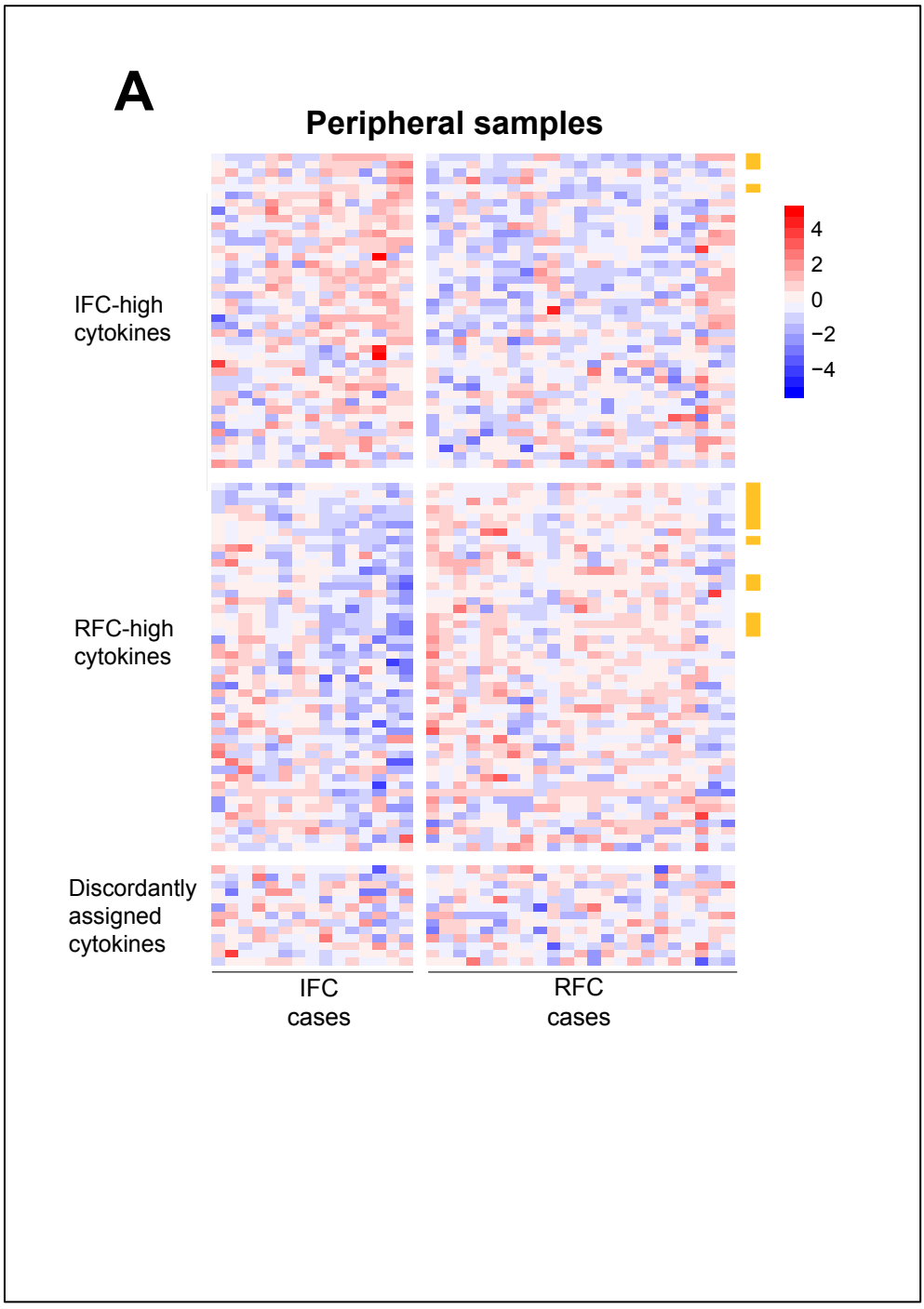

Figure 40: Heatmaps of the cytokines differentially expressed between the two plaque pathologies within peripheral samples as described above

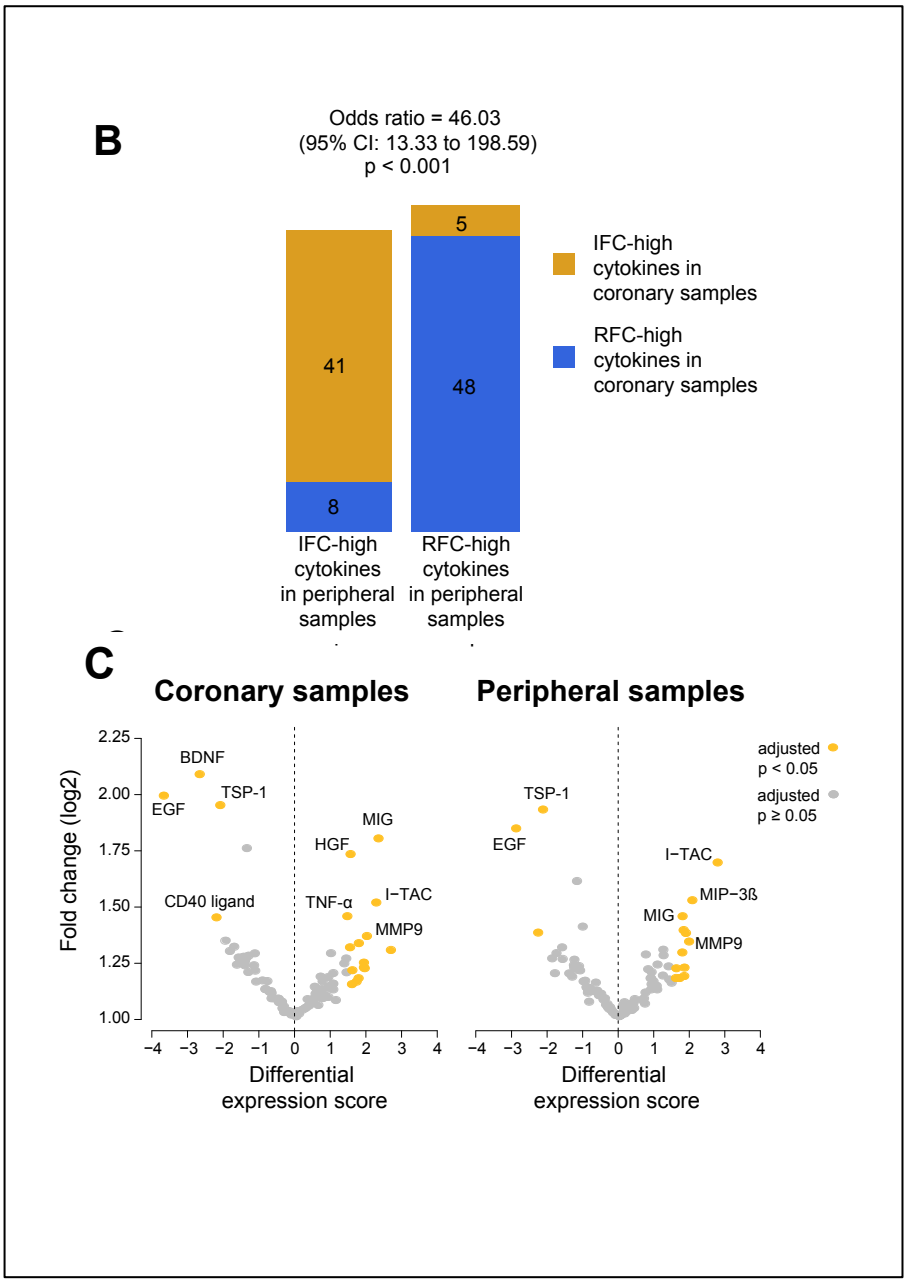

Figure 41: Mosaic plot of concordance between preferential expression assignments for coronary samples (rows) and peripheral samples (columns). Odds ratio, 95% CI and p-value are reported for Fisher's exact test.

Figure 42: C Volcano plots of the $\log_2$ fold change of expression for all cytokines against the SAM differential expression score for the coronary (left plot) and peripheral (right plot) samples. Positive differential expression scores indicate an association to the group more highly expressed in RFC cases than in IFC cases, whereas negative D-scores represent an association to the group more highly expressed in IFC cases. Cytokines that were significantly associated with either plaque type (adjusted p <0.05; SAM) are coloured in gold, whereas non-significant associations are in grey. RFC – ruptured fibrous cap; IFC – intact fibrous cap.

Coronary RFC	Peripheral RFC	Coronary IFC	Peripheral IFC
HGF	MIG	HGF	MIG
FGF-7	IP-10	FGF-7	BDNF
IL-1ra	Leptin	IL-3	IL-8
Growth hormone	MIP-3α	IP-10	RAGE
IL-19	IL-8	IL-1a	Angiopoietin-1
IL-4	BAFF	Fas ligand	Flt-3 ligand
uPAR	ST2	IL-2	G-CSF
TARC	TFF3	GM-CSF	Adiponectin
ICAM-1	Resistin	Complement factor D	IL-1ra
	VEGF	FGF basic	MIP-3α
	Relaxin-2	C5a	MCP-1
		EGF	PAI-1
		IL-19	Dkk-1
		IFN-γ	CD147
		TGF-α	PDGF-AA
		Cystatin C	Cripto-1
		PDGF-AB/BB	Chitinase 3-like 1
		IGFBP-3	CD30
		IL-10	DPPIV
		CRP	IL-5

Table 13: Table summarising differential expression analysis between coronary and peripheral samples

This highlights cytokines that are preferentially expressed in the coronary circulation and those that are preferentially expressed in the peripheral circulation when compared against each other.

HGF, FGF-7 and IL-19 were expressed in both the RFC and IFC groups within the coronary samples. MIG and MIP-3α were expressed in both the RFC and IFC groups within the peripheral samples.

4.2 ELISA validation

The cytokine array analysis identified two cytokines (EGF + TSP-1) demonstrating significantly higher expression in IFC cases in both the coronary and peripheral samples. By contrast, ten cytokines (MIG, I-TAC, MMP-9, aggrecan, lipocalin-2, IL-18/BPα, TFF3, complement factor D, RANTES and adiponectin) demonstrated significant preferential expression in RFC cases for both coronary and peripheral samples.

To validate the results of the cytokine array analysis, we performed ELISA on five of these twelve cytokines. We therefore sought to validate higher expressions of EGF and TSP-1 in the IFC group and MIG, I-TAC, MMP-9 within the RFC group. We also performed ELISA on BDNF since it demonstrated preferential expression for IFC within coronary samples and the scientific literature suggesting links to atherosclerosis and endothelial apoptosis (121). The ELISA for MPO was undertaken given the potential relevance to plaque erosion (122). To address the possibility of artefactually higher expression in one set of cases over the other, we additionally selected two cytokines that were not significantly differentially expressed and could, in essence, serve as negative controls: leptin and growth hormone.

None of the negative controls exhibited any significant difference between IFC and RFC cases for both coronary and peripheral samples ($p > 0.05$) (Figures 43, 44 and 45). For EGF, we observed a significantly higher expression in both coronary and peripheral IFC samples as compared with RFC samples ($p < 0.05$) (Figures 43, 44 and 45). By contrast, for TSP-1, a significantly higher expression in IFC patients was only found for coronary samples ($p = 0.0041$). No significant differences were observed for MIG ($p > 0.05$). I-TAC was the only cytokine that was significantly higher in RFC cases, albeit only for coronary samples ($p = 0.042$) (Figures 43, 44, 45 and Table 14).

A full list of the mean spot pixel densities for the cytokine arrays (arbitrary units – AU) and ELISA-calculated mean plasma concentrations (pg/mL or ng/mL) for each

cytokine validated are listed in the Appendix. This includes values for both the coronary and peripheral samples for the cytokine tested and separated into pathological adjudication for array and ELISA.

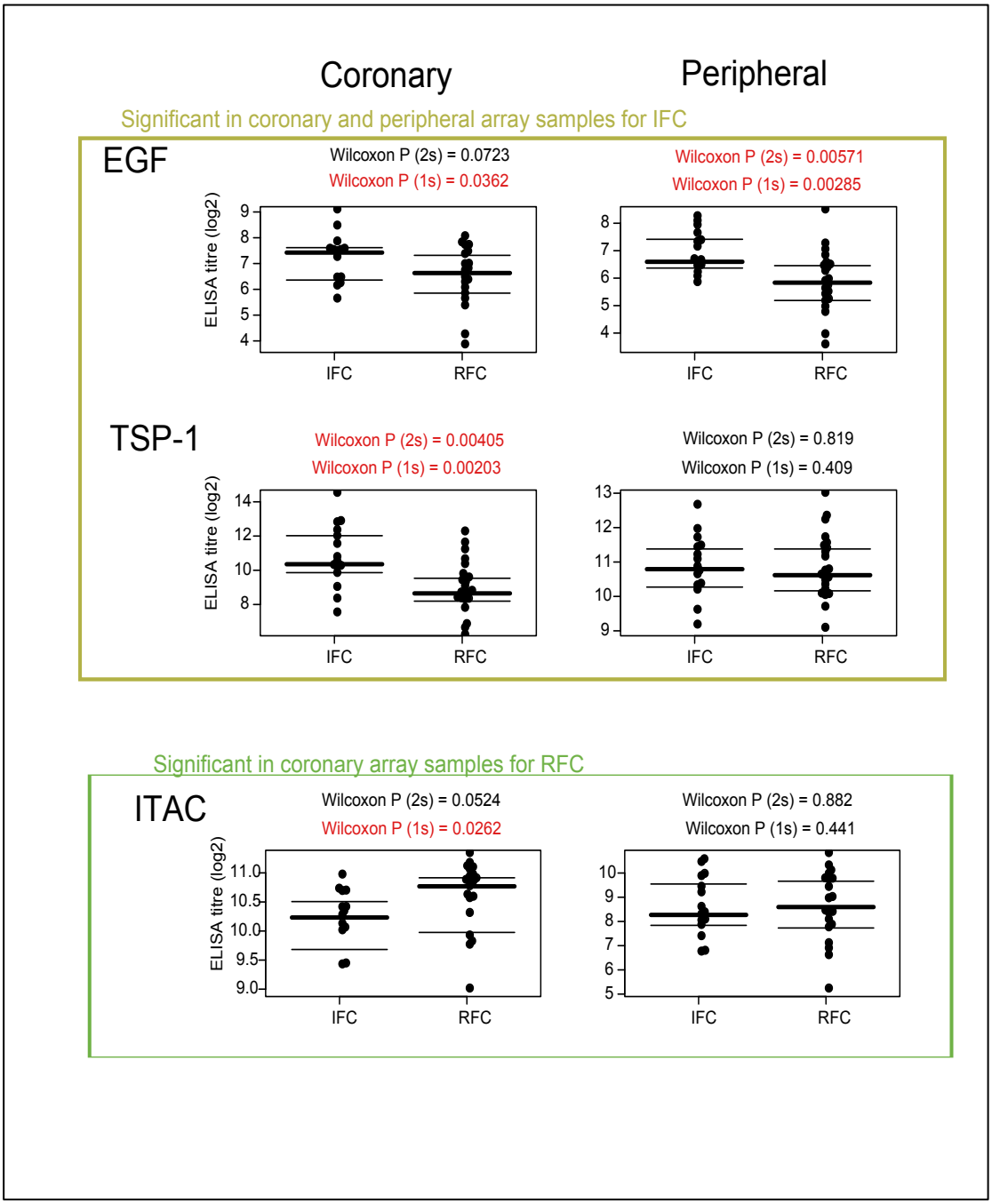

Figure 43: Plasma ELISA analysis

Plasma titres according to plaque pathology and sample site for positively validated ELISAs – EGF, TSP-1 and I-TAC. Horizontal lines indicate median $\log_2$ values and interquartile ranges. Strip plots show the ELISA titre values between IFC and RFC cases for both the coronary and peripheral samples of 11 cytokines. P-values are computed using one-sided and two-sided Wilcoxon rank-sum tests.

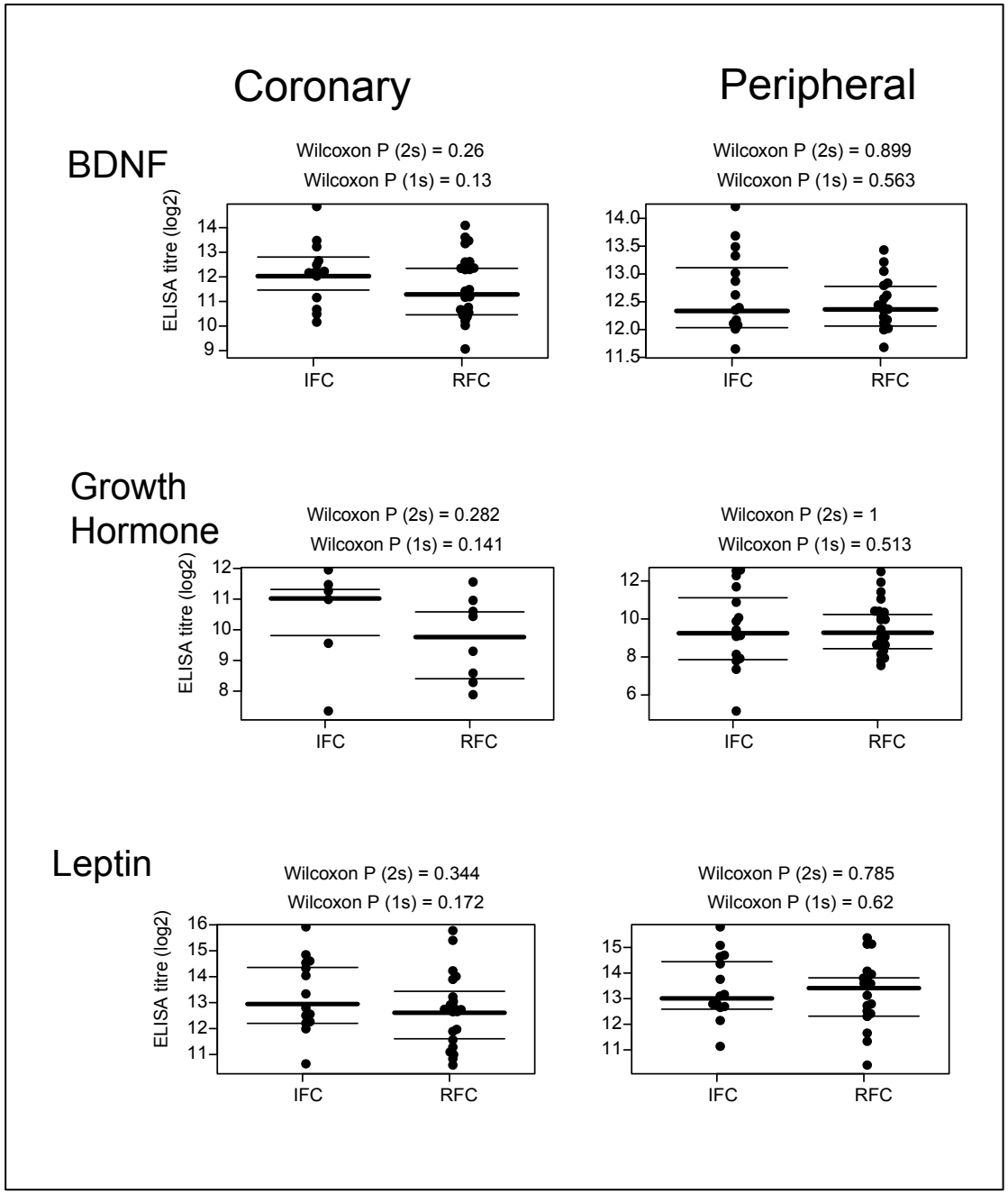

Figure 44: Plasma titres according to plaque pathology and sample site for BDNF, growth hormone and leptin

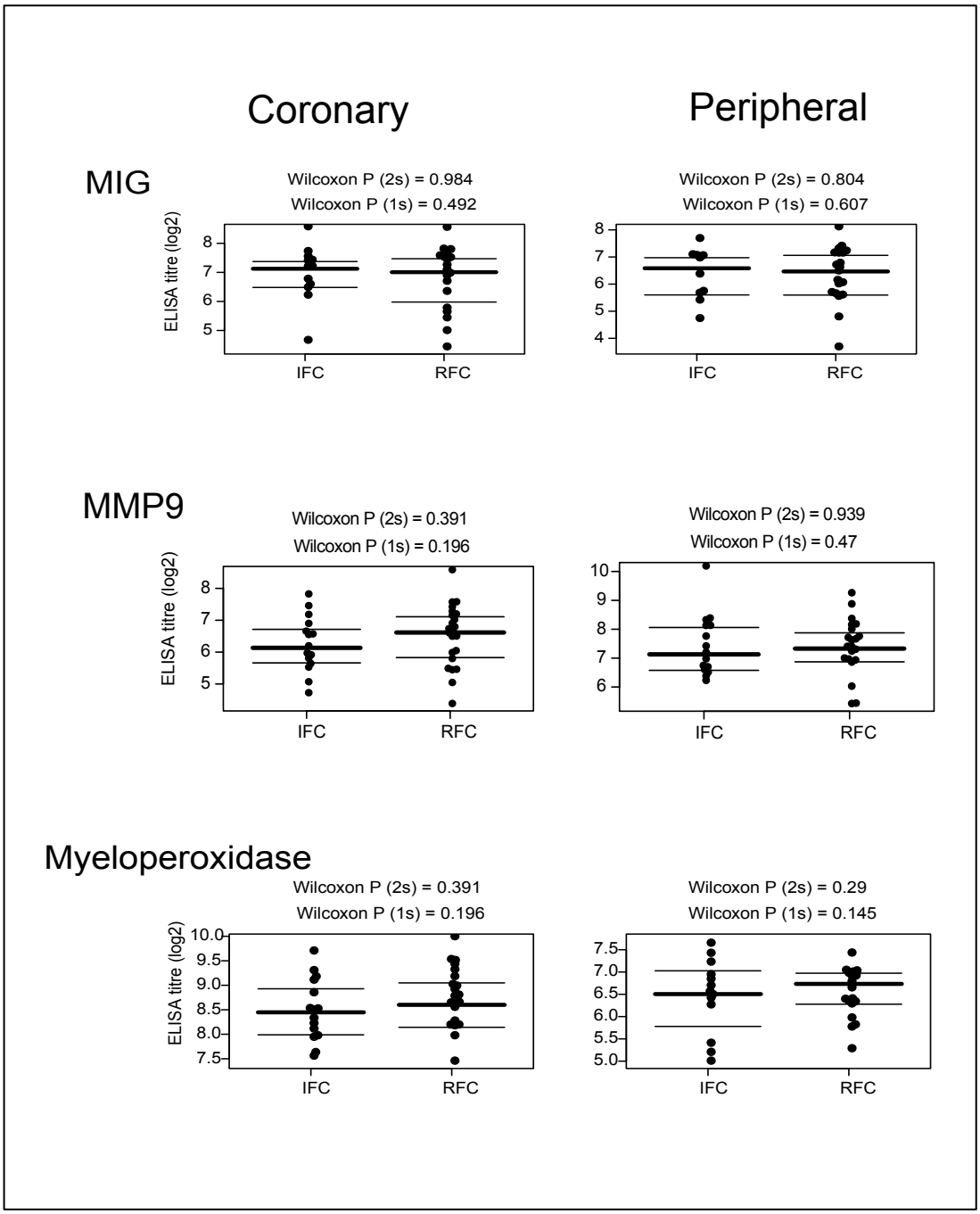

Figure 45: Plasma titres according to plaque pathology and sample site for MIG, MMP-9, myeloperoxidase

Coronary IFC	Coronary RFC	Peripheral IFC	Peripheral RFC
BDNF	MIG	EGF	I-TAC
EGF	I-TAC	TSP-1	MIP-3α
TSP-1	MMP-9	CD40 ligand	MIG
ENA-78	Aggrecan		CD30
	Lipocalin-2		Aggrecan
	IL-18 BPα		MMP-9
	Osteopontin		IL-18 BPα
	TFF3		TFF3
	Complement factor D		Complement factor D
	Chitinase 3-like 1		RANTES
	HGF		Lipocalin-2
	TNF-α		Adiponectin
	FGF-7		
	RANTES		
	Adiponectin		

Table 14: Summary of preferential expression of cytokines in both coronary and peripheral samples for either IFC or RFC from cytokine array analysis

Cytokines highlighted as to whether ELISA validation was significant or not.

RED = Significant in ELISA

BLUE = Non-significant in ELISA

Black = Not tested by ELISA

4.3 Thrombectomy RT-PCR analysis

Thrombectomy yielded analysable samples in 18 RFC and 13 IFC cases. Expression of I-TAC mRNA was significantly increased in RFC samples compared to IFC (p = 0.001), while the opposite was true of EGF expression (p = 0.0264). There were no differences in the expression of TSP-1 (p = 0.6505) or MPO (p = 0.2978) between groups (Figure 46). A full list of the dCT values of mRNA specimens normalised to GADPH or β actin are listed in the Appendix (section 9.0, Table 22).

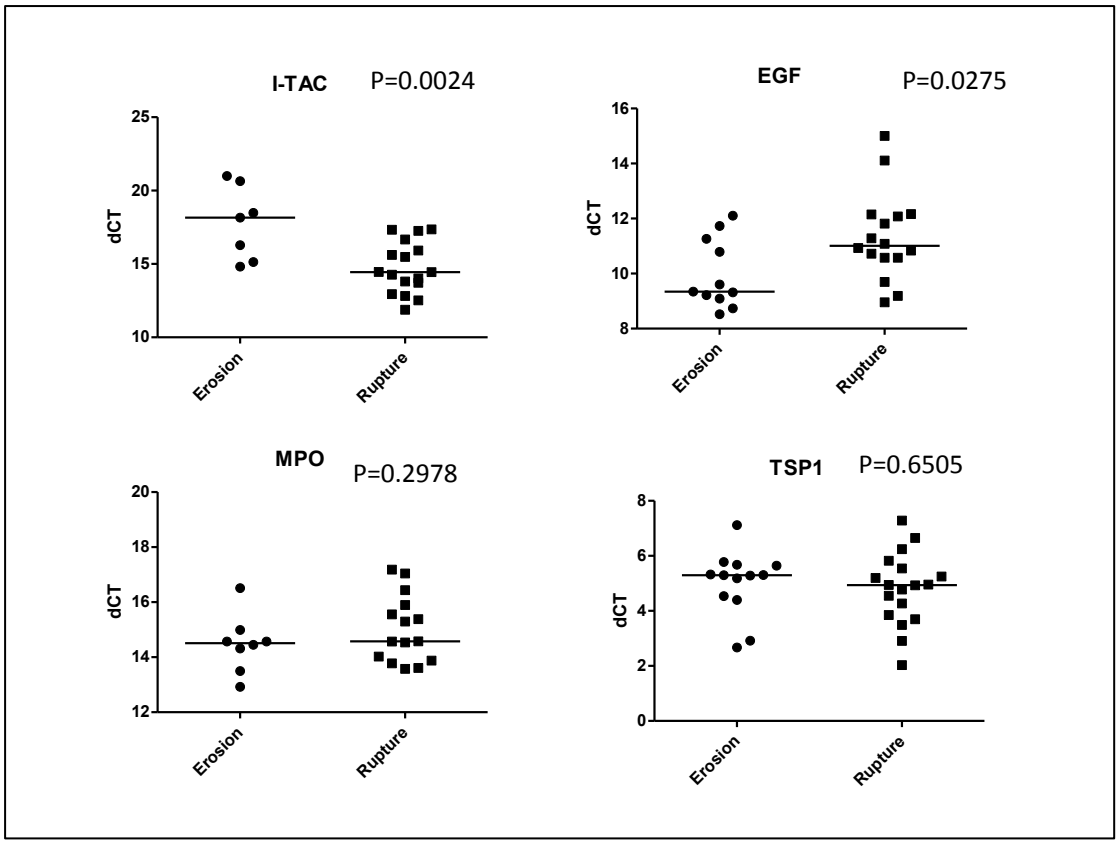

Figure 46: Relative mRNA expression in coronary thrombectomy specimens normalised to GAPDH Lower dCT values indicate higher expression. dCT – delta cycle threshold.

Chapter 5: Discussion

5.1 Principal findings

The principal findings from our study are:

1) An IFC was present in the culprit lesion in fifteen patients (38%) of the 40 cases of STEMI recruited to the PEPS study.
2) Cytokine array data demonstrated 12 (12%) cytokines whose expression differed significantly between IFC and RFC. Two cytokines were preferentially expressed in IFC and 10 cytokines in RFC.
3) We confirmed elevated EGF (coronary and peripheral samples) and TSP-1 (coronary samples) in IFC, and elevated I-TAC (coronary samples) in RFC using ELISAs.
4) These findings were replicated, with the exception of TSP-1, in the analysis of mRNA for EGF, I-TAC and TSP-1 expression from thrombectomy samples.

5.2 Feasibility of the study

An important objective was to demonstrate the utility and feasibility of our methodology. We targeted patients presenting with short ischaemic times in order to reflect the inflammatory process at the onset of the myocardial infarction and minimise the impact of secondary inflammatory changes.

We successfully recruited our target of 40 patients to the study with no complications from performing OCT or delay in treatment as a result. Indeed, as a result of the patients being included in the PEPS study, OCT was frequently used as a further adjunct for PPCI to help size the vessel and therefore appropriately select the required balloon or stent.

5.3 Clinical characteristics

5.3.1 Baseline characteristics

In our study, the incidence of IFC was 38%, while RFC was observed in 58%. These findings are consistent with post mortem data and other OCT studies (16,21,123),

which have previously described approximately two-thirds of cases of coronary thrombosis in STEMI patients due to plaque rupture and one-third secondary to plaque erosion. However, a recent study by Kajander et al. (124) evaluated 93 patients undergoing OCT and thrombectomy as part of a prospective sub-study of the TOTAL (ThrOmbecTomy versus PCI ALone) trial. Culprit lesion morphology was assessable by OCT in 70/93 cases (75.3%). IFC was found in 31 (44.3%) patients, RFC in 34 (48.6%) and calcified nodule in five (7.1%). This suggests that the incidence of IFC is higher than previously reported.

We found no differences in sex between the two groups, although autopsy studies have previously suggested that plaque erosion occurs more frequently in women than in men (21,23,125).

We did find a statistical difference in age between the two groups, with patients in the IFC group being younger than those in the RFC group (RFC median age – 65years, IFC median age – 60 years, p = 0.03). Studies by Arbustini et al. (average age 68 years in plaque rupture cases and 70 years in plaque erosion) (125) and Sato et al. (average age 70 years in plaque rupture cases and 68 years in plaque erosion) (84) describe similar age profiles to our study, with no significant difference in age between the two groups. Farb et al. (23) studied 50 cases of sudden cardiac death due to coronary artery thrombosis. The mean ages of men and women were similar (49 ± 9 and 49 ± 13 years, respectively). They found the mean age at death was 53 ± 10 years in plaque rupture cases versus 44 ± 7 years in eroded plaques without rupture (P = 0.02). Burke et al. (126) examined 51 cases of sudden coronary death in women. They also found an increased proportion of erosions responsible for coronary thrombotic events for women less than 50 years old (58 ± 12 years in plaque rupture cases and 45 ± 8 years in plaque erosion (p = 0.01)). Although both of these studies describe a younger cohort of patients compared to our study, the high proportion of erosions in premenopausal women might be due to an active process precipitated by the effects of oestrogen and progesterone.

It should also be noted that the median ischaemic times were well below the cut-off of six hours, and there were no significant differences between the two groups, therefore fulfilling our aim of recruiting patients as early as possible.

There were no significant differences between the groups with regard to baseline echo and blood test characteristics.

5.3.2 Angiographic characteristics

There were no significant differences found in angiographic and procedural characteristics between the RFC and IFC groups.

In almost every case, only the culprit artery was treated, with only one case of a second artery treated in the RFC group. The RCA was the most commonly treated artery in the RFC group and the LAD in the IFC group.

Thrombectomy was performed in every patient in order to obtain a coronary sample from the vicinity of the culprit plaque and was a key requirement for satisfying entry into the study. Thrombectomy also served as a therapeutic strategy to mechanically dislodge the thrombus and re-establish TIMI 3 flow.

Although we did not find any significant differences in the number of stents implanted per patient or stent length between the two groups, the results did suggest a lower use of stents in the IFC group. This would corroborate the findings from the studies by Prati et al. (91) and Souteyrand et al. (127), who respectively suggested an alternative treatment strategy for OCT-verified IFC in which non-obstructive lesions might be managed without stenting and that un-stented IFC plaques showed features suggesting partial incorporation of the deepest layers of thrombus in the plaque. The potential to avoid stent deployment in this group of patients could reflect the theory that luminal thrombosis in plaque erosion is secondary to apoptosis or endothelial degradation. Treatment with anti-platelet drugs may allow healing of the endothelial layer and therefore avoid the requirement for stents, reducing the risks of both early and late complications associated with stent implantation. Jia et al. (110) also demonstrated that, in ACS patients identified with plaque erosion using OCT, thrombus removal without stent implantation and effective anti-thrombotic therapy may be sufficient to restore coronary artery patency and allow healing of the endothelial layer. They also demonstrated a reduction in thrombus volume and an increase in minimal flow area with antithrombotic therapy alone. Possible explanations for the rationale behind the alternative treatment strategies can be

explained by the distinctive pathophysiology of plaque erosion compared to plaque rupture.

Eroded plaques do not contain a large necrotic core but exhibit a proteoglycan-rich matrix and smooth muscle cells, which have less tissue factor and inflammation (macrophages and C-reactive protein), resulting in lower local thrombogenicity (84,85).

The stenosis of a coronary artery lumen may not always be significant in eroded plaques. Farb et al. (23) demonstrated that plaque rupture was associated with an average area stenosis of 77%, whereas plaque erosion had an average 70% area stenosis ($p < 0.03$) in the coronary arteries of post mortem sudden cardiac death patients. Kramer et al. (85) studied coronary lesions with thrombi (ruptures, n=65; erosions, n=50) from 111 sudden cardiac death victims. They demonstrated that plaque erosion (60%) had a higher incidence of <75% area stenosis when compared with plaque rupture (35.4%) ($p = 0.02$). Saia et al. (87), studied 140 STEMI patients with OCT of the IRA before PCI. They described an IFC presenting more frequently with a patent IRA when compared to an RFC (56.2% vs. 34.9%; $p = 0.047$).

Kajander et al. (124) used OCT to compare stenosis severity between STEMI culprit lesions with IFC and those with RFC. They found contrasting results. Following thrombectomy, OCT demonstrated similar lumen area stenosis in IFC (79.3%) and PR (79.6%) ($p = 0.88$). Lumen area stenosis <50% was observed in none of the patients with RFC and in one patient with IFC.

In our study, we were unable to demonstrate a difference between minimal luminal diameter and diameter stenosis using QCA or OCT analysis between the RFC and IFC groups.

It is also worth mentioning that drug-coated balloons were used in some cases, instead of stents. This is primarily attributable to the preferred strategy of a specific interventionalist with the principle of trying to avoid the potential early and late sequelae of stent deployment.

5.3.3 OCT data

OCT analysis revealed residual thrombus in the majority of cases, with no significant differences between the two groups. The thrombus types were also similar between the groups, with white thrombus the most common in both groups. This contrasts with the findings in other studies (87,102). Saia et al. (87) demonstrated in their study of 140 patients that IFC had residual thrombus less frequently compared to RFC before stent implantation (84.4% vs. 98.4%; p = 0.016). There was a significant difference in the presence of white thrombus between IFC and RFC (78.1% vs. 98.4%; p = 0.002). Niccoli et al. (102) also demonstrated a significant difference between residual thrombus across IFC and RFC (56.1% vs. 75.6%; p = 0.05). In addition, there was a significant difference in the presence of white thrombus (96.6% vs. 29.2%) and red thrombus (3.4% vs .70.8%) between IFC and RFC (p <0.001).

We found that the predominant plaque characteristic of both groups was lipid-rich, with 40% of the IFC cases also having a fibrous plaque phenotype. This would be in keeping with the thick fibrous cap model for plaque erosion and the lipid core representative of plaque rupture. We found differences for minimum and mean cap thicknesses between the two groups, with RFC having significantly smaller measurements.

Some of these findings are consistent with the studies mentioned above, which also looked at plaque characteristics in their analysis (87, 102). Saia et al. (87) found that IFC had fewer lipid areas (75% vs. 100%; p <0.001) and more fibrotic areas (25.0% vs. 0.0%; p = 0.005) at the culprit site. They also found that RFC had a smaller mean fibrous cap thickness (171 μm vs. 203 μm; p = 0.002) and a minimal fibrous cap thickness (47 μm vs. 69 μm; p = 0.02). Niccoli et al. (102) found that patients with RFC had a lipid-rich plaque at the culprit lesion (70 (85.4%) vs. 31 (71.9%), p = 0.001) compared with IFC patients. They also found that patients with RFC had a significantly thinner fibrous cap (76.2 μm vs. 87.0 μm; p = 0.04).

Kajander et al. (124) compared plaque content between IFC and RFC in STEMI patients. They found that IFC had fewer quadrants with lipid plaque compared to RFC (28.16 vs. 39.12; p = 0.004). However, in both lesion types, lipid was the predominant plaque type (83.9% vs. 63.7% of diseased quadrants). They also found

the minimal fibrous cap thickness to be significantly less in RFC (62.05 μm vs 91.03 μm; p <0.001).

5.3.4 Clinical outcomes

Clinical follow-up data revealed only one transient ischaemic attack and one death in our cohort of 40 patients. Our small data set and limited follow-up time makes it difficult to draw meaningful conclusions about long-term differences between the two groups, which is also alluded to in other studies (102,103).

Niccoli et al. (102) followed up 139 ACS patients over an approximate three-year period. Eighty-two patients (59%) were categorised as having RFC and the remaining 37 (41%) patients with IFC. MACCE occurred more frequently in patients with RFC compared with those having IFC (39.0 vs. 14.0%; p <0.001).

Yonetsu et al. (103) also sought to evaluate the morphological features and clinical outcomes of patients with ACS caused by lesions with RFC and IFC. 318 patients with ACS underwent OCT before PCI. Culprit lesions were categorised into 141 RFCs and 131 IFCs, with 46 in an undefined group. 307 patients were followed for a median follow-up duration of 576 days. Adverse cardiac events were observed in 93 patients (30.3%). Kaplan–Meier analysis demonstrated a significantly lower event rate in the IFC group compared with the RFC and undefined groups.

Kajander et al. (124) showed a low MACCE rate in their OCT analysable data of 70 patients and no difference between RFC and IFC (0 vs. 2, p = 0.22). There were two cases of recurrent myocardial infarction, which were in the IFC group.

There were no complications arising from the OCT procedure in our study, further highlighting the safety of this procedure.

5.4 Cytokine analysis

An important objective of our study was to explore whether there was a difference in the expression of cytokines between the RFC and IFC groups in STEMI patients. Using our novel methodology and proteomic arrays, we were able to identify a number of cytokines displaying preferential expression for RFC and IFC within both the coronary and peripheral circulation. We selected BDNF, MMP-9, MIG, EGF,

TSP-1 and I-TAC for ELISA validation based on a combination of the strength of the log fold changes from the array analysis and background literature proposing a likely causative role.

We confirmed elevated EGF and TSP-1 in IFC and elevated I-TAC in RFC using ELISAs. To put our results in context, the levels of EGF, TSP-1, I-TAC in IFC are approximately 14, 4.8, and 1.6 times higher, respectively, compared to median values in healthy volunteers reported in other studies (128–130). The values for RFC are approximately 8, 1.4 and 2.4 times higher, respectively.

These observations could be interpreted as reflecting primary differences between the two different atherosclerotic pathologies or could simply reflect a secondary response to myocardial infarction.

5.4.1 Positively validated ELISAs

5.4.1.1 Epidermal growth factor (EGF)

EGF is a common mitogenic growth factor that stimulates cell growth, proliferation and differentiation by binding to its receptor, EGFR, which in turn initiates intracellular signalling (131). The EGFR is widely studied in cancer biology, with EGFR antagonism by antibodies and receptor inhibitors having had numerous beneficial effects in patients with non-small-cell lung, colorectal and pancreatic cancers (132,133).

Vascular remodelling plays a key role in the development of atherosclerosis and involves hypertrophy, hyperplasia, migration and phenotypic alterations of vascular smooth muscle cells (VSMCs). There is strong evidence that EGFR is critical in mediating vascular remodelling. All members of EGFR, as well as most of their ligands, are expressed by VSMCs (134).

EGF is an SMC antigen, the effects of which can be enhanced by TGF-β, angiotensin II and IGF-1, and inhibited by HDL (135). EGF stimulation of the EGFR in VSMCs activates the mitogen-activated protein kinase (MAPK) pathway, and inhibits angiotensin II action (136). Although platelets are a putative source of EGF during atherogenesis, they lack protein biosynthetic capability, and are involved late in the atherogenic process. It is possible that EGF is synthesised in megakaryocytes and

stored in platelets, or that EGF is derived from some other source and is subsequently taken up by platelets (137).

Studies have demonstrated the abolition of EGFR in vascular smooth muscle to be beneficial in treating animal models of hypertension and atherosclerosis (138).

A study by Kagiyama et al. investigated the role of EGFR in hypertensive rats (139). They showed that antisense directed to EGFR demonstrated suppression of left ventricular hypertrophy in hypertensive rats infused with angiotensin II. This implies that EGFR plays a critical role in the development of LVH induced by angiotensin II.

Chan et al. investigated the role of EGFR in an animal model of atherosclerosis (140). They induced arterial intimal hyperplasia in rat carotid arteries by the passage of a balloon catheter into the vessel. The animals were given a monoclonal blocking antibody to EGFR. Blocking the EGFR antibody inhibited medial SMC proliferation, indicating that activation of EGFR is important for induction of SMC proliferation and subsequent intimal thickening.

Other observations have also suggested a potential role for EGFR signalling in atherosclerosis. The expression of the EGFR and its ligands (heparin-binding EGF (HB-EGF), betacellulin (BTC) and epiregulin (EREG)) are elevated in the vascular lesions of humans with atherosclerosis (137). In addition to vascular cells, infiltrating monocytes and macrophages are another important source of EGF-like ligands in atherosclerosis (137). Furthermore, plasma levels of HB-EGF are increased in patients with coronary artery disease and correlate with serum cholesterol (141).

Increased EGF expression in IFC could be an important stimulus for VSMC proliferation and maintenance of a thick fibrous cap. Rattik et al. aimed to investigate whether plasma levels of EGF, heparin-binding EGF (HB-EGF) and platelet-derived growth factor correlated with plaque phenotype and incidence of acute coronary events (142). HB-EGF, EGF and platelet-derived growth factor were measured in plasma from 202 patients undergoing carotid endarterectomy and in 384 acute coronary event cases and 409 matched controls recruited from the Malmö Diet and Cancer cohort. Significant positive associations were found between the plasma levels of all three growth factors and the collagen and elastin contents of the removed plaques from the carotid arteries, indicating an association with a more fibrous phenotype in carotid arteries. Acute coronary event cases had lower levels of HB-

EGF in plasma, whereas no significant differences were found for EGF and platelet-derived growth factor. These findings suggest a clinically important role for smooth muscle cell growth factors in plaque stabilisation and protection against development of acute coronary events. We demonstrated significant expression of EGF in patients with IFC in both the coronary and peripheral samples. Our findings could also be consistent with EGF as a marker of a more fibrous thick-capped plaque. It is also plausible that elevated plasma levels of EGF may simply reflect release from granules of activated platelet.

5.4.1.2 Thrombospondin-1 (TSP-1)

The TSP family consists of five multidomain calcium-binding glycoproteins that act as regulators of cell–cell and cell–matrix associations (143). TSP-1 is a potent endogenous inhibitor of angiogenesis, and is expressed in endothelial cells, VSMC, vascular fibroblasts and platelets. Plasma concentration is low but is increased rapidly by the release of stored TSP-1 from platelet α-granules following platelet activation.

TSP-1 has many modulatory effects on endothelial cell adhesion, motility, growth and apoptosis. It has been shown to inhibit the formation of focal adhesions by endothelial cells and disrupts endothelial cell focal adhesions, leading to cell detachment in vitro (144). TSP-1 inhibits endothelial cell proliferation (145) and can induce cellular quiescence (146) or apoptosis via CD36 signalling (147,148). Inhibitory effects on endothelial progenitor cell angiogenesis have also been described (149).

TSP-1 inhibits NO production by endothelial cells by indirect inhibition of eNOS: this is mediated by disrupting the interaction of CD47 with vascular endothelial growth factor receptor 2 (VEGFR2), which reduces calmodulin-mediated activation of eNOS due to altered calcium transients (150). Reduced NO may contribute to endothelial dysfunction, impaired vasodilatation and a predisposition to vasospasm.

In contrast to the effects on endothelial cells, TSP-1 enhances the proliferation and migration of vascular smooth muscle cells (151,152). VSMC proliferation in response to balloon angioplasty appears to be TSP-1 dependent and can be blocked by antibodies to CD47 and $\alpha_{IIb}\beta$ integrins (153–155).

TSP-1 also inhibits NO-stimulated activation of guanylyl cyclase in vascular smooth muscle cells, resulting in reduced cGMP levels and impaired vasodilatation. This is mediated via CD47 signalling (156).

TSP-1 constitutes one-third of the protein in platelet α-granules, and is released during platelet activation. Although it is not essential for thrombosis, it plays an important role in potentiating platelet activation and stabilisation of platelet thrombi in high shear stress (157,158).

There are, therefore, multiple aspects of atherosclerosis that could be explained by the effects of TSP-1 through inflammation, thrombosis, inhibition of angiogenesis, cell apoptosis, inhibition of nitric oxide and vasoconstriction.

Genetic association studies have reported a variable association of myocardial infarction with polymorphisms of TSP-1, TSP-2 and TSP-4. A meta-analysis of 13 studies involving 10,801 cases and 9,381 controls confirmed an association of the THBS-1 N700S polymorphism with coronary artery disease (heterozygote model: Odds Ratio (OR) = 1.14, 95% CI: 1.03-1.26; dominant model: OR = 1.13, 95% CI: 1.00-1.29) (159). This study, however, did not distinguish between plaque erosion and rupture. A separate study of sudden death patients suggested that a single nucleotide polymorphism of the TSP-2 gene was decreased in plaque erosion compared to other forms of coronary artery disease (160).

The literature, in addition to our demonstration of preferential expression of TSP-1 in the IFC group in the coronary sample, supports the theory that there is a potential relationship between TSP-1 and plaque erosion.

5.4.1.3 Interferon-inducible T-cell alpha chemoattractant (I-TAC)

Array analysis confirmed that multiple cytokines that are known to be important in plaque rupture were preferentially expressed in the RFC group. These included MIG, I-TAC, MMP-9, aggrecan, lipocalin-2, IL-18/BPα, TFF3, complement factor D, RANTES and adiponectin. It was not feasible to validate all of these cytokines with ELISA due to lack of sample and expense. We performed ELISAs on MIG, I-TAC and MMP-9. ELISA validation demonstrated the novel observation that I-TAC was the only cytokine that was significantly higher in coronary samples in RFC cases.

I-TAC is a chemokine that is significantly increased in response to interferon-γ and exclusively uses CXC chemokine receptor 3 (CXCR3) (161). Activated T-lymphocytes accumulate early in atheroma formation and persist at sites of lesion growth and rupture, suggesting that they play an important role in the pathogenesis of atherosclerosis and plaque rupture (162). Studies have shown that I-TAC plays a key role in the recruitment and retention of activated T lymphocytes observed at sites of inflammation during atherogenesis (51). A study by Mach et al. (51) demonstrated increased expression of I-TAC by endothelial cells and macrophages within human atherosclerotic lesions in situ.

A study by Kao et al. looked at CXCR3 chemokines as causative factors in transplant coronary artery disease (TCAD). Levels of I-TAC were found to be elevated in patients with severe TCAD compared with long-term survivors of transplantation without TCAD and with healthy volunteers who had not undergone transplantation (130). This supports our finding that I-TAC has a role in atherosclerotic heart disease.

A study by Saxena et al. looked at the possible anti-fibrotic role of CXCR3 signalling in myocardial infarction (163). They found that in reperfused mouse infarcts, expression of CXCL9 and CXC11/I-TAC was extremely low. Low levels of both of these CXCR3 ligands did not affect the scar size, geometric ventricular modelling, collagen deposition or systolic dysfunction of the infarcted heart. They did, however, find that the other ligand of CXCR3, CXCL10, was markedly induced in infarcted myocardium. CXCL10 is known to limit cardiac fibrosis by inhibiting growth-factor-mediated fibroblast migration. Their findings suggest that CXCR3 signalling does not critically regulate cardiac remodelling and dysfunction following myocardial infarction, and the anti-fibrotic effects of CXCL10 in the healing infarct are CXCR3 independent.

5.4.2 Negatively validated ELISAs

5.4.2.1 Brain-derived neurotropic factor (BDNF)

Brain-derived neurotrophic factor is a member of the neurotrophin family of proteins and has a favourable neuroprotective effect against oxygen-glucose deprivation (164). It is well recognised that BDNF specifically binds to the tropomyosin-related

kinase receptor B (TrkB) and further modulates downstream intracellular signalling pathways, thereby affecting the development and function of the nervous system (165). Endothelial cells lining the arteries and capillaries of the heart muscle also express BDNF and its receptor TrkB (166). Studies have reported that increased levels of exogenous and endogenous BDNF confer a protective effect on cerebral ischaemia (167). These concepts have extended the roles of BDNF to atherosclerosis and ischaemic heart disease. A study by Okada et al. reported that upregulation of BDNF protected against cardiac dysfunction post MI (168), while other studies have demonstrated that advanced atherosclerosis displays reduced circulating BDNF levels (121) and proposed that reduced BDNF levels improve post-MI survival and reduce left ventricular remodelling by attenuating inflammation and angiogenesis (169).

It would, therefore, seem very reasonable to expect BDNF to have a role in the aetiology of ischaemic heart disease and specifically plaque erosion. We know that BDNF is expressed in the endothelium of coronary arteries and deficient levels have been proposed as a mechanism of endothelial apoptosis (170). Although our cytokine array analysis demonstrated preferential expression of BDNF in the IFC group from coronary samples, ELISA did not validate this.

5.4.2.2 Matrix metalloproteinase-9 (MMP-9)

Atherosclerotic plaques contain numerous macrophages, providing a prominent source of matrix metalloproteinases (MMPs). MMPs play a role in the degradation of the extracellular matrix (ECM) resulting in destabilisation of the atherosclerotic plaque.

MMP-9 plays a key role in the degradation of ECM and plaque ruptures are associated with increased MMP-9 proteolytic activity (171). In the plaque, the major source for MMP-9 is macrophage-derived foam cells, and MMP-9 associates with the formation of a vulnerable thin fibrous cap (172). In a study by Gough et al., it was found that, in apolipoprotein E-null mice, MMP-9 levels were highly correlated with incidence of plaque rupture (173). An increase in systemic MMP-9 levels has also been shown to be highly correlated with cardiovascular mortality in patients

with atherosclerosis (174). These findings suggest deleterious effects of MMP-9 overexpression on the progression of atherosclerosis.

Higher MMP-9 levels also play an important role during the early stages of acute MI. MMP-9 levels increase as early as several minutes post MI and remain increased for the first week in many animal models of MI (175,176). The early increases in MMP-9 levels post MI correlate with increased numbers of neutrophils, and later increase at *days 2–4* with the infiltration of macrophages. These changes show an important role of MMP-9 at different stages of the inflammatory response.

Given the extensive evidence base for the role of MMP-9 in atherosclerotic plaque rupture and MI, we sought to validate its expression with ELISA in our study. Cytokine array analysis identified preferential expression of MMP-9 in the RFC group within the coronary samples, but ELISA did not validate this finding. Although our study did not confirm this expression in our cohort of STEMI patients, the literature suggests that MMPs and indeed MMP-9 clearly have a role in atherosclerosis and degradation of the thin fibrous cap. Indeed, MMP levels might not correlate with MMP activity, which might also provide an explanation as to why we did not find elevated levels in our cohort.

Within the original protocol, our initial aim was to analyse the coronary and peripheral samples for expression of more MMPs and analysis of thrombi to identify differences between plaque rupture and erosion.

As described above, there is a substantial body of evidence implicating MMPs in the degradation of the fibrous cap (15) and, therefore, likely that there are differences in the spectrum of MMP expression between rupture and erosion. Unfortunately, due to time constraints, resources and limited samples, we were unable to perform cytokine array screening for more MMPs or histological/immunohistochemistry analysis on our retained samples and coronary thrombi.

5.4.2.3 Monokine induced by gamma interferon (MIG)

Chemokines are a group of small secreted proteins that exert their effects through seven transmembrane-domain G-protein-coupled receptors and are active as chemotactic factors and regulators of cell growth (177).

CXCL9/Mig is an IFN-γ-inducible chemokine produced mainly by dendritic cells, B-lymphocytes and macrophages (178). It perpetuates IFN-γ-producing immune responses by the recruitment of T-cells that selectively express its cognate receptor, CXCR3. IFN-γ is a proatherogenic cytokine that is expressed in arterial plaques (179) and by circulating T-cells in patients with coronary atherosclerosis (180). There are some studies in patients with myocarditis which report that CXCL9 is expressed in the heart during acute infection and remains upregulated in chronic infection (181,182).

Very little is known about the relationship between CXCL9 and coronary artery disease, but, essentially, it plays a role in inflammation; it could, therefore, be postulated that this relationship may have a role in the inflammatory processes involved with plaque rupture. Indeed, CXCL9 was identified by cytokine analysis as showing preferential expression for RFC in the coronary and peripheral samples, suggesting that it may have a systemic role. However, this was not corroborated with the ELISA.

5.4.3 Controls

5.4.3.1 Myeloperoxidase (MPO)

We did not find any association between MPO levels and plaque erosion. This was relatively surprising given previous studies demonstrating a role for MPO in erosion. MPO is an abundant leucocyte enzyme and is released on neutrophil activation. Serum levels of MPO in ACS patients are considered a marker of plaque vulnerability (183). A study by Ferrante et al. (122) showed increased systemic levels of MPO in patients with plaque erosion compared to plaque rupture in a small study of 25 patients with acute coronary syndromes. In addition, the density of MPO-positive cells within thrombi retrieved from sudden death patients was significantly higher in lesions with erosion (n=11) than rupture (n=11). Niccoli et al. looked at 84 patients presenting with ACS and stable angina, followed by OCT of the culprit coronary stenosis. They also found that patients presenting with plaque erosion presented with higher MPO levels (104). However, these findings are discordant with the study by Saia et al. (87). In their study of 140 STEMI patients, culprit plaque morphology was adjudicated in 97 patients. Patients with IFC and RFC had

similar serum inflammatory and platelet biomarkers. Specifically, there was no difference in MPO expression between the two groups.

These discrepancies could reflect differences in the type of acute coronary syndrome, sample sites and timings of samples. The studies above reflect patients with sudden cardiac death, angina and STEMI. Our cohort is a small STEMI population and it might, therefore, be difficult to draw meaningful conclusions regarding the lack of MPO expression.

5.5 Thrombectomy analysis

To confirm and validate the data generated by cytokine array analysis and ELISA, we performed RT-PCR for EGF, TSP-1, I-TAC and MPO on messenger RNA extracted from the thrombectomy specimens. MPO was analysed given the previous literature demonstrating increased levels in plaque erosion cases.

Thrombectomy yielded an analysable sample in 31 out of 38 (two patients were undefined) patient samples. Of these, 18 were RFC cases and 13 IFC. This retrieval of coronary thrombotic aspirate (81.5%) is higher than other studies, which have also sought to study the composition of the thrombus sample, with 72.9% in the TAPAS trial (n=1,080) and 74% in a study by Kramer et al. (n=1,362), respectively (81,184) – although our numbers are much smaller in comparison.

Expression of I-TAC mRNA was significantly increased in RFC samples compared to IFC, while the opposite was true of EGF expression. There were no differences in the expression of TSP-1 or MPO between groups.

Both EGF and TSP-1 are stored in platelet granules (185) and elevated plasma levels could reflect differences in thrombus composition and platelet activation (84,104). This possibility is supported by the concordance of EGF expression in plasma and thrombectomy samples. It is also possible that differences in thrombus type are not responsible for these findings. We did not observe significant differences in thrombus type on OCT, nor did the array analysis identify differences in other platelet-related molecules such as platelet factor 4 or platelet-derived growth factor. The discordance between TSP-1 expression in plasma and thrombectomy samples may, therefore, reflect local expression of TSP-1 within the coronary artery.

Increased I-TAC mRNA in thrombectomy specimens could reflect expression by inflammatory cells trapped in thrombus, or aspirated atherosclerotic material.

Post mortem studies had suggested that coronary thrombi might differ depending on the underlying plaque pathology. In thrombi associated with plaque erosion, platelets were found to be more abundant than fibrin (84), MPO positive cells more numerous (75) and the thrombi were found to be older (>4 days) (85). However, a study of thrombectomy samples from patients undergoing PPCI had failed to confirm these differences (87).

5.6 Coronary versus peripheral circulation

In addition to comparing RFC vs IFC within either the coronary or peripheral samples, we also were able to directly compare the coronary and peripheral circulations, to assess for differential cytokine expression between the two sampling pools.

To reiterate our methodology, peripheral samples were arterial samples taken from the access route, which was almost exclusively the radial arterial sheath, and coronary samples were taken as close to the culprit lesion as possible by thrombectomy of the culprit artery. To be able to compare cytokine expression between two distinct sampling sites provides insight into the factors involved in a more systemic, general process as well as hopefully representing more localised interactions within the heart.

Most studies that have looked to focus more clearly on the coronary vasculature have used selective coronary sinus (CS) catheterisation as a well-established method to reflect the coronary microenvironment (186). Though the venous system of the heart comprises variable anatomical branches, drainage is primarily via the CS into the right atrium (RA). In addition to electrophysiological mapping and pacing, the CS can be cannulated and used to study changes in flow, temperature and, more commonly, blood sampling. Limited studies do suggest that during regional ischaemic injury, sampling of CS blood does appear to define early and accurate measurements of myocardial metabolism in contrast with concomitant peripheral blood samples, which show no change (187).

The factors triggering coronary plaque destabilisation have traditionally been defined by peripheral blood sampling, which has defined a range of indices reflecting pathophysiological processes within the systemic circulation. Investigations using regional CS blood sampling have played an important role in providing a quantitative assessment of the various systems involved in the pathogenesis of ACS, including endogenous platelet activation (188) and thrombogenesis (189).

CS sampling does have disadvantages, with the invasive nature of CS catheterisation carrying a risk of supraventricular arrhythmias and difficulty achieving a stable catheter position. In addition, activation of platelet and thrombin production remains a potential drawback (190). However, obtaining samples from the coronary artery appears to be an attractive alternative in qualifying the local environment, as it can be included in left-heart catheterisation or during PCI without the need for additional right-sided instrumentation.

A study by Ko et al. (191) investigated the presence in STEMI patients of locally increased inflammatory factors in the culprit artery and compared this with samples taken from the peripheral arterial circulation – in this, the femoral artery. They found increased levels of soluble CD40 ligand, IL-6, serotonin, tissue factor and factor VII in the culprit coronary artery compared to those from the femoral artery. This study demonstrated the feasibility of obtaining blood from the coronary artery, similar to our study, by using a thrombectomy catheter and also highlighting differential expression in the coronary circulation confirmed with ELISA.

Studies have also looked at circulating microRNAs (miRs) in transcoronary (between coronary sinus and aorta) settings. MiRs are small non-coding RNAs that control gene expression by binding to target mRNAs, thereby inducing mRNA degradation or repression of protein translation (192). Circulating miRs have been detected in the blood in cases of acute myocardial infarction (AMI) (193), and, specifically, miR-1, miR-133, miR-208a/b and miR-499 are predominantly increased in patients with ACS (194–196). Leistner et al. assessed coronary atherosclerotic plaque burden by OCT in patients with stable angina and measured the levels of circulating miRs across the CS and femoral arterial samples (197). They found that, in patients with a high incidence of TCFAs, there were significantly increased transcoronary gradients (aortic levels subtracted from CS) of miR-126-3p, miR-126-5p and miR-145-5p.

All of these studies indicate alternative methodologies and ways of quantifying transcoronary differences. In our specific study, we identified numerous cytokines in each plaque morphology group from within either the coronary or peripheral circulation. Subsequently, we identified HGF, FGF-7 and IL-19 as shared cytokines expressed in the both the RFC and IFC groups but from within the coronary sample, and, similarly, MIG and MIP-3α from the peripheral circulation. Wykrzykowska et al. also found up-regulation of HGF, FGF-7 and MIG in a pilot study (IBIS-1) undertaken to correlate coronary imaging with circulating biomarker expression in patients with stable angina, unstable angina and AMI (198).

These cytokines were identified by cytokine array analysis, but we did not validate with ELISA due to lack of samples. However, the preliminary identification of these cytokines in the respective coronary and peripheral samples could be justified by their biological roles.

5.6.1 Molecules preferentially expressed in coronary samples

HGF has mitogenic and unique morphoregulatory functions, and is considered to act as a hepatotrophic and a renotrophic factor for regeneration of the liver and kidney subjected to various insults (199). Previous studies have shown that expression of HGF and its receptor, c-Met, are transiently up-regulated in the myocardium of developing hearts in mice (200) and HGF plasma levels are markedly elevated in patients with AMI (201). There is, therefore, evidence to explain why HGF might be locally upregulated in the coronary artery. Further support for higher local expression of HGF comes from the evidence that heparin is a potent inducer of HGF production. Matsumoto et al. showed that the addition of heparin to a culture of human embryonic lung fibroblasts increased the HGF concentration in the conditioned medium, in a dose-dependent manner (202). In our study, unfractionated heparin (UH) was administered after peripheral sampling and before coronary sampling. There is literature to suggest that the concentration of HGF is higher after administration of UH. A study by Seidel et al. (203) compared the levels of HGF after injections of unfractionated and low-molecular-weight heparin (LMWH) in healthy individuals. They found a significant increase in HGF from pre-treatment values, with the increase in HGF greater in individuals receiving UH than LMWH.

The timing of UH administration and literature supporting HGF concentrations with UH offers a plausible explanation for the increased levels of HGF in our study within the coronary circulation.

FGF-7 plays an important role in the regulation of embryonic development, but perhaps relevant to our finding is that it is a heparin-binding protein (204), which might also be explained by the timing of the administration of heparin.

IL-19 has recently been identified as an anti-inflammatory interleukin (205) and there is some evidence to suggest that it is mitogenic and chemotactic for endothelial cells (ECs) and can induce the angiogenic potential of ECs (206). Therefore, it might feasibly have a local role within the context of an acute inflammatory process.

5.6.2 Molecules preferentially expressed in peripheral samples

As described above, MIG/CXCL9 is an IFN-γ-inducible chemokine, with IFN-γ a proatherogenic cytokine expressed in atherosclerosis and arterial plaques. It is well described in this setting and therefore could very feasibly be a marker of systemic inflammation in the context of STEMI patients.

MIP-3α/CCL-19 is a homeostatic chemokine and, via its receptor CCR7, is an important regulator of lymphocyte and dendritic cell trafficking during immune surveillance (207). There is limited data directly supporting the relationship between this chemokine and cardiac patients, but studies have implicated its expression in vascular inflammation in the skin of patients with systemic sclerosis (208).

5.7 Study limitations

The most obvious limitations of our study are the small sample size and the single-centre design: larger studies would be required to validate our findings.

In order to minimise disruption to the normal PPCI procedure, peripheral and coronary arterial blood samples were not taken simultaneously. Therefore, the time delay between sampling of both the peripheral and coronary samples was not recorded or controlled for. In addition, all of the coronary samples were taken after the administration of heparin, again representing a potential confounder of our results. This in particular might explain some of the differences we observed

between cytokines preferentially expressed in either the coronary or peripheral circulation.

We were only able to validate a small number of the array findings with ELISAs due to limited plasma samples. Ideally, we would have performed ELISAs on all of the cytokines identified by array analysis, which might have confirmed further cytokines showing preferential expression to RFC or IFC, as well as being able to validate the transcoronary differences we observed.

Out of the 7 cytokines tested with ELISA, only 3 were positively validated. It is important to validate arrays with cytokine specific ELISA as there is always the possibility of getting false positives with the array. Although the data sets derived from the arrays were complete, there is always the possibility of experimental user error, therefore justifying the use of ELISA to reduce human error as much as possible. The antibody array only detects relative expression and differences between samples. The density of chemoluminescence as quantified by imaging software determines the amount of expression for a particular antibody. ELISA is a more precise method for the detection and quantification of the specific protein. The array does not specifically quantify the amount of protein in a sample as opposed to ELISA. Another possibility for the differences seen could be that both the cytokine array and ELISA were not done simultaneously. ELISAs were only done after all of the cytokine arrays were completed. This would have meant that the samples were thawed initially for the cytokine array, refrozen and then thawed again for the ELISA. This process might have influenced the specific quantity of protein measured and detected by ELISA. Finally, the ELISA data did mostly mirror the array data, so although statistical significance was not achieved with all of the ELISAs, this could be purely down to the numbers derived and not reaching enough statistical significance with that particular test.

Our study cohort did not represent the entire STEMI population. We had specific exclusion criteria to ensure we were only recruiting patients on whom it was safe to perform OCT while only slightly delaying the overall procedure time. Therefore, we were unable to include every STEMI patient; but, given the nature of the study, this was the only feasible, safe approach we could use. For example, patients presenting with cardiogenic shock were not included in the study, primarily for safety reasons. There also would have been some patients who did not even make it to hospital and

died before arrival. Had data from these patients been included, this might have also changed our results, as this would be incorporating a more representative STEMI population. In real terms however, this was a pilot study and it would not have been ethical or feasible to include the entire STEMI population.

We had to exclude patients for whom we were unable to adequately perform thrombectomy or OCT, in addition to the patients we were unable to classify due to excess residual thrombus. Therefore, we eliminated patients from subsequent analysis that could have made our findings more generalisable, although this is a recognised problem in other OCT-based studies, with up to 25% of plaque morphology unclassifiable due to residual thrombus (86,87).

It is also worth noting the small possibility that OCT/thrombectomy might traumatise the vessel and lead to misclassification of pathology. This issue affects the majority of studies in this field of research, and only a minority of patients do not require thrombectomy (209). In addition, our protocol permitted the use of a small predilatation balloon to facilitate OCT acquisition in cases in which sufficient TIMI flow had not been re-established, in keeping with other studies (102). Some studies had specifically excluded patients if thrombus aspiration alone had not established good coronary flow, in order to reduce the possibility of misclassification (87,209).

Plaque erosion is essentially a histological diagnosis and, although our OCT findings classified morphologies, there was no pathological validation. True pathological validation is impossible because studying the samples post mortem of patients who had died from ACS is fundamentally very different from classifying in vivo those who have survived and have been treated with antithrombotics. The absence of endothelial cells is a key pathological criterion for plaque erosion, but OCT cannot detect endothelial cell loss. In conjunction with other OCT-based studies, the OCT definition of plaque erosion is based primarily on a diagnosis of exclusion requiring the absence of a fibrous cap rupture, and we have used the term IFC as a surrogate for this (97).

Another limitation of our study was the omission of body mass index data. During the PPCI procedure, weight was estimated but not routinely recorded. Height was not recorded in any of the patients meaning that there was no assessment of body mass index. Given the recent data suggesting that there is an association between obesity

and a vulnerable lipid rich plaque, it would have been worthwhile to see whether we could have found any similar associations.

Although the assessment of left ventricular systolic function post myocardial infarction was not the main focus of our study, a further limitation was that there was no measure taken to investigate the intra and inter operator reproducibility between the different sonographers responsible for performing transthoracic echocardiography and reporting left ventricular function. If the study were repeated, ideally only one sonographer would be used to perform and report the echocardiograms for all of the patients recruited to reduce variability in assessment.

Patients on immune modulating drugs e.g steroids, methotrexate or monoclonal antibody medications were not excluded from the study. The medications patients were taking prior to presenting with an acute STEMI were not recorded. This is a limitation of the study since pre-existing medications used for chronic inflammatory conditions might have affected the results and these patient samples, thereby potentially demonstrating a predilection for pro inflammatory cytokines on the arrays.

In our study, we did not record an admission cholesterol level. This was primarily because it was felt that there was variation in cholesterol with an acute myocardial infarction and that this was not the key parameter we were addressing in our study. However, it might have been worthwhile to measure, record and compare baseline total cholesterol, LDL and HDL between plaque rupture and erosion to determine if there was any significant association with either pathology. Given that ruptured plaques are lipid-rich and eroded plaques tend to be more fibrous, there might have been an association between elevated cholesterol and plaque rupture. Similarly, the admission statin use for each patient recruited into the study was not recorded. Because of the increasing success of LDL-lowering therapies associated with statin use, one might expect a rise in the proportion of ACS caused by erosion. In our relatively small study, we may have been able to demonstrate possible associations between statin therapy and plaque erosions had we recorded statin use for each patient.

With regards to events adjudication, there was no independent, blinded, events adjudication committee. This is a limitation of the study and going forward, if the study was to be repeated, an independent blinded committee would be in place to review events and adjudicate whether any events that did occur during the follow-up phase were cardiac or non-cardiac. This would then act as a more robust measure to determine whether an event should be included in MACCE.

5.8 Implications

Our study has several unique features that distinguish it from previous studies. Our observations are novel and support the concept that different atherosclerotic pathologies may be associated with distinct intracoronary inflammatory profiles.

We have demonstrated the feasibility of studying different plaque pathologies using intracoronary blood sampling, OCT and multiplex arrays to screen for molecular differences. The cytokines identified have been shown to be involved in mechanisms that make them plausible candidates for driving or facilitating plaque destabilisation. This supports the validity of our approach to studying potential triggers of plaque erosion and rupture.

Large-scale proteomic studies would also be worthwhile now that we have demonstrated that our approaches to sample collection, intravascular imaging, cytokine arrays and ELISAs have been feasible and reproducible. Our methodology could also be extended to other ACS patients (NSTEMI/unstable angina). Both of these approaches might provide further validation of our findings, as well as allowing the identification of further novel biomarkers for plaque erosion or rupture. This may facilitate the ability to screen high-risk patients, as well as customisation of treatment according to the underlying pathology (91,210).

We sampled coronary blood from the infarct-related artery, which appears to provide a more accurate reflection of the inflammatory processes within the culprit lesion compared to peripheral samples. We also demonstrated preferential expression of some cytokines for the coronary circulation, which might be explained by the timing of administration of heparin.

However, it is worth noting that any future studies would have to refer to the latest European Society of Cardiology guidelines, which suggest that routine thrombus

aspiration is not recommended, except in the cases of large residual thrombus burden (211). This follows on from the safety concerns raised from the TOTAL trial, which demonstrated an increase in the risk of stroke when comparing routine aspiration thrombectomy with PCI versus PCI alone in STEMI patients (212). Patients would therefore have to be informed about the potential risks of thrombectomy prior to obtaining verbal assent whilst also explaining that it is not routine practice to perform thrombectomy anymore. This new guidance may affect patient recruitment in the future and the ability to perform a similar study.

5.9 Future directions for research

5.9.1 Endothelial cells

The leading hypothesis for plaque erosion is endothelial cell loss of an atherosclerotic plaque, which thereby exposes a thrombogenic extracellular matrix to blood. The vascular endothelium is an interface between the blood stream and vessel wall. Any changes in this layer are believed to be of primary importance in the pathogenesis of atherosclerosis and in acute thrombosis. The balance of cell loss and cell replacement maintains the healthy, intact endothelium.

Endothelial cell loss may be due to cell death (e.g. apoptosis, necrosis) or detachment of viable cells. Replacement is due to proliferation of differentiated endothelial cells as well as recruitment of endothelial progenitor cells (EPCs) and to sites of injury (213).

Circulating apoptotic EPCs ($CD34^+$, Annexin V^+, 7-ADD^-) are increased in ACS compared to healthy subjects and correlate with the burden of coronary atheroma (214). Prospective studies in stable coronary artery disease have shown that subjects with lower circulating EPC numbers generally have worse outcomes than those with higher EPC numbers (215,216).

EMPs ($CD31^+$, Annexin V^+) have also been demonstrated in patients both with stable coronary disease and ACS (216–218), and levels correlate with cardiovascular outcomes, disease severity and endothelial dysfunction.

CECs are increased in many conditions associated with vascular injury, including myocardial infarction and unstable angina, but are not increased in stable coronary artery disease (219).

Flow cytometry is an established methodology for identifying all three cell fragments – EPCs, EMPs and CECs, and determining cell counts in the studies mentioned above.

Endothelial cell apoptosis is an attractive explanation for the disappearance of endothelial cells in plaque erosion. There is circumstantial evidence, including studies of chemically induced endothelial cell apoptosis in a rabbit femoral artery model, which results in vessel thrombosis and a histological appearance similar to plaque erosion (62,220). Using an endothelial marker, CD31, Quillard et al. (70) found that clusters of apoptotic endothelial cells were evident in smooth muscle (characteristic of erosion) rich atheromatous plaques in patients who had died after myocardial infarction.

It therefore seems very plausible that all three cell types – EMPs, EPCs and CECs – are likely to be present in both plaque rupture and erosion, but it is not known whether there are any qualitative or quantitative differences.

An extension of our study would therefore be to undertake a prospective observational study of endothelial cells using flow cytometry of blood samples from patients undergoing PPCI in a similar way to the PEPs study. The aim would then be to correlate these findings with plaque morphology to increase our understanding of the endothelium and, ultimately, plaque erosion.

5.9.2 Thrombospondin-1

We have demonstrated significantly increased levels of TSP-1 in the coronary circulation of patients with plaque erosion compared to rupture. Our data is purely observational and the significance of elevated TSP-1 in IFC is unclear. Proving a causal role requires additional evidence. TSP-1 has many modulatory roles within the endothelium but specifically has been shown to induce endothelial cell apoptosis in cultured cell and animal models (148,149). It would therefore seem sensible to pursue the investigation of TSP-1 in its potential role of plaque erosion.

Animal models where rapid atherosclerosis can develop are very useful for understanding this pathological process. Apolipoprotein E (Apo E) knockout mice show impaired clearing of plasma lipoproteins and develop atherosclerosis in a short time.

We could therefore investigate the effect of TSP-1 infusion in Apo E mice to determine the time course of plasma levels achieved and also assess arterial histology with a particular emphasis on vascular structure and endothelial apoptosis. We could also apply the model of measuring endothelial cell fragments to see if there is a relationship between TSP-1 and, for example, circulating EPCs. Infusion of TSP-1 might also affect the incidence of plaque morphologies such that we might see an increased frequency of plaque erosion, given that we think TSP-1 might primarily act on the endothelium.

5.9.3 Multicentre work

Subsequent to the publication of the work from this thesis, multicentre collaborations would be a logical step in helping to understand further about the aetiology of plaque erosion. Our methodology has been shown to be feasible and reproducible for a small cohort of patients. A larger cohort of patients from numerous centres would provide more robust data with which stronger inferences and conclusions could be drawn regarding preferential cytokine expression. Our method of cytokine arrays, followed by ELISA is reproducible but onerous. Using alternative techniques such as mass spectrometry might enable screening of a much larger range of cytokines. In addition, further work defining the influence of shear stress on the incidence of endothelial erosion in coronary arteries needs to be undertaken in order to try and understand the specific conditions in which erosion is likely to occur. Combining models of elevated and reduced shear stress in conjunction with mass spectrometry might yield more specific cytokines particular to plaque erosion.

Chapter 6: Conclusion

We have demonstrated a significant difference in the cytokine profiles of RFC and IFC in vivo, including the novel findings that I-TAC is preferentially expressed in RFC and IFC is associated with elevated intracoronary EGF and TSP-1 levels. Some of these differences are also reflected in the mRNA analysis of thrombectomy samples. These results may help to further understand the pathophysiology of plaque erosion and potentially tailor future treatment strategies. Our results suggest that our methodology is a safe and feasible approach for studying the potential triggers of plaque erosion.

We have achieved our primary objectives of demonstrating the utility, safety and feasibility of this combined methodology and correlating expression of cytokines with plaque morphology. As a result, we have improved our understanding of the pathophysiology of plaque erosion.

Further work including larger trials is required to establish whether or not these differences play a causal role in the different pathologies, or simply reflect different secondary responses.

References

1. Melorose J, Perroy R, Careas S. CVD statistics - UK factsheet. Statew Agric L Use Baseline 2015. 2015;1(Cvd).

2. Bhatnagar P, Wickramasinghe K, Williams J, Rayner M, Townsend N. The epidemiology of cardiovascular disease in the UK 2014. Heart (British Cardiac Society). 2015. p. heartjnl-2015-307516-.

3. Heidenreich PA, Trogdon JG, Khavjou OA, Butler J, Dracup K, Ezekowitz MD, et al. Forecasting the future of cardiovascular disease in the United States. Circulation. 2011. p. 933–44.

4. Libby P. Molecular bases of the acute coronary syndromes. Circulation. 1995;91(11):2844–50.

5. Li JJ, Fang CH. Atherosclerosis is a more rational term for the pathological entity currently known as atherosclerosis. Medical Hypotheses. 2004. p. 100–2.

6. Singh RB, Mengi SA, Xu YJ, Arneja AS, Dhalla NS. Pathogenesis of atherosclerosis: A multifactorial process. Experimental and Clinical Cardiology. 2002. p. 40–53.

7. Tegos TJ, Kalodiki E, Sabetai MM, Nicolaides AN. The Genesis of Atherosclerosis and Risk Factors: A Review. Angiology. 2001;52(2):89–98.

8. Wentzel JJ, Chatzizisis YS, Gijsen FJH, Giannoglou GD, Feldman CL, Stone PH. Endothelial shear stress in the evolution of coronary atherosclerotic plaque and vascular remodelling: Current understanding and remaining questions. Cardiovascular Research. 2012. p. 234–43.

9. Chatzizisis YS, Coskun AU, Jonas M, Edelman ER, Feldman CL, Stone PH. Role of Endothelial Shear Stress in the Natural History of Coronary Atherosclerosis and Vascular Remodeling. Molecular, Cellular, and Vascular Behavior. J Am Coll Cardiol. 2007;49(25):2379–93.

10. Stary HC, Chandler a B, Dinsmore RE, Fuster V, Glagov S, Insull W, et al. A definition of advanced types of atherosclerotic lesions and a histological classification of atherosclerosis. A report from the Committee on Vascular

Lesions of the Council on Arteriosclerosis, American Heart Association. Arterioscler Thromb Vasc Biol. 1995;15(9):1512–31.

11. Virmani R, Virmani R, Kolodgie FD, Kolodgie FD, Burke AP, Burke AP, et al. Lessons From Sudden Coronary Death. Arterioscler Thromb. 2000;1262–75.

12. van der Wal a C, Becker a E, van der Loos CM, Das PK. Site of intimal rupture or erosion of thrombosed coronary atherosclerotic plaques is characterized by an inflammatory process irrespective of the dominant plaque morphology. Circulation. 1994. p. 36–44.

13. Fan J, Watanabe T. Inflammatory reactions in the pathogenesis of atherosclerosis. J Atheroscler Thromb. 2003;10(2):63–71.

14. Kolodgie FD, Gold HK, Burke AP, Fowler DR, Kruth HS, Weber DK, et al. Intraplaque hemorrhage and progression of coronary atheroma. N Engl J Med. 2003;349(24):2316–25.

15. Libby P. Mechanisms of Acute Coronary Syndromes and Their Implications for Therapy. N Engl J Med. 2013;368(21):2004–13.

16. Virmani R, Burke AP, Willerson JT, Farb A, Narula J, Kolodgie FD. The Pathology of Vulnerable Plaque. In: The Vulnerable Atherosclerotic Plaque: Strategies for Diagnosis and Management. 2007. p. 19–36.

17. Schaar JA, Muller JE, Falk E, Virmani R, Fuster V, Serruys PW, et al. Terminology for high-risk and vulnerable coronary artery plaques. Eur Heart J. 2004;25(12):1077–82.

18. Burke AP, Farb A, Malcom GT, Liang Y, Smialek JE, Virmani R. Plaque rupture and sudden death related to exertion in men with coronary artery disease. Jama. 1999;281(10):921–6.

19. Yonetsu T, Kakuta T, Lee T, Takahashi K, Kawaguchi N, Yamamoto G, et al. In vivo critical fibrous cap thickness for rupture-prone coronary plaques assessed by optical coherence tomography. Eur Heart J. 2011;32(10):1251–9.

20. Burke a P, Weber DK, Kolodgie FD, Farb a, Taylor a J, Virmani R. Pathophysiology of calcium deposition in coronary arteries. Herz. 2001;26(4):239–44.

21. Falk E, Nakano M, Bentzon JF, Finn A V., Virmani R. Update on acute coronary syndromes: The pathologists' view. Eur Heart J. 2013;34(10):719–28.

22. van der Wal a C, Becker a E, van der Loos CM, Das PK. Site of intimal rupture or erosion of thrombosed coronary atherosclerotic plaques is characterized by an inflammatory process irrespective of the dominant plaque morphology. Circulation. 1994;89(1):36–44.

23. Farb A, Burke AP, Tang AL, Liang TY, Mannan P, Smialek J, et al. Coronary plaque erosion without rupture into a lipid core. A frequent cause of coronary thrombosis in sudden coronary death. Circulation. 1996;93(7):1354–63.

24. Muller JE, Tofler GH, Stone PH. Circadian variation and triggers of onset of acute cardiovascular disease. Circulation. 1989;79(4):733–43.

25. Xu Y, Mintz GS, Tam A, Mcpherson JA, Iñiguez A, Fajadet J, et al. Prevalence, distribution, predictors, and outcomes of patients with calcified nodules in native coronary arteries: A 3-vessel intravascular ultrasound analysis from providing regional observations to study predictors of events in the coronary tree (PROSPE. Circulation. 2012;126(5):537–45.

26. Kolodgie FD, Virmani R, Burke a P, Farb a, Weber DK, Kutys R, et al. Pathologic assessment of the vulnerable human coronary plaque. Heart. 2004;90(12):1385–91.

27. Stone GW, Maehara A, Lansky AJ, de Bruyne B, Cristea E, Mintz GS, et al. A prospective natural-history study of coronary atherosclerosis. N Engl J Med. 2011;364(3):226–35.

28. Calvert PA, Obaid DR, O'Sullivan M, Shapiro LM, McNab D, Densem CG, et al. Association between IVUS findings and adverse outcomes in patients with coronary artery disease: The VIVA (VH-IVUS in vulnerable atherosclerosis) study. JACC Cardiovasc Imaging. Elsevier Inc.; 2011;4(8):894–901.

29. Kubo T, Maehara A, Mintz GS, Doi H, Tsujita K, Choi SY, et al. The Dynamic Nature of Coronary Artery Lesion Morphology Assessed by Serial Virtual Histology Intravascular Ultrasound Tissue Characterization. J Am Coll Cardiol. Elsevier Inc.; 2010;55(15):1590–7.

30. Burke AP, Kolodgie FD, Farb A, Weber DK, Malcom GT, Smialek J, et al. Healed Plaque Ruptures and Sudden Coronary Death : Evidence That Subclinical Rupture Has a Role in Plaque Progression. Circulation. 2001;103(7):934–40.

31. Sakakura K, Nakano M, Otsuka F, Ladich E, Kolodgie FD, Virmani R. Pathophysiology of Atherosclerosis Plaque. Hear Lung Circ. Australian and New Zealand Society of Cardiac and Thoracic Surgeons (ANZSCTS) and the Cardiac Society of Australia and New Zealand (CSANZ); 2013;22(6):399–411.

32. Lafont A. Basic aspects of plaque vulnerability. Heart. 2003;89(10):1262–7.

33. Libby P, Ridker PM, Maseri A. Inflammation and atherosclerosis. Circulation. 2002;105(9):1135–43.

34. Cybulsky MI, Gimbrone M a. Endothelial expression of a mononuclear leukocyte adhesion molecule during atherogenesis. Science. 1991;251(4995):788–91.

35. Berliner JA, Leitinger N, Tsimikas S. The role of oxidized phospholipids in atherosclerosis. J Lipid Res. 2008;50(Supplement):S207–12.

36. Gu L, Okada Y, Clinton SK, Gerard C, Sukhova GK, Libby P, et al. Absence of monocyte chemoattractant protein-1 reduces atherosclerosis in low density lipoprotein receptor-deficient mice. Mol Cell. 1998;2(2):275–81.

37. Smith JD, Trogan E, Ginsberg M, Grigaux C, Tian J, Miyata M. Decreased atherosclerosis in mice deficient in both macrophage colony-stimulating factor (op) and apolipoprotein E. Proc Natl Acad Sci U S A. 1995;92(18):8264–8.

38. Quinn KL, Henriques M, Tabuchi A, Han B, Yang H, Cheng WE, et al. Human neutrophil peptides mediate endothelial-monocyte interaction, foam cell formation, and platelet activation. Arterioscler Thromb Vasc Biol. 2011;31(9):2070–9.

39. Vidal F, Colomé C, Martínez-González J, Badimon L. Atherogenic concentrations of native low-density lipoproteins down- regulate nitric-oxide-synthase mRNA and protein levels in endothelial cells. Eur J Biochem. 1998;252(3):378–84.

40. Vorchheimer D a, Becker R. Platelets in atherothrombosis. Mayo Clin Proc. 2006;81(1):59–68.

41. Crola Da Silva C, Lamerant-Fayel N, Paprocka M, Mitterrand M, Gosset D, Dus D, et al. Selective human endothelial cell activation by chemokines as a guide to cell homing. Immunology. 2009;126(3):394–404.

42. Huo Y, Ley K. Adhesion molecules and atherogenesis. Acta Physiologica Scandinavica. 2001. p. 35–43.

43. Tobar N, Villar V, Santibanez JF. ROS-NFκB mediates TGF-β1-induced expression of urokinase-type plasminogen activator, matrix metalloproteinase-9 and cell invasion. Mol Cell Biochem. 2010;340(1–2):195–202.

44. Li AC, Glass CK. The macrophage foam cell as a target for therapeutic intervention. Nat Med. 2002;8(11):1235–42.

45. Badimon L, Storey RF, Vilahur G. Update on lipids, inflammation and atherothrombosis. Thromb Haemost. 2011;105(SUPPL. 1):34–42.

46. Falck-Hansen M, Kassiteridi C, Monaco C. Toll-like receptors in atherosclerosis. International Journal of Molecular Sciences. 2013. p. 14008–23.

47. Muzio M, Mantovani a. Toll-like receptors (TLRs) signalling and expression pattern. J Endotoxin Res. 2001;7(4):297–300.

48. Ashida K, Miyazaki K, Takayama E, Tsujimoto H, Ayaori M, Yakushiji T, et al. Characterization of the expression of TLR2 (toll-like receptor 2) and TLR4 on circulating monocytes in coronary artery disease. J Atheroscler Thromb. 2005;12(1):53–60.

49. Grenier D, Grignon L. Response of human macrophage-like cells to stimulation by Fusobacterium nucleatum ssp. nucleatum lipopolysaccharide. Oral Microbiol Immunol. 2006;21(3):190–6.

50. Ishikawa Y, Satoh M, Itoh T, Minami Y. Local expression of Toll-like receptor 4 at the site of ruptured plaques in patients with acute myocardial infarction. 2008;140:133–40.

51. Mach F, Sauty A, Iarossi AS, Sukhova GK, Neote K, Libby P, et al.

Differential expression of three T lymphocyte-activationg CXC chemokines by human atheroma-associated cells. JClinInvest. 1999;104(8):1041–50.

52. Hansson GK. Immune mechanisms in atherosclerosis. Arterioscler Thromb Vasc Biol. 2001;21(12):1876–90.

53. Koenig W, Khuseyinova N. Biomarkers of atherosclerotic plaque instability and rupture. Arterioscler Thromb Vasc Biol. 2007;27(1):15–26.

54. Galis ZS, Sukhova GK, Lark MW, Libby P. Increased expression of matrix metalloproteinases and matrix degrading activity in vulnerable regions of human atherosclerotic plaques. J Clin Invest. 1994;94(6):2493–503.

55. Schönbeck U, Mach F, Sukhova GK, Herman M, Graber P, Kehry MR, et al. CD40 ligation induces tissue factor expression in human vascular smooth muscle cells. Am J Pathol. 2000;156(1):7–14.

56. Müller A, Krämer SD, Meletta R, Beck K, Selivanova S V., Rancic Z, et al. Gene expression levels of matrix metalloproteinases in human atherosclerotic plaques and evaluation of radiolabeled inhibitors as imaging agents for plaque vulnerability. Nucl Med Biol. Elsevier Inc.; 2014;41(7):562–9.

57. Ohayon J, Finet G, Gharib AM, Herzka D a, Tracqui P, Heroux J, et al. Necrotic core thickness and positive arterial remodeling index: emergent biomechanical factors for evaluating the risk of plaque rupture. Am J Physiol Heart Circ Physiol. 2008;295(2):H717–27.

58. Davies MJ, Thomas AC. Plaque fissuring--the cause of acute myocardial infarction, sudden ischaemic death, and crescendo angina. Br Heart J. 1985;53(December 1984):363–73.

59. Zaman AG, Helft G, Worthley SG, Badimon JJ. The role of plaque rupture and thrombosis in coronary artery disease. Atherosclerosis. 2000;149(2):251–66.

60. Fulton FM. Concepts in Acute Coronary Thrombosis: Relevance To Treatment. Rev Lit Arts Am. 1993;403–8.

61. Campbell IC, Suever JD, Timmins LH, Veneziani A, Vito RP, Virmani R, et al. Biomechanics and Inflammation in Atherosclerotic Plaque Erosion and Plaque Rupture: Implications for Cardiovascular Events in Women. PLoS

One. 2014;9(11):e111785.

62. Durand E. In Vivo Induction of Endothelial Apoptosis Leads to Vessel Thrombosis and Endothelial Denudation: A Clue to the Understanding of the Mechanisms of Thrombotic Plaque Erosion. Circulation. 2004;109(21):2503–6.

63. Nerem RM. Vascular fluid mechanics, the arterial wall, and atherosclerosis. J Biomech Eng. 1992;114(3):274–82.

64. Dimmeler S, Hermann C, Zeiher AM. Apoptosis of endothelial cells. Contribution to the pathophysiology of atherosclerosis? In: European Cytokine Network. 1998. p. 697–8.

65. Tricot O, Mallat Z, Heymes C, Belmin J, Lesèche G, Tedgui a. Relation between endothelial cell apoptosis and blood flow direction in human atherosclerotic plaques. Circulation. 2000;101(21):2450–3.

66. Campbell IC, Timmins LH, Giddens DP, Virmani R, Veneziani A, Rab ST, et al. Computational Fluid Dynamics Simulations of Hemodynamics in Plaque Erosion. Cardiovasc Eng Technol. 2013;4(4):464–73.

67. White SJ, Newby AC, Johnson TW. Endothelial erosion of plaques as a substrate for coronary thrombosis. Thromb Haemost. 2016;115(3):509–19.

68. Suhr F, Bloch W. Endothelial cell apoptosis: A new focal adhesion assembly makes the difference. Circ Res. 2012;111(12):1488–90.

69. Dimmeler S, Zeiher AM. Endothelial cell apoptosis in angiogenesis and vessel regression. Circ Res. 2000;87(6):434–9.

70. Quillard T, Araújo HA, Franck G, Shvartz E, Sukhova G, Libby P. TLR2 and neutrophils potentiate endothelial stress, apoptosis and detachment: Implications for superficial erosion. Eur Heart J. 2015;36(22):1394–404.

71. Dollery CM, Libby P. Atherosclerosis and proteinase activation. Cardiovascular Research. 2006. p. 625–35.

72. Saffarzadeh M, Juenemann C, Queisser MA, Lochnit G, Barreto G, Galuska SP, et al. Neutrophil extracellular traps directly induce epithelial and endothelial cell death: A predominant role of histones. PLoS One. 2012;7(2).

73. Butler LM, Rainger GE, Nash GB. A role for the endothelial glycosaminoglycan hyaluronan in neutrophil recruitment by endothelial cells cultured for prolonged periods. Exp Cell Res. 2009;315(19):3433–41.

74. Sugiyama S, Kugiyama K, Aikawa M, Nakamura S, Ogawa H, Libby P. Hypochlorous acid, a macrophage product, induces endothelial apoptosis and tissue factor expression: Involvement of myeloperoxidase-mediated oxidant in plaque erosion and thrombogenesis. Arterioscler Thromb Vasc Biol. 2004;24(7):1309–14.

75. Ferrante G, Nakano M, Prati F, Niccoli G, Mallus MT, Ramazzotti V, et al. High Levels of Systemic Myeloperoxidase Are Associated. 2010;2505–13.

76. Zijlstra F, Hoorntje JC, de Boer MJ, Reiffers S, Miedema K, Ottervanger JP, et al. Long-term benefit of primary angioplasty as compared with thrombolytic therapy for acute myocardial infarction. N Engl J Med. 1999;341(19):1413–9.

77. Henriques JPS, Zijlstra F, Ottervanger JP, de Boer M-J, van 't Hof a WJ, Hoorntje JC a, et al. Incidence and clinical significance of distal embolization during primary angioplasty for acute myocardial infarction. Eur Heart J. 2002;23(14):1112–7.

78. Reffelmann T, Kloner RA. The no-reflow phenomenon: A basic mechanism of myocardial ischemia and reperfusion. Basic Research in Cardiology. 2006. p. 359–72.

79. Jolly SS, James S, Džavík V, Cairns JA, Mahmoud KD, Zijlstra F, et al. Thrombus Aspiration in ST-Segment–Elevation Myocardial Infarction An Individual Patient Meta-Analysis: Thrombectomy Trialists Collaboration. Circulation. 2017 Jan 9;135(2):143 LP-152.

80. Svilaas T, Vlaar PJ, van der Horst IC, Diercks GFH, de Smet BJGL, van den Heuvel AFM, et al. Thrombus aspiration during primary percutaneous coronary intervention. N Engl J Med. 2008;358(6):557–67.

81. Kramer MC, van der Wal AC, Koch KT, Rittersma SZ, Li X, Ploegmakers HP, et al. Histopathological features of aspirated thrombi after primary percutaneous coronary intervention in patients with ST-elevation myocardial

infarction. PLoS One. 2009;4(6):e5817.

82. Rittersma SZH, Van Der Wal AC, Koch KT, Piek JJ, Henriques JPS, Mulder KJ, et al. Plaque instability frequently occurs days or weeks before occlusive coronary thrombosis: A pathological thrombectomy study in primary percutaneous coronary intervention. Circulation. 2005;111(9):1160–5.

83. Carol A, Bernet M, Curos A, Rodriguez-Leor O, Serra J, Fernandez-Nofrerias E, et al. Thrombus age, clinical presentation, and reperfusion grade in myocardial infarction. Cardiovasc Pathol. Elsevier Inc.; 2014;23(3):126–30.

84. Sato Y, Hatakeyama K, Yamashita a, Marutsuka K, Sumiyoshi a, Asada Y. Proportion of fibrin and platelets differs in thrombi on ruptured and eroded coronary atherosclerotic plaques in humans. Heart. 2005;91(4):526–30.

85. Kramer MC a, Rittersma SZH, de Winter RJ, Ladich ER, Fowler DR, Liang YH, et al. Relationship of thrombus healing to underlying plaque morphology in sudden coronary death. J Am Coll Cardiol. Elsevier Inc.; 2010;55(2):122–32.

86. Guagliumi G, Capodanno D, Saia F, Musumeci G, Tarantini G, Garbo R, et al. Mechanisms of atherothrombosis and vascular response to primary percutaneous coronary intervention in women versus men with acute myocardial infarction: results of the OCTAVIA study. JACC Cardiovasc Interv. 2014;7(9):958–68.

87. Saia F, Komukai K, Capodanno D, Sirbu V, Musumeci G, Boccuzzi G, et al. Eroded Versus Ruptured Plaques at the Culprit Site of STEMI. JACC Cardiovasc Imaging. 2015;8(5):566–75.

88. Tearney GJ, Brezinski ME, Boppart SA, Bouma BE, Weissman N, Southern JF, et al. Catheter-Based Optical Imaging of a Human Coronary Artery. Circulation. 1996 Dec 1;94(11):3013–3013.

89. Prati F, Regar E, Mintz GS, Arbustini E, Di Mario C, Jang I-K, et al. Expert review document on methodology, terminology, and clinical applications of optical coherence tomography: physical principles, methodology of image acquisition, and clinical application for assessment of coronary arteries and atherosclerosis. Eur Heart J. 2010;31(4):401–15.

90. Kume T, Akasaka T, Kawamoto T, Watanabe N, Toyota E, Neishi Y, et al. Assessment of coronary intima--media thickness by optical coherence tomography: comparison with intravascular ultrasound. Circ J. 2005;69(8):903–7.

91. Prati F, Uemura S, Souteyrand G, Virmani R, Motreff P, Di Vito L, et al. OCT-based diagnosis and management of STEMI associated with intact fibrous cap. JACC Cardiovasc Imaging. 2013;6(3):283–7.

92. Rollins AM, Simon DI. Intracoronary Optical Coherence Tomography : A Comprehensive Review. JCIN. Elsevier Inc.; 2009;2(11):1035–46.

93. Yabushita H, Bouma BE, Houser SL, Aretz HT, Jang IK, Schlendorf KH, et al. Characterization of human atherosclerosis by optical coherence tomography. Circulation. 2002;106(13):1640–5.

94. Kubo T, Imanishi T, Takarada S, Kuroi A, Ueno S, Yamano T, et al. Assessment of Culprit Lesion Morphology in Acute Myocardial Infarction. Ability of Optical Coherence Tomography Compared With Intravascular Ultrasound and Coronary Angioscopy. J Am Coll Cardiol. 2007;50(10):933–9.

95. Kume T, Akasaka T, Kawamoto T, Ogasawara Y, Watanabe N, Toyota E, et al. Assessment of coronary arterial thrombus by optical coherence tomography. Am J Cardiol. 2006;97(12):1713–7.

96. Otsuka F, Joner M, Prati F, Virmani R, Narula J. Clinical classification of plaque morphology in coronary disease. Nat Rev Cardiol. Nature Publishing Group; 2014;11(7):379–89.

97. Tearney GJ, Regar E, Akasaka T, Adriaenssens T, Barlis P, Bezerra HG, et al. Consensus Standards for Acquisition, Measurement, and Reporting of Intravascular Optical Coherence Tomography Studies. J Am Coll Cardiol. Elsevier Inc.; 2012;59(12):1058–72.

98. Tanaka A, Imanishi T, Kitabata H, Kubo T, Takarada S, Tanimoto T, et al. Morphology of exertion-triggered plaque rupture in patients with acute coronary syndrome: an optical coherence tomography study. Circulation. 2008;118(23):2368–73.

99. Kubo T, Ino Y, Tanimoto T, Kitabata H, Tanaka A, Akasaka T. Optical coherence tomography imaging in acute coronary syndromes. Cardiol Res Pract. 2011;2011:312978.

100. Ozaki Y, Okumura M, Ismail TF, Motoyama S, Naruse H, Hattori K, et al. Coronary CT angiographic characteristics of culprit lesions in acute coronary syndromes not related to plaque rupture as defined by optical coherence tomography and angioscopy. Eur Heart J. 2011;32(22):2814–23.

101. Kubo T, Tanaka A, Ino Y, Kitabata H, Shiono Y, Akasaka T. Assessment of coronary atherosclerosis using optical coherence tomography. J Atheroscler Thromb. 2014;21(9):895–903.

102. Niccoli G, Montone RA, Di Vito L, Gramegna M, Refaat H, Scalone G, et al. Plaque rupture and intact fibrous cap assessed by optical coherence tomography portend different outcomes in patients with acute coronary syndrome. Eur Heart J. 2015;36(22):1377–84.

103. Yonetsu T, Lee T, Murai T, Suzuki M, Matsumura A, Hashimoto Y, et al. Plaque morphologies and the clinical prognosis of acute coronary syndrome caused by lesions with intact fibrous cap diagnosed by optical coherence tomography. Int J Cardiol. Elsevier Ireland Ltd; 2016;203:766–74.

104. Niccoli G, Montone RA, Cataneo L, Cosentino N, Gramegna M, Refaat H, et al. Morphological-biohumoral correlations in acute coronary syndromes: Pathogenetic implications. Int J Cardiol. Elsevier Ireland Ltd; 2014;171(3):463–6.

105. Edirisinghe I, Rahman I. Cigarette smoke-mediated oxidative stress, shear stress, and endothelial dysfunction: Role of VEGFR2. In: Annals of the New York Academy of Sciences. 2010. p. 66–72.

106. Tavora F, Cresswell N, Li L, Ripple M, Fowler D, Burke A. Sudden coronary death caused by pathologic intimal thickening without atheromatous plaque formation. Cardiovasc Pathol. 2011;20(1):51–7.

107. Burke AP, Farb A, Pestaner J, Malcom GT, Zieske A, Kutys R, et al. Traditional Risk Factors and the Incidence of Sudden Coronary Death With and Without Coronary Thrombosis in Blacks. Circulation. 2002 Jan

29;105(4):419 LP-424.

108. Libby P, Theroux P. Pathophysiology of coronary artery disease. Circulation. 2005;111(25):3481–8.

109. Rosa R De, Vasa-Nicotera M, Leistner DM, Reis SM, Thome CE, Boeckel J, et al. Coronary Atherosclerotic Plaque Characteristics and Cardiovascular Risk Factors —. 2017;81(August):1165–73.

110. Jia H, Dai J, Hou J, Xing L, Ma L, Liu H, et al. Effective anti-thrombotic therapy without stenting : intravascular optical coherence tomography-based management in plaque erosion (the EROSION study). Eur Heart J. 2016;0:1–9.

111. Ridker PM, Thuren T, Zalewski A, Libby P. Interleukin-1β inhibition and the prevention of recurrent cardiovascular events: Rationale and Design of the Canakinumab Anti-inflammatory Thrombosis Outcomes Study (CANTOS). Am Heart J. 2011;162(4):597–605.

112. Wharton G, Steeds R, Allen J, Phillips H, Jones R, Kanagala P, et al. A minimum dataset for a standard adult transthoracic echocardiogram: a guideline protocol from the British Society of Echocardiography. Echo Res Pract. 2015;2(1):G9–24.

113. Masani N, Wharton G, Author L, Allen J, Chambers J, Graham J, et al. Echocardiography : Guidelines for Chamber Quantification British Society of Echocardiography Education Committee. 2010.

114. Abdul-Aziz AM, Shafat MS, Mehta TK, Di Palma F, Lawes MJ, Rushworth SA, et al. MIF-Induced Stromal PKCβ/IL8 Is Essential in Human Acute Myeloid Leukemia. Cancer Res. 2017 Jan 16;77(2):303 LP-311.

115. Ary CN. Proteome Profiler Array. 2012;16.

116. Zhang S, Garcia-D'Angeli A, Brennan JP, Huo Q. Predicting detection limits of enzyme-linked immunosorbent assay (ELISA) and bioanalytical techniques in general. Analyst. 2014;139(2):439–45.

117. Orlando C, Pinzani P, Pazzagli M. Developments in quantitative PCR. Clinical Chemistry and Laboratory Medicine. 1998. p. 255–69.

118. R&D Systems. Proteome ProfilerTM Array: Human XL Cytokine Array Kit. 2014.

119. Bolstad BM, Irizarry R., Astrand M, Speed TP. A comparison of normalization methods for high density oligonucleotide array data based on variance and bias. Bioinformatics. 2003;19(2):185–93.

120. Tibshirani R, Chu G, Narasimhan B, Li J. samr: SAM: Significance Analysis of Microarrays. 2011.

121. Chaldakov GN, Fiore M, Stankulov IS, Manni L, Hristova MG, Antonelli A, et al. Neurotrophin presence in human coronary atherosclerosis and metabolic syndrome: A role for NGF and BDNF in cardiovascular disease? Prog Brain Res. 2004;146:279–89.

122. Ferrante G, Nakano M, Prati F, Niccoli G, Mallus MT, Ramazzotti V, et al. High levels of systemic myeloperoxidase are associated with coronary plaque erosion in patients with acute coronary syndromes: A clinicopathological study. Circulation. 2010;122(24):2505–13.

123. Kubo T, Imanishi T, Takarada S, Kuroi A, Ueno S, Yamano T, et al. Assessment of Culprit Lesion Morphology in Acute Myocardial Infarction. J Am Coll Cardiol. 2007;50(10):933–9.

124. Kajander OA, Pinilla-Echeverri N, Jolly SS, Bhindi R, Huhtala H, Niemela KO, et al. Culprit plaque morphology in STEMI – an optical coherence tomography study: insights from the TOTAL-OCT substudy. EuroIntervention. Europa Digital & Publishing SE - CORONARY INTERVENTIONS; 2016 Aug 20;12(6):716–23.

125. Arbustini E, Dal Bello B, Morbini P, Burke a P, Bocciarelli M, Specchia G, et al. Plaque erosion is a major substrate for coronary thrombosis in acute myocardial infarction. Heart. 1999;82(3):269–72.

126. Burke AP, Farb A, Malcom GT, Liang Y, Smialek J, Virmani R. Effect of Risk Factors on the Mechanism of Acute Thrombosis and Sudden Coronary Death in Women. Circulation. 1998 Jun 2;97(21):2110 LP-2116.

127. Souteyrand G, Arbustini E, Motreff P, Gatto L, Vito L Di, Marco V, et al. Serial optical coherence tomography imaging of ACS-causing culprit plaques.

2015;319–24.

128. Berrahmoune H, Lamont J V, Herbeth B, FitzGerald PS, Visvikis-Siest S. Biological Determinants of and Reference Values for Plasma Interleukin-8, Monocyte Chemoattractant Protein-1, Epidermal Growth Factor, and Vascular Endothelial Growth Factor: Results from the STANISLAS Cohort. Clin Chem. 2006 Feb;52(3):504 LP-510.

129. Barclay JL, Keshvari S, Whitehead JP, Inder WJ. Development of an enzyme-linked immunosorbent assay for thrombospondin-1 and comparison of human plasma and serum concentrations. Ann Clin Biochem An Int J Biochem Lab Med . 2016 Sep;53(5):606–10.

130. Kao J, Kobashigawa J, Fishbein MC, Robb MacLellan W, Burdick MD, Belperio JA, et al. Elevated serum levels of the CXCR3 chemokine ITAC are associated with the development of transplant coronary artery disease. Circulation. 2003;107(15):1958–61.

131. Wong RWC, Guillaud L. The role of epidermal growth factor and its receptors in mammalian CNS. Cytokine and Growth Factor Reviews. 2004. p. 147–56.

132. Wieduwilt MJ, Moasser MM. The epidermal growth factor receptor family: Biology driving targeted therapeutics. Cellular and Molecular Life Sciences. 2008. p. 1566–84.

133. Arteaga CL, Engelman JA. ERBB receptors: From oncogene discovery to basic science to mechanism-based cancer therapeutics. Cancer Cell. 2014. p. 282–303.

134. Makki N, Thiel KW, Miller FJ. The epidermal growth factor receptor and its ligands in cardiovascular disease. International Journal of Molecular Sciences. 2013. p. 20597–613.

135. Ko Y, Haring R, Stiebler H, Wieczorek AJ, Vetter H, Sachinidis A. High-density lipoprotein reduces epidermal growth factor-induced DNA synthesis in vascular smooth muscle cells. Atherosclerosis. 1993;99(2):253–9.

136. Gui Y, Zheng XL. Epidermal growth factor induction of phenotype-dependent cell cycle arrest in vascular smooth muscle cells is through the mitogen-activated protein kinase pathway. J Biol Chem. 2003;278(52):53017–25.

137. Dreux AC, Lamb DJ, Modjtahedi H, Ferns GAA. The epidermal growth factor receptors and their family of ligands: Their putative role in atherogenesis. Atherosclerosis. 2006;186(1):38–53.

138. Forrester SJ, Kawai T, O'Brien S, Thomas W, Harris RC, Eguchi S. Epidermal Growth Factor Receptor Transactivation: Mechanisms, Pathophysiology, and Potential Therapies in the Cardiovascular System. Annu Rev Pharmacol Toxicol. 2016;56(1):annurev-pharmtox-070115-095427.

139. Kagiyama S, Eguchi S, Frank GD, Inagami T, Zhang YC, Phillips MI. Angiotensin II-induced cardiac hypertrophy and hypertension are attenuated by epidermal growth factor receptor antisense. Circulation. 2002;106(8):909–12.

140. Chan AK, Kalmes A, Hawkins S, Daum G, Clowes AW. Blockade of the epidermal growth factor receptor decreases intimal hyperplasia in balloon-injured rat carotid artery. J Vasc Surg. 2003;37(3):644–9.

141. Sánchez-Vizcaíno E, Vehí C, Campreciós G, Morcillo C, Soley M, Ramírez I. Heparin-binding EGF-like growth factor in human serum. Association with high blood cholesterol and heart hypertrophy. Growth Factors. Taylor & Francis; 2010 Apr 1;28(2):98–103.

142. Rattik S, Wigren M, Björkbacka H, Fredrikson GN, Hedblad B, Siegbahn A, et al. High plasma levels of heparin-binding epidermal growth factor are associated with a more stable plaque phenotype and reduced incidence of coronary events. Arterioscler Thromb Vasc Biol. 2015;35(1):222–8.

143. Adams JC, Lawler J. The Thrombospondins. Cold Spring Harb Perspect Biol. 2011;3(10):a009712–a009712.

144. Murphy-Ullrich JE, Hook M. Thrombospondin modulates focal adhesions in endothelial cells. J Cell Biol. 1989;109(3):1309–19.

145. Bagavandoss P, Wilks JW. Specific inhibition of endothelial cell proliferation by thrombospondin. BiochemBiophysResCommun. 1990;170(2):867–72.

146. Rostama B, Turner JE, Seavey GT, Norton CR, Gridley T, Vary CPH, et al. DLL4/Notch1 and BMP9 Interdependent Signaling Induces Human Endothelial Cell Quiescence via P27KIP1 and Thrombospondin-1.

Arterioscler Thromb Vasc Biol . 2015 Dec 1;35(12):2626–37.

147. Guo NH, Krutzsch HC, Inman JK, Roberts DD. Thrombospondin 1 and type I repeat peptides of thrombospondin 1 specifically induce apoptosis of endothelial cells. Cancer Res. 1997;57(9):1735–42.

148. Jiménez B, Volpert O V, Crawford SE, Febbraio M, Silverstein RL, Bouck N. Signals leading to apoptosis-dependent inhibition of neovascularization by thrombospondin-1. Nat Med. 2000;6(1):41–8.

149. Smadja DM, d'Audigier C, Bièche I, Evrard S, Mauge L, Dias J-V, et al. Thrombospondin-1 Is a Plasmatic Marker of Peripheral Arterial Disease That Modulates Endothelial Progenitor Cell Angiogenic Properties. Arterioscler Thromb Vasc Biol . 2011 Mar 1;31(3):551–9.

150. Bauer EM, Qin Y, Miller TW, Bandle RW, Csanyi G, Pagano PJ, et al. Thrombospondin-1 supports blood pressure by limiting eNOS activation and endothelial-dependent vasorelaxation. Cardiovasc Res. 2010;88(3):471–81.

151. Majack R a, Cook SC, Bornstein P. Control of smooth muscle cell growth by components of the extracellular matrix: autocrine role for thrombospondin. Proc Natl Acad Sci U S A. 1986;83(23):9050–4.

152. Yabkowitz R, Dixit VM, Guo N, Roberts DD, Shimizu Y. Activated T-cell adhesion to thrombospondin is mediated by the alpha 4 beta 1 (VLA-4) and alpha 5 beta 1 (VLA-5) integrins. J Immunol. 1993;151(1):149–58.

153. Roth JJ, Gahtan V, Brown JL, Gerhard C, Swami VK, Rothman VL, et al. Thrombospondin-1 is elevated with both intimal hyperplasia and hypercholesterolemia. J Surg Res. 1998;74(1):11–6.

154. Stouffer GA, Hu Z, Sajid M, Li H, Jin G, Nakada MT, et al. Beta3 integrins are upregulated after vascular injury and modulate thrombospondin- and thrombin-induced proliferation of cultured smooth muscle cells. Circulation. 1998;97(9):907–15.

155. Chen D, Asahara T, Krasinski K, Witzenbichler B, Yang J, Magner M, et al. Antibody blockade of thrombospondin accelerates reendothelialization and reduces neointima formation in balloon-injured rat carotid artery. Circulation. 1999;100(8):849–54.

156. Isenberg JS, Wink DA, Roberts DD. Thrombospondin-1 antagonizes nitric oxide-stimulated vascular smooth muscle cell responses. Cardiovasc Res. 2006;71(4):785–93.

157. Bonnefoy A, Legrand C. Proteolysis of subendothelial adhesive glycoproteins (fibronectin, thrombospondin, and von Willebrand factor) by plasmin, leukocyte cathepsin G, and elastase. Thromb Res. 2000;98(4):323–32.

158. Bonnefoy A, Daenens K, Feys HB, De Vos R, Vandervoort P, Vermylen J, et al. Thrombospondin-1 controls vascular platelet recruitment and thrombus adherence in mice by protecting (sub)endothelial VWF from cleavage by ADAMTS13. Blood. 2006;107(3):955–64.

159. Zhang X-J, Wei C-Y, Li W-B, Zhang L-L, Zhou Y, Wang Z-H, et al. Association between single nucleotide polymorphisms in thrombospondins genes and coronary artery disease: A meta-analysis. Thromb Res. 2015;136(1):45–51.

160. Burke A, Creighton W, Tavora F, Li L, Fowler D. Decreased frequency of the 3'UTR T>G single nucleotide polymorphism of thrombospondin-2 gene in sudden death due to plaque erosion. Cardiovasc Pathol. Elsevier B.V.; 2010;19(3):e45–9.

161. Cole KE, Strick CA, Paradis TJ, Ogborne KT, Loetscher M, Gladue RP, et al. Interferon-inducible T cell alpha chemoattractant (I-TAC): a novel non-ELR CXC chemokine with potent activity on activated T cells through selective high affinity binding to CXCR3. J Exp Med. 1998;187(12):2009–21.

162. Hansson GK, Jonasson L, Lojsthed B, Stemme S, Kocher O, Gabbiani G. Localization of T lymphocytes and macrophages in fibrous and complicated human atherosclerotic plaques. Atherosclerosis. 1988;72(2–3):135–41.

163. Saxena A, Bujak M, Frunza O, Dobaczewski M, Gonzalez-Quesada C, Lu B, et al. CXCR3-independent actions of the CXC chemokine CXCL10 in the infarcted myocardium and in isolated cardiac fibroblasts are mediated through proteoglycans. Cardiovasc Res. 2014;103(2):217–27.

164. Van Kanegan MJ, He DN, Dunn DE, Yang P, Newman R a, West AE, et al. BDNF mediates neuroprotection against oxygen-glucose deprivation by the

cardiac glycoside oleandrin. J Neurosci. 2014;34(3):963–8.

165. Numakawa T, Suzuki S, Kumamaru E, Adachi N, Richards M, Kunugi H. BDNF function and intracellular signaling in neurons. Histology and Histopathology. 2010. p. 237–58.

166. Donovan MJ, Lin MI, Wiegn P, Ringstedt T, Kraemer R, Hahn R, et al. Brain derived neurotrophic factor is an endothelial cell survival factor required for intramyocardial vessel stabilization. Development. 2000;127(21):4531–40.

167. Larsson E, Nanobashvili a, Kokaia Z, Lindvall O. Evidence for neuroprotective effects of endogenous brain-derived neurotrophic factor after global forebrain ischemia in rats. J Cereb Blood Flow Metab. 1999;19(11):1220–8.

168. Okada S, Yokoyama M, Toko H, Tateno K, Moriya J, Shimizu I, et al. Brain-derived neurotrophic factor protects against cardiac dysfunction after myocardial infarction via a central nervous system-mediated pathway. Arterioscler Thromb Vasc Biol. 2012;32(8):1902–9.

169. Halade G V, Ma Y, Ramirez T a, Zhang J, Dai Q, Hensler JG, et al. Reduced BDNF attenuates inflammation and angiogenesis to improve survival and cardiac function following myocardial infarction in mice. Am J Physiol Heart Circ Physiol. 2013;305(41):H1830-42.

170. Donovan M, Lin M, Wiegn P, Ringstedt T, Kraemer R, Hahn R, et al. Brain derived neurotrophic factor is an endothelial cell survival factor required for intramyocardial vessel stabilization. Development. 2000;127(21):4531–40.

171. Brown DL, Hibbs MS, Kearney M, Loushin C, Isner JM. Identification of 92-kD gelatinase in human coronary atherosclerotic lesions. Association of active enzyme synthesis with unstable angina. Circulation. 1995.

172. Wågsäter D, Zhu C, Björkegren J, Skogsberg J, Eriksson P. MMP-2 and MMP-9 are prominent matrix metalloproteinases during atherosclerosis development in the Ldlr(-/-)Apob(100/100) mouse. Int J Mol Med. 2011;28(2):247–53.

173. Gough PJ, Gomez IG, Wille PT, Raines EW. Macrophage expression of active MMP-9 induces acute plaque disruption in apoE-deficient mice. J Clin Invest.

2006;116(1):59–69.

174. Blankenberg S, Rupprecht HJ, Poirier O, Bickel C, Smieja M, Hafner G, et al. Plasma concentrations and genetic variation of matrix metalloproteinase 9 and prognosis of patients with cardiovascular disease. Circulation. 2003;107(12):1579–85.

175. Etoh T, Joffs C, Deschamps a M, Davis J, Dowdy K, Hendrick J, et al. Myocardial and interstitial matrix metalloproteinase activity after acute myocardial infarction in pigs. Am J Physiol Heart Circ Physiol. 2001;281(3):H987–94.

176. Romanic AM, Burns-Kurtis CL, Gout B, Berrebi-Bertrand I, Ohlstein EH. Matrix metalloproteinase expression in cardiac myocytes following myocardial infarction in the rabbit. Life Sci. 2001;68(7):799–814.

177. Miller MD, Krangel MS. Biology and biochemistry of the chemokines: a family of chemotactic and inflammatory cytokines. Crit Rev Immunol. 1992;12(1–2):17–46.

178. Loetscher M, Gerber B, Loetscher P, Jones S a, Piali L, Clark-Lewis I, et al. Chemokine receptor specific for IP10 and mig: structure, function, and expression in activated T-lymphocytes. J Exp Med. 1996;184(3):963–9.

179. Frostegård J, Ulfgren AK, Nyberg P, Hedin U, Swedenborg J, Andersson U, et al. Cytokine expression in advanced human atherosclerotic plaques: Dominance of pro-inflammatory (Th1) and macrophage-stimulating cytokines. Atherosclerosis. 1999;145(1):33–43.

180. Fernandes JL, Mamoni RL, Orford JL, Garcia C, Selwyn AP, Coelho OR, et al. Increased Th1 activity in patients with coronary artery disease. Cytokine. 2004;26(3):131–7.

181. Talvani A, Ribeiro CS, Aliberti JCS, Michailowsky V, Santos PVA, Murta SMF, et al. Kinetics of cytokine gene expression in experimental chagasic cardiomyopathy: Tissue parasitism and endogenous IFN-γ as important determinants of chemokine mRNA expression during infection with Trypanosoma cruzi. Microbes Infect. 2000;2(8):851–66.

182. Hardison JL, Wrightsman RA, Carpenter PM, Lane TE, Manning JE. The

chemokines CXCL9 and CXCL10 promote a protective immune response but do not contribute to cardiac inflammation following infection with Trypanosoma cruzi. Infect Immun. 2006;74(1):125–34.

183. Brennan M-L, Penn MS, Van Lente F, Nambi V, Shishehbor MH, Aviles RJ, et al. Prognostic value of myeloperoxidase in patients with chest pain. N Engl J Med. 2003;349(17):1595–604.

184. Svilaas T, van der Horst IC, Zijlstra F. Thrombus Aspiration during Percutaneous coronary intervention in Acute myocardial infarction Study (TAPAS)--study design. Am Hear J. 2006;151(3):597.e1-597.e7.

185. Burkhart JM, Gambaryan S, Watson SP, Jurk K, Walter U, Sickmann A, et al. What Can Proteomics Tell Us About Platelets? Circ Res. 2014;114(7):1204–19.

186. Jaumdally R, Varma C, Macfadyen RJ, Lip GYH. Coronary sinus blood sampling : an insight into local cardiac pathophysiology and treatment ? 2007;929–40.

187. Lantos J, Temes G, Göbölös L, Jaberansari MT, Roth E. Is peripheral blood a reliable indicator of acute oxidative stress following heart ischemia and reperfusion? Med Sci Monit. 2001;7(6):1166–70.

188. Craft J a, Masci PP, Roberts MS, Brighton T a, Garrahy P, Cox S, et al. Increased platelet-derived microparticles in the coronary circulation of percutaneous transluminal coronary angioplasty patients. Blood Coagul Fibrinolysis. 2004;15(6):475–82.

189. Watkins MW, Luetmer PA, Schneider DJ, Witmer WT, Vaitkus PT, Sobel BE. Determinants of rebound thrombin activity after cessation of heparin in patients undergoing coronary interventions. Cathet Cardiovasc Diagn. 1998;44(3):257–66.

190. Nichols AB, Owen J, Grossman BA, Marcella JJ, Fleisher LN, Lee MM. Effect of heparin bonding on catheter-induced fibrin formation and platelet activation. Circulation. 1984;70(5):843–50.

191. Ko Y, Jung J, Park S, Choi E, Joung B. Inflammatory and vasoactive factors in the aspirate from the culprit coronary artery of patients with acute

myocardial infarction. Int J Cardiol. 2006;112:66–71.

192. Thum T. MicroRNA therapeutics in cardiovascular medicine. EMBO Molecular Medicine. 2012. p. 3–14.

193. Fichtlscherer S, Zeiher AM, Dimmeler S. Circulating MicroRNAs: Biomarkers or mediators of cardiovascular diseases? Arterioscler Thromb Vasc Biol. 2011;31(11):2383–90.

194. D'Alessandra Y, Devanna P, Limana F, Straino S, Di Carlo A, Brambilla PG, et al. Circulating microRNAs are new and sensitive biomarkers of myocardial infarction. Eur Heart J. 2010;31(22):2765–73.

195. Cheng Y, Tan N, Yang J, Liu X, Cao X, He P, et al. A translational study of circulating cell-free microRNA-1 in acute myocardial infarction. Clin Sci (Lond). 2010;119(2):87–95.

196. Ji X, Takahashi R, Hiura Y, Hirokawa G, Fukushima Y, Iwai N. Plasma miR-208 as a biomarker of myocardial injury. Clin Chem. 2009;55(11):1944–9.

197. Leistner DM, Boeckel J, Reis SM, Thome CE, Rosa R De, Keller T, et al. Transcoronary gradients of vascular miRNAs and coronary atherosclerotic plaque characteristics. 2016;

198. Wykrzykowska JJ, Garcia-Garcia HM, Goedhart D, Zalewski A, Serruys PW. Differential protein biomarker expression and their time-course in patients with a spectrum of stable and unstable coronary syndromes in the Integrated Biomarker and Imaging Study-1 (IBIS-1). Int J Cardiol. Elsevier; 2017 Jul 2;149(1):10–6.

199. Lindroos PM, Zarnegar R, Michalopoulos GK. Hepatocyte growth factor (hepatopoietin A) rapidly increases in plasma before DNA synthesis and liver regeneration stimulated by partial hepatectomy and carbon tetrachloride administration. Hepatology. 1991;13:743–50.

200. Rappolee DA, Iyer A, Patel Y. Hepatocyte growth factor and its receptor are expressed in cardiac myocytes during early cardiogenesis. Circ Res. 1996;78(6):1028–36.

201. Matsumori a, Furukawa Y, Hashimoto T, Ono K, Shioi T, Okada M, et al. Increased circulating hepatocyte growth factor in the early stage of acute

myocardial infarction. Biochemical and biophysical research communications. 1996. p. 391–5.

202. Matsumoto K, Tajima H, Okazaki H, Nakamura T. Heparin as an inducer of hepatocyte growth factor. J Biochem. 1993;114(6):820–6.

203. Seidel C, Hjorth-Hansen H, Bendz B, Borset M, Sandset PM, Hansen JB, et al. Hepatocyte growth factor in serum after injection of unfractionated and low molecular weight heparin in healthy individuals. Br J Haematol. 1999;105(3):641–7.

204. Fannon M, Forsten KE, Nugent MA. Potentiation and inhibition of bFGF binding by heparin: A model for regulation of cellular response. Biochemistry. 2000;39(6):1434–45.

205. Jordan WJ, Eskdale J, Boniotto M, Lennon GP, Peat J, Campbell JDM, et al. Human IL-19 regulates immunity through auto-induction of IL-19 and production of IL-10. Eur J Immunol. 2005;35(5):1576–82.

206. Jain S, Gabunia K, Kelemen SE, Panetti TS, Autieri M V. The anti-inflammatory cytokine interleukin 19 is expressed by and angiogenic for human endothelial cells. Arterioscler Thromb Vasc Biol. 2011;31(1):167–75.

207. Sallusto F, Lanzavecchia a. Understanding dendritic cell and T-lymphocyte traffic through the analysis of chemokine receptor expression. Immunol Rev. 2000;177(1):134–40.

208. Mathes AL, Christmann RB, Stifano G, Affandi AJ, Radstake TRDJ, Farina GA, et al. Global chemokine expression in systemic sclerosis (SSc): CCL19 expression correlates with vascular inflammation in SSc skin. Ann Rheum Dis. 2013;73(10):1–9.

209. Jia H, Abtahian F, Aguirre AD, Lee S, Chia S, Lowe H, et al. In vivo diagnosis of plaque erosion and calcified nodule in patients with acute coronary syndrome by intravascular optical coherence tomography. J Am Coll Cardiol. 2013;62(19):1748–58.

210. Ridker PM, Howard CP, Walter V, Everett B, Libby P, Hensen J, et al. Effects of interleukin-1β inhibition with canakinumab on hemoglobin A1c, lipids, C-reactive protein, interleukin-6, and fibrinogen a phase IIb randomized,

placebo-controlled trial. Circulation. 2012;126(23):2739–48.

211. Ibanez B, James S, Agewall S, Antunes MJ, Bucciarelli-Ducci C, Bueno H, et al. 2017 ESC Guidelines for the management of acute myocardial infarction in patients presenting with ST-segment elevation. Eur Heart J. 2017;(November):1–66.

212. Jolly SS, Cairns J a, Yusuf S, Meeks B, Pogue J, Rokoss MJ, et al. Randomized trial of primary PCI with or without routine manual thrombectomy. N Engl J Med. 2015;372(15):1389–98.

213. Cahill PA, Redmond EM. Vascular endothelium - Gatekeeper of vessel health. Atherosclerosis. 2016. p. 97–109.

214. Schwartzenberg S, Deutsch V, Maysel-Auslender S, Kissil S, Keren G, George J. Circulating apoptotic progenitor cells: A novel biomarker in patients with acute coronary syndromes. Arterioscler Thromb Vasc Biol. 2007;27(5).

215. Schmidt-Lucke C, Fichtlscherer S, Aicher A, Tschöpe C, Schultheiss HP, Zeiher AM, et al. Quantification of circulating endothelial progenitor cells using the modified ISHAGE Protocol. PLoS One. 2010;5(11).

216. Werner N, Kosiol S, Schiegl T, Ahlers P, Walenta K, Link A, et al. Circulating endothelial progenitor cells and cardiovascular outcomes. N Engl J Med. 2005;353(10):999–1007.

217. Bernal-Mizrachi L, Jy W, Jimenez JJ, Pastor J, Mauro LM, Horstman LL, et al. High levels of circulating endothelial microparticles in patients with acute coronary syndromes. Am Heart J. 2003;145(6):962–70.

218. Sinning JM, Losch J, Walenta K, Böhm M, Nickenig G, Werner N. Circulating CD31 +/Annexin V + microparticles correlate with cardiovascular outcomes. Eur Heart J. 2011;32(16):2034–41.

219. Regueiro A, Cuadrado-Godia E, Bueno-Betí C, Diaz-Ricart M, Oliveras A, Novella S, et al. Mobilization of endothelial progenitor cells in acute cardiovascular events in the PROCELL study: Time-course after acute myocardial infarction and stroke. J Mol Cell Cardiol. 2015;80:146–55.

220. Xu F, Sun Y, Chen Y, Sun Y, Li R, Liu C, et al. Endothelial cell apoptosis is responsible for the formation of coronary thrombotic atherosclerotic plaques.

Tohoku J Exp Med. 2009;218(1):25–33.

APPENDIX

TABLE OF CONTENTS

1.0 Research and ethics committee letter of approval

NHS
Health Research Authority
NRES Committee London - Camden & Islington
Room 001
Jarrow Business Centre
Rolling Mill Road
Jarrow
Tyne & Wear
NE32 3DT

Telephone: 0191 428 3476

24 November 2014

Dr Alisdair Ryding
Norfolk and Norwich University Hospital NHS Foundation Trust
Department of Cardiology
Norfolk and Norwich University Hospital
Level 3, East Block
Norwich
NR4 7UY

Dear Dr Ryding

Study title:	**Plaque Erosion Pilot Study: A single centre, prospective observational pilot study comparing the molecular biology of plaque rupture and plaque erosion in patients with ST elevation myocardial infarction undergoing Primary PCI.**
REC reference:	**14/LO/1901**
IRAS project ID:	**161361**

Thank you for your letter of 17 November 2014, responding to the Committee's request for further information on the above research and submitting revised documentation.

The further information has been considered on behalf of the Committee by the Chair and Committee Member, Dr Andy Petros.

We plan to publish your research summary wording for the above study on the HRA website, together with your contact details. Publication will be no earlier than three months from the date of this opinion letter. Should you wish to provide a substitute contact point, require further information, or wish to make a request to postpone publication, please contact the REC Assistant, Miss Donna Bennett, nrescommittee.london-camdenandislington@nhs.net.

Confirmation of ethical opinion

On behalf of the Committee, I am pleased to confirm a favourable ethical opinion for the above research on the basis described in the application form, protocol and supporting documentation as revised, subject to the conditions specified below.

2.0 Patient information sheet and consent form

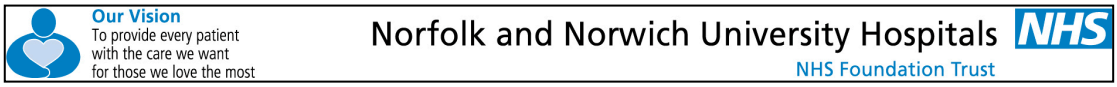

Title: The PEP Study – Plaque Erosion Pilot Study

PEPS: A single-centre, prospective observational pilot study comparing the molecular biology of plaque rupture and plaque erosion in patients with ST Elevation Myocardial Infarction undergoing primary PCI.

Information sheet for PEP Study patients

PART 1

1. Invitation

You are being invited to take part in a research study called 'The PEP study'. Before you decide, it is important for you to know why the research is being done and what it will involve. Please take time to read the following information carefully. Feel free to discuss it with others if you wish.

Part 1 tells you the purpose of this study and what will happen to you if you take part.

Part 2 gives you more detailed information about the conduct of the study.

Ask us if there is anything that is not clear or if you want more information. Take your time to decide if you wish to participate.

2. Aim of the study

The aim of this study is to investigate the different causes of heart attack.

3. What is the purpose of the study?

The study is being conducted in patients who have had a heart attack. We know that heart attacks are caused by the sudden blockage of an artery supplying blood to the heart. In most cases, the artery is furred up due to fatty material, known as atherosclerosis. In about two-thirds of heart attacks, the fatty material suddenly bursts (known as plaque rupture) and this triggers a blood clot that blocks the artery.

In the other one-third of cases, there appears to be a more subtle trigger for clotting/blockage (known as plaque erosion). Very little is known about the causes of this, and the purpose of this study is to improve our understanding. Eventually, this may help us to improve the treatment and prevention of heart attacks in the future.

4. Why have I been invited?

You have just suffered a heart attack, and an emergency procedure to unblock one of your heart arteries has been successfully performed. During this procedure the doctor removed a blood clot from the blocked artery as well as a small amount of blood. Normally, this is discarded, but in your case, we have stored the samples so that, with your permission, we can analyse these for specific molecules that we think might be important. In addition, we have taken very detailed pictures of the inside of one of your heart arteries using a special camera, so that we can work out what triggered the heart attack.

5. Do I have to take part?

No. Your participation in this study is entirely voluntary and you are under no pressure to take part. If you agree to enter the study and later change your mind, you may withdraw from the study at any time, without affecting your routine treatment or care in any way.

6. What will happen to me if I take part?

A member of the research team will talk to you about the study to see if you are interested in taking part. If you say yes, you will be provided with this patient information sheet, which you should read and discuss with your family and friends. If you are still interested in taking part you will be asked to give written consent about 24 hours later. Your blood samples and heart artery pictures from the procedure will then be retained and analysed for research purposes.

Before you are discharged you will have a comprehensive medical history and clinical examination, blood tests to assess the degree of heart damage, electrocardiograms (ECG) and an echocardiogram, which are part of normal clinical practice.

After you have been discharged home, a member of the research team will contact you on the telephone at intervals of three, six and twelve months to see how you are managing following your heart attack. Each telephone conversation will last for anything between five to fifteen minutes. We will discuss whether you have encountered any symptoms such as chest pain, shortness of breath or any other medical problems you may have encountered since your heart attack. If we cannot contact you for any reason, we may contact your GP for the same information.

You will not need to re-attend the hospital after you have been discharged for the purposes of the research study.

7. Expenses and payments

There are no payments for taking part in this study. You will not incur any expenses by participating in this study.

8. What will I have to do?

If you participate in this study, we will analyse your blood samples and heart artery pictures. You will not have to do anything, but we will contact you over the telephone for updates on your health. Apart from this, you will receive the same treatment as someone who has had similar treatment for a heart attack but is not participating in the study.

9. What are the possible disadvantages and risks of taking part

There are no obvious disadvantages or risks to taking part in this study.
The emergency treatment that you have received is essentially the same as you would otherwise have received if you had not been in this study. The only differences are that more detailed pictures of your heart arteries were taken, and the blood clot/blood samples removed from your blocked artery have been saved for analysis. These procedures are often used as part of standard care in selected cases, and do not add any significant risk to the procedure with only a minor increase in your exposure to x-rays.
No aspect of this study will compromise or delay your treatment. Also, it should not unnecessarily inconvenience you after discharge.

10. What are the possible benefits of taking part?

We cannot guarantee any personal benefit from participating in this study. However, if you participate in this study you will have the advantage that your health and your heart will be monitored more closely than patients who do not take part.

By taking part in this study you will also be contributing to the improvement and understanding of patients who present with acute heart attacks.

11. What if there is a problem?

Any complaint about the way you have been treated during the study or any possible harm you might suffer will be addressed. (Further detailed information in Part 2.)

12. Will my taking part in this study be kept confidential?

Yes. All the information about your participation in this study will be kept confidential. The details are included in Part 2.

Thank you for taking the time to read this.

This completes Part 1 of the Information Sheet.

If the information in Part 1 has interested you and you are considering participating, please read the additional information in Part 2 before making a decision.

PART 2

1. What if relevant new information becomes available?

The study will be scrutinised by an independent data monitoring committee. Its role is to check that the study is run correctly and to ensure that patients remain safe. If this committee or the research doctors hear of relevant new information during the course of this study, they will tell you about it. If the study is stopped for any reason, we will tell you and arrange for your care to continue.

2. What will happen if I don't want to carry on with the study?

If you wish us to stop collecting your medical information then we will do so. However, we will need to use the information collected up until the time that you decided to withdraw from the study, unless you tell us you want all your information withdrawn.

3. What if there is a problem?

If you are concerned about any aspect of this study, you should ask to speak to one of the researchers who will do their best to answer your questions.

If you remain unhappy and wish to complain formally, you can do this through the NHS Complaints Procedure. Details can be obtained from the Patient Advice and Liaison Service (PALS) (01603 289036).

If something goes wrong and you are harmed during the study due to someone's negligence, then you may have grounds for a legal action for compensation against the hospital involved, but you may have to pay your legal costs. The normal NHS complaints mechanisms will still be available to you.

NHS hospitals are unable to agree in advance to pay compensation for non-negligent harm (situations where no one can be blamed for what happened). However, NHS Trusts are able to consider offering an ex gratia payment in the case of a claim.

4. Will my taking part in this study be kept confidential?

All information that is collected about you during the course of this study will be kept strictly confidential according to the Data Protection Act 1998. Information on paper will be kept in locked filing cabinets and, where possible, behind security-coded, locked doors. Electronic information will be kept on computers that are protected by passwords.

The electronic data we store for this study will be kept on a database. You will be assigned a unique study code in place of your name. Only members of the research team will have

access to your name and address from the study code, so that you can be contacted as part of the follow-up.

Any information about you that leaves the hospital will be anonymous and anything that could identify you (name, date of birth, address, hospital number) will be removed and you will only be identified by a study code. When the study is reported to the funding body, published in medical journals or presented at conferences, it will not be possible to identify you personally.

Representatives from regulatory authorities may need to look at your medical records and the data collected in the study to check that the study was carried out correctly. All will have a duty of confidentiality to you.

6. What will happen to the results of the research study?

Once the study is complete and analysed, the results will be submitted for publication in a scientific journal and presented at scientific conferences. Your confidentiality will be maintained and you will not be identified in any report or publication of this study. If you wish to see the results when they are published, let the researcher who obtains consent from you know and a copy of the results can be sent to you.

7. Who is organising and funding the research?

The research is organised and sponsored by Norfolk and Norwich University Hospitals NHS Trust.

8. Who has reviewed the study?

The study was reviewed by independent experts and has been given a favourable ethical opinion by the NRES Committee London – Camden and Islington Research Ethics Committee. It has been reviewed and gained Trust approval from Norfolk and Norwich University Hospital Research & Development Department.

9. Further information and contact details

If you have any questions about this study please contact:

Co-investigator: Dr Sujay Chandran, Cardiology Research Fellow

Norfolk and Norwich University Hospital, Colney Lane, Norwich, Norfolk

NR 4 7UY. United Kingdom

Local Principal Investigator contact details: Dr Alisdair Ryding 01603 387930

Thank you for considering taking part in this study.

If you decide to participate, you will be asked to sign a consent form and will be given a copy of this information sheet and the consent form to keep.

Consent Form

Study Title: *Plaque Erosion Pilot Study* – PEP Study

Study Number: 2014CARD06L

Principal Investigator: *Dr Alisdair Ryding*

Patient name:	CRF ID:

	Please read the following statements and put your initials in the box to show that you have read and understood them and that you agree with them.	**Please initial each box**
1	I confirm that I have read and understand the information sheet dated 3 September 2014 for the above study. I have had the opportunity to consider the information, ask questions and have had these answered satisfactorily.	
2	I understand that my involvement is voluntary and that I am free to withdraw at any time, without giving any reason and without my medical care or legal rights being affected.	
3	I understand that relevant sections of any of my medical notes and data collected during the study may be looked at by responsible individuals from the Sponsor or authorised by the Sponsor, from regulatory authorities or from the NHS Trust, where it is relevant to my taking part in this research. I give permission for these individuals to have access to my records.	
4	I understand that a member of the research team will contact my GP informing them of my participation the study.	

5	I understand that if I withdraw from the study early, or the study staff are unable to contact me, the study site (study doctor and/or staff) would like permission to make the following contacts. **PLEASE TICK THE BOXES IF YOU AGREE:** ☐ The study site has my permission to contact me to collect information or to review publically available records (if available and allowed by local law) on how I am doing at what would have been the end of the study. ☐ The study site has my permission to contact my GP (General Practitioner) who will review my medical records and tell the study staff how I am doing at what would have been the end of the study.	☐
6	In the event that I withdraw from the study early, I understand that the information collected about me cannot and will not be used in the study.	☐

To be filled in by the patient

I agree to take part in the above study

Your name **Date** (Day/Month/Year) e.g. 14/July/2006) **Signature**

To be filled in by the person obtaining consent (investigator)

I confirm that I have explained the nature, purposes and possible effects of the research study to the person whose name is printed above. They agreed to take part by signing and dating above.

Name of Investigator (or person obtaining consent if different from Investigator)

Date (Day/Month/Year) e.g. 14/July/2006)

Signature

Impartial Witness

*At least one **impartial** witness is mandatory when the patient is unable to read or write. An **impartial** witness must be present during the entire informed consent discussion.*

I confirm that the information in the consent form was accurately explained to, and apparently understood by, the patient, and that consent was freely given by the patient.

Name of Impartial Witness

Date (Day/Month/Year) e.g. 14/July/2006)

Signature

Instructions to Study Staff

- File one copy in the patient's notes
- File one copy in the trial folder
- Give one copy to the patient

3.0 List of cytokines from Proteome Profiler™ Human XL Cytokine Array Kit (R&D Systems, Abingdon, UK) ARY022

Adiponectin/Acrp30

Aggrecan

Angiogenin

Angiopoietin-1

Angiopoietin-2

BAFF/BLyS/TNFSF13B – B-cell activating factor/B lymphocyte stimulator/tumor necrosis factor ligand SuperFamily member 13B

BDNF – Brain-derived neurotrophic factor

C5a – Complement factor 5a

CCL2/MCP-1 – CC chemokine ligand 2/monocyte chemoattractant protein-1
CCL3/CCL4 (MIP-1α/ MIP-1β) – CC chemokine ligand 3/chemokine ligand 4 (macrophage inflammatory protein-1α/macrophage inflammatory protein 1β
CCL5/RANTES – CC chemokine ligand 5/regulated on activation normal T-cell expressed and secreted

CCL7/MCP-3 – CC chemokine ligand 7/monocyte chemoattractant protein-3
CCL17/TARC – CC chemokine ligand 17/thymus-and activation-regulated chemokine

CCL19/MIP-3β – CC chemokine ligand 19/macrophage inflammatory protein-3β
CCL20/MIP-3α – CC chemokine ligand 20/macrophage inflammatory protein-3α
CD14 - Cluster of differentiation 14

CD30/TNFRSF8 – Cluster of differentiation 30/tumour necrosis factor ligand SuperFamily member 8

CD40 Ligand/TNFSF5 – Cluster of differentiation 40/tumour necrosis factor ligand SuperFamily member 5

Chitinase 3-like 1, Complement Factor D, CRP – C-reactive protein, Cripto-1
CXCL1/GROa – CXC chemokine ligand 1/growth-regulated protein α

CXCL4/PF4 – CXC chemokine ligand 4/platelet factor 4

CXCL5/ENA-78 – CXC chemokine ligand 5/epithelial neutrophil-activating peptide-78

CXCL8/IL-8 CXC chemokine ligand 8/interleukin-8

CXCL9/MIG – CXC chemokine ligand 9/monokine induced by interferon-gamma
CXCL10/IP-10 – CXC chemokine ligand 10/interferon gamma-induced protein 10
CXCL11/ I-TAC – CXC chemokine ligand 11/interferon-inducible T-cell alpha chemoattractant

CXCL12/SDF-1a - CXC chemokine ligand 12/stromal cell-derived factor 1 cystatin C

Dkk-1 – Dickkopf-related protein-1

DPPIV/CD26 – Dipeptidyl peptidase 4/cluster of differentiation 26

EGF – Epidermal growth factor

Endoglin/CD105 – Cluster of differentiation 105

EMMPRIN/CD147 – Extracellular matrix metalloproteinase inducer/cluster of differentiation 147

Fas Ligand/TNFSF6 - Tumour necrosis factor ligand SuperFamily member 6

FGF basic – Fibroblast growth factor basic

KGF/FGF-7 – Keratinocyte growth factor/fibroblast growth factor-19

FGF-19 – Fibroblast growth factor-19,

Flt-3 Ligand – Fms-related tyrosine kinase 3 ligand

G-CSF – Granulocyte-colony stimulating factor

GDF-15 – Growth differentiation factor-15

GM-CSF – Granulocyte-macrophage colony-stimulating factor

Growth hormone

HGF – Hepatocyte growth factor

ICAM-1/CD54 – Intercellular adhesion molecule-1/cluster of differentiation 54

IFN-γ – Interferon-γ

IGFBP-2 – Insulin-like growth factor binding protein-2

IGFBP-3 – Insulin-like growth factor binding protein-3

IL-1α /IL-1F1 – Interleukin-1α

IL-1β/IL-1F2 – Interleukin-1β

IL-1ra/IL-1F3 – Interleukin-1 receptor antagonist

IL-2 – Interleukin-2

IL-3 – Interleukin-3

IL-4 – Interleukin-4

IL-5 – Interleukin-5

IL-6 – Interleukin-6

IL-10 – Interleukin-10

IL-11 – Interleukin-11

IL-12 p70 – Interleukin-12

IL-13 – Interleukin-13

IL-15 – Interleukin-15

IL-16 – Interleukin-16

IL-17A – Interleukin-17A

IL-18 BPα – Interleukin-18 binding protein α

IL-19 – Interleukin-19

IL-22 – Interleukin-22

IL-23 – Interleukin-23

IL-24 – Interleukin-24

IL-27 – Interleukin-27

IL-31 – Interleukin-31

IL-32a/β/γ – Interleukin-32α/β/γ

IL-33 – Interleukin-33

IL-34 – Interleukin-34

Kallikrein 3/ PSA – Prostate-specific antigen

Leptin

LIF – Leukaemia inhibitory factor

Lipocalin-2/NGAL – Neutrophil gelatinase-associated lipocalin

M-CSF – Macrophage colony stimulating factor

MIF – Macrophage migration inhibitory factor

MMP-9 – Matrix metalloproteinase-9

Myeloperoxidase

Osteopontin

PDGF-AA – Platelet-derived growth factor-AA

PDGF-AB/BB – Platelet-derived growth factor –AB/BB

Pentraxin 3/TSG-14 – Tumour necrosis factor stimulating gene-14

RAGE – Receptor for advanced glycation endproducts

RBP4 – Retinol binding protein 4

Relaxin-2

Resistin

Serpin E1/PAI-1 – Plasmin activator inhibitor type 1

SHBG – Sex hormone binding globulin

ST2/IL-1 R4 – Interleukin-1 receptor-like 4

TFF3 – Trefoil factor 3

TfR – Transferrin receptor

TGF-α – Transforming growth factor-α

TSP-1 - Thrombospondin-1

TNF-α – Tumour necrosis factor-α

uPAR – Urokinase-type plasminogen activator receptor

VEGF – Vascular endothelial growth factor

Vitamin D BP – Vitamin D binding protein

4.0 Table 1: Cytokines within peripheral samples demonstrating preferential expression

Cytokine	D score	Numerator (r)	Denominator (s+s0)	Fold change	Q value	Local fdr	PE expression	PR expression	Regulation
EGF	-2.87	-0.88	0.31	1.84	0.00	30.34	12.64	11.76	Erosion
Thrombospondin-1	-2.11	-0.94	0.45	1.92	4.31	28.94	14.07	13.12	Erosion
CD40 ligand	-2.25	-0.46	0.20	1.38	4.31	28.63	12.07	11.61	Erosion
ENA-78	-1.58	-0.39	0.25	1.31	10.78	35.67	13.75	13.35	Erosion
IL-24	-1.73	-0.36	0.21	1.29	10.78	32.26	10.30	9.94	Erosion
IL-11	-1.85	-0.34	0.18	1.26	10.78	30.53	11.09	10.75	Erosion
Angiopoietin-2	-1.56	-0.33	0.21	1.26	10.78	36.11	11.54	11.21	Erosion
MIF	-1.78	-0.26	0.15	1.20	10.78	31.55	13.87	13.61	Erosion
Endoglin	-1.37	-0.26	0.19	1.20	10.78	41.69	14.79	14.53	Erosion
Leptin	-1.16	-0.68	0.59	1.61	25.61	50.31	13.55	12.86	Erosion
BDNF	-0.99	-0.49	0.49	1.40	25.61	57.66	12.79	12.30	Erosion
Dkk-1	-1.23	-0.33	0.27	1.26	25.61	47.20	10.76	10.44	Erosion
IFN-?	-1.24	-0.30	0.24	1.23	25.61	46.61	10.48	10.18	Erosion
DPPIV	-1.10	-0.30	0.27	1.23	25.61	52.83	14.84	14.54	Erosion
IL-31	-1.24	-0.29	0.23	1.22	25.61	46.91	9.64	9.35	Erosion
LIF	-1.17	-0.28	0.24	1.21	25.61	49.88	9.93	9.66	Erosion

Cytokine	D score	Numerator (r)	Denominator (s+s0)	Fold change	Q value	Local fdr	PE expression	PR expression	Regulation
IL-10	-1.07	-0.27	0.26	1.21	25.61	54.20	10.26	9.99	Erosion
MCP-3	-1.29	-0.24	0.19	1.18	25.61	44.71	9.76	9.53	Erosion
IL-1a	-0.92	-0.22	0.23	1.16	29.79	60.94	10.44	10.22	Erosion
TGF-a	-0.97	-0.21	0.22	1.16	29.79	58.89	9.81	9.59	Erosion
Serpin E1	-0.89	-0.18	0.20	1.13	29.79	62.64	15.42	15.23	Erosion
MIP-3a	-0.82	-0.18	0.22	1.13	29.79	65.86	9.58	9.40	Erosion
IL-6	-0.86	-0.18	0.20	1.13	29.79	63.89	10.72	10.55	Erosion
IL-27	-0.81	-0.17	0.21	1.13	29.79	66.47	10.58	10.41	Erosion
PDGF-AA	-0.84	-0.17	0.20	1.12	29.79	64.82	15.04	14.87	Erosion
FGF-19	-0.82	-0.17	0.20	1.12	29.79	66.09	12.45	12.28	Erosion
IL-13	-0.80	-0.16	0.20	1.12	29.79	67.09	9.47	9.31	Erosion
IL-32a/ÃŸ/?	-0.85	-0.15	0.18	1.11	29.79	64.63	10.12	9.97	Erosion
Angiogenin	-0.81	-0.10	0.12	1.07	29.79	66.22	15.51	15.41	Erosion
IL-1ÃŸ	-0.73	-0.17	0.23	1.12	30.84	69.93	9.87	9.71	Erosion
MIP-1a/MIP-1ÃŸ	-0.70	-0.16	0.23	1.12	31.86	71.54	9.18	9.02	Erosion
Myeloperoxidase	-0.62	-0.21	0.33	1.15	33.33	74.87	10.66	10.45	Erosion
IL-15	-0.59	-0.16	0.28	1.12	34.77	76.59	9.68	9.52	Erosion
PDGF-AB/BB	-0.54	-0.13	0.25	1.10	36.16	78.73	14.59	14.46	Erosion

Cytokine	D score	Numerator (r)	Denominator (s+s0)	Fold change	Q value	Local fdr	PE expression	PR expression	Regulation
BAFF	-0.48	-0.14	0.30	1.10	47.22	81.36	13.39	13.25	Erosion
IP-10	-0.40	-0.12	0.29	1.09	49.38	84.40	10.32	10.20	Erosion
G-CSF	-0.41	-0.11	0.27	1.08	49.38	84.17	9.51	9.40	Erosion
IL-1ra	-0.37	-0.12	0.32	1.08	51.43	85.93	10.31	10.19	Erosion
IL-4	-0.34	-0.08	0.23	1.06	52.42	87.15	10.83	10.76	Erosion
TARC	-0.30	-0.08	0.28	1.06	54.57	88.74	11.77	11.69	Erosion
GRO-a	-0.29	-0.06	0.22	1.05	54.57	89.09	10.51	10.45	Erosion
IL-33	-0.25	-0.05	0.21	1.04	56.71	90.51	9.50	9.45	Erosion
GDF-15	-0.22	-0.06	0.28	1.04	57.60	91.46	13.79	13.72	Erosion
IL-23	-0.20	-0.05	0.25	1.03	58.38	92.39	9.62	9.57	Erosion
RAGE	-0.16	-0.04	0.23	1.03	60.70	93.49	11.05	11.02	Erosion
M-CSF	-0.14	-0.03	0.22	1.02	60.70	93.95	10.35	10.32	Erosion
IL-34	-0.11	-0.03	0.24	1.02	61.40	94.65	8.99	8.97	Erosion
IL-5	-0.08	-0.02	0.28	1.01	61.47	95.37	8.94	8.92	Erosion
Cripto-1	-0.07	-0.01	0.21	1.01	61.47	95.45	9.82	9.80	Erosion
I-TAC	2.80	0.76	0.27	1.69	0.00	20.12	11.29	12.04	Rupture
MIP-3ÃŸ	2.09	0.60	0.29	1.52	0.00	23.61	10.51	11.12	Rupture
MIG	1.82	0.54	0.29	1.45	0.00	34.11	10.50	11.04	Rupture

Cytokine	D score	Numerator (r)	Denominator (s+s0)	Fold change	Q value	Local fdr	PE expression	PR expression	Regulation
CD30	1.85	0.47	0.26	1.39	0.00	32.68	10.27	10.74	Rupture
Aggrecan	1.91	0.46	0.24	1.37	0.00	29.80	13.98	14.44	Rupture
MMP-9	2.00	0.42	0.21	1.34	0.00	26.42	13.49	13.91	Rupture
IL-18 BPa	1.81	0.37	0.20	1.29	0.00	34.45	11.85	12.21	Rupture
TFF3	1.87	0.29	0.15	1.22	0.00	31.68	13.47	13.76	Rupture
Complement Factor D	1.86	0.24	0.13	1.18	0.00	31.94	14.67	14.91	Rupture
RANTES	1.64	0.28	0.17	1.22	4.98	42.39	14.68	14.97	Rupture
Lipocalin-2	1.63	0.23	0.14	1.17	4.98	42.79	14.88	15.11	Rupture
Adiponectin	1.73	0.23	0.13	1.17	4.98	38.07	15.02	15.26	Rupture
MCP-1	1.42	0.29	0.21	1.23	7.19	51.44	11.70	11.99	Rupture
Osteopontin	1.44	0.22	0.16	1.17	7.19	50.78	13.70	13.93	Rupture
Chitinase 3-like 1	1.51	0.21	0.14	1.15	7.19	48.08	15.29	15.50	Rupture
IL-2	1.28	0.38	0.30	1.30	10.78	56.41	9.53	9.90	Rupture
Resistin	1.28	0.35	0.27	1.28	10.78	56.20	12.75	13.10	Rupture
TfR	1.26	0.25	0.19	1.19	10.78	56.83	11.59	11.83	Rupture
IL-3	1.11	0.30	0.27	1.23	15.62	61.66	8.79	9.09	Rupture
CD14	1.09	0.19	0.17	1.14	15.62	62.41	13.00	13.19	Rupture

Cytokine	D score	Numerator (r)	Denominator (s+s0)	Fold change	Q value	Local fdr	PE expression	PR expression	Regulation
GM-CSF	1.03	0.19	0.18	1.14	15.62	64.32	10.38	10.57	Rupture
Cystatin C	1.10	0.17	0.15	1.12	15.62	61.93	14.25	14.42	Rupture
ST2	0.94	0.26	0.28	1.20	17.97	67.43	12.91	13.18	Rupture
Fas Ligand	0.92	0.23	0.25	1.17	17.97	68.46	10.74	10.97	Rupture
IL-19	0.93	0.23	0.25	1.17	17.97	67.92	9.86	10.09	Rupture
Relaxin-2	1.00	0.21	0.22	1.16	17.97	65.54	10.27	10.48	Rupture
uPAR	0.94	0.20	0.21	1.15	17.97	67.49	11.81	12.01	Rupture
IL-17A	0.93	0.17	0.18	1.12	17.97	68.02	12.41	12.58	Rupture
Kallikrein 3	0.85	0.28	0.33	1.21	20.99	71.11	10.51	10.79	Rupture
TNF-alpha	0.78	0.36	0.45	1.28	25.61	73.61	10.57	10.93	Rupture
ICAM-1	0.77	0.15	0.20	1.11	25.61	74.01	14.37	14.52	Rupture
Complement Component C5/C5a	0.73	0.12	0.16	1.08	25.61	75.66	13.51	13.62	Rupture
C-Reactive Protein	0.76	0.08	0.11	1.06	25.61	74.53	15.51	15.59	Rupture
IGFBP-3	0.68	0.11	0.16	1.08	29.79	77.70	13.96	14.07	Rupture
FGF basic	0.47	0.11	0.24	1.08	47.22	85.78	11.38	11.49	Rupture
EMMPRIN	0.43	0.09	0.20	1.06	47.22	87.15	13.89	13.98	Rupture
VEGF	0.40	0.09	0.22	1.06	47.22	88.50	10.05	10.14	Rupture

Cytokine	D score	Numerator (r)	Denominator (s+s0)	Fold change	Q value	Local fdr	PE expression	PR expression	Regulation
Vitamin D BP	0.45	0.06	0.13	1.04	47.22	86.45	15.36	15.41	Rupture
RBP4	0.39	0.05	0.12	1.03	47.22	88.80	15.78	15.83	Rupture
SHBG	0.33	0.04	0.14	1.03	51.43	90.86	14.30	14.35	Rupture
FGF-7	0.26	0.07	0.27	1.05	54.57	92.87	9.72	9.79	Rupture
Flt-3 Ligand	0.23	0.06	0.28	1.05	54.57	93.81	10.48	10.54	Rupture
IGFBP-2	0.27	0.04	0.16	1.03	54.57	92.76	13.94	13.99	Rupture
HGF	0.18	0.09	0.52	1.07	56.71	94.85	11.50	11.59	Rupture
Angiopoietin-1	0.17	0.05	0.29	1.03	56.71	95.08	11.98	12.03	Rupture
IL-12 p70	0.16	0.03	0.21	1.02	56.71	95.19	10.00	10.04	Rupture
PF4	0.19	0.02	0.13	1.02	56.71	94.66	15.41	15.44	Rupture
Growth Hormone	0.14	0.07	0.55	1.05	57.60	95.60	11.53	11.61	Rupture
Pentraxin-3	0.07	0.01	0.19	1.01	59.89	96.23	11.50	11.52	Rupture
SDF-1a	0.09	0.01	0.17	1.01	59.89	96.15	12.29	12.31	Rupture
IL-22	0.05	0.01	0.26	1.01	60.70	96.33	11.10	11.11	Rupture
IL-8	0.03	0.01	0.21	1.01	60.70	96.33	10.00	10.01	Rupture
IL-16	0.03	0.01	0.22	1.00	60.70	96.33	9.46	9.46	Rupture

5.0 Table 2: Cytokines within coronary samples demonstrating preferential expression

Cytokine	D score	Numerator (r)	Denominator (s+s0)	Fold change	Q value	Local fdr	CE expression	CR expression	Regulation
BDNF	-2.65	-1.06	0.40	2.08	0.00	33.72	13.30	12.25	Erosion
EGF	-3.66	-0.99	0.27	1.99	0.00	33.51	12.70	11.72	Erosion
Thrombospondin-1	-2.08	-0.96	0.46	1.94	3.05	35.04	13.98	13.02	Erosion
ENA-78	-2.18	-0.53	0.24	1.44	3.05	34.55	13.67	13.14	Erosion
IL-24	-1.94	-0.42	0.22	1.34	7.16	36.25	10.26	9.83	Erosion
IL-10	-1.69	-0.39	0.23	1.31	7.16	40.48	10.27	9.88	Erosion
PDGF-AA	-1.81	-0.37	0.21	1.29	7.16	38.18	15.07	14.70	Erosion
Dkk-1	-1.56	-0.34	0.22	1.27	7.16	43.22	10.82	10.48	Erosion
IL-11	-1.61	-0.30	0.19	1.23	7.16	42.09	10.94	10.64	Erosion
Leptin	-1.33	-0.81	0.61	1.75	9.41	48.55	13.20	12.39	Erosion
Myeloperoxidase	-1.28	-0.35	0.27	1.27	9.41	49.74	10.51	10.16	Erosion
Angiopoietin-1	-1.42	-0.34	0.24	1.27	9.41	46.48	12.14	11.79	Erosion
PDGF-AB/BB	-1.35	-0.34	0.25	1.26	9.41	48.04	14.62	14.28	Erosion
Serpin E1	-1.53	-0.33	0.22	1.26	9.41	44.02	15.48	15.14	Erosion
FGF-19	-1.39	-0.32	0.23	1.25	9.41	47.28	12.45	12.13	Erosion
IFN-?	-1.38	-0.30	0.22	1.23	9.41	47.32	10.53	10.23	Erosion
Angiopoietin-2	-1.29	-0.26	0.20	1.20	9.41	49.57	11.48	11.22	Erosion

Cytokine	D score	Numerator (r)	Denominator (s+s0)	Fold change	Q value	Local fdr	CE expression	CR expression	Regulation
BAFF	-1.11	-0.36	0.33	1.28	16.81	54.05	13.29	12.93	Erosion
DPPIV	-1.13	-0.30	0.27	1.23	16.81	53.51	14.85	14.55	Erosion
IL-1a	-1.10	-0.27	0.25	1.21	16.81	54.35	10.61	10.34	Erosion
Endoglin	-1.07	-0.21	0.20	1.16	16.81	55.00	14.69	14.48	Erosion
IL-31	-0.89	-0.22	0.24	1.16	27.87	60.24	9.56	9.34	Erosion
TARC	-0.76	-0.22	0.28	1.16	34.12	65.08	11.65	11.43	Erosion
IL-27	-0.81	-0.17	0.21	1.13	34.12	63.02	10.46	10.29	Erosion
TGF-a	-0.81	-0.17	0.21	1.12	34.12	63.22	9.84	9.67	Erosion
CD40 ligand	-0.66	-0.16	0.24	1.12	37.31	68.93	11.89	11.73	Erosion
IL-13	-0.70	-0.16	0.22	1.11	37.31	67.13	9.41	9.25	Erosion
IL-4	-0.67	-0.15	0.23	1.11	37.31	68.61	10.62	10.47	Erosion
IL-19	-0.64	-0.15	0.23	1.11	37.31	69.62	9.92	9.77	Erosion
IL-32a/ÃŸ/?	-0.64	-0.12	0.18	1.08	37.31	69.58	9.88	9.76	Erosion
MCP-3	-0.56	-0.12	0.21	1.08	41.18	72.97	9.62	9.50	Erosion
IL-22	-0.46	-0.11	0.25	1.08	43.14	76.82	11.09	10.98	Erosion
MIP-1a/MIP-1ÃŸ	-0.44	-0.11	0.26	1.08	43.14	77.50	9.14	9.03	Erosion
Flt-3 Ligand	-0.48	-0.11	0.23	1.08	43.14	75.98	10.63	10.52	Erosion
LIF	-0.43	-0.09	0.21	1.07	43.14	77.60	9.59	9.49	Erosion
GDF-15	-0.35	-0.10	0.28	1.07	47.66	80.35	13.78	13.69	Erosion

Cytokine	D score	Numerator (r)	Denominator (s+s0)	Fold change	Q value	Local fdr	CE expression	CR expression	Regulation
G-CSF	-0.35	-0.09	0.25	1.06	47.66	80.30	9.62	9.53	Erosion
GRO-a	-0.29	-0.07	0.23	1.05	47.66	81.95	10.39	10.32	Erosion
IL-33	-0.34	-0.06	0.17	1.04	47.66	80.78	9.33	9.28	Erosion
MIF	-0.30	-0.05	0.17	1.04	47.66	81.63	13.70	13.64	Erosion
Angiogenin	-0.29	-0.03	0.11	1.02	47.66	82.05	15.49	15.46	Erosion
RAGE	-0.15	-0.04	0.26	1.03	52.01	84.72	11.22	11.19	Erosion
IL-15	-0.14	-0.03	0.24	1.02	52.01	84.78	9.62	9.59	Erosion
IL-1ÃŸ	-0.16	-0.03	0.19	1.02	52.01	84.56	9.75	9.72	Erosion
IL-34	-0.10	-0.02	0.24	1.02	52.01	85.19	8.96	8.94	Erosion
Pentraxin-3	-0.09	-0.02	0.19	1.01	52.01	85.26	11.47	11.45	Erosion
MIG	2.36	0.84	0.36	1.80	0.00	19.86	11.62	12.46	Rupture
I-TAC	2.29	0.59	0.26	1.51	0.00	20.22	11.27	11.86	Rupture
MMP-9	2.03	0.44	0.22	1.36	0.00	21.86	13.43	13.88	Rupture
Aggrecan	1.81	0.41	0.23	1.33	0.00	23.93	13.95	14.36	Rupture
Lipocalin-2	2.70	0.38	0.14	1.30	0.00	17.57	14.70	15.08	Rupture
IL-18 BPa	1.95	0.31	0.16	1.24	0.00	22.51	11.74	12.05	Rupture
Osteopontin	1.95	0.29	0.15	1.22	0.00	22.51	13.55	13.84	Rupture
TFF3	1.97	0.28	0.14	1.22	0.00	22.33	13.31	13.59	Rupture
Complement Factor D	1.80	0.23	0.13	1.17	0.00	24.01	14.76	14.99	Rupture

Cytokine	D score	Numerator (r)	Denominator (s+s0)	Fold change	Q value	Local fdr	CE expression	CR expression	Regulation
Chitinase 3-like 1	1.74	0.21	0.12	1.16	0.00	24.73	15.31	15.53	Rupture
HGF	1.57	0.79	0.50	1.73	3.05	27.52	13.89	14.68	Rupture
TNF-alpha	1.48	0.54	0.36	1.45	3.05	29.46	10.41	10.94	Rupture
FGF-7	1.56	0.39	0.25	1.31	3.05	27.79	10.30	10.69	Rupture
RANTES	1.62	0.27	0.17	1.21	3.05	26.56	14.67	14.94	Rupture
Adiponectin	1.61	0.20	0.12	1.15	3.05	26.76	15.12	15.31	Rupture
Resistin	1.45	0.33	0.23	1.26	7.16	30.21	12.53	12.86	Rupture
TfR	1.40	0.31	0.22	1.24	7.16	31.67	11.45	11.76	Rupture
CD14	1.46	0.26	0.18	1.20	7.16	30.01	12.99	13.25	Rupture
IP-10	1.03	0.36	0.35	1.28	14.64	46.21	10.55	10.91	Rupture
CD30	1.09	0.26	0.24	1.20	14.64	43.13	10.28	10.54	Rupture
IL-2	0.95	0.24	0.25	1.18	14.64	50.02	9.67	9.91	Rupture
uPAR	1.09	0.20	0.18	1.15	14.64	43.13	11.56	11.76	Rupture
IL-16	1.08	0.20	0.19	1.15	14.64	43.75	9.29	9.49	Rupture
Relaxin-2	0.95	0.18	0.19	1.14	14.64	49.93	10.09	10.28	Rupture
IL-12 p70	0.96	0.17	0.18	1.13	14.64	49.56	9.79	9.97	Rupture
Cystatin C	1.09	0.17	0.15	1.12	14.64	43.15	14.28	14.45	Rupture
IGFBP-2	0.86	0.13	0.15	1.10	14.64	55.24	13.89	14.02	Rupture
SHBG	0.95	0.12	0.13	1.09	14.64	50.01	14.16	14.29	Rupture

Cytokine	D score	Numerator (r)	Denominator (s+s0)	Fold change	Q value	Local fdr	CE expression	CR expression	Regulation
C-Reactive Protein	1.16	0.11	0.09	1.08	14.64	39.97	15.52	15.62	Rupture
IL-1ra	0.74	0.24	0.32	1.18	20.59	61.82	10.39	10.63	Rupture
ST2	0.79	0.21	0.27	1.16	20.59	58.78	12.72	12.93	Rupture
MIP-3ÃŸ	0.77	0.17	0.22	1.13	20.59	60.11	10.59	10.76	Rupture
GM-CSF	0.69	0.14	0.20	1.10	20.59	64.37	10.48	10.61	Rupture
SDF-1a	0.77	0.13	0.17	1.10	20.59	59.75	12.04	12.17	Rupture
Complement Component C5/C5a	0.77	0.12	0.16	1.09	20.59	59.74	13.58	13.70	Rupture
IGFBP-3	0.80	0.12	0.15	1.09	20.59	58.54	13.98	14.10	Rupture
RBP4	0.67	0.08	0.11	1.05	20.59	65.35	15.74	15.82	Rupture
Kallikrein 3	0.57	0.18	0.32	1.14	24.88	70.40	10.46	10.65	Rupture
FGF basic	0.62	0.17	0.28	1.13	24.88	68.09	11.46	11.63	Rupture
Fas Ligand	0.59	0.14	0.24	1.10	24.88	69.22	10.89	11.03	Rupture
ICAM-1	0.57	0.12	0.21	1.09	24.88	70.55	14.24	14.36	Rupture
VEGF	0.55	0.12	0.21	1.08	24.88	71.10	9.80	9.91	Rupture
IL-17A	0.53	0.11	0.20	1.08	24.88	72.19	12.33	12.43	Rupture
EMMPRIN	0.42	0.08	0.19	1.06	31.96	76.67	13.93	14.01	Rupture
MIP-3a	0.41	0.07	0.18	1.05	31.96	77.15	9.45	9.52	Rupture
IL-8	0.37	0.11	0.30	1.08	34.12	78.53	10.24	10.35	Rupture

Cytokine	D score	Numerator (r)	Denominator (s+s0)	Fold change	Q value	Local fdr	CE expression	CR expression	Regulation
Vitamin D BP	0.33	0.06	0.19	1.04	37.31	79.77	15.27	15.33	Rupture
M-CSF	0.29	0.06	0.19	1.04	37.31	80.84	10.13	10.18	Rupture
MCP-1	0.23	0.05	0.21	1.03	41.18	82.48	11.76	11.81	Rupture
IL-23	0.13	0.02	0.17	1.02	47.66	84.30	9.56	9.58	Rupture
Growth Hormone	0.07	0.04	0.55	1.03	48.93	85.03	11.14	11.18	Rupture
IL-3	0.07	0.02	0.25	1.01	48.93	85.04	9.05	9.07	Rupture
IL-5	0.05	0.02	0.33	1.01	48.93	85.19	8.95	8.97	Rupture
Cripto-1	0.06	0.01	0.20	1.01	48.93	85.13	9.84	9.86	Rupture
IL-6	0.04	0.01	0.21	1.01	48.93	85.27	10.66	10.67	Rupture
PF4	0.05	0.01	0.11	1.00	48.93	85.18	15.42	15.43	Rupture

6.0 Tables of mean spot pixel densities for cytokine arrays (Arbitrary units – AU)

Table 3: Array data for BDNF

Coronary rupture	Coronary erosion	Coronary undecided	Peripheral rupture	Peripheral erosion	Peripheral undecided
1619.81	34882.7	10611.21	625.96	22387.3	6584.81
2900.17	7953.29	11809.96	3198.86	3106.48	11850.66
14412.46	7474.32		7397.75	2138.67	
6313.98	4950.92		62597.48	2467.05	
2261.5	27665.25		1927.61	15541.2	
1084.91	24715.14		2064.87	27184.01	
15995.32	951.16		17955.76	557.99	
19724.66	10074.41		36269.89	4876.81	
9124.26	8611.12		8436.85	4238.2	
11342.13	8184.71		10837.17	4414.36	
5074.6	6354.13		3657.79	3100.11	
4365.72	1857.12		4056.15	2117.43	
334.23	2885.64		223.08	2814.95	
2916.09	48498.59		1920.4	61561.85	
1823.58	27293.94		1419.39	62653.56	
2005.26			1042.42		

2242.82	2522.41
142.2	285.92
6510.73	4337.81
4212.31	1722.9
7934.75	5129.92
7934.98	5272.96
6559.58	7361.38

Units – AU

Table 4: Array data for EGF

Coronary rupture	Coronary erosion	Coronary undecided	Peripheral rupture	Peripheral erosion	Peripheral undecided
2326.81	9272.93	3550.51	1361.29	7232.25	3869.76
3772.61	4522.81	4045.41	4502.77	2865.22	7440.79
2862.49	4163.73		2600.15	2451.77	
3007.71	1620.87		12221.79	1369.51	
2266.21	32054.28		2406.92	19868.02	
1581.47	20553.85		2187.31	19380.51	
3908.14	556.53		4691.3	303.68	
5438.94	2697.65		8546.47	2591.55	
8485.33	11124.82		11108.86	7330.25	
9479.08	4501.11		8373.49	5991.25	
3934.28	6266.03		3317	3907.67	
2522.89	3213.84		1145.95	3404.23	
397.81	3204.68		287.38	2887.97	
1150.81	23602.6		767.13	31159.27	
794.9	4823.03		992.4	39510.35	
507.36			593.2		
2196.52			2445.85		
125.54			291.08		

4296.46	2706.76
4003.94	1030.4
5363.12	2590.27
9712.49	6273.17
7711.31	8543.58

Units – AU

Table 5: Array data for growth hormone

Coronary rupture	Coronary erosion	Coronary undecided	Peripheral rupture	Peripheral erosion	Peripheral undecided
1295.41	-27.49	1431.87	1751.43	0	2959.93
2337.51	-32.26	6636.22	2004.95	0	19481.59
2689.24	22107.31		2117.76	31403.07	
624.31	166.86		813.15	221.56	
2589.72	3345.95		3376.93	3403.58	
4419.59	36846.44		2659.92	29909.37	
1574.57	157.07		4534.97	126.72	
5040.98	2608.95		8425.94	2550.31	
12629.46	3859.59		17101.87	3626.55	
9770.6	3135.81		14421.06	4336.64	
744.45	5061.06		488.56	4011.19	
946.59	1366.53		1439.8	3832.81	
601.02	7922.73		469.29	10757.1	
225.22	696.87		455.43	1393.84	
3576.55	403.03		6817.9	1709.58	
219.55			307.78		
245.74			1686.36		
-23.8			304.63		

8595.15	960.98
1146.91	1275.05
2360.49	2616.01
29282.67	24200.11
2027.7	2753.97

Units – AU

Table 6: Array data for I-TAC

Coronary rupture	Coronary erosion	Coronary undecided	Peripheral rupture	Peripheral erosion	Peripheral undecided
2769.5	3929.57	4972.33	2629.14	2267.23	13536.88
5542.18	689.09	2405.83	8372.38	407.14	3507.24
1696.11	1942.51		1709.71	1503.3	
2099.4	917.68		5292.45	565.95	
1961.26	6077.83		1987.2	4652.25	
1420.99	3128.27		2828.07	2966.16	
4258.77	599.54		8403.77	255.66	
9634.59	2694.57		11102.02	2566.6	
5335.2	4203.71		5099.78	4271.09	
4514.21	4371.79		3239.86	4315.52	
7335.61	2377.67		7413.57	1497.87	
6227.13	912.46		4598.52	1691.41	
1135.43	2670.21		874.45	2860.09	
1701.07	2462.83		1372.99	2162.06	
1686.48	330.99		1796.62	5211.31	
1290.08			1874.63		
2188.8			2462.8		
443.19			1158.11		

8222.57	2739.51
1882.37	780.54
5025.32	4966.05
6617.63	3987.87
5169.16	4257.22

Units – AU

Table 7: Array data for leptin

Coronary rupture	Coronary erosion	Coronary undecided	Peripheral rupture	Peripheral erosion	Peripheral undecided
964.36	22648.9	2171.05	760.78	21506.17	3578.29
6439.48	62565.64	417.99	10258.45	64598.21	405.85
1200.5	6484.07		1418.95	8263.95	
8736.71	396.55		17406.63	610.86	
2245.11	60337.31		2195.63	60264.58	
1305.41	6957.84		2630.87	7532.96	
3255.23	681.02		5291.62	1136.07	
62196.88	2559.21		63964.47	2488.17	
5382.79	48973.89		5004.79	48165.9	
15995.39	7726.82		22520.5	23675.66	
8559.84	9788.26		11180.98	8926.56	
1847.45	417.99		2365.87	405.85	
677.65	6459.81		1047.43	8663.79	
2866.77	62466.85		5303.3	62185.14	
2171.05	62635.38		3578.29	62564.12	
6482.07			10446.84		
2463.5			4459.29		
1772.7			6685.71		

7839.14	3533.62
4087.96	4086.77
2708.76	3564.83
5609.5	3146.09
20884.45	50485.65

Units – AU

Table 8: Array data for MIG

Coronary rupture	Coronary erosion	Coronary undecided	Peripheral rupture	Peripheral erosion	Peripheral undecided
6135.87	9798.82	7343.11	1148.68	0	3229.3
6036.23	9757.27	2311.18	1401.08	0	1024.2
3805.21	3634.98		1213.1	1206.8	
3777.42	636.01		14081.69	156.24	
4002.06	10501.55		953.44	3378.76	
652.43	2454.92		4394.25	6962.06	
4435.54	1418.71		1416.42	198.58	
17581.2	6223.13		3462.04	1068.13	
7292.04	4450.08		3463.08	3490.26	
5372.56	3883.64		2215.72	1577.84	
11921.69	2943.74		3776.57	806.78	
7876.05	1255.6		1600.26	732.32	
1602.16	2891.81		148.36	2808.32	
2452.12	1394.28		257.27	2865.7	
2112.33	272.43		459.12	6589.06	
2484.21			224.11		
2492.27			605.93		
596.11			229.96		

7805.03	4313.94
2922.44	505.57
7959.36	2728.25
6182.64	1982.71
6357.29	2969.62

Units – AU

Table 9: Array data for MMP-9

Coronary rupture	Coronary erosion	Coronary undecided	Peripheral rupture	Peripheral erosion	Peripheral undecided
14528.18	16842.64	15607.43	13139.94	26058.18	18557.57
15528.38	30635.46	10025.58	26663.69	28935.68	19003.05
22519.34	20023.77		16890.95	19649.23	
14238.92	4118.79		14969.37	4474.22	
19133.94	25411.66		15720.05	29006.91	
18490.28	34471.46		19206.19	26986.91	
17221.47	4327.05		19245.15	2431.89	
15246.75	7989.08		17249.65	6011.31	
17613.9	8483.97		16640.38	8510.19	
24714.01	11876.43		19562.98	9367.94	
11724.75	4744.85		10907.21	3423.36	
18619.38	3696.76		16550.59	8851.63	
5264.44	8921.48		3931.53	8144.92	
6004.41	8824.01		5910.08	10386.98	
4239.39	3529.85		5541.76	12647.78	
2029.91			4550.15		
6732.89			7546.45		
2341.96			4148.85		

18480.58	8159.34
11445.79	8107.75
7903.1	13433.78
21315.71	13287.5
21963.2	27658.39

Units – AU

Table 10: Array data for MPO

Coronary rupture	Coronary erosion	Coronary undecided	Peripheral rupture	Peripheral erosion	Peripheral undecided
1306.07	206.18	925.85	215.27	36.12	622.52
380.27	-32.26	636.5	947.8	405.08	1297.15
1572.03	1055.11		1603.51	832.16	
444	230.53		1410.1	154.67	
697.62	5610.64		516.25	3219.13	
672.17	2718.72		727.45	4757.67	
386.06	608.27		941.39	193.31	
681.33	785.03		719.79	152.6	
3641	4118.03		2860.48	4044.52	
2840.23	894.8		22857.44	2468.54	
1011.99	1020.73		731.08	933.34	
1552.57	666.34		1105.04	1082.85	
334.02	2848.43		194.17	2840.89	
172.93	1740.9		184.41	5160.4	
162.47	748.83		143.91	4181.84	
105.05			62.01		
-14.93			1079.91		
16.28			164.28		

1256.58	229.44
975.47	488.65
2641.2	2531.37
4053.44	3176.12
4192.22	4635.62

Units – AU

Table 11: Array data for TSP-1

Coronary rupture	Coronary erosion	Coronary undecided	Peripheral rupture	Peripheral erosion	Peripheral undecided
8257.4	9241.64	6054.08	5114.97	12195.22	6701.52
7136.03	6862.71	3052.92	9445.47	6413.61	5367.53
5603.82	6862.57		4301.36	5594.82	
3526.71	2281.59		8937.88	1624.18	
6453.15	59975.95		5192.5	56975.7	
4506.43	59256.93		6475.84	59909.15	
6108.54	1520.53		6293.87	707.35	
5512.13	2632.09		6231.38	2573.12	
56102.85	40504.06		55441.48	31267.32	
49974.52	29624.28		51469.16	33089.75	
7927.83	22357.72		6054.97	16762.2	
7335.13	14580.73		5927.34	21266.9	
1139.1	27464.6		788.79	30974.9	
1956.74	34900.9		1466.08	48785.6	
1480.92	12229.03		1832.24	43450.82	
630.75			1105.9		
2429.5			2542.53		
339			1044.95		

5646.12	3384.68
4321.67	2897.46
37550.13	38972.28
60441.75	49551.61
58379.57	60568.34

Units – AU

7.0 Tables of ELISA calculated mean plasma concentrations (pg/mL or ng/mL)

Table 12: ELISA data for BDNF

Coronary rupture	Coronary erosion	Coronary undecided	Peripheral rupture	Peripheral erosion	Peripheral undecided
1455.37	8736.55	2964.35	865.31	7952.3	3695.82
4763.24		16209.65	5070.37		13351.1
4591.71	1044.48		5331.57	542.13	
2136.77	27131.24		23361.29	12653.77	
5720.46			5265.46		
1079.75	4357.33		1293.79	9860.33	
11405.85	1308.89		Invalid Result	4234.85	
15925.6	5865.95		20877.48	18239.24	
1210.02			9135.94		
4785.39	2084.04		8137	4153.8	
5669.31			3991.35		
	4150.93			5015.8	
1579.75	1492.72		4279.1	3086.61	
9539.01			7018.89		
2498.23			3926.14		
10325.19			4443.13		

950.96	5784.48
1478.11	4994.7
4610.18	10602.97
2107.23	6028.6
2605.86	6814.87
1269.24	4598.89
1357.94	3150.85

Units - pg/mL

Table 13: ELISA data for EGF

Coronary rupture	Coronary erosion	Coronary undecided	Peripheral rupture	Peripheral erosion	Peripheral undecided
13.575	177.875	96.5625	11.25	286.3875	68.6625
104.5125	166.375	478.0625	40.025	186.775	236.3375
99.1375	82.2875		55.775	54.1875	
Invalid Result	216.475		452.825	149.7125	
62.425	171.8375		58.5	94.4125	
46.4875	70.3625		14.5625	156.025	
165.1625	46.4875		Invalid Result	96.675	
210.6125	171.825		339.1125	228.3625	
82.9625	177.875		33.75	83.3875	
77.325	66.025		78.475	62.7625	
197.0125	331.2875		71.9	132.825	
Invalid Result	142.3125		42.6	81.7875	
Invalid Result	81.95		35.2875	69.75	
118.8875	510.2125		123.7625	91.0875	
72.4875	919.55		29.1625	254.4625	

249	84.475
Invalid Result	88.875
17.7875	46.275
117.5875	143.8375
154.0875	106.875
196.9125	25.4875
53.4625	81.9125
38.7	49.7625

Units – pg/mL

Table 14: ELISA data for growth hormone

Coronary rupture	Coronary erosion	Coronary undecided	Peripheral rupture	Peripheral erosion	Peripheral undecided
Invalid Result	Invalid Result	Invalid Result	450.496	145.064	216.512
Invalid Result	Invalid Result	2606.345	251.91	608.34	4923.846
Invalid Result	2283.07		1157.05	5448.648	
Invalid Result	Invalid Result		200.164	31.648	
Invalid Result	Invalid Result		1043.576	215.086	
289.605	3683.62		1204.72	5259.304	
Invalid Result	Invalid Result		Invalid Result	197.468	
Invalid Result	Invalid Result		1213.394	951.84	
1287.565	Invalid Result		2433.512	482.26	
585.585	151.745		1885.174	833.89	
Invalid	1889.61		Invalid	2938.49	

Result		Result	
Invalid Result	701.415	473.258	1673.792
Invalid Result	2642.71	896.03	4408.366
Invalid Result	Invalid Result	166.298	499.122
1848.4	Invalid Result	3472.87	249.95
Invalid Result		346.172	
Invalid Result		352.764	
356.915		218.66	
1442.39		356.074	
219.445		619.582	
Invalid Result		886.912	
2805.85		5115.456	
Invalid Result		286.124	

Units – pg/mL

Table 15: ELISA data for I-TAC

Coronary rupture	Coronary erosion	Coronary undecided	Peripheral rupture	Peripheral erosion	Peripheral undecided
115.716	1607.456	2555.94	127.672	290.22	439.78
877.132		1526.46	216.38		943.086
2122.368	1319.64		90.572	250.76	
2236.496	1001.338		Invalid Result	100.272	
1494.022			200.684		
1692.73	1034.612		34.822	243.89	
Invalid Result	1322.498		Invalid Result	927.956	
941.468	260.7		324.1	214.924	
1231.414			109.858		
2070.426	1599.668		Invalid Result	360.784	
2513.242			637.798		
	674.112			545.888	
253.616	666.42		305.448	642.242	
1469.642			478.326		
1530.758			788.308		
1861.306			807.742		

500.044	251.184
843.282	312.15
1801.202	931.394
1826.04	817.032
1799.044	1680.53
1896.428	1182.008
2150.958	1023.402

Units – pg/mL

Table 16: ELISA data for leptin

Coronary rupture	Coronary erosion	Coronary undecided	Peripheral rupture	Peripheral erosion	Peripheral undecided
2785.9	15475.6	7094.6	2366.6	19246.8	11398.9
13995.3	56922.8	Invalid Result	13100.5	52387.2	Invalid Result
2288	9510.8		617.7	6515.5	
17637.1	4516.4		32946.1	4160.9	
6592.2	27087.2		8207.4	31814.3	
3683.9	1466.1		5387	2067.6	
3485.3	4343.6		Invalid Result	8075.4	
88382.5	3732.6		88446.8	6071.4	
2010.1	18766.4		1245.3	23398.8	
6247.6	5330.7		6228.7	12685.5	
15146.6	6544.3		13887.1	5919.3	
1676.2	Invalid Result		2956.9	Invalid Result	
5912.9	5532.4		5006.8	8427	
6164.6	21781.9		15830	24392.2	
7094.6	22903.9		11398.9	6433.3	

39691.6	32836.7
7738.5	14562.8
51625	39056.2
8782.7	11311.5
5893.7	10503
1876.6	6514.4
1417.8	4647
6303.8	12336.5

Units – pg/mL

Table 17: ELISA data for MIG

Coronary rupture	Coronary erosion	Coronary undecided	Peripheral rupture	Peripheral erosion	Peripheral undecided
20.462	159.476	144.84	26.121	78.093	152.226
Invalid Result		101.013	Invalid Result		65.277
40.896	90.998		47.23	125.886	
200.445	Invalid Result		98.425	25.049	
112.05	70.301		92.614	50.226	
76.921	84.388		103.06	47.988	
Invalid Result	140.425		Invalid Result	117.863	
211.715	103.06		133.239	Invalid Result	
Invalid Result	162.426		66.551	128.203	
Invalid Result	199.661		45.692	124.954	
354.941	Invalid Result		260.976	Invalid Result	
128.664	Invalid Result			Invalid Result	
51.689	23.949		44.125	Invalid	

			Result
97.904	176.081	84.388	Invalid Result
144.401	359.278	148.768	40.067
164.52		140.869	
47.23		Invalid Result	
30.186		12.118	
174.446		134.146	
118.819		48.741	
172.395		159.053	
209.01		60.708	
180.147		62.687	

Units – pg/mL

Table 18: ELISA data for MMP-9

Coronary rupture	Coronary erosion	Coronary undecided	Peripheral rupture	Peripheral erosion	Peripheral undecided
31.6	25.3	29.25	62.1	140.1	89.05
86.75	168.15	225.4	206.35	206.65	1040.8
182.1	96.45		584.45	101.85	
86.45	53.6		23.25	79.15	
101.85	47.8		150.6	98.7	
164.3	59.95		193.45	86.75	
124.1	114.3		Invalid Result	162.8	
183	216.9		116.45	119.55	
63.2	44.15		40.85	267.4	
135.9	138.9		110.6	266.75	
20	32.1		41.3	71.3	
98.05	91		271.85	1112	
140.4	57.75		121.7	92.3	
42.1	70.25		187.8	317.95	
42.95	89.7		160.4	305.15	
53.2			161.3		
367.35			144		

148.8	245.1
106.25	314.9
60.65	199.75
41.7	118.95
92.6	276.35
114.95	447.3

Units – ng/mL

Table 19: ELISA data for MPO

Coronary rupture	Coronary erosion	Coronary undecided	Peripheral rupture	Peripheral erosion	Peripheral undecided
386	288.1	391.15	Invalid Result	40.75	101.6
702.4	609.65	718.95	104.75	118.2	Invalid Result
500.65	356.35		611.7	143.9	
984.9	181.8		482.5	30.85	
712.5	445.75		101.15	14.8	
431.1	266.26		213.75	193.15	
362.45	242.5		Invalid Result	86.85	
559.95	532.55		124.35	82.25	
298.6	310.35		48.25	74	
489.75	191.15		149.7	90.8	
423.95	349.15		67.65	35.35	
617.2	237.2		163.3	957	
665.3	354.6		137.15	99.7	
1.9	804.75		162	165.05	
242.6	557.9		100.05	110.3	
27.45			155.9		

388.15	104.15
382.75	69.95
466.35	479.7
282.55	96.8
282.5	149.4
279.25	77.9
169.25	158.9

Units - ng/mL

Table 20: ELISA data for TSP-1

Coronary rupture	Coronary erosion	Coronary undecided	Peripheral rupture	Peripheral erosion	Peripheral undecided
282.3	1046.5	420.78	789.72	2053.14	1187.1
687.34		7963.98	1419.96		9697.78
483.08	166.96		1634.46	1216.12	
89.7	3684.64		7829.98	3185.7	
374.82			1509.8		
303.96	469.94		516.66	2708.26	
4439.38	293.3		Invalid Result	742.6	
570.58	1140.38		4567.64	6156.98	
295.54			3201.76		
201	4680.72		2559.82	2619.64	
401.52			1018.92		
	2680.62			1113.46	
104.14	1578.5		1233.4	1256.06	
795.9			2166.64		
613.26			1118.42		
2143.08			1352.02		
290.56			2373.72		

359.42	1488.78
689	4938.58
1183.34	2856.54
2837.86	1676.54
366.3	998.38
1442.12	1030.24

Units – ng/mL

8.0 Table 21: Cytokines within erosion cases demonstrating preferential expression for coronary or peripheral circulation

CYTOKINE	D SCORE	NUMERATOR(R)	DENOMINATOR (S+S0)	FOLD CHANGE	Q VALUE	LOCAL FDR	CE EXPRESSION	PE EXPRESSION	REGULATION
HGF	2.69	2.39	0.89	5.25	0.00	100.00	11.50	13.89	CE
FGF-7	2.90	0.58	0.20	1.50	0.00	100.00	9.72	10.30	CE
IL-3	1.29	0.26	0.20	1.20	0.00	100.00	8.79	9.05	CE
IP-10	0.90	0.23	0.26	1.17	0.00	100.00	10.32	10.55	CE
IL-1A	1.08	0.17	0.16	1.12	0.00	100.00	10.44	10.61	CE
FAS LIGAND	0.81	0.15	0.19	1.11	0.00	100.00	10.74	10.89	CE
IL-2	1.08	0.14	0.13	1.11	0.00	100.00	9.53	9.67	CE
GM-CSF	0.61	0.09	0.15	1.07	0.00	100.00	10.38	10.48	CE
COMPLEMENT FACTOR D	1.16	0.09	0.08	1.06	0.00	100.00	14.67	14.76	CE
FGF BASIC	0.40	0.08	0.20	1.06	0.00	100.00	11.38	11.46	CE
COMPLEMENT COMPONENT C5/C5A	0.74	0.07	0.09	1.05	0.00	100.00	13.51	13.58	CE

CYTOKINE	D SCORE	NUMERATOR(R)	DENOMINATOR (S+S0)	FOLD CHANGE	Q VALUE	LOCAL FDR	CE EXPRESSION	PE EXPRESSION	REGULATION
EGF	0.43	0.06	0.14	1.04	0.00	100.00	12.64	12.70	CE
IL-19	0.31	0.06	0.18	1.04	0.00	100.00	9.86	9.92	CE
IFN-?	0.28	0.04	0.15	1.03	0.00	100.00	10.48	10.53	CE
TGF-A	0.25	0.04	0.15	1.03	0.00	100.00	9.81	9.84	CE
CYSTATIN C	0.40	0.03	0.08	1.02	0.00	100.00	14.25	14.28	CE
PDGF-AB/BB	0.21	0.03	0.12	1.02	0.00	100.00	14.59	14.62	CE
IGFBP-3	0.20	0.02	0.09	1.01	0.00	100.00	13.96	13.98	CE
IL-10	0.06	0.01	0.17	1.01	0.00	99.25	10.26	10.27	CE
C-REACTIVE PROTEIN	0.12	0.01	0.06	1.01	0.00	100.00	15.51	15.52	CE
PF4	0.07	0.01	0.08	1.00	0.00	99.31	15.41	15.42	CE
GROWTH HORMONE	-2.31	-0.39	0.17	1.31	8.43	40.35	11.53	11.14	CE
IL-32A/ÃŸ/?	-1.98	-0.24	0.12	1.18	8.43	44.00	10.12	9.88	CE
LIPOCALIN-2	-2.18	-0.17	0.08	1.13	8.43	42.01	14.88	14.70	CE
MIF	-2.36	-0.17	0.07	1.12	8.43	39.56	13.87	13.70	CE

CYTOKINE	D SCORE	NUMERATOR(R)	DENOMINATOR (S+S0)	FOLD CHANGE	Q VALUE	LOCAL FDR	CE EXPRESSION	PE EXPRESSION	REGULATION
LEPTIN	-1.78	-0.35	0.20	1.27	14.05	45.05	13.55	13.20	CE
SDF-1A	-1.67	-0.25	0.15	1.19	14.05	45.63	12.29	12.04	CE
RESISTIN	-1.76	-0.22	0.13	1.17	14.05	45.14	12.75	12.53	CE
OSTEOPONTIN	-1.57	-0.16	0.10	1.11	14.05	46.48	13.70	13.55	CE
IL-12 P70	-1.32	-0.21	0.16	1.16	24.09	51.44	10.00	9.79	CE
SHBG	-1.44	-0.14	0.10	1.10	24.09	48.67	14.30	14.16	CE
ENDOGLIN	-1.36	-0.09	0.07	1.07	24.09	50.28	14.79	14.69	CE
CD40 LIGAND	-0.96	-0.18	0.19	1.13	30.11	63.51	12.07	11.89	CE
IL-27	-0.98	-0.12	0.13	1.09	30.11	62.70	10.58	10.46	CE
MCP-3	-0.78	-0.15	0.19	1.11	41.08	71.03	9.76	9.62	CE
MIP-3A	-0.83	-0.13	0.15	1.09	41.08	68.91	9.58	9.45	CE
IL-18 BPA	-0.74	-0.11	0.15	1.08	41.08	72.79	11.85	11.74	CE
THROMBOSPONDIN-1	-0.85	-0.09	0.11	1.06	41.08	68.23	14.07	13.98	CE
ENA-78	-0.64	-0.08	0.12	1.06	41.08	77.29	13.75	13.67	CE
TNF-ALPHA	-0.58	-0.16	0.28	1.12	48.44	79.92	10.57	10.41	CE
IL-1ÃŸ	-0.51	-0.12	0.24	1.09	48.44	82.78	9.87	9.75	CE
IL-6	-0.54	-0.06	0.11	1.04	48.44	81.53	10.72	10.66	CE
IL-23	-0.46	-0.06	0.13	1.04	48.44	84.44	9.62	9.56	CE
MMP-9	-0.34	-0.06	0.17	1.04	52.90	88.36	13.49	13.43	CE

CYTOKINE	D SCORE	NUMERATOR(R)	DENOMINATOR (S+S0)	FOLD CHANGE	Q VALUE	LOCAL FDR	CE EXPRESSION	PE EXPRESSION	REGULATION
KALLIKREIN 3	-0.39	-0.04	0.11	1.03	52.90	86.59	10.51	10.46	CE
IL-15	-0.21	-0.06	0.31	1.04	56.72	92.20	9.68	9.62	CE
MIP-1A/MIP-1ÃŸ	-0.20	-0.04	0.18	1.03	56.72	92.25	9.18	9.14	CE
PENTRAXIN-3	-0.24	-0.03	0.13	1.02	56.72	91.33	11.50	11.47	CE
I-TAC	-0.12	-0.02	0.17	1.01	56.72	94.69	11.29	11.27	CE
RANTES	-0.22	-0.02	0.07	1.01	56.72	91.77	14.68	14.67	CE
IL-22	-0.05	-0.01	0.24	1.01	56.72	96.56	11.10	11.09	CE
MIG	2.83	1.12	0.39	2.17	0.00	100.00	10.50	11.62	PE
BDNF	2.91	0.51	0.18	1.43	0.00	100.00	12.79	13.30	PE
IL-8	0.71	0.23	0.33	1.18	0.00	100.00	10.00	10.24	PE
RAGE	0.93	0.17	0.18	1.13	0.00	100.00	11.05	11.22	PE
ANGIOPOIETIN-1	0.97	0.15	0.16	1.11	0.00	100.00	11.98	12.14	PE
FLT-3 LIGAND	0.82	0.15	0.18	1.11	0.00	100.00	10.48	10.63	PE
G-CSF	0.71	0.11	0.15	1.08	0.00	100.00	9.51	9.62	PE
ADIPONECTIN	1.28	0.09	0.07	1.07	0.00	100.00	15.02	15.12	PE

CYTOKINE	D SCORE	NUMERATOR(R)	DENOMINATOR (S+S0)	FOLD CHANGE	Q VALUE	LOCAL FDR	CE EXPRESSION	PE EXPRESSION	REGULATION
IL-1RA	0.35	0.08	0.23	1.06	0.00	100.00	10.31	10.39	PE
MIP-3ÃŸ	0.34	0.07	0.22	1.05	0.00	100.00	10.51	10.59	PE
MCP-1	0.45	0.06	0.14	1.05	0.00	100.00	11.70	11.76	PE
SERPIN E1	0.57	0.06	0.11	1.04	0.00	100.00	15.42	15.48	PE
DKK-1	0.45	0.05	0.12	1.04	0.00	100.00	10.76	10.82	PE
EMMPRIN	0.41	0.04	0.10	1.03	0.00	100.00	13.89	13.93	PE
PDGF-AA	0.34	0.04	0.10	1.02	0.00	100.00	15.04	15.07	PE
CRIPTO-1	0.16	0.03	0.18	1.02	0.00	100.00	9.82	9.84	PE
CHITINASE 3-LIKE 1	0.35	0.02	0.07	1.02	0.00	100.00	15.29	15.31	PE
CD30	0.06	0.01	0.21	1.01	0.00	99.27	10.27	10.28	PE
DPPIV	0.15	0.01	0.07	1.01	0.00	100.00	14.84	14.85	PE
IL-5	0.03	0.01	0.18	1.00	0.00	98.54	8.94	8.95	PE
FGF-19	0.03	0.00	0.12	1.00	0.00	98.44	12.45	12.45	PE

CYTOKINE	D SCORE	NUMERATOR(R)	DENOMINATOR (S+S0)	FOLD CHANGE	Q VALUE	LOCAL FDR	CE EXPRESSION	PE EXPRESSION	REGULATION
UPAR	-2.22	-0.25	0.11	1.19	8.43	41.50	11.81	11.56	PE
ST2	-2.08	-0.20	0.09	1.15	8.43	43.12	12.91	12.72	PE
LIF	-1.38	-0.35	0.25	1.27	24.09	49.92	9.93	9.59	PE
IL-4	-1.45	-0.21	0.15	1.16	24.09	48.33	10.83	10.62	PE
TFF3	-1.43	-0.16	0.11	1.12	24.09	48.77	13.47	13.31	PE
IL-11	-1.21	-0.15	0.12	1.11	24.09	54.37	11.09	10.94	PE
ICAM-1	-1.25	-0.13	0.10	1.09	24.09	53.30	14.37	14.24	PE
VITAMIN D BP	-1.34	-0.09	0.07	1.06	24.09	50.78	15.36	15.27	PE
VEGF	-1.09	-0.25	0.23	1.19	28.10	58.23	10.05	9.80	PE
M-CSF	-1.10	-0.23	0.21	1.17	28.10	58.07	10.35	10.13	PE
IL-33	-1.12	-0.17	0.15	1.12	28.10	57.19	9.50	9.33	PE
TFR	-1.11	-0.13	0.12	1.10	28.10	57.58	11.59	11.45	PE
IL-16	-1.04	-0.17	0.16	1.12	30.11	60.19	9.46	9.29	PE
TARC	-0.93	-0.12	0.13	1.09	30.11	64.44	11.77	11.65	PE
RELAXIN-2	-0.81	-0.18	0.22	1.13	41.08	70.05	10.27	10.09	PE
MYELOPEROXIDASE	-0.74	-0.14	0.19	1.10	41.08	73.11	10.66	10.51	PE
GRO-A	-0.77	-0.12	0.16	1.09	41.08	71.72	10.51	10.39	PE
IL-17A	-0.78	-0.08	0.11	1.06	41.08	71.34	12.41	12.33	PE
IGFBP-2	-0.67	-0.06	0.08	1.04	41.08	75.98	13.94	13.89	PE

CYTOKINE	D SCORE	NUMERATOR(R)	DENOMINATOR (S+S0)	FOLD CHANGE	Q VALUE	LOCAL FDR	CE EXPRESSION	PE EXPRESSION	REGULATION
BAFF	-0.52	-0.10	0.20	1.07	48.44	82.20	13.39	13.29	PE
IL-31	-0.45	-0.08	0.17	1.06	48.44	84.67	9.64	9.56	PE
ANGIOPOIETIN-2	-0.61	-0.06	0.10	1.04	48.44	78.87	11.54	11.48	PE
RBP4	-0.56	-0.04	0.07	1.03	48.44	80.61	15.78	15.74	PE
IL-13	-0.40	-0.06	0.15	1.04	52.90	86.54	9.47	9.41	PE
IL-24	-0.28	-0.05	0.16	1.03	56.72	90.18	10.30	10.26	PE
AGGRECAN	-0.33	-0.04	0.11	1.03	56.72	88.68	13.98	13.95	PE
IL-34	-0.14	-0.03	0.20	1.02	56.72	94.09	8.99	8.96	PE
ANGIOGENIN	-0.30	-0.02	0.06	1.01	56.72	89.37	15.51	15.49	PE
CD14	-0.15	-0.01	0.08	1.01	56.72	93.81	13.00	12.99	PE
GDF-15	-0.05	-0.01	0.10	1.00	56.72	96.37	13.79	13.78	PE

9.0 Table 22: Cytokines within rupture cases demonstrating preferential expression for coronary or peripheral circulation

Cytokine	D Score	Numerator (r)	Denominator (s+s0)	Fold Change	Q Value	Local Fdr	CR expression	PR expression	Regulation
HGF	7.58	3.09	0.41	8.49	0.00	72.23	11.59	14.68	CR
FGF-7	4.46	0.90	0.20	1.87	0.00	72.34	9.79	10.69	CR
IL-1ra	2.49	0.44	0.18	1.35	0.00	70.62	10.19	10.63	CR
Growth Hormone	-2.20	-0.42	0.19	1.34	0.00	18.08	11.61	11.18	CR
IL-19	-2.94	-0.32	0.11	1.25	0.00	13.88	10.09	9.77	CR
IL-4	-2.68	-0.29	0.11	1.22	0.00	14.46	10.76	10.47	CR
uPAR	-2.53	-0.25	0.10	1.19	0.00	15.11	12.01	11.76	CR
TARC	-2.11	-0.25	0.12	1.19	3.30	19.49	11.69	11.43	CR
ICAM-1	-2.16	-0.16	0.07	1.12	3.30	18.63	14.52	14.36	CR
Angiopoietin-1	-1.47	-0.24	0.16	1.18	5.70	36.17	12.03	11.79	CR
IL-32a/ÃŸ/?	-1.67	-0.20	0.12	1.15	5.70	29.51	9.97	9.76	CR
MCP-1	-1.56	-0.18	0.12	1.14	5.70	32.82	11.99	11.81	CR
LIF	-1.48	-0.16	0.11	1.12	5.70	35.74	9.66	9.49	CR
ENA-78	-1.24	-0.22	0.18	1.16	13.21	45.06	13.35	13.14	CR
PDGF-AB/BB	-1.17	-0.18	0.15	1.13	13.21	47.95	14.46	14.28	CR
PDGF-AA	-1.26	-0.17	0.13	1.13	13.21	43.92	14.87	14.70	CR
IL-17A	-1.20	-0.14	0.12	1.10	13.21	46.47	12.58	12.43	CR
Kallikrein 3	-1.32	-0.14	0.11	1.10	13.21	41.86	10.79	10.65	CR
SDF-1a	-1.40	-0.13	0.10	1.10	13.21	38.52	12.31	12.17	CR

Cytokine	D Score	Numerator (r)	Denominator (s+s0)	Fold Change	Q Value	Local Fdr	CR expression	PR expression	Regulation
IL-27	-1.06	-0.13	0.12	1.09	13.21	52.24	10.41	10.29	CR
Thrombospondin-1	-1.31	-0.10	0.08	1.07	13.21	42.05	13.12	13.02	CR
Aggrecan	-1.29	-0.09	0.07	1.06	13.21	42.89	14.44	14.36	CR
Serpin E1	-0.95	-0.09	0.09	1.06	17.11	57.02	15.23	15.14	CR
IL-10	-0.78	-0.11	0.14	1.08	19.10	63.85	9.99	9.88	CR
SHBG	-0.90	-0.06	0.06	1.04	19.10	58.86	14.35	14.29	CR
TfR	-0.59	-0.07	0.11	1.05	27.89	70.84	11.83	11.76	CR
IL-13	-0.36	-0.05	0.15	1.04	36.33	77.89	9.31	9.25	CR
EGF	-0.34	-0.05	0.14	1.03	36.33	78.46	11.76	11.72	CR
MMP-9	-0.27	-0.03	0.11	1.02	36.33	80.10	13.91	13.88	CR
IL-3	-0.17	-0.03	0.16	1.02	36.33	82.35	9.09	9.07	CR
Flt-3 Ligand	-0.13	-0.02	0.19	1.02	36.33	83.03	10.54	10.52	CR
MCP-3	-0.17	-0.02	0.14	1.02	36.33	82.25	9.53	9.50	CR
IL-31	-0.04	-0.01	0.19	1.01	36.33	84.33	9.35	9.34	CR
RAGE	1.57	0.17	0.11	1.12	38.95	75.46	11.02	11.19	CR
Complement Factor D	1.28	0.08	0.06	1.05	41.48	78.52	14.91	14.99	CR
G-CSF	0.89	0.13	0.14	1.09	43.20	82.85	9.40	9.53	CR
IL-6	0.93	0.12	0.13	1.09	43.20	82.47	10.55	10.67	CR
IL-1a	0.89	0.11	0.13	1.08	43.20	82.94	10.22	10.34	CR
Fas Ligand	0.58	0.06	0.11	1.05	43.20	85.72	10.97	11.03	CR
CD14	0.65	0.06	0.10	1.04	43.20	85.15	13.19	13.25	CR

Cytokine	D Score	Numerator (r)	Denominator (s+s0)	Fold Change	Q Value	Local Fdr	CR expression	PR expression	Regulation
Cripto-1	0.38	0.06	0.15	1.04	43.20	86.66	9.80	9.86	CR
IFN-?	0.33	0.05	0.13	1.03	43.20	86.74	10.18	10.23	CR
IL-5	0.24	0.04	0.18	1.03	43.20	86.65	8.92	8.97	CR
MIF	0.39	0.04	0.09	1.03	43.20	86.65	13.61	13.64	CR
Chitinase 3-like 1	0.66	0.03	0.05	1.02	43.20	85.10	15.50	15.53	CR
EMMPRIN	0.39	0.03	0.08	1.02	43.20	86.65	13.98	14.01	CR
IGFBP-3	0.31	0.03	0.09	1.02	43.20	86.74	14.07	14.10	CR
TNF-alpha	0.06	0.02	0.26	1.01	43.20	85.57	10.93	10.94	CR
IL-23	0.07	0.01	0.17	1.01	43.20	85.69	9.57	9.58	CR
Angiopoietin-2	0.07	0.01	0.11	1.01	43.20	85.68	11.21	11.22	CR
IL-2	0.03	0.00	0.14	1.00	43.20	85.26	9.90	9.91	CR
MIG	5.20	1.42	0.27	2.68	0.00	73.33	11.04	12.46	PR
IP-10	3.21	0.71	0.22	1.64	0.00	70.44	10.20	10.91	PR
Leptin	-4.01	-0.47	0.12	1.39	0.00	14.30	12.86	12.39	PR
MIP-3ÃŸ	-2.75	-0.36	0.13	1.28	0.00	14.25	11.12	10.76	PR
IL-8	2.81	0.34	0.12	1.26	0.00	70.24	10.01	10.35	PR
BAFF	-2.69	-0.32	0.12	1.25	0.00	14.42	13.25	12.93	PR
ST2	-4.13	-0.25	0.06	1.19	0.00	14.40	13.18	12.93	PR
TFF3	-2.43	-0.16	0.07	1.12	0.00	15.80	13.76	13.59	PR
Resistin	-2.06	-0.24	0.12	1.18	3.30	20.27	13.10	12.86	PR
VEGF	-1.97	-0.23	0.11	1.17	3.30	21.87	10.14	9.91	PR

Cytokine	D Score	Numerator (r)	Denominator (s+s0)	Fold Change	Q Value	Local Fdr	CR expression	PR expression	Regulation
Relaxin-2	-1.86	-0.21	0.11	1.15	3.30	24.38	10.48	10.28	PR
I-TAC	-1.71	-0.18	0.11	1.13	5.70	28.13	12.04	11.86	PR
IL-18 BPa	-1.58	-0.17	0.10	1.12	5.70	32.17	12.21	12.05	PR
Myeloperoxidase	-1.22	-0.29	0.23	1.22	13.21	45.72	10.45	10.16	PR
IL-33	-1.37	-0.17	0.13	1.13	13.21	39.61	9.45	9.28	PR
FGF-19	-1.32	-0.15	0.12	1.11	13.21	41.79	12.28	12.13	PR
M-CSF	-1.12	-0.14	0.13	1.10	13.21	49.93	10.32	10.18	PR
IL-11	-1.08	-0.12	0.11	1.08	13.21	51.70	10.75	10.64	PR
Osteopontin	-1.25	-0.09	0.07	1.06	13.21	44.60	13.93	13.84	PR
CD30	-1.05	-0.20	0.19	1.15	17.11	53.01	10.74	10.54	PR
IL-22	-1.02	-0.14	0.14	1.10	17.11	54.07	11.11	10.98	PR
GRO-a	-0.88	-0.13	0.14	1.09	19.10	59.68	10.45	10.32	PR
Vitamin D BP	-0.78	-0.09	0.11	1.06	19.10	63.97	15.41	15.33	PR
Endoglin	-0.74	-0.05	0.07	1.03	19.10	65.29	14.53	14.48	PR
IL-24	-0.68	-0.11	0.16	1.08	27.89	67.80	9.94	9.83	PR
IL-12 p70	-0.62	-0.07	0.12	1.05	27.89	69.74	10.04	9.97	PR
Pentraxin-3	-0.60	-0.06	0.10	1.04	27.89	70.41	11.52	11.45	PR
GDF-15	-0.60	-0.04	0.06	1.03	27.89	70.49	13.72	13.69	PR
Lipocalin-2	-0.49	-0.03	0.06	1.02	31.37	74.16	15.11	15.08	PR
RANTES	-0.49	-0.03	0.05	1.02	31.37	74.25	14.97	14.94	PR
BDNF	-0.33	-0.06	0.17	1.04	36.33	78.57	12.30	12.25	PR

Cytokine	D Score	Numerator (r)	Denominator (s+s0)	Fold Change	Q Value	Local Fdr	CR expression	PR expression	Regulation
IL-34	-0.15	-0.02	0.16	1.02	36.33	82.61	8.97	8.94	PR
PF4	-0.24	-0.01	0.06	1.01	36.33	80.89	15.44	15.43	PR
RBP4	-0.15	-0.01	0.04	1.00	36.33	82.56	15.83	15.82	PR
FGF basic	0.69	0.14	0.20	1.10	43.20	84.82	11.49	11.63	PR
CD40 ligand	1.09	0.12	0.11	1.09	43.20	80.71	11.61	11.73	PR
MIP-3a	0.84	0.12	0.14	1.09	43.20	83.36	9.40	9.52	PR
TGF-a	0.58	0.08	0.14	1.06	43.20	85.70	9.59	9.67	PR
Complement Component C5/C5a	1.02	0.07	0.07	1.05	43.20	81.48	13.62	13.70	PR
IL-15	0.36	0.06	0.18	1.05	43.20	86.71	9.52	9.59	PR
Adiponectin	1.09	0.06	0.05	1.04	43.20	80.66	15.26	15.31	PR
Angiogenin	0.80	0.05	0.06	1.03	43.20	83.79	15.41	15.46	PR
GM-CSF	0.38	0.04	0.12	1.03	43.20	86.68	10.57	10.61	PR
Dkk-1	0.30	0.04	0.14	1.03	43.20	86.74	10.44	10.48	PR
IGFBP-2	0.50	0.03	0.07	1.02	43.20	86.20	13.99	14.02	PR
Cystatin C	0.44	0.03	0.07	1.02	43.20	86.50	14.42	14.45	PR
C-Reactive Protein	0.68	0.03	0.04	1.02	43.20	84.90	15.59	15.62	PR
IL-16	0.20	0.03	0.13	1.02	43.20	86.52	9.46	9.49	PR
IL-1ÃŸ	0.10	0.01	0.12	1.01	43.20	85.94	9.71	9.72	PR
MIP-1a/MIP-1ÃŸ	0.05	0.01	0.18	1.01	43.20	85.45	9.02	9.03	PR
DPPIV	0.06	0.01	0.10	1.00	43.20	85.55	14.54	14.55	PR

10.0 Table 23: dCT values of mRNA specimens normalised to GADPH or β actin

Plaque Morphology	B-Actin				GADPH			
	I-TAC	**EGFb**	**MPO**	**TSP1**	**I-TAC**	**EGFb**	**MPOa**	**TSP1**
RFC	11.875	10.575	14.57	2.03	9.08	7.78	11.93	-0.92
RFC	12.525	12.165	13.875	7.285	11.02	10.66	12.37	5.78
RFC	14.02		13.61	4.775	9.45		9.04	0.205
RFC		8.955		5.82		2.935		-0.2
RFC	17.36	11.285	16.435	4.27	12.37	6.295	11.445	-0.72
RFC	17.25	11.085	14.58	4.945	12.29	5.99	9.485	-0.15
RFC	17.325	10.575	13.775	5.2	11.635	4.885	8.085	-0.49
RFC	13.72	10.93	15.295	4.93	8.78	5.99	10.355	-0.01
RFC	16.67	14.11	15.38	5.545	11.96	9.4	10.81	0.835
RFC	14.46	10.835	14.02	3.695	9.535	5.91	9.08	-1.23
RFC	15.92	11.815	14.535	5.25	10.32	6.645	9.365	0.08
RFC	12.945	15	17.18	6.245	8.67	10.725	13.37	1.97
RFC	15.615	12.15	15.9	6.65	11.595	8.13	12.03	2.63
RFC	15.48	12.08	13.58	4.55	12.01	8.61	10.35	1.08
RFC	14.27	9.19		3.85	9.25	3.9		-1.44
RFC	14.45	10.725	15.555	3.49	11.025	7.3	12.13	0.065
RFC	13.805	9.695	17.04	2.91	11.13	7.02	14.365	0.235
RFC	12.815			4.955	10.665			2.805
IFC		11.265		5.325		5.02		-0.92

IFC	16.28	12.1	16.51	5.185	13.56	9.37	13.79	2.455
IFC	18.475	9.32	14.99	5.295	13.275	4.12	9.66	0.095
IFC	18.16	9.34		5.645	12.56	3.81		0.115
IFC		8.525	14.57	5.305		2.66	8.63	-0.56
IFC		8.735		5.68		3.6		0.545
IFC	15.125		13.5	7.115	12.225		10.73	4.215
IFC		11.73	14.315	2.915		6.95	9.535	-1.865
IFC	20.99	10.79		5.28	16.24	6.04		0.53
IFC	20.65	9.09	14.45	4.535	14.91	3.57	8.71	-0.985
IFC				5.775				0.025
IFC		9.605	14.57	4.395		4.37	9.3	-0.84
IFC	14.825	9.215	12.925	2.67	11.755	6.145	9.855	-0.4

JAHA Published Paper: ‘Inflammatory Difference in Plaque Erosion and Rupture in Patients with ST-Segment Elevation Myocardial Infarction’

ORIGINAL RESEARCH

American Heart Association | American Stroke Association

Inflammatory Differences in Plaque Erosion and Rupture in Patients With ST-Segment Elevation Myocardial Infarction

Sujay Chandran, BSc, MBBS, MRCP; Johnathan Watkins, MA, PhD; Amina Abdul-Aziz, BSc, MRes; Manar Shafat, BSc, MSc; Patrick A. Calvert, BM, BCh, MA, PhD, MRCP, FACC; Kristian M. Bowles, MBBS, PhD, FRCP, FRCPath; Marcus D. Flather, MBBS, FRCP; Stuart A. Rushworth, BSc, PhD;* Alisdair D. Ryding, MB ChB, MRCP, PhD*

***Background*—**Plaque erosion causes 30% of ST-segment elevation myocardial infarctions, but the underlying cause is unknown. Inflammatory infiltrates are less abundant in erosion compared with rupture in autopsy studies. We hypothesized that erosion and rupture are associated with significant differences in intracoronary cytokines in vivo.

***Methods and Results*—**Forty ST-segment elevation myocardial infarction patients with <6 hours of chest pain were classified as ruptured fibrous cap (RFC) or intact fibrous cap (IFC) using optical coherence tomography. Plasma samples from the infarct-related artery and a peripheral artery were analyzed for expression of 102 cytokines using arrays; results were confirmed with ELISA. Thrombectomy samples were analyzed for differential mRNA expression using quantitative real-time polymerase chain reaction. Twenty-three lesions were classified as RFC (58%), 15 as IFC (38%), and 2 were undefined (4%). In addition, 12% (12 of 102) of cytokines were differentially expressed in both coronary and peripheral plasma. I-TAC was preferentially expressed in RFC (significance analysis of microarrays adjusted $P<0.001$; ELISA IFC 10.2 versus RFC 10.8 $\log_2$ pg/mL; $P=0.042$). IFC was associated with preferential expression of epidermal growth factor (significance analysis of microarrays adjusted $P<0.001$; ELISA IFC 7.42 versus RFC 6.63 $\log_2$ pg/mL, $P=0.036$) and thrombospondin 1 (significance analysis of microarrays adjusted $P=0.03$; ELISA IFC 10.4 versus RFC 8.65 $\log_2$ ng/mL, $P=0.0041$). Thrombectomy mRNA showed elevated I-TAC in RFC ($P=0.0007$) epidermal growth factor expression in IFC ($P=0.0264$) but no differences in expression of thrombospondin 1.

***Conclusions*—**These results demonstrate differential intracoronary cytokine expression in RFC and IFC. Elevated thrombospondin 1 and epidermal growth factor may play an etiological role in erosion. **(*J Am Heart Assoc*. 2017;6:e005868. DOI: 10.1161/JAHA.117.005868.)**

Key Words: coronary artery disease • erosion • inflammation • myocardial infarction • optical coherence tomography • thrombospondin 1

Plaque erosion is a major cause of ST-segment elevation myocardial infarction (STEMI), accounting for ≈30% to 40% of cases,[1–3] yet little is known about the triggers for this pathological process, in contrast to a more detailed understanding of the complex inflammatory processes leading to atherosclerotic plaque rupture.[4] There is increasing interest in plaque erosion, and tailored treatments for this pathology are being tested.[5]

Autopsy studies suggest that markers of inflammation are significantly lower in plaque erosion compared with plaque rupture, with sparse infiltration of macrophages and T lymphocytes within the vessel wall.[6,7] Other studies, however, have suggested an important role for neutrophil infiltrates at sites of plaque erosion.[8] Demonstrating inflammatory profiles of patients that are concordant with autopsy data is important to validate clinical research aiming to identify the triggers of plaque erosion. Nevertheless, evidence that inflammatory differences between erosion and rupture are detectable in patients at the time of myocardial infarction is contradictory.[9–11] We designed a study to optimize the assessment of intracoronary inflammation in patients with STEMI by using multiplex arrays to screen a wide range of inflammatory mediators in plasma samples taken from the culprit vessel.

From the Norfolk and Norwich University Hospital, Norwich, United Kingdom (S.C., K.M.B., M.D.F., A.D.R.); Norwich Medical School, University of East Anglia, Norwich, United Kingdom (S.C., A.A.-A., M.S., K.M.B., M.D.F., S.A.R.); PILAR Research and Education, Cambridge, United Kingdom (J.W.); Papworth Hospital NHS Foundation Trust, Papworth Everard, Cambridge, United Kingdom (P.A.C.).

*Dr Rushworth and Dr Ryding contributed equally to this work.

Correspondence to: Alisdair D. Ryding, MBBS, MRCP, PhD, Cardiology Department, Norfolk and Norwich University Hospital, Colney Lane, Norwich, Norfolk NR4 7UY, United Kingdom. E-mail: alisdair.ryding@nnuh.nhs.uk

Received February 23, 2017; accepted March 15, 2017.

We hypothesized that differential cytokine expression would provide insights into the underlying cause of plaque erosion and could validate our methodology as an approach to studying the etiology of plaque erosion.

Methods

Study Design and Population

We prospectively enrolled consecutive patients undergoing primary percutaneous coronary intervention for STEMI at the Norfolk and Norwich University Hospital. All patients provided written informed consent, and the study was approved by the local ethics committee. Eligible patients included those presenting within 6 hours of the onset of pain, with ST-segment elevation of >1 mm in at least 2 contiguous leads, new left bundle-branch block, or true posterior myocardial infarction on the 12-lead ECG. Exclusion criteria were mechanical ventilation, cardiogenic shock, stent thrombosis, failed thrombectomy, renal insufficiency (estimated glomerular filtration rate <30 mL/min per 1.73 m^2) and failed optical coherence tomography (OCT) imaging of the culprit lesion. All patients received prehospital aspirin 300 mg and clopidogrel 600 mg. All aspects of the primary percutaneous coronary intervention procedure were at the discretion of the interventionalist responsible for the patient's procedure. Gentle predilatation (≤2.0 mm) was permitted to facilitate passage of the OCT catheter.

Blood and Thrombectomy Samples

Thrombectomy was performed in all patients (Pronto catheter; Aquilant International), and aspirates were filtered to separate particulate matter (thrombus with or without plaque fragments) and blood. Particulate matter was stored in Allprotect tissue reagent (Qiagen GmbH) at −70°C. Coronary and peripheral plasma were stored at −70°C.

Clinical and Angiographic Data

Baseline demographics, patient characteristics, angiographic data, procedural details, and clinical outcomes up to 12 months were recorded for each patient. Quantitative coronary angiography was performed using the Quantitative Vascular Analysis package (Siemens) by 2 independent operators.

Optical Coherence Tomography

OCT of the culprit lesion was performed after thrombectomy using a Frequency Domain OCT System (C7-XRTM OCT Intravascular Imaging System; St Jude Medical). OCT images were anonymized and analyzed on a St Jude OCT Offline Review Workstation by 3 independent observers (S.C., P.C., and A.R.) blinded to other data. Established definitions of plaque pathology (ruptured fibrous cap [RFC] and intact fibrous cap [IFC]), plaque constituents and thrombus types were used.[11,12] Discordant results were resolved by consensus or categorized as *undefined*. Measurements were performed with dedicated OCT system software (B.0.1; Light Lab Imaging). Minimum fibrous cap thickness was measured at the thinnest point of the cap, whereas mean cap thickness was computed as the mean of 3 evenly distributed measurements along the fibrous cap.

Cytokine Arrays

Coronary and peripheral arterial plasma samples were analyzed using the Proteome Profiler Human XL Cytokine Array Kit (ARY022; R&D Systems), according to the manufacturer's instructions. Quantification of cytokine optical densities were obtained with the HLImage++ software (Western Vision).

ELISA

ELISAs for epidermal growth factor (EGF; DEG00; R&D Systems), interferon-inducible T-cell alpha chemoattractant (I-TAC; DCX110; R&D Systems), monokine induced by γ-interferon (DCX900; R&D Systems), myeloperoxidase (DMYE00B; R&D Systems), and thrombospondin 1 (TSP-1; DTSP10; R&D Systems) were performed according to the manufacturer's instructions.

Thrombectomy Analysis

Total RNA was extracted from homogenized thrombectomy specimens using the ReliaPrep RNA extraction kit (Promega). Reverse transcription was performed using a cDNA synthesis Kit (PCR Biosystems). Relative quantitative real-time polymerase chain reaction used SYBR green technology (PCR Biosystems) on cDNA reverse transcribed from purified RNA. After preamplification (95°C for 2 minutes), the PCRs were amplified for 45 cycles (95°C for 15 seconds, 60°C for 10 seconds, and 72°C for 10 seconds) on a 384-well LightCycler 480 (Roche). mRNA was analyzed for EGF, myeloperoxidase, I-TAC, and TSP1 expression and normalized to GAPDH or β-actin mRNA expression using the comparative cycle threshold method. Primer sequences were designed using KicqStart (Sigma-Aldrich).

Primer sequences for quantitative real-time polymerase chain reaction were as follows (forward/reverse): β-actin, gacgacatggagaaaatctg/atgatctgggtcatcttctc; EGF, ggtggtga agttgatctaaag/tagcatgtgttgagattctg; GAPDH, ctccttgttcgacagt

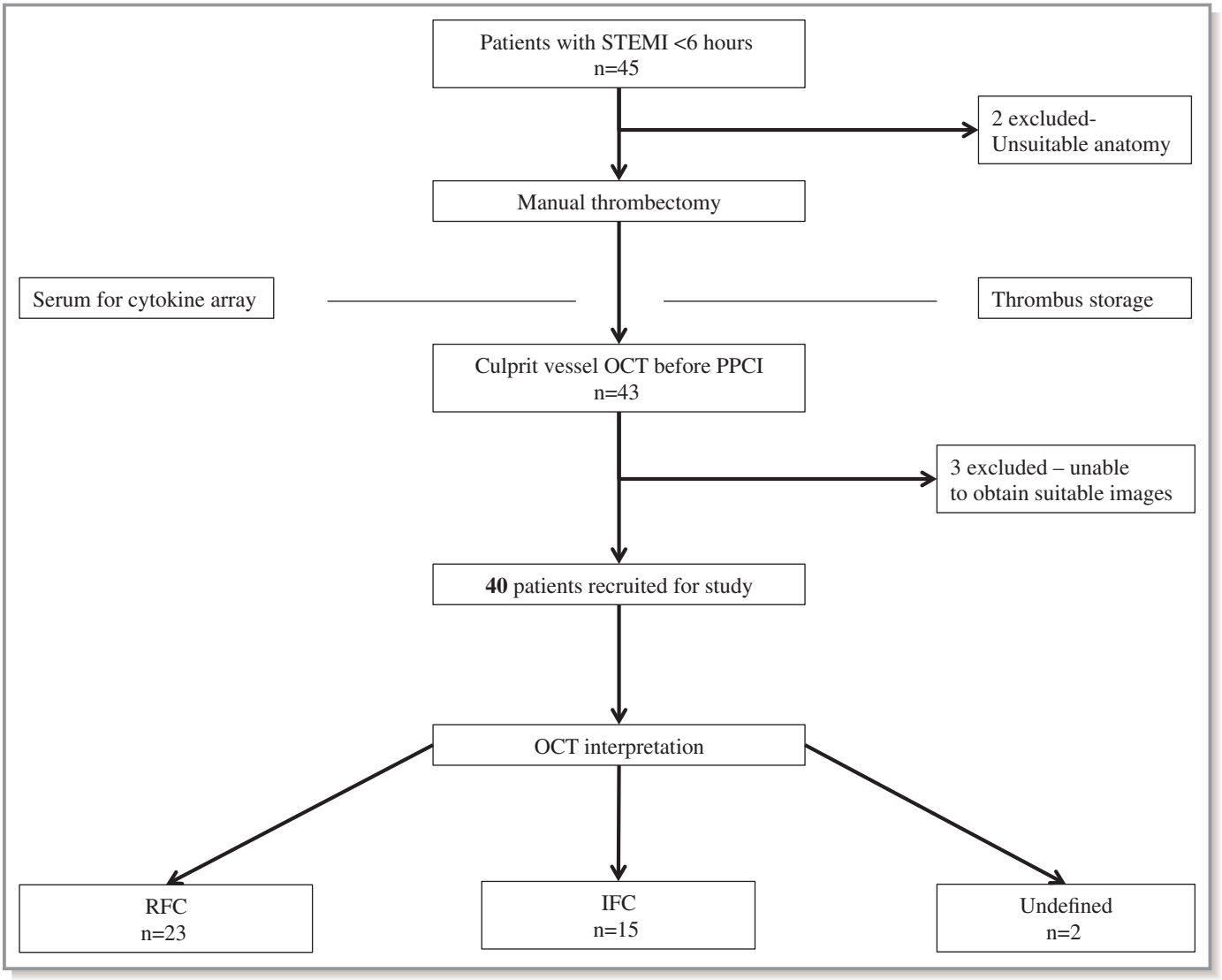

Figure 1. Study enrollment. IFC indicates intact fibrous cap; OCT, optical coherence tomography; PPCI, primary percutaneous coronary intervention; RFC, ruptured fibrous cap; STEMI, ST-segment elevation myocardial infarction.

cagcc/gactccgaccttcaccttcc; I-TAC, ctacagttgttcaaggcttc/cac tttcactgcttttaccc; myeloperoxidase, ccatggaactcctatcctac/ttg acttggacaacacattc; TSP-1, gtgactgaagagaacaaagag/cagctatca acagtccattc.

Cytokine Array Analysis

Intensities of the negative control of each sample were subtracted from the intensity of each cytokine-sample pair,[13] and relative intensity values were quantile-normalized.[14] To allow for direct comparisons to be made between cytokines, values were $\log_2$ transformed. Differential expression was assessed using the significance analysis of microarrays method,[15] with *P* values corrected for multiple testing using the Benjamini–Hochberg procedure.[16] The output of this included assignment to either a group comprising cytokines with an average expression higher in patients with IFC or a group comprising cytokines with an average expression higher in patients with RFC. Significance analysis of microarrays was conducted for coronary and peripheral blood samples separately. A differential expression score (D-score) and average $\log_2$ fold change in expression were captured for each cytokine in addition to the adjusted *P* value. Analyses were performed in the R statistical language environment, version 3.1.2, using several Bioconductor packages.[17]

Statistical Analysis

Continuous variables were reported as median and first to third quartiles. Categorical data were reported as numbers and relative percentages. Overall comparisons across groups

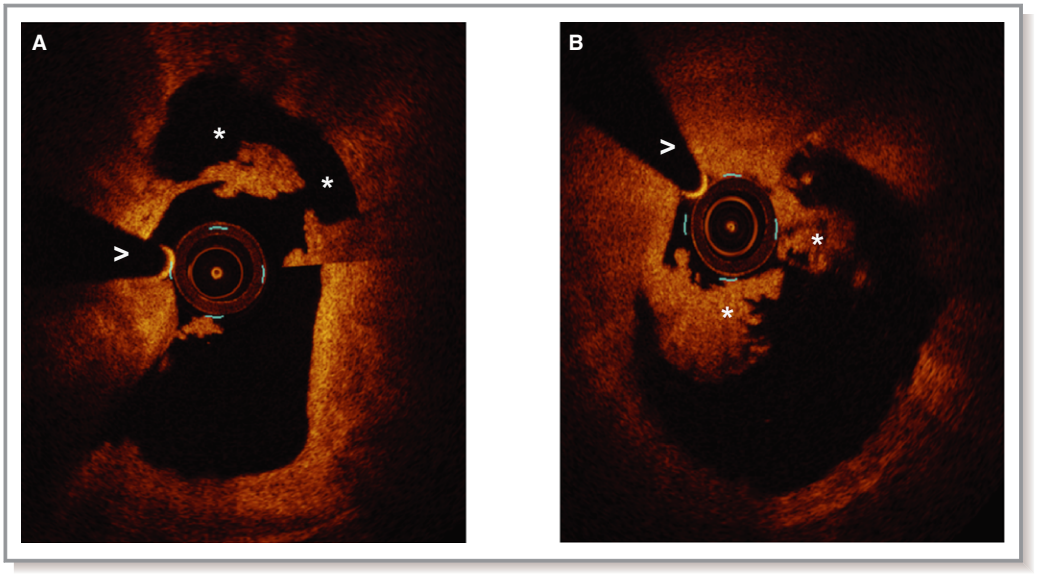

Figure 2. Ruptured and intact fibrous cap appearance using optical coherence tomography. A, Ruptured fibrous cap. *Rupture cavity. >Wire artifact. B, Intact fibrous cap.*Thrombus. >Wire artifact.

were based on the nonparametric Wilcoxon rank sum test for continuous variables and the Fisher exact test for categorical variables. All *P* values are 2-sided. *P* values were corrected for multiple testing using the Benjamini–Hochberg procedure.[16] Adjusted *P* values <0.05 were considered significant unless otherwise stated.

Results

Baseline and Angiographic Characteristics

Between February 2, 2015, and October 14, 2015, 40 STEMI patients were recruited into the Plaque Erosion Pilot Study (Figure 1), representing ≈30% of all potentially eligible

Table 1. Baseline Characteristics

	RFC (n=23)	IFC (n=15)	*P* Value	Adjusted *P* Value
Age, y	65 (59.5–75)	60 (52–64.5)	0.03	0.36
Sex (male)	16 (69.6)	10 (66.7%)	1.00	1.00
Hypertension	8 (34.8%)	3 (20%)	0.47	0.71
Hyperlipidemia	8 (34.8%)	4 (26.7%)	0.44	0.71
Smoker	12 (52.2%)	8 (53.3%0	1.00	1.00
Diabetes mellitus	0 (0%)	2 (13.3%)	0.15	0.60
Previous MI	0 (0%)	0 (0%)	. . .	. . .
Previous PCI	0 (0%)	0 (0%)	. . .	. . .
Symptom onset to lab, minutes	160 (125–207.5)	190 (145–247.5)	0.24	0.71
Door to balloon time, minutes	37 (29–61)	44 (29–46)	0.47	0.71
Call to balloon time, minutes	125 (95–147)	134 (99–142)	0.71	0.95
Killip class			0.15	0.60
Class 1	23 (100%)	13 (86.7%)		
Class 2	0 (0%)	2 (13.3%)		
TIMI risk score	2 (1–4)	2 (1–2)	0.46	0.71
Anemia	0 (0%)	0 (0%)	1.00	1.00

Values are median (first to third quartile) or n (%). Both unadjusted and Benjamini–Hochberg-adjusted *P* values are shown. IFC indicates intact fibrous cap; MI, myocardial infarction; PCI, percutaneous coronary intervention; RFC, ruptured fibrous cap; TIMI, Thrombolysis in Myocardial Infarction.

Table 2. Angiographic and Procedural Characteristics

	RFC (n=23)	IFC (n=15)	*P* Value	Adjusted *P* Value
Number of lesions treated			1.00	1.00
1	22 (95.7%)	15 (100%)		
2	1 (4.3%)	0 (0%)		
Infarct related artery			0.64	0.94
LAD	7 (30.4%)	9 (60%)		
LCX	4 (17.4%)	2 (13.3%)		
RCA	12 (52.2%)	4 (26.7%)		
Multivessel disease	9 (39.1%)	4 (26.7%)	0.5	0.88
Thrombectomy	23 (100%)	15 (100%)	1.00	1.00
Gp2b3a use	9 (39.1%)	8 (53.3%)	0.51	0.88
Radial access	23 (100%)	14 (93.3%)	0.39	0.88
Stent used	18 (78.3%)	8 (53.3%)	0.16	0.88
Total stent length, mm	27 (22–38)	23 (17–28)	0.06	0.88
Drug coated balloon angioplasty	5 (21.7%)	6 (40%)	0.28	0.88
Direct stenting	11 (47.8%)	5 (33.3%)	0.51	0.88
Maximum balloon/stent diameter, mm	4 (3.375–4)	3.5 (3.125–3.875)	0.20	0.88
Base TIMI flow			0.63	0.94
0	14 (60.9%)	10 (66.7%)		
1	0 (0%)	0 (0%)		
2	3 (13.3%)	3 (20%)		
3	6 (26.8%)	2 (13.3%)		
Final TIMI flow			0.82	1.00
0	0 (0%)	0 (0%)		
1	1 (4.3%)	0 (0%)		
2	0 (0%)	0 (0%)		
3	22 (95.6%)	15 (100%)		
Procedural success	22 (95.6%)	15 (100%)		
QCA at baseline				
Reference vessel diameter, mm	3.28 (2.81–3.62)	3.17 (2.73–3.33)	0.44	0.88
Minimal luminal diameter, mm	0 (0–0.97)	0 (0–0.84)	0.96	1.00
Diameter stenosis (%)	100 (75.6–100)	100 (75.2–100)	0.88	1.00
QCA after thrombectomy				
Reference vessel diameter, mm	3.38 (2.85–3.76)	3.22 (2.58–3.49)	0.39	0.88
Minimal luminal diameter	1.1 (0.88–1.45)	0.94 (0.7–1.2)	0.40	0.88
Diameter stenosis	66.5 (46.4–77.3)	68.8 (62.3–73.6)	0.75	1.00

Values are median (first to third quartile) or n (%). Both unadjusted and Benjamini–Hochberg-adjusted *P* values are shown. Gp2b3a indicates glycoprotein$_{IIbIIIa}$; IFC, intact fibrous cap; LAD, left anterior descending; LCX, left circumflex; QCA, quantitative coronary angiography; RCA, right coronary artery; RFC, ruptured fibrous cap; TIMI, Thrombolysis in Myocardial Infarction.

patients. An additional 5 patients were not enrolled in the study because of unsuitable anatomy and inability to obtain adequate OCT images. A fully identifiable culprit plaque was adjudicated in 38 patients, with RFC identified in 23 (57.5%) and IFC in 15 (37.5%); 2 (5%) were undefined (Figure 2).

There were no differences in baseline characteristics between patients with RFC and IFC (Table 1). Both groups

Table 3. OCT Analysis

	RFC (n=23)	IFC (n=15)	*P* Value	Adjusted *P* Value
Minimum cap thickness, μm	40 (30–40)	80 (70–95)	<0.001	0.006
Mean cap thickness, μm	52 (40–59)	100 (99–134)	<0.001	0.006
Length of lesion, mm	11.3 (9.75–12.55)	11.4 (9.9–15.1)	0.82	1
Plaque characteristics			0.93	1
Fibrocalcific	1 (4.34%)	1 (4.34%)		
Fibrous	2 (8.7%)	6 (40%)		
Lipid-rich	20 (86.7%)	8 (53.3%)		
Area stenosis (%)	79.0 (52.5–83.1)	74.3 (70.4–77.1)	0.16	0.64
Residual thrombus characteristics			0.54	1
Red	1 (4)	1 (7)		
White	12 (52)	5 (33)		
Mixed	9 (39)	5 (33)		
None	1 (4)	4 (27)		

Values are median (first to third quartile) or n (%). Both unadjusted and Benjamini–Hochberg-adjusted *P* values are shown. IFC indicates intact fibrous cap; RFC, ruptured fibrous cap.

had very similar ischemic times and angiographic findings. Although there was lower use of stents in the IFC group, this result was nonsignificant (78.3% RFC versus 53.3% IFC, adjusted *P*=0.88) (Table 2).

Optical Coherence Tomography Data

Cap thickness was significantly lower in the RFC group (minimum cap thickness: RFC 40 μm [range 30–40 μm] versus IFC 80 μm [range 70–95 μm], adjusted *P*=0.006: mean cap thickness RFC 52 μm [range 40–59 μm] versus IFC 100 μm [range 99–134 μm], adjusted *P*=0.006) (Table 3). There were no significant differences in other plaque parameters, although there was a trend toward a more fibrous phenotype in IFC. The residual thrombus burden after thrombectomy and thrombus types were similar between groups, with white thrombus and mixed thrombus predominating (Table 3).

Clinical Outcomes

At 12 months, 1 death occurred in the RFC group and 1 transient ischemic attack in the IFC group, with no statistical differences between the 2 groups.

Cytokine Analysis

Just under 40.2% (41 of 102) of cytokines were more highly expressed on average in patients with IFC than RFC for both coronary and peripheral samples. By contrast, 47.1% (48 of 102) were more highly expressed on average in RFC patients than in IFC patients for both coronary and peripheral samples (Figure 3A and 3B). For the remaining cytokines (12.7%, 13 of 102), preferential expression was discordant between coronary and peripheral samples (Figure 3A and 3B). Despite this, the preferential expressions of cytokines (higher in either RFC or IFC) were, for the most part, consistent between coronary and peripheral samples (odds ratio 46.03, 95% CI 13.33–198.59, *P*<0.001) (Figure 3B).

EGF and TSP-1 were the only molecules with significantly higher expression in IFC patients than in RFC patients in both coronary and peripheral samples (adjusted *P*<0.05) (Figure 3C). The average $\log_2$ fold change in expression was >1.75 for both (Figure 3C). By contrast, 10 molecules demonstrated significant preferential expression in patients with RFC for both coronary and peripheral samples, including monokine induced by γ-interferon, I-TAC, matrix metalloproteinase-9 (MMP-9), aggrecan, lipocalin 2, interleukin 18 binding protein, trefoil factor 3, complement factor D, RANTES, and adiponectin (adjusted *P*<0.05) (Figure 3C).

ELISA Validation

For each lesion group, we selected 2 cytokines with significant differential expression in both coronary and peripheral data sets and an average $\log_2$ fold change of at least 1.5 (Figure 3C). Therefore, we sought to orthogonally validate higher expressions of EGF and TSP-1 among IFC cases and monokine induced by γ-interferon and I-TAC among rupture cases using ELISA. ELISA for myeloperoxidase was also undertaken, given the potential relevance to plaque erosion.

EGF expression was significantly higher in both coronary and peripheral IFC samples compared with RFC samples ($P<0.05$) (Figure 4). By contrast, TSP-1 was significantly higher only in IFC coronary samples ($P=0.0041$), and I-TAC was significantly higher only in RFC coronary samples ($P=0.042$) (Figure 4). No significant differences were observed for monokine induced by γ-interferon or myeloperoxidase expression between IFC and RFC cases for coronary or peripheral samples ($P>0.05$).

Thrombectomy Quantitative Real-Time Polymerase Chain Reaction Analysis

Thrombectomy yielded an analyzable sample in 18 RFC and 13 IFC cases. Expression of I-TAC mRNA was significantly increased in RFC samples compared with IFC ($P=0.0007$), whereas the opposite was true of EGF expression ($P=0.0264$). There were no differences in the expression of TSP-1 or myeloperoxidase between groups ($P>0.05$) (Figure 5).

Discussion

We detected multiple differences in the inflammatory profiles of IFC and RFC in patients with STEMI, using cytokine arrays. We confirmed elevated EGF and TSP-1 in IFC and elevated I-TAC in RFC using ELISAs. Most of these differences were demonstrable only in coronary plasma samples. In addition, we demonstrated that these findings were replicated, with the exception of TSP-1, in analysis of mRNA in thrombectomy samples. These observations are new and support the

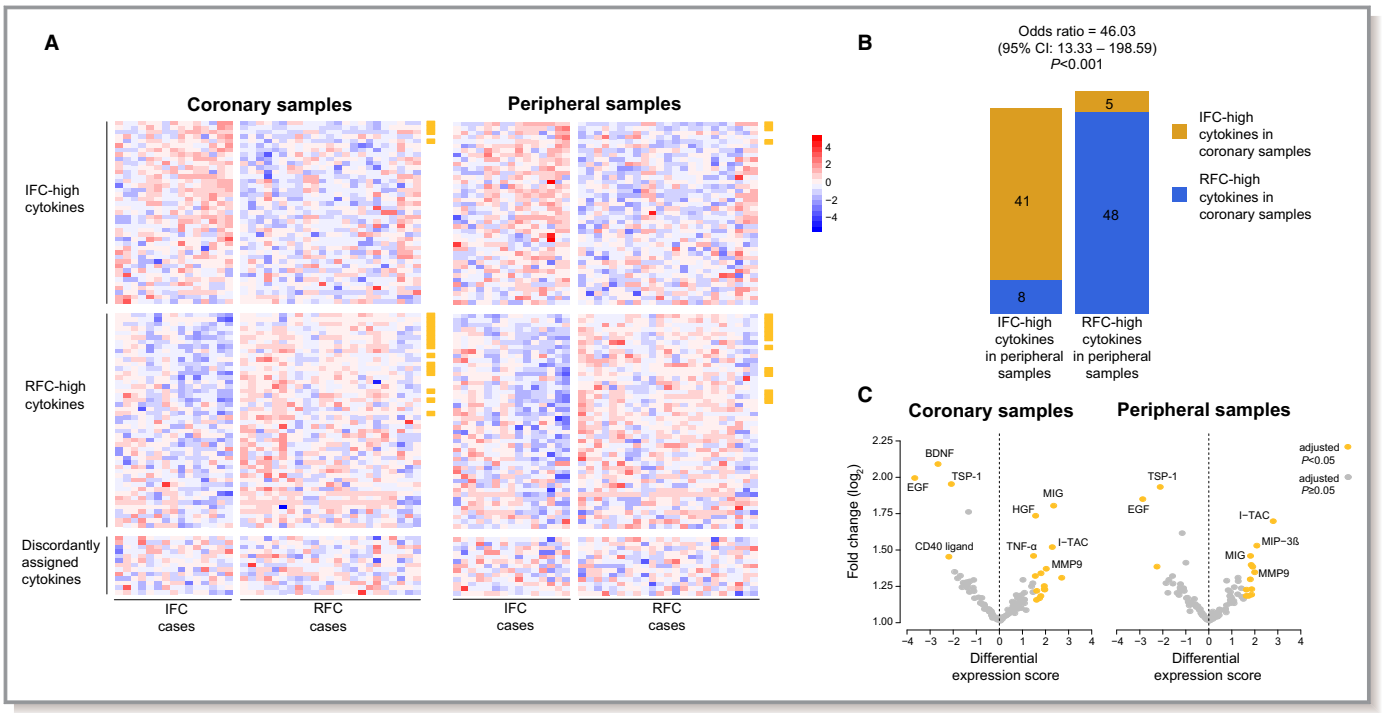

Figure 3. Differential expression analysis of cytokines. A, Heat maps of the cytokines differentially expressed between the 2 plaque pathologies. The coronary samples are shown in the left heat map and peripheral samples on the right heat map. Samples (columns) are sorted from left to right in ascending order within the IFC (left-hand panels) and RFC (right-hand panels) groups. The cytokines (rows) are ordered from top to bottom by descending average fold change within the IFC-assigned cytokine group (top panels), the RFC-assigned group (middle panels), and discordantly assigned group (bottom panels). Heat map colors represent $\log_2$ expression values standardized across the data set. A legend that maps color to standardized expression value is shown to the side of the heat maps. The golden bars on the side of each heat map indicate significant hits. B, Bar plots of concordance between preferential expression assignments for coronary samples and peripheral samples. For peripheral samples, cytokines are stratified by bar: IFC-high cytokines in the left bar and RFC-high cytokines in the right bar. For coronary samples, cytokines are stratified by color: IFC-high cytokines in orange and RFC-high cytokines in blue. Odds ratio, 95% CI, and *P* value are reported for Fisher exact test. C, Volcano plots of the $\log_2$ fold change of expression for all cytokines against the significance analysis of microarrays differential expression score for the coronary (left plot) and peripheral (right plot) samples. Positive differential expression scores indicate an association to the group more highly expressed in RFC cases than in IFC cases, whereas negative D-scores represent an association to the group more highly expressed in IFC cases. Cytokines that were significantly associated with either plaque type (adjusted $P<0.05$; significance analysis of microarrays) are colored in gold, whereas nonsignificant associations are in grey. BDNF indicates brain-derived neurotrophic factor; EGF, epidermal growth factor; HGF, hepatocyte growth factor; IFC, intact fibrous cap; I-TAC, interferon-inducible T cell alpha chemoattractant; MIG, monokine induced by γ-interferon; MIP-3α, macrophage inflammatory protein 3α; MMP-9, matrix metalloprotein 9; MPO, myeloperoxidase; RFC, ruptured fibrous cap; TNFα, tumor necrosis factor α; TSP-1, thrombospondin 1.

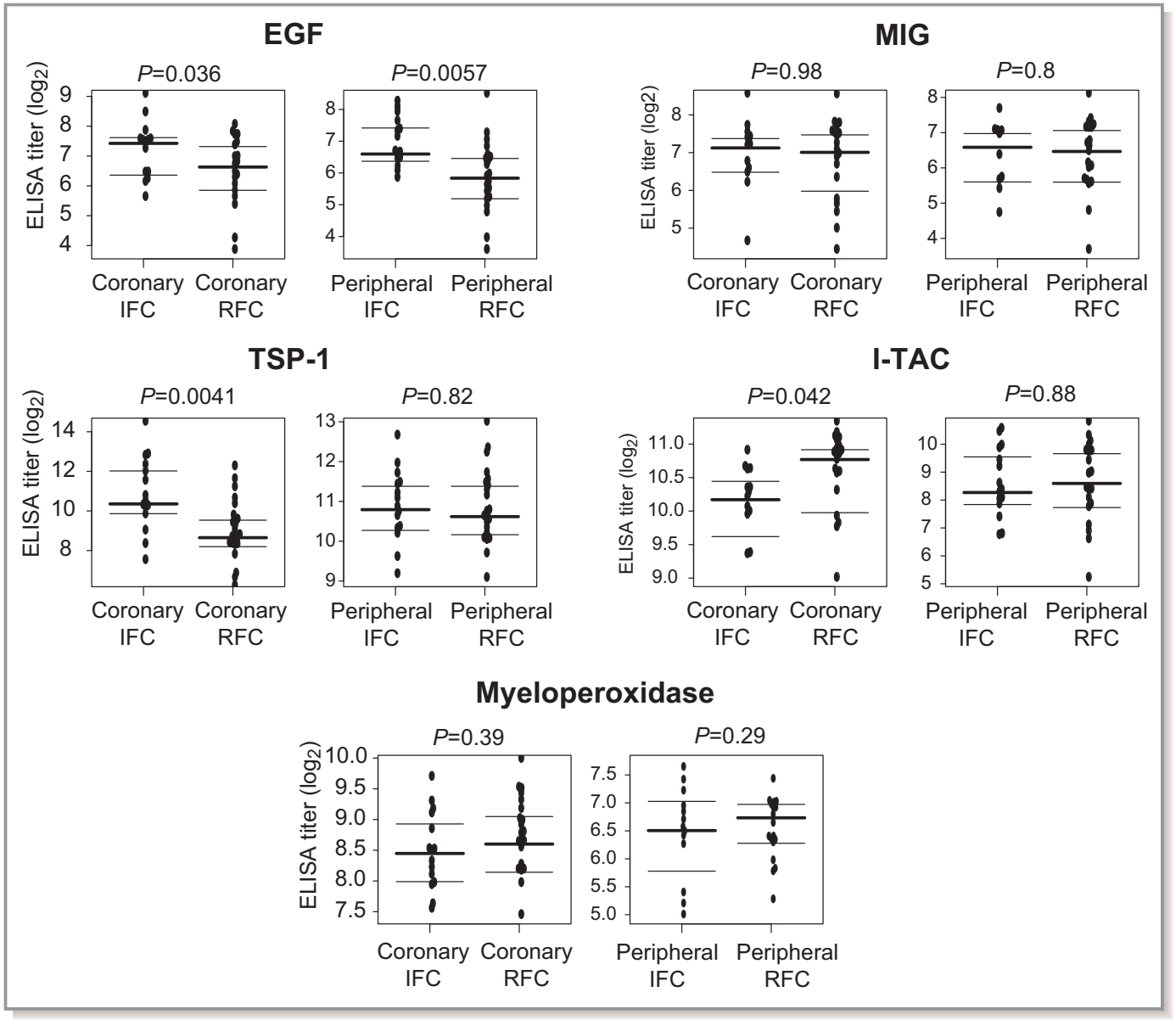

Figure 4. Plasma ELISA analysis. Plasma titers according to plaque pathology and sample site. Horizontal lines indicate median $\log_2$ values and interquartile ranges. EGF indicates epidermal growth factor; IFC, intact fibrous cap; I-TAC, interferon-inducible T cell alpha chemoattractant; MIG, monokine induced by γ-interferon; TSP-1, thrombospondin 1; RFC, ruptured fibrous cap.

concept that different atherosclerotic pathologies may be associated with distinct intracoronary inflammatory profiles.

Previous comparative studies of inflammation in plaque erosion and rupture have yielded conflicting results. Some reports suggest significant elevation of myeloperoxidase in erosion,[9,10] and elevated high-sensitivity C-reactive protein and matrix metalloproteinase 9 in rupture.[10] In contrast other studies have not found any difference in the levels of myeloperoxidase, thromboxane B2, eosinophilic cationic protein,[11] or high-sensitivity C-reactive protein.[2,11,18] Our study is unique in that we sampled both coronary and peripheral arterial plasma, screened a much larger range of inflammatory molecules, and enrolled only patients with short ischemic times presenting with STEMI.

To put our results in context, the levels of EGF, TSP-1, and I-TAC in IFC are ≈14-, 4.8-, and 1.6-fold higher, respectively, compared with median values in healthy volunteers reported in other studies.[19–21] The respective values for RFC are ≈8-, 1.4- and 2.4-fold higher.

The significance of elevated EGF and TSP-1 in IFC compared with RFC is unclear. Both EGF and TSP-1 are stored in platelet granules,[22] and elevated plasma levels may simply reflect differences in thrombus composition and platelet activation.[3,10,23] This possibility is supported by the

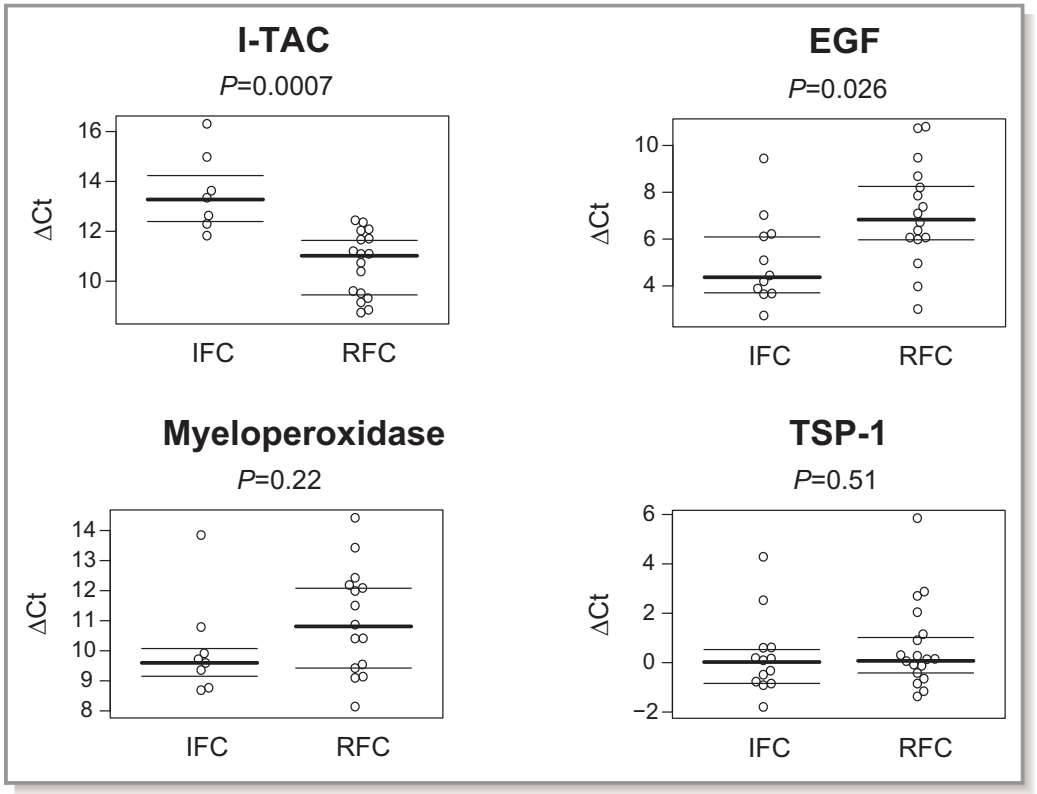

Figure 5. Quantitative real-time polymerase chain reaction analysis of thrombectomy specimens. Relative mRNA expression in coronary thrombectomy specimens. Lower ΔCt values indicate higher expression. EGF, epidermal growth factor; IFC, intact fibrous cap; I-TAC, interferon-inducible T cell alpha chemoattractant; TSP-1, thrombospondin 1; RFC, ruptured fibrous cap.

concordance of EGF expression in plasma and thrombectomy samples. It is also possible that differences in thrombus type are not responsible for these findings. We did not observe significant differences in thrombus type on OCT, nor did the array analysis identify differences in other platelet-related molecules such as platelet factor 4 or platelet-derived growth factor (unpublished data). The discordance between TSP-1 expression in plasma and thrombectomy samples may reflect local expression of TSP-1 within the coronary artery.

TSP-1 has complex biological effects that may be relevant to plaque erosion. It is a matricellular glycoprotein that is expressed in platelets, vascular smooth muscle cells, endothelial cells, and vascular fibroblasts and is present in the extracellular matrix of vessels.[24] It impairs endothelial cell adhesion, motility, growth, and survival[25–27] and stabilizes thrombi.[28] Interestingly a polymorphism of the gene encoding TSP-2 has been associated with plaque erosion in a cohort of patients with sudden death.[29] Studies of TSP-1 and TSP-2 expression in autopsy specimens might clarify whether TSPs are relevant to plaque erosion.

Array analysis confirmed that multiple molecules thought to be important in plaque rupture were preferentially expressed in the RFC group, including matrix metalloproteinase 9, lipocalin 2, and RANTES.[30–32] We also confirmed significantly increased I-TAC/CXCL11 in coronary plasma samples in RFC, which is a new finding. I-TAC plays a key role in the recruitment and retention of activated T lymphocytes at sites of inflammation during atherogenesis and is known to be expressed by neovascular endothelial cells and macrophages in the shoulder regions of advanced atherosclerotic lesions.[33] We do not know whether increased I-TAC mRNA in thrombectomy specimens reflects expression by inflammatory cells trapped in thrombus or aspirated atherosclerotic material.

Implications

We demonstrated the feasibility of studying different plaque pathologies using intracoronary blood sampling, OCT, and multiplex arrays to screen for molecular differences. The cytokines identified have been shown to be involved in mechanisms that make them plausible candidates for driving or facilitating plaque destabilization. This supports the validity of our approach to studying potential triggers of plaque erosion and rupture. Larger studies might refine the identification of novel biomarkers for such lesions and facilitate the customization of treatment according to the underlying pathology.[5]

Study Limitations

This is a single-center study, and larger studies are required to confirm our findings. To minimize disruption to the normal primary percutaneous coronary intervention procedure, peripheral and coronary arterial blood samples were not taken simultaneously. We were able to validate only a small number of the array findings with ELISAs because of limited plasma samples. In common with other studies,[3,10,34] predilatation was permitted before OCT and could have led to misclassification of pathology. We have used IFC as an OCT surrogate for plaque erosion, but direct histological confirmation is not possible.[12]

Conclusions

We demonstrated significant differences in the inflammatory profiles of RFC and IFC in patients with STEMI, using cytokine arrays. Novel findings include elevated intracoronary EGF and TSP-1 with IFC and elevated intracoronary I-TAC with RFC. Some of the differences are also reflected in mRNA analysis of thrombectomy samples. These results may help to further understand the pathophysiology of plaque erosion and to potentially tailor future treatment strategies.

Acknowledgments

OCT catheters were donated by St Jude Medical. St Jude, Norwich Research Park, and the Norfolk Heart Trust were not involved with any of the study processes. We are grateful to Professor Roger Hall, Professor Andreas Baumbach, and Dr Thomas Johnson for their oversight of the study.

Sources of Funding

The study was supported by the Norwich Research Park (Science Link Seed Fund) and the Norfolk Heart Trust.

Disclosures

None.

References

1. Guagliumi G, Capodanno D, Saia F, Musumeci G, Tarantini G, Garbo R, Tumminello G, Sirbu V, Coccato M, Fineschi M, Trani C, De Benedictis M, Limbruno U, De Luca L, Niccoli G, Bezerra H, Ladich E, Costa M, Biondi Zoccai G, Virmani R. Mechanisms of atherothrombosis and vascular response to primary percutaneous coronary intervention in women versus men with acute myocardial infarction: results of the OCTAVIA study. *JACC Cardiovasc Interv*. 2014;7:958–968.
2. Jia H, Abtahian F, Aguirre AD, Lee S, Chia S, Lowe H, Kato K, Yonetsu T, Vergallo R, Hu S, Tian J, Lee H, Park SJ, Jang YS, Raffel OC, Mizuno K, Uemura S, Itoh T, Kakuta T, Choi SY, Dauerman HL, Prasad A, Toma C, McNulty I, Zhang S, Yu B, Fuster V, Narula J, Virmani R, Jang IK. In vivo diagnosis of plaque erosion and calcified nodule in patients with acute coronary syndrome by intravascular optical coherence tomography. *J Am Coll Cardiol*. 2013;62:1748–1758.
3. Niccoli G, Montone RA, Di Vito L, Gramegna M, Refaat H, Scalone G, Leone AM, Trani C, Burzotta F, Porto I, Aurigemma C, Prati F, Crea F. Plaque rupture and intact fibrous cap assessed by optical coherence tomography portend different outcomes in patients with acute coronary syndrome. *Eur Heart J*. 2015;36:1377–1384.
4. Libby P. Mechanisms of acute coronary syndromes and their implications for therapy. *N Engl J Med*. 2013;368:2004–2013.
5. Jia H, Dai J, Hou J, Xing L, Ma L, Liu H, Xu M, Yao Y, Hu S, Yamamoto E, Lee H, Zhang S, Yu B, Jang I. Effective anti-thrombotic therapy without stenting: intravascular optical coherence tomography-based management in plaque erosion (the EROSION study). *Eur Heart J*. 2016;38:1–9.
6. Campbell IC, Suever JD, Timmins LH, Veneziani A, Vito RP, Virmani R, Oshinski JN, Taylor WR. Biomechanics and inflammation in atherosclerotic plaque erosion and plaque rupture: implications for cardiovascular events in women. *PLoS One*. 2014;9:e111785.
7. Falk E, Nakano M, Bentzon JF, Finn AV, Virmani R. Update on acute coronary syndromes: the pathologists' view. *Eur Heart J*. 2013;34:719–728.
8. Quillard T, Araújo HA, Franck G, Shvartz E, Sukhova G, Libby P. TLR2 and neutrophils potentiate endothelial stress, apoptosis and detachment: implications for superficial erosion. *Eur Heart J*. 2015;36:1394–1404.
9. Ferrante G, Nakano M, Prati F, Niccoli G, Mallus MT, Ramazzotti V, Montone RA, Kolodgie FD, Virmani R, Crea F. High levels of systemic myeloperoxidase are associated with coronary plaque erosion in patients with acute coronary syndromes: a clinicopathological study. *Circulation*. 2010;122:2505–2513.
10. Niccoli G, Montone RA, Cataneo L, Cosentino N, Gramegna M, Refaat H, Porto I, Burzotta F, Trani C, Leone AM, Severino A, Crea F. Morphological-biohumoral correlations in acute coronary syndromes: pathogenetic implications. *Int J Cardiol*. 2014;171:463–466.
11. Saia F, Komukai K, Capodanno D, Sirbu V, Musumeci G, Boccuzzi G, Tarantini G, Fineschi M, Tumminello G, Bernelli C, Niccoli G, Coccato M, Bordoni B, Bezerra H, Biondi-Zoccai G, Virmani R, Guagliumi G. Eroded versus ruptured plaques at the culprit site of STEMI: in vivo pathophysiological features and response to primary PCI. *JACC Cardiovasc Imaging*. 2015;8:566–575.
12. Tearney GJ, Regar E, Akasaka T, Adriaenssens T, Barlis P, Bezerra HG, Bouma B, Bruining N, Cho JM, Chowdhary S, Costa MA, De Silva R, Dijkstra J, Di Mario C, Dudeck D, Falk E, Feldman MD, Fitzgerald P, Garcia H, Gonzalo N, Granada JF, Guagliumi G, Holm NR, Honda Y, Ikeno F, Kawasaki M, Kochman J, Koltowski L, Kubo T, Kume T, Kyono H, Lam CCS, Lamouche G, Lee DP, Leon MB, Maehara A, Manfrini O, Mintz GS, Mizuno K, Morel MA, Nadkarni S, Okura H, Otake H, Pietrasik A, Prati F, Rber L, Radu MD, Rieber J, Riga M, Rollins A, Rosenberg M, Sirbu V, Serruys PWJC, Shimada K, Shinke T, Shite J, Siegel E, Sonada S, Suter M, Takarada S, Tanaka A, Terashima M, Troels T, Uemura S, Ughi GJ, Van Beusekom HMM, Van Der Steen AFW, Van Es GA, Van Soest G, Virmani R, Waxman S, Weissman NJ, Weisz G. Consensus standards for acquisition, measurement, and reporting of intravascular optical coherence tomography studies: a report from the International Working Group for Intravascular Optical Coherence Tomography Standardization and Validation. *J Am Coll Cardiol*. 2012;59:1058–1072.
13. R&D Systems. Proteome ProfilerTM Array: human XL cytokine array kit. 2014.
14. Bolstad BM, Irizarry R, Astrand M, Speed TP. A comparison of normalization methods for high density oligonucleotide array data based on variance and bias. *Bioinformatics*. 2003;19:185–193.
15. Tibshirani R, Chu G, Narasimhan B, Li J. samr: SAM: significance analysis of microarrays. 2011.
16. Benjamini Y, Hochberg Y. Controlling the false discovery rate: a practical and powerful approach to multiple testing. *J R Stat Soc B*. 1995;57:289–300.
17. R Core Team. *R: A Language and Environment for Statistical Computing*. Vienna, Austria: R Found. Stat. Comput.; 2014. {ISBN} 3-900051-07-0.
18. Vergallo R, Ren X, Yonetsu T, Kato K, Uemura S, Yu B, Jia H, Abtahian F, Aguirre AD, Tian J, Hu S, Soeda T, Lee H, McNulty I, Park SJ, Jang Y, Prasad A, Lee S, Zhang S, Porto I, Biasucci LM, Crea F, Jang IK. Pancoronary plaque vulnerability in patients with acute coronary syndrome and ruptured culprit plaque: a 3-vessel optical coherence tomography study. *Am Heart J*. 2014;167:59–67.
19. Berrahmoune H, Lamont JV, Herbeth B, FitzGerald PS, Visvikis-Siest S. Biological determinants of and reference values for plasma interleukin-8, monocyte chemoattractant protein-1, epidermal growth factor, and vascular endothelial growth factor: results from the STANISLAS cohort. *Clin Chem*. 2006;52:504–510.
20. Barclay JL, Keshvari S, Whitehead JP, Inder WJ. Development of an enzyme-linked immunosorbent assay for thrombospondin-1 and comparison of human plasma and serum concentrations. *Ann Clin Biochem*. 2016;53:606–610.
21. Kao J, Kobashigawa J, Fishbein MC, Robb MacLellan W, Burdick MD, Belperio JA, Strieter RM. Elevated serum levels of the CXCR3 chemokine ITAC are associated with the development of transplant coronary artery disease. *Circulation*. 2003;107:1958–1961.

22. Burkhart JM, Gambaryan S, Watson SP, Jurk K, Walter U, Sickmann A, Heemskerk JWM, Zahedi RP. What can proteomics tell us about platelets? *Circ Res*. 2014;114:1204–1219.

23. Sato Y, Hatakeyama K, Yamashita A, Marutsuka K, Sumiyoshi A, Asada Y. Proportion of fibrin and platelets differs in thrombi on ruptured and eroded coronary atherosclerotic plaques in humans. *Heart*. 2005;91:526–530.

24. Roberts DD, Miller TW, Rogers NM, Yao M, Isenberg JS. The matricellular protein thrombospondin-1 globally regulates cardiovascular function and responses to stress via CD47. *Matrix Biol*. 2012;31:162–169.

25. Murphy-Ullrich JE, Hook M. Thrombospondin modulates focal adhesions in endothelial cells. *J Cell Biol*. 1989;109:1309–1319.

26. Bagavandoss P, Wilks JW. Specific inhibition of endothelial cell proliferation by thrombospondin. *Biochem Biophys Res Commun*. 1990;170:867–872.

27. Jiménez B, Volpert OV, Crawford SE, Febbraio M, Silverstein RL, Bouck N. Signals leading to apoptosis-dependent inhibition of neovascularization by thrombospondin-1. *Nat Med*. 2000;6:41–48.

28. Bonnefoy A, Daenens K, Feys HB, De Vos R, Vandervoort P, Vermylen J, Lawler J, Hoylaerts MF. Thrombospondin-1 controls vascular platelet recruitment and thrombus adherence in mice by protecting (sub)endothelial VWF from cleavage by ADAMTS13. *Blood*. 2006;107:955–964.

29. Burke A, Creighton W, Tavora F, Li L, Fowler D. Decreased frequency of the 3′UTR T>G single nucleotide polymorphism of thrombospondin-2 gene in sudden death due to plaque erosion. *Cardiovasc Pathol*. 2010;19:e45–e49.

30. Hemdahl A-L, Gabrielsen A, Zhu C, Eriksson P, Hedin U, Kastrup J, Thorén P, Hansson GK. Expression of neutrophil gelatinase–associated lipocalin in atherosclerosis and myocardial infarction. *Arterioscler Thromb Vasc Biol*. 2006;26:136–142.

31. te Boekhorst BC, Bovens SM, Hellings WE, van der Kraak PH, van de Kolk KW, Vink A, Moll FL, van Oosterhout MF, de Vries JP, Doevendans PA, Goumans M-J, de Kleijn DP, van Echteld CJ, Pasterkamp G, Sluijter JP. Molecular MRI of murine atherosclerotic plaque targeting NGAL: a protein associated with unstable human plaque characteristics. *Cardiovasc Res*. 2011;89:680–688.

32. Shalhoub J, Viiri LE, Cross AJ, Gregan SM, Allin DM, Astola N, Franklin IJ, Davies AH, Monaco C. Multi-analyte profiling in human carotid atherosclerosis uncovers pro-inflammatory macrophage programming in plaques. *Thromb Haemost*. 2016;115:1064–1072.

33. Mach F, Sauty A, Iarossi AS, Sukhova GK, Neote K, Libby P, Luster AD. Differential expression of three T lymphocyte-activationg CXC chemokines by human atheroma-associated cells. *J Clin Invest*. 1999;104:1041–1050.

34. Higuma T, Soeda T, Abe N, Yamada M, Yokoyama H, Shibutani S, Vergallo R, Minami Y, Ong DS, Lee H, Okumura K, Jang IK. A combined optical coherence tomography and intravascular ultrasound study on plaque rupture, plaque erosion, and calcified nodule in patients with ST-segment elevation myocardial infarction: incidence, morphologic characteristics, and outcomes after percutaneous coronary intervention. *JACC Cardiovasc Interv*. 2015;8:1166–1176.

Inflammatory Differences in Plaque Erosion and Rupture in Patients With ST–Segment Elevation Myocardial Infarction

Sujay Chandran, Johnathan Watkins, Amina Abdul-Aziz, Manar Shafat, Patrick A. Calvert, Kristian M. Bowles, Marcus D. Flather, Stuart A. Rushworth and Alisdair D. Ryding

J Am Heart Assoc. 2017;6:e005868; originally published May 3, 2017;
doi: 10.1161/JAHA.117.005868
The *Journal of the American Heart Association* is published by the American Heart Association, 7272 Greenville Avenue, Dallas, TX 75231
Online ISSN: 2047-9980